

GSK CONFIDENTIAL

UNIVERSITY OF STRATHCLYDE

DEPARTMENT OF PURE AND APPLIED CHEMISTRY

Preclinical Development of a Treatment for Systemic Lupus Erythematosus

Erin Murray

2014



Declaration of Authenticity and Author's Rights

This thesis is the result of the author's original research. It has been composed by the author and has not been previously submitted for examination which has led to the award of a degree.

The copyright of this thesis belongs to GSK in accordance with the author's contract of employment with GSK under the terms of the United Kingdom Copyright Acts. Due acknowledgement must always be made of the use of any material contained in, or derived from, this thesis.

Signed:

Date:

Contents

Declaration of Authenticity and Author's Rights	i
Abbreviations	v
Abstract	1
1 Introduction	2
1.1 Systemic Lupus Erythematosus	3
1.2 Protein kinases	3
1.3 Janus Kinases	6
1.4 Kinase inhibitors	7
1.5 Aryl-Aryl Cross Coupling	9
1.5.1 The Suzuki-Miyaura Cross Coupling	12
1.5.2 Oxidative addition	14
1.5.3 Transmetalation	18
1.5.4 Reductive elimination	19
1.5.5 Active palladium species	20
1.5.6 Boronic Coupling Partners	22
1.5.7 Side reactions observed during Suzuki-Miyaura couplings	25
1.5.8 Palladium Removal	30
1.5.9 The future of aryl-aryl cross coupling reactions	32
1.5.10 Conclusions	34
2 Development of a New Route to Drug Substance for the Treatment of Systemic Lupus Erythematosus	35
2.1 Introduction	36
2.1.1 Medicinal Chemistry Route (Route A)	36
2.1.2 Improvements Made to the Route A	37

2.1.3	Controlling the Polymorph of 1	39
2.1.4	Objectives for Route B.....	40
2.1.5	Reaction Optimisation using Design of Experiments	41
2.2	Results & Discussion.....	44
2.2.1	Development of Route B Stage 2.....	44
2.2.2	Identification of Reaction Conditions for Route B Stage 3	45
2.2.3	Optimisation of Sodium Carbonate/Methanol Reaction Conditions ...	49
2.2.4	Investigation of Palladium Removal Methods.....	54
2.2.5	Development of Stage 3 <i>n</i> -Butanol Reaction Conditions	57
2.2.6	Scale-up of Sodium Carbonate/ <i>n</i> -Butanol Process	60
2.2.7	Development of Stage 3 Process using Potassium Bicarbonate	66
2.2.8	Identification of Late Running Impurities.....	67
2.2.9	Optimisation of Potassium Bicarbonate Reaction Conditions with DoE 69	
2.2.10	Optimisation of Reaction Work-up to Control Impurities	76
2.2.11	Transfer of Route B Suzuki-Miyaura Coupling to Pilot Plant.....	80
2.3	Conclusions	87
3	Synthesis of Metabolites	88
3.1	Introduction	89
3.2	Synthesis of Metabolite 157	89
3.2.1	Retrosynthetic Analysis of 157	89
3.2.2	Synthesis of 157	91
3.3	Synthesis of Metabolite 167	94
3.3.1	Retrosynthetic Strategy for Metabolite 167	94
3.3.2	Testing the Endgame strategy	97
3.3.3	Route 1 to Azetidine 175.....	97

3.3.4	Route 2 to Azetidine 175.....	102
3.3.5	End game.....	107
3.3.6	Improvements to the Synthesis of Metabolite 167.....	109
3.4	Conclusions	110
4	Experimental	113
4.1	General Experimental Details.....	114
4.2	Experimental Details for Chapter 2.....	117
4.3	Experimental Details for Chapter 3.....	139
5	References	155
6	Appendices.....	169
6.1	Route A Stage 2 Palladium Source, Base and Solvent Screen.....	170
6.2	Working Directions for Route B Processes.....	173
6.2.1	Working Directions For the Preparation of IG 1	174
6.2.2	Working Directions for Preparation of API 1	180
7	Acknowledgments.....	184

Abbreviations

Å	Ångstrom
Ac	Acetyl
ADP	Adenosine 5`-diphosphate
Ar	Aryl
API	Active Pharmaceutical Ingredient
ATP	Adenosine 5`-triphosphate
BINAP	2,2'-Bis(diphenylphosphino)-1,1'-binaphthyl
Bn	Benzyl
BOP	(Benzotriazo-1-yloxy)trisdimethylamino)phosphonium hexafluorophosphate
Bu	Butyl
^t Bu	<i>tert</i> -Butyl
CDI	1,1'-Carbonyldiimidazole
CLR	Controlled Laboratory Reactor
conc.	Concentrated
CPME	Cyclopentyl methyl ether
Cy	Cyclohexyl
DavePhos	2-Dicyclohexylphosphino-2'-(<i>N,N</i> -dimethylamino)biphenyl
dba	Dibenzylideneacetone
DIPEA	<i>Diisopropylethylamine</i>
DMA	<i>N,N</i> -Dimethylacetamide

GSK CONFIDENTIAL

DME	1,2-Dimethoxyethane
DMF	<i>N,N</i> -Dimethylformamide
DMPK	Drug Metabolism and Pharmacokinetics
DMSO	Dimethyl Sulfoxide
DNA	Deoxyribonucleic Acid
DoE	Design of Experiments
DPP	Diphenylphosphine
dppf	1,1'-Bis(diphenylphosphino)ferrocene
DPPP	1,3-Bis(diphenylphosphino)propane
EDC	1-Ethyl-3-(3-dimethylaminopropyl)carbodiimide
<i>e.g.</i>	<i>Exemplia gratia</i>
eOVI	Electronic Organic Volatile Impurities
eq	Equivalents
ESI-MS	Electrospray Ionization Mass Spectrometry
Et	Ethyl
<i>et al.</i>	<i>et alii</i>
EtOAc	Ethyl acetate
FDA	Food and Drug Administration
GSK	GlaxoSmithKline
h	Hours
HOBt	1-Hydroxybenzotriazole
HPLC	High Pressure Liquid Chromatography

GSK CONFIDENTIAL

HRMS	High Resolution Mass Spectrometry
ICP-AES	Inductively Coupled Plasma-Atomic Emission Spectroscopy
IG	Intermediate Grade
IMS	Industrial Methylated Spirits
IPM	In Process Monitoring
IR	Infra Red
JAK	Janus Kinase
KF	Karl Fischer
L	Ligand
LA	Lewis Acid
LC-MS	Liquid Chromatography-Mass Spectrometry
M	Molar
MDAP	Mass Directed Autopreparation
Me	Methyl
MeOH	Methanol
MET	Met proto-oncogene
MIDA	<i>N</i> -methyliminodiacetic acid
min	Minutes
mp.	Melting Point
Ms	Methanesulfonyl
N	Normal
N/A	Not Applicable

GSK CONFIDENTIAL

NaTMT	Trithiocyanuric acid, trisodium salt
ND	Not Detected
NE	Not Examined
NMP	<i>N</i> -methyl-2-pyrrolidone
NMR	Nuclear Magnetic Resonance
OVAT	One Variable At a Time
PAR	Peak Area Ratio
PDE-V	Phosphodiesterase V
Ph	Phenyl
PhMe	Toluene
ppm	Parts Per Million
<i>i</i> Pr	<i>iso</i> -Propyl
RRT	Relative Retention Time
rt	Room Temperature
S	Solvent
SIPr	(1,3-Bis(2,6- <i>diiso</i> propylphenyl)imidazolidene)
SLE	Systemic Lupus Erythematosus
S _N 1	Unimolecular nucleophilic substitution
S _N 2	Bimolecular nucleophilic substitution
SPhos	2-Dicyclohexylphosphino-2',6'-dimethoxybiphenyl
STAT	Signal Transducers and Activator of Transcription
TBAB	Tetrabutylammonium Bromide

GSK CONFIDENTIAL

TBME	<i>tert</i> -butyl methyl ether
TEA	Triethylamine
Temp.	Temperature
Tf	Trifluoromethane sulfonyl
THF	Tetrahydrofuran
TMS	Tetramethylsilane
TMT	Trithiocyanuric acid
Ts	Tosylate
TYK	Tyrosine-protein kinase
US	United States of America
vol	Solvent volumes with respect to the mass of the limiting reagent
wt	weight with respect to mass of limiting reagent used in procedure

Abstract

Janus Kinase 1 (JAK1) inhibitor **1** is being developed between GlaxoSmithKline (GSK) and Galapagos for the treatment of systemic lupus erythematosus (SLE). The medicinal chemistry route to **1** has been scaled up to provide kilogram quantities of **1** for clinical trials. A new sustainable route to **1** is required to fund larger clinical studies and enable commercial manufacture.

A new route was identified to prepare **1** using a Suzuki-Miyaura coupling in the final synthetic step. For the new route to be carried out in the pilot plant, it was necessary to develop the final synthetic step to control palladium and impurity levels in order for **1** to be prepared in acceptable quality for clinical use. The new Suzuki-Miyaura coupling has been scaled up using an 45 Kg input of **149** preparing a total of 165 Kg **1** containing <10ppm Pd and all impurities within specification.

Metabolism of drug substance **1** has been investigated in order to develop **1** into a medicine. The synthesis of metabolites **157** and **167** was carried out to provide analytical markers for a clinical study.

1 Introduction

1.1 Systemic Lupus Erythematosus

Systemic lupus erythematosus (SLE) is a chronic autoimmune disease, where the immune system attacks healthy tissues. The exact causes of SLE are still unknown, but it is thought that several genetic and environmental factors are responsible.¹ SLE is significantly more prevalent in women who make up around 90% of SLE sufferers.²

It is difficult to diagnose SLE, as the symptoms can vary from person to person.³ The main symptoms of SLE are skin rashes, joint pain and fatigue. It is common for the severity of the symptoms to vary over time, so a patient may experience 'flare-ups' of severe symptoms as well as long periods with little or no symptoms. Close monitoring of SLE patients is required, as SLE can also cause inflammation in organs, such as the heart and kidneys leading to an increased risk of cardiovascular and kidney disease.

The subject of this thesis is the preclinical development of drug substance **1** (Figure 1), which is being investigated as a potential the treatment of systemic lupus erythematosus.

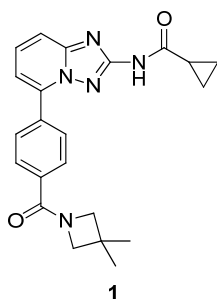


Figure 1: Drug substance 1.

Drug substance **1** is a Janus kinase 1 (JAK1) inhibitor. JAK1 is a protein kinase belonging to the Janus kinase (JAK) family of protein kinases.

1.2 Protein kinases

There are 518 genes for kinases representing 1.7% of the human genome.⁴ Protein kinases are involved in a wide variety of cellular processes, including transcription, differentiation, cell migration, the cell cycle, cell communication, metabolism and apoptosis. Protein kinases are enzymes which respond to external chemical

messengers, to control the activity of other enzymes through phosphorylation. The response of protein kinases to the external chemical messengers, initiates signalling cascades which in turn drive cellular processes.

Protein kinases initiate and regulate enzyme activity by phosphorylation of amino acids in enzymes.⁵ Protein kinases phosphorylate alcohols in the amino acids serine **2** and threonine **3** (Figure 2) as well as the phenol present in tyrosine **4**.

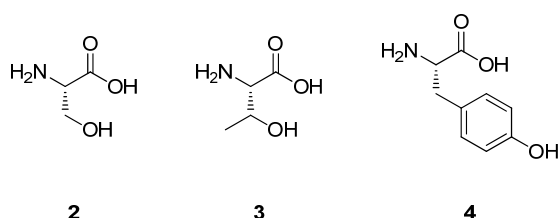
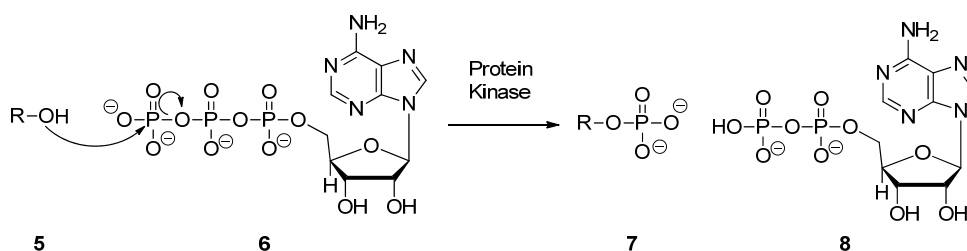


Figure 2: Amino acids serine 2, threonine 3 and tyrosine 4.

The phosphate ion which reacts with hydroxyl from the amino acid, is provided by the co-factor adenosine 5'-triphosphate (ATP) **6** (Scheme 1). The formation of the negatively charged phosphoric acid ester (*e.g.* **7**) can change the hydrogen bonding interactions of the parent protein, which can initiate a signalling cascade.



Scheme 1: Phosphorylation of hydroxyl groups.

Under physiological conditions, the phosphorylation and dephosphorylation of amino acids is catalysed by enzymes (Figure 3). The hydrolysis of the phosphoric acid esters to give the free hydroxyl in the amino acid, is catalysed by phosphatase enzymes. Together, protein kinases and phosphatases to regulate many aspects of cell activity.

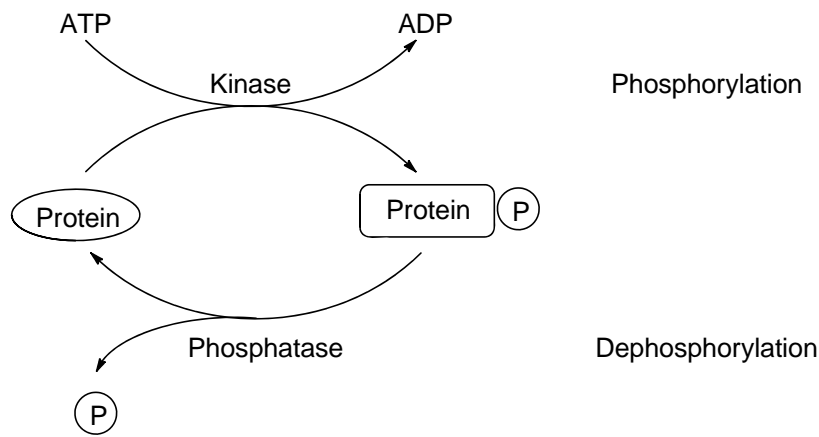


Figure 3: Phosphorylation and dephosphorylation of proteins.

Phosphorylation of the amino acid residues disrupts the hydrogen bonding patterns of an enzyme and offers alternative ionic bonding interactions, which can lead to changes in the tertiary structure of an enzyme. For example, hydrogen bonds between the hydroxyl groups from the amino acids are broken and the negatively charged phosphate group can typically form ionic bonds with positively charged amino acid residues such as ammonium ions (Figure 4).

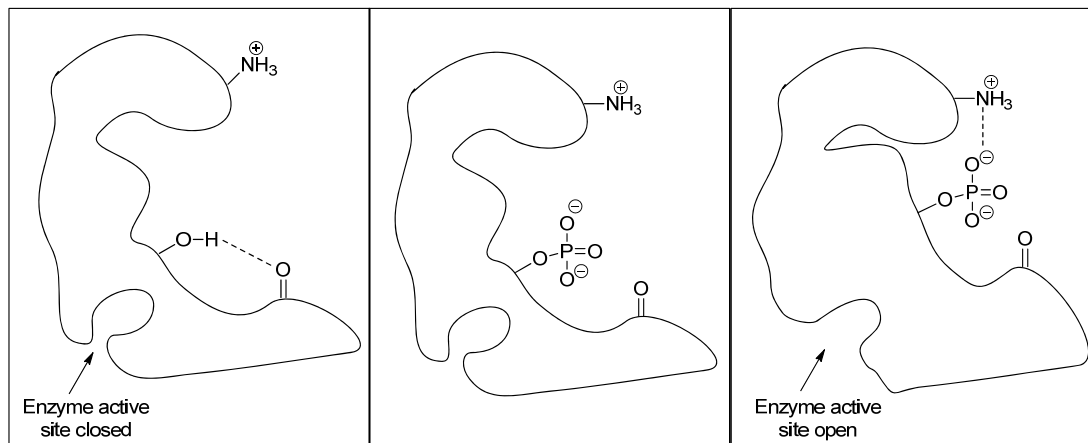


Figure 4: Conformational changes in an enzyme, induced by phosphorylation.⁵

A potential effect of conformational changes in an enzyme, is the exposure, or closure of the active site of the enzyme. The activation or deactivation of the enzyme will cascade further reactions within the cell. Protein kinases are involved in cell signalling cascades and this will be exemplified for Janus kinases in the following section.

1.3 Janus Kinases

The Janus kinase (JAK) family is a group of 4 tyrosine kinases, JAK1, JAK2, JAK 3 and TYK2, which are associated with receptors at the cell membrane. Cytokines are the chemical messengers of the immune system and bind to receptors, activating the associated JAKs by phosphorylation of the tyrosine residues (Figure 5). Once activated, JAKs selectively phosphorylate the STAT (signal transducers and activator of transcription) group of proteins, enabling their activation. The phosphorylated STATs bind to DNA in the nucleus which impacts gene transcription processes. The modulation of gene transcription leads to changes in cellular function.

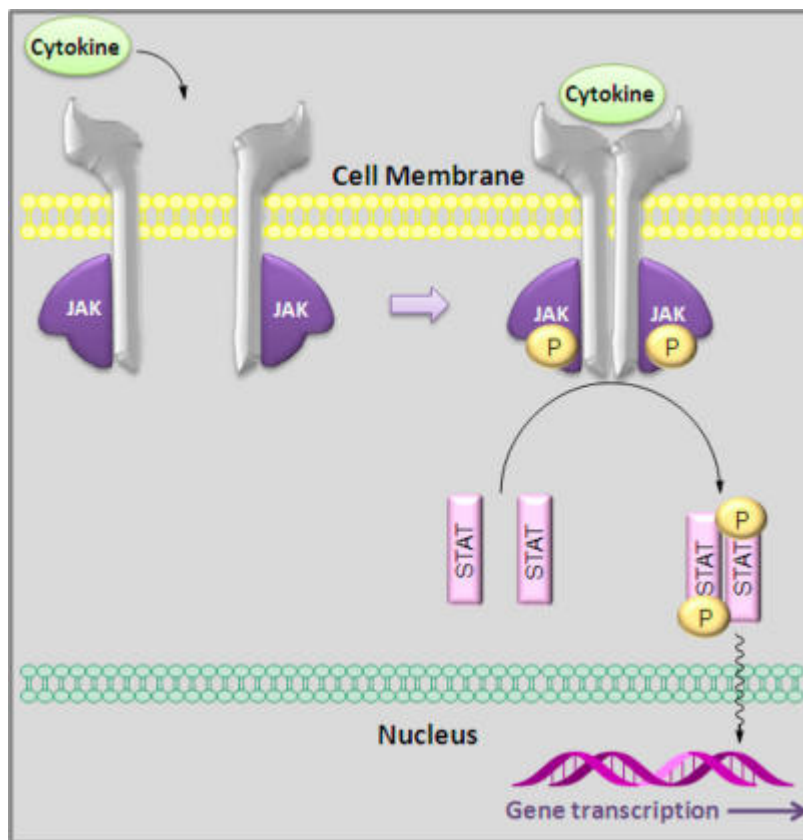


Figure 5: Cytokine signaling through the JAK/STAT pathway.⁶

In the activated state, STATs have a critical role in regulating innate and acquired host immune responses.⁷ JAKs are activated by multiple cytokines involved in the pathogenesis of inflammatory diseases,⁶ so inhibition of JAK phosphorylation using a small molecule could provide new medicines for autoimmune and inflammatory diseases.

1.4 Kinase inhibitors

An inhibitor binds to a protein preventing the protein from carrying out its function. Small molecules can bind to a kinase at the ATP binding site by forming hydrogen bonds and hydrophobic interactions. When the ATP binding site is blocked, the kinase cannot carry out its function of phosphorylating amino acids, preventing further signal transduction processes.

ATP binds to all protein kinases to phosphorylate proteins, so understanding this binding interaction has enabled selective kinase inhibitors to be developed. Figure 6 shows the typical binding interactions of ATP in the kinase active site.

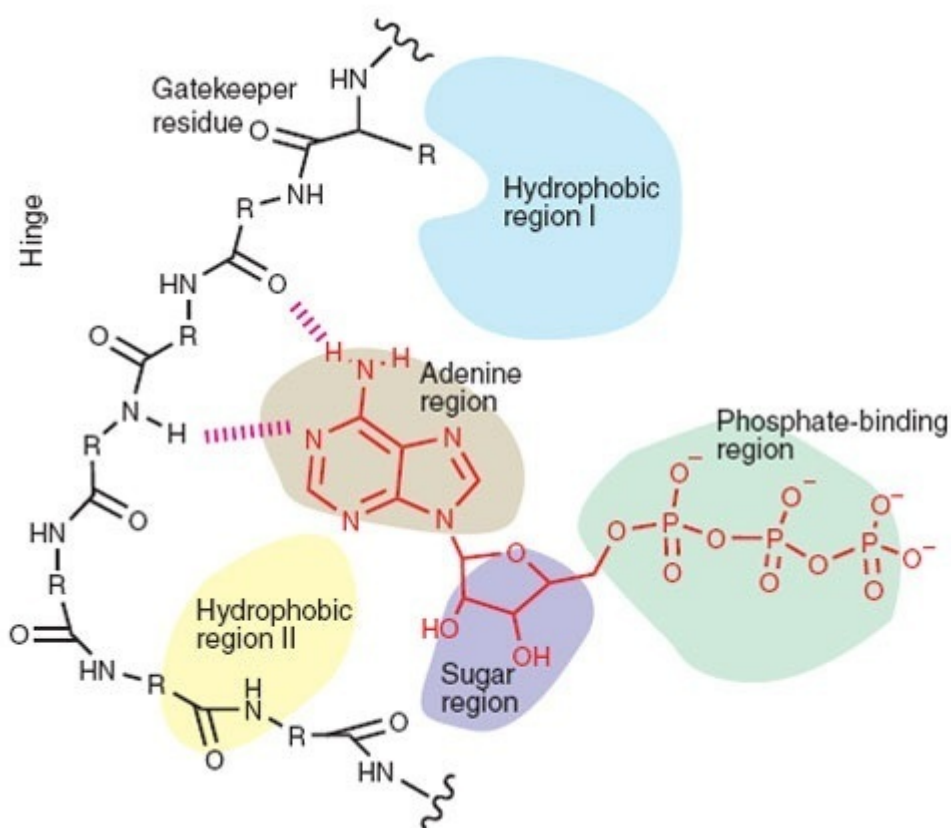


Figure 6: Binding of ATP to the active site of a kinase. ⁸

ATP contains three distinct structural motifs; the adenine region, the sugar region and the phosphate binding region, which have different interactions with the active site to allow binding. The adenine in ATP makes two hydrogen bonds to the amino acids in a specific area of the protein kinase, which is known as the 'hinge'. Protein kinase inhibitors are designed to contain heterocycles similar to adenine to make

hydrogen bonds at the same amino acid residues. The strongly ionic phosphate groups bind to metal ions present in proteins, as well as amino acid residues. ATP is loosely bound in the active site leaving the hydrophobic regions, areas where small molecules can bind to amino acids specific to a particular kinase. At the entrance of one of these hydrophobic regions (Hydrophobic region I in Figure 6), there is an amino acid residue known as the gatekeeper residue. In some protein kinases, the gatekeeper residue is large and therefore blocks the entrance to the active site, however when the gatekeeper residue is smaller, a kinase inhibitor can be designed to have bonding interactions with this amino acid residue. Understanding the relationship between the structure of a particular kinase and the amino acids present within the active site has enabled the rational design of selective kinase inhibitors.

Currently there are two JAK inhibitors Ruxolitinib **9** and Tofactinib **10**, which have received approval for use as medicines from the FDA (Figure 7). Ruxolitinib **9** is a JAK1/JAK2 inhibitor developed by Incyte and Novartis to treat myelofibrosis, which was approved by FDA in 2011.⁹ Pfizer have developed Tofactinib **10**, a JAK3 inhibitor for the treatment of rheumatoid arthritis, which received approval from the FDA in 2012.¹⁰

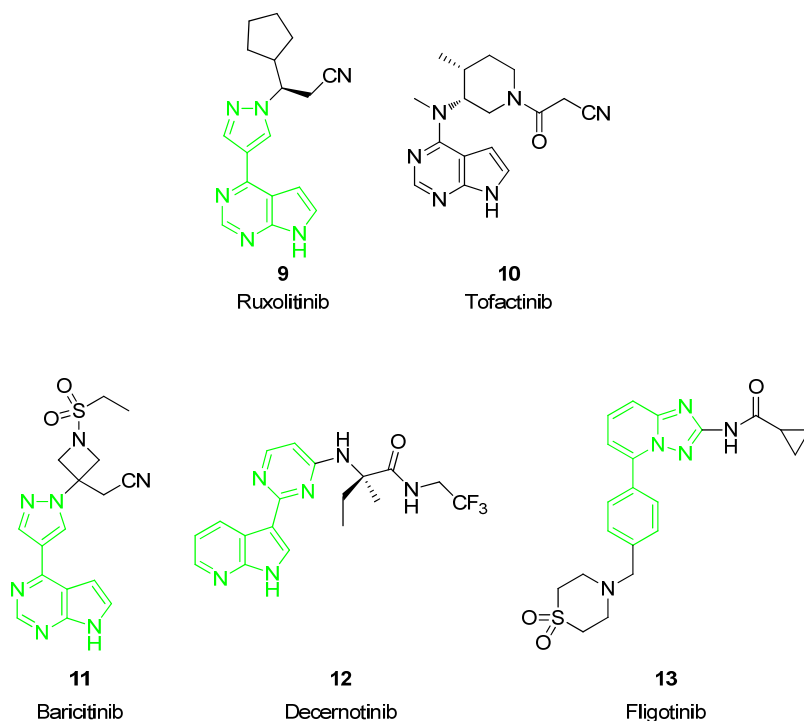
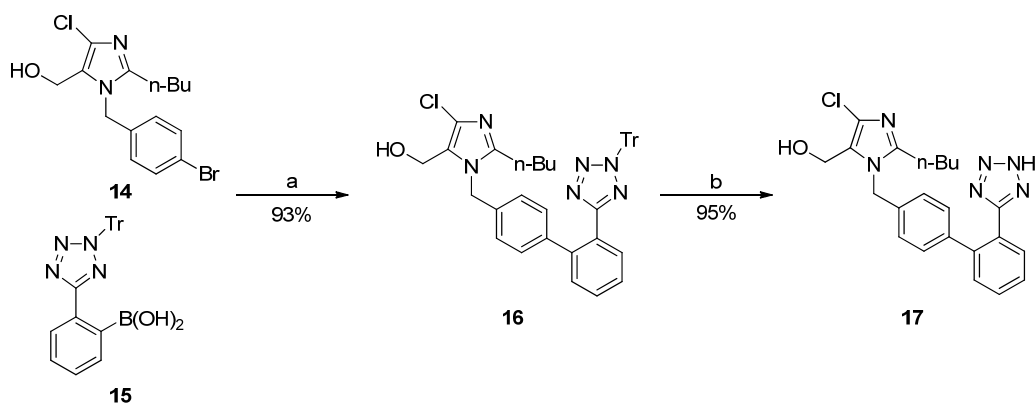


Figure 7: JAK Inhibitors.

Along with the FDA approved compounds, there are several JAK inhibitors in clinical trials for rheumatoid arthritis, including Baricitinib **11**,¹¹ Decernotinib **12**,¹² and Fligotinib **13**¹³ (Figure 7). A key structural motif in many of these JAK inhibitors is a biaryl group. Biaryl groups are present in a significant numbers of drug substances. There are many reasons for this, but one explanation is the ease with which this bond can be constructed, specifically using the Suzuki-Miyaura reaction, providing the product in kilogram to tonne quantities in high purity and yield. The following section will describe the key features of this pivotal C-C bond forming process.

1.5 Aryl-Aryl Cross Coupling

Aryl-aryl cross coupling methodology enables access to biaryl compounds which are a common structural motif in many drug molecules and agrochemicals. Biphenyl groups can interact with aromatic, hydrophobic, polar and positively charged residues in proteins, which in turn leads to a therapeutic effect.¹⁴ Losartan **17** is a treatment for hypertension developed by Merck, which contains a biphenyl group.¹⁵ The biphenyl group is prepared from aryl bromide **14** and boronic acid **15** *via* a Suzuki-Miyaura cross coupling (Scheme 2).¹⁶



Conditions: a) Aryl bromide **14** (1.0 eq), arylboronic acid **15** (1.05 eq), palladium(II) acetate (1 mol%), triphenylphosphine (4 mol%), potassium carbonate (2.5 eq), 4:1 diethoxymethane/THF(11 vol), water (0.1 vol), reflux, 3-6 hours; b) **16** (1.0 eq), 0.75 M H₂SO₄ in 1:1 acetonitrile/water (5 vol), rt, 35 minutes.

Scheme 2: Synthesis of Losartan 17.

A significant number of synthetic methods for forming biaryl bonds were developed throughout the 20th century, starting with the Ullman coupling¹⁷ in 1901 (Figure 8). Between 1972 and 1981, Kumada,¹⁸ Corriu,¹⁹ Negishi,²⁰ Stille²¹ and Suzuki²² published different methods for preparing cross coupled products. The contributions

of Negishi and Suzuki were recognized with the part award of the Nobel Prize for Chemistry in 2010.²³⁻²⁵

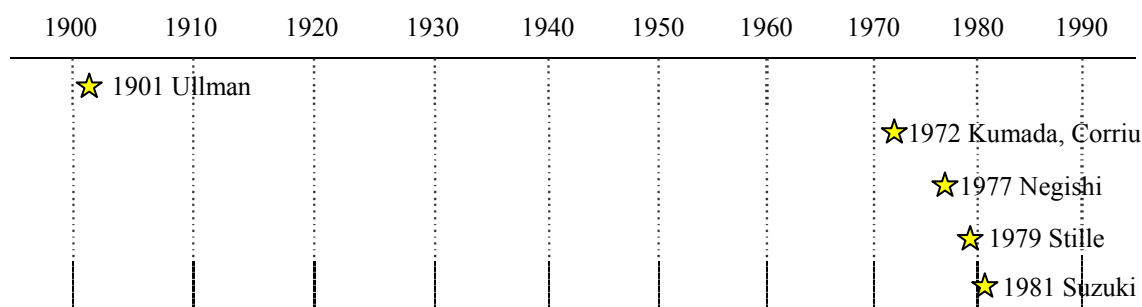
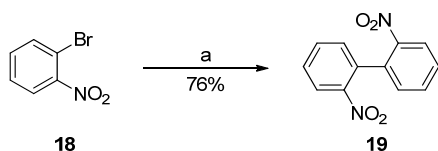


Figure 8: Timeline of publication of synthetic methods.

First reported in 1901, the Ullman reaction formed the homocoupled biaryl product **19** by heating *o*-bromonitrobenzene **18** with stoichiometric copper powder (Scheme 3).¹⁷

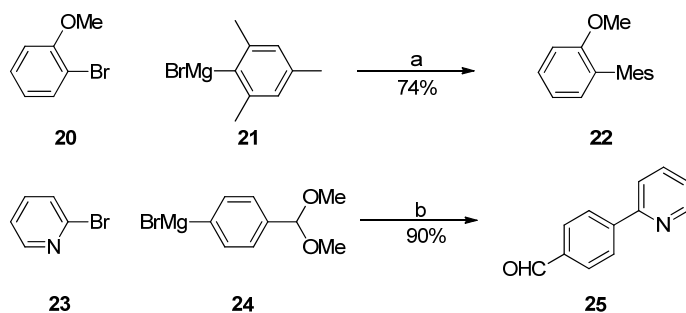


Conditions: a) **18** (1.0 eq), copper powder (1.9 eq), 210-220 °C.

Scheme 3: The Ullman reaction.

The Ullman reaction demonstrates the feasibility of preparing homo-coupled biphenyl products. However a method was required which could deliver cross coupled products. For this reason, alternative methodologies were developed, where the cross coupling partners contain different functional groups.

Kumada and Corriu independently developed methods for cross coupling aryl halides and organomagnesium compounds. The first reported cross coupling reactions of aryl halides with Grignard reagents were catalysed by nickel (Scheme 4).^{18,19,26}

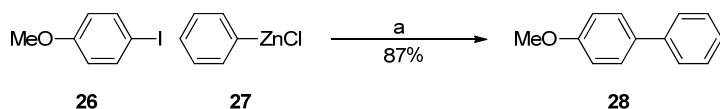


Conditions: a) Aryl halide **20** (1.0 eq), Grignard reagent **21** (1.24 eq), dichloro[1,3-bis(diphenylphosphino)propane]nickel(II) (0.25 mol%), diethyl ether, reflux, 3 – 20 hours; b) i. Aryl halide **23** (1.0 eq), Grignard reagent **24** (1.07 eq), [1,3-bis(diphenylphosphino)propane]nickel(II) chloride (0.6 mol%), *diisobutylaluminium hydride* (0.19 vol, 20% in hexanes), rt, 90 minutes; ii. HCl.

Scheme 4: Kumada-Corriu reaction examples.

This reaction has been scaled up in order to produce 1.82 Kg **25** (Scheme 4).²⁷ The Kumada-Corriu reaction has also been shown to be catalysed by palladium.²⁸ Compared with the Ullman coupling, the Kumada-Corriu coupling has the advantages of enabling access to cross coupled products with catalytic amounts of transition metals, rather than stoichiometric copper. However using Grignard reagents limits the scope of this reaction, as these reagents are incompatible with many functional groups, such as esters and ketones.

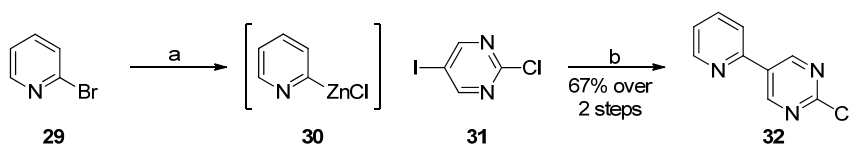
Negishi developed a palladium catalysed method for aryl-aryl cross coupling involving the reaction of aryl halides with arylzinc reagents (Scheme 5).²⁰



Conditions: a) Aryl iodide **26** (1.0 eq), organozinc chloride **27**, $\text{Cl}_2\text{Pd}(\text{PPh}_3)_2$ (5 mol%), *diisobutylaluminium hydride* (10 mol%), THF, 25 °C, 1-2 hours.

Scheme 5: Negishi reaction.

The organozinc reagent is usually formed *in situ* through addition of zinc chloride or zinc bromide to an organolithium formed by halogen/lithium exchange. Forming the organozinc coupling partner using this method prohibits the use of substrates with acidic protons, such as aldehydes and alcohols, due to the potential for side reactions. The Negishi cross coupling has been scaled up to prepare 16 Kg of biaryl **32** across six batches, which was required for the synthesis of a PDE-V inhibitor (Scheme 6).²⁹

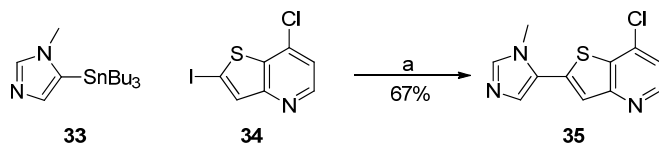


Conditions: a) Aryl bromide **29** (2.08 eq), hexyllithium (2.18 eq), solution in hexanes, zinc(II) chloride (2.08 eq), THF, -65 to -55 °C; b) Pd(PPh₃)₄ (20 mol%), aryl iodide **31** (1.0 eq), THF, rt, 1 hour.

Scheme 6: Negishi reaction carried out on kilogram scale.

A consideration for scaling up a Negishi reaction to kilogram scale is the generation of a significant amount of zinc waste, which requires expensive disposal methods.

The limited functional group tolerance of the Kumada-Corriu and Negishi cross couplings was addressed by development of the Stille reaction in the late 1970s.²¹ In the Stille reaction, cross coupled products are obtained by the palladium catalysed reaction of aryl halides with organostannanes. Organostannanes are mild organometallic reagents, enabling cross coupling to be carried out in the presence of functional groups which are not tolerated by the Kumada-Corriu and Negishi reactions. The tolerance of functional groups in the Stille reaction has made this reaction a popular choice for palladium catalysed C-C bond formations.²⁵ A team from Pfizer have scaled up a Stille coupling to produce 302 g of key intermediate **35** (Scheme 7).³⁰



Conditions: a) Aryl iodide **34** (1.0 eq), stannane **33** (1.0 eq), Pd(PPh₃)₄ (5 mol%), DMF, 95 °C, 40 hours.

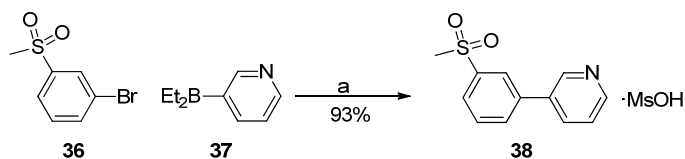
Scheme 7: Stille reaction.

A disadvantage of the Stille coupling is the production of stoichiometric organotin by-products along with the desired cross coupled products. The organotin by-products are highly toxic, making this method less favourable for scaling up to kilogram scale.³¹

1.5.1 The Suzuki-Miyaura Cross Coupling

The Suzuki-Miyaura reaction is an established methodology used for cross coupling reactions, which is convenient for use in academic and industrial settings. In the pharmaceutical industry, it is used widely during drug discovery and development

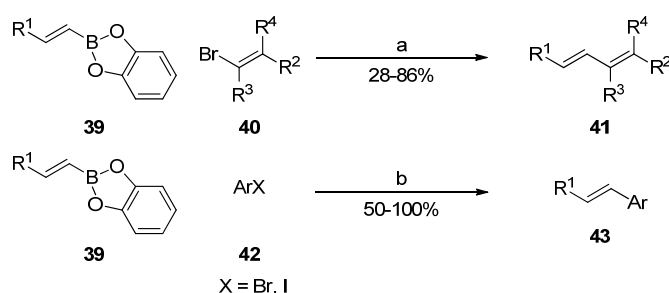
and has been successfully scaled up to prepare hundreds of kilograms of biaryl products such as **38** (Scheme 8).³²



Conditions: a) i. Aryl halide **36** (1.0 eq), organoborane **37** (1.0 eq), TBAB (9 mol%), Pd(PPh₃)₄ (0.7 mol%), potassium carbonate (3.0 eq), toluene, water, 84 °C, 12 hours; ii. Methanesulfonic acid (1.0 eq).

Scheme 8: Suzuki-Miyaura coupling scaled up to 215 Kg input of 36.

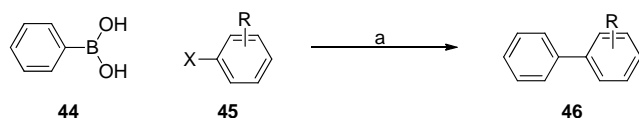
The first publications of cross coupling reactions with organoboron reagents and catalysed by palladium were published in 1979 by Suzuki and Miyaura.^{33,34} In these reactions, the cross coupled product is obtained by combination of an aryl, alkenyl or alkynyl halide and an alkenylborane in the presence of a palladium catalyst and a base (Scheme 9).



Conditions: a) Vinyl bromide **40** (1.0 eq), benzodioxaborole **39** (1.1 eq), Pd(PPh₃)₄ (1 mol%), sodium ethoxide in ethanol (2.0 eq), benzene, reflux, 2 hours; b) Aryl halide **42** (1.0 eq), benzodioxaborole **39** (1.1 eq), Pd(PPh₃)₄ (1-5 mol%), sodium ethoxide in ethanol (2.2 eq), benzene, reflux, 2 hours.

Scheme 9: Suzuki-Miyaura sp²-sp² cross coupling.

The first example of an aryl-aryl cross coupling using organoboronic acids was first reported in 1981 by Suzuki and Miyaura (Scheme 10).²²

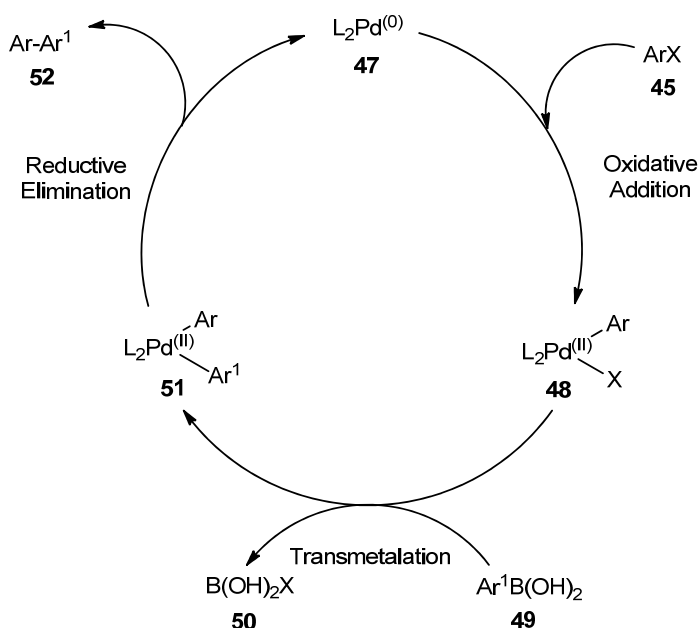


Conditions: a) Aryl halide **45**, phenylboronic acid **44**, Pd(PPh₃)₄, sodium carbonate, benzene, reflux.

Scheme 10: Suzuki-Miyaura aryl-aryl cross coupling.

Scheme 11 depicts the general catalytic cycle for the Suzuki-Miyaura cross coupling.³⁵ The first step is oxidative addition of aryl halide **45** (where X = I, Br, Cl or OTf) to palladium(0) **47**. This is followed by transmetalation of **48** with **49** to

give **51**. Reductive elimination generates the cross coupled product **52** and regenerates palladium(0) **47**.

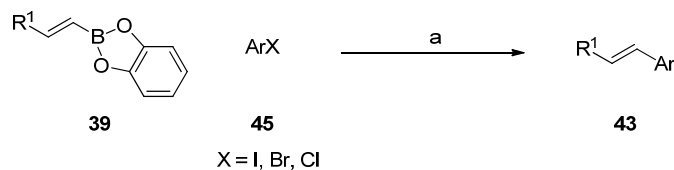


Scheme 11: A general catalytic cycle for the Suzuki-Miyaura Cross Coupling.³⁵

The catalytic cycle in Scheme 11 is supported by the observation of **48** and **51** in electrospray ionization mass spectrometry (ESI-MS) analysis of reaction mixtures.³⁶ The intermediate formed by oxidative addition **48**, has also been observed using electrochemical methods.³⁷

1.5.2 Oxidative addition

The first step of the catalytic cycle in a Suzuki-Miyaura coupling is the oxidative addition of the aryl halide **45** to the palladium(0) species **47**, forming a palladium(II) complex **48**. Oxidative addition of the aryl halide **45** to the palladium(0) species is also the first step in the other aryl-aryl cross coupling reactions, such as the Stille coupling and the Buchwald-Hartwig amination. Oxidative addition of the aryl halide **45** to the palladium(0) species is often the rate limiting step of cross coupling reactions.³⁵ The rate of oxidative addition is influenced significantly by the aryl halide **45** used in the cross coupling (Table 1).

Table 1: Comparison of Suzuki-Miyaura reaction using different aryl halides. ^a

Entry	ArX (45)	Reaction time (h)	Yield (%)
1	PhI	2	100
2	PhBr	2	63
3	PhBr	4	98
4	PhCl	2	3

^a Conditions: a) Aryl halide **45** (1.0 eq), benzodioxaborole **39** (1.1 eq), Pd(PPh₃)₄ (1-5 mol%), sodium ethoxide in ethanol (2.2 eq), benzene, reflux.

Table 1 shows aryl iodides (entry 1) are more reactive than aryl bromides (entries 2 and 3), which are more reactive than aryl chlorides (entry 4). This trend had also been observed when aryl halides were added to tetrakis(triphenylphosphine)palladium(0).^{38,39} Using phenyliodide, the oxidative addition product Ph(PPh₃)₂Pd^{II}I was formed at room temperature. To form the corresponding product Ph(PPh₃)₂Pd^{II}Br from phenyl bromide, temperatures of 80 °C were required. Using phenyl chloride, the product of oxidative addition, Ph(PPh₃)₂Pd^{II}Cl, was not formed at 135 °C. These experimental results are consistent with the bond strengths observed for the C-X bond, as more energy is required to break C-Cl bonds, than C-I bonds (Table 2).⁴⁰

Table 2: Carbon-halide bond dissociation energies.

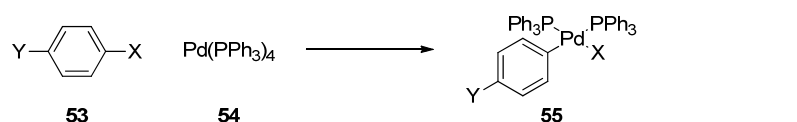
C-X	Bond dissociation energy kcal/mol at 298 K
C-F	126
C-Cl	96
C-Br	81
C-I	65

Aryl chlorides are more attractive as starting materials for cross coupling reactions than aryl iodides and bromides, because aryl chlorides are cheaper and more readily available than the corresponding iodides and bromides.⁴⁰ Using aryl chlorides also increases the mass efficiency of a reaction, because the mass of the halide by-products are lower. As oxidative addition had been shown to be the rate limiting

step for the cross coupling of aryl bromides, it was anticipated oxidative addition would be slower still for aryl chlorides.^{41,42}

Substituents on the aryl ring can activate or deactivate an aryl halide towards oxidative addition.³⁷ Electron donating groups on an aryl halide can reduce the rate of oxidative addition. The presence of a para electron withdrawing group can improve the reactivity of the aryl halide. For example, 4-nitrophenyl iodide undergoes oxidative addition at a faster rate than phenyl iodide. Nitro groups can also improve the reactivity of aryl chlorides (Table 3). For example, 4-nitrophenyl chloride can undergo oxidative addition at 80 °C (entry 2), whereas phenyl chloride does not undergo oxidative addition at 135 °C (entry 1).³⁹

Table 3: Effect of substituents on oxidative addition.^a



Entry	X	Y	Temperature (°C)	Isolated yield
1	Cl	H	135	0
2	Cl	NO ₂	80	86

^a Conditions: Aryl halide **53** (1.0 eq), Pd(PPh₃)₄ (0.2-0.3 eq), benzene.

Choice of ligand has been shown to be a key factor in developing a general method for the Suzuki-Miyaura coupling of aryl chlorides. Fu,⁴³ Buchwald⁴² and Hartwig⁴¹ have shown oxidative addition of aryl chlorides to palladium(0) is possible using the ligands shown in Figure 9.

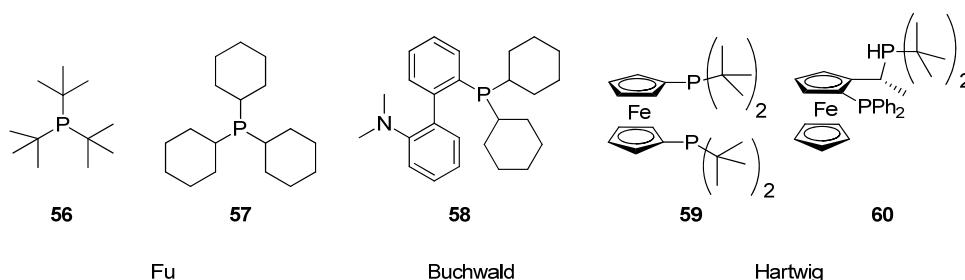


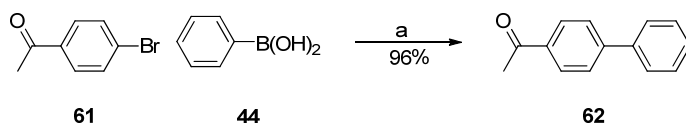
Figure 9: Ligands used for cross coupling reactions of aryl chlorides.

Fu reported using P^tBu₃ **56** and PCy₃ **57** with Pd₂(dba)₃, enabled cross coupling of 4-chlorotoluene with phenylboronic acid **44**.⁴³ This method was shown to be applicable to electron-rich aryl chlorides as well as electron poor aryl chlorides. Around the

same time, the dialkylbiaryl phosphine ligand **58** developed by Buchwald was shown to enable cross coupling of various aryl chlorides.⁴² Hartwig demonstrated the use of ferrocene derived ligands **59** and **60**, enabling aryl chlorides to undergo oxidative addition and subsequent amination.⁴¹ The ligands used by Fu, Buchwald and Hartwig contain alkyl groups and are therefore more electron rich than the aryl phosphine ligands which had been used prior to this work. These electron rich ligands enable a more active catalytic palladium(0) species to be generated, which can undergo oxidative addition with an aryl chloride.

Littke and Fu have carried out further mechanistic investigations⁴⁴ into the catalytically active species generated from Pd₂(dba)₃ and P^tBu₃ **56**, which suggested a monoligated palladium(0) may be the catalytically active species. As well as being electron rich, the ligands used to enable cross coupling of aryl chlorides are also bulky. The steric bulk of the ligand is also important in stabilising the reactive monoligated palladium(0) species.⁴⁵

Using more active palladium catalysts is also beneficial for other aryl halides such as bromides and iodides, as this enables the Suzuki coupling to be carried out under milder conditions, or enables palladium loadings to be reduced. Buchwald and Fu have shown the palladium species generated from the alkylphosphine ligands can undergo oxidative addition with aryl bromides at room temperature.^{46, 44} Buchwald has also shown using the more active catalysts with aryl bromides enables the palladium and ligand loading to be reduced to 0.001 mol% in the coupling of **61** with **44** (Scheme 12).⁴⁶



Conditions: a) Aryl bromide **61** (1.0 eq), phenylboronic acid **44** (1.5 eq), K₃PO₄ (2.0 eq), Pd₂(dba)₃ (0.001 mol%), (*o*-biphenyl)P(^tBu)₂ (0.002 mol%), toluene, 100 °C, 19 hours.

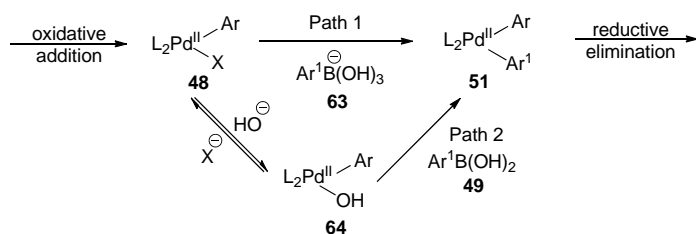
Scheme 12: Suzuki-Miyaura reaction using 0.001 mol% palladium.

The dialkylbiaryl phosphine ligands developed by Buchwald such as **58** are more complex and consequently more expensive than ligands such as triphenylphosphine. This could be seen as a disadvantage of using these ligands, however Colacot *et al.*

argue the savings gained by use of an aryl chloride over an aryl bromide or iodide, should be considered as these savings could outweigh the costs of the ligand.²⁵

1.5.3 Transmetalation

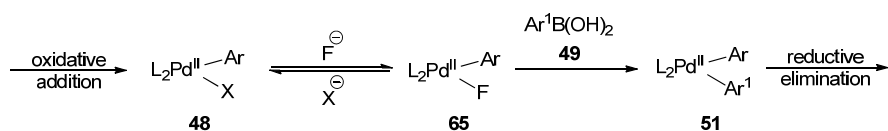
Two pathways have been proposed for transmetalation (Scheme 13). Path 1 suggests the oxidative addition product **48** is attacked by the nucleophilic boronate species **63**. Path 2 suggests the halide in the oxidative addition product **48** undergoes ligand exchange with hydroxide ions to give the oxo-palladium complex **64**. The oxo-palladium complex **64** formed undergoes transmetalation with the aryl boronic acid **49**. Several computational studies were performed to investigate the preferred route of transmetalation and all of these studies showed the preferred pathway was Path 2.⁴⁷⁻⁴⁹



Scheme 13: Alternative pathways for transmetalation.

The transmetalation process has been explored experimentally by Jutand *et al.*⁵⁰ and Hartwig *et al.*⁵¹ in 2011. Jutand and co-workers used cyclic voltammetry to demonstrate the preferred pathway is reaction of the oxo-palladium complex **64** with the boronic acid **49** (Path 2, Scheme 13). The cross coupled product was not observed when the oxidative addition product **48** was combined with aryl boronate **63** (Path 1, Scheme 13). Hartwig's group also showed using NMR spectroscopy, no reaction was observed between **48** and **63**.⁵¹ They also showed the rate of reaction of the boronic acid **49** with **64** (Path 2, Scheme 13) was significantly faster than path 1.

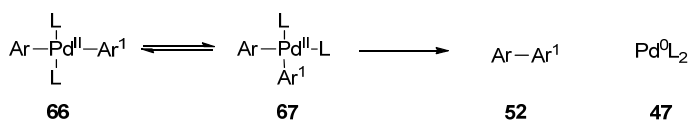
Potassium fluoride and caesium fluoride have been investigated as alternative bases to hydroxide in the Suzuki-Miyaura reaction, in order to provide an alternative when functional groups which are incompatible with hydroxide are present.⁵² Jutand has demonstrated fluoride ions undergo exchange with the halide in the oxidative addition product **48** to give **65** (Scheme 14).⁵³ The complex **65** obtained also undergoes transmetalation with arylboronic acid **49**.



Scheme 14: Transmetalation involving fluoride ions.

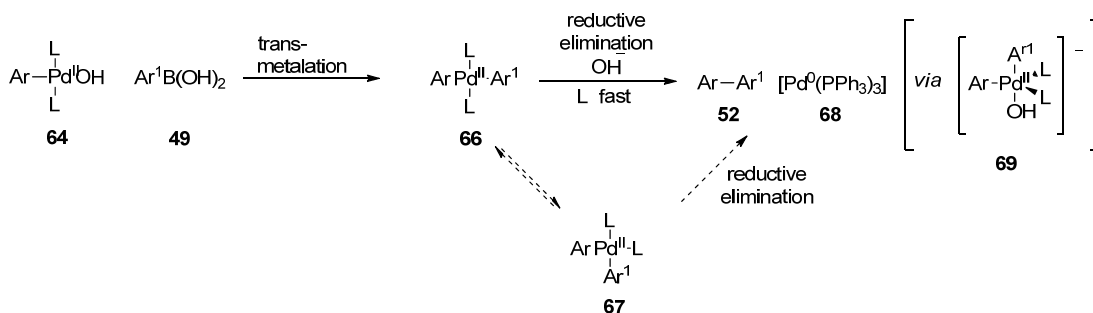
1.5.4 Reductive elimination

The final step in the catalytic cycle of the Suzuki-Miyaura coupling is the reductive elimination of the biaryl product **52**, which also regenerates the palladium(0) catalyst **47**. Early studies showed the coordination geometry at palladium was important in order for reductive elimination to proceed. Several studies showed dialkyl and biaryl products were reductively eliminated from *cis*-palladium species.^{54,55} *Trans*-palladium species **66** were shown to undergo isomerisation to *cis*-palladium species **67**, before the dialkyl/biaryl product **52** could be reductively eliminated (Scheme 15).



Scheme 15: *Trans-cis* isomerisation leading to reductive elimination.

Recently Jutand *et al.* have proposed a base is required in order for reductive elimination to occur.⁵⁰ Having demonstrated the preferred pathway for transmetalation is by reaction of aryl boronic acid **49** with the oxo-palladium complex **64**, it was expected the transmetalation product **51** would reductively eliminate (Scheme 13). Using cyclic voltammetry methods, it was expected the palladium species Pd⁰(PPh₃)₃ would be detected, but this was not observed. The *trans*-complex **66** was isolated and characterized by ¹H and ³¹P NMR spectroscopy. Slow conversion of the *trans*-complex **66** to the biaryl product **52** was observed when one of the aryl groups contained an electron donating group e.g. methoxy. Addition of hydroxide to the *trans*-complex **66** significantly increased the rate of reductive elimination, so it is proposed reductive elimination occurs *via* an anionic 5-coordinate palladium species **69** (Scheme 16).



Scheme 16: Proposed pathways for reductive elimination.

As fluoride ions have been shown to be effective bases for the Suzuki-Miyaura coupling, the role of fluoride ions was investigated in the reductive elimination step.⁵³ Fluoride ions were also shown to increase the rate of reductive elimination, so it is proposed reductive elimination occurs *via* formation of the analogous anionic 5-coordinate palladium species **70** (Figure 10).

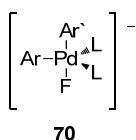


Figure 10: Anionic 5-coordinate palladium species formed with fluoride ions.

1.5.5 Active palladium species

In the first reports of the Suzuki-Miyaura reaction, Pd(PPh₃)₄ was the catalyst used for the transformation.^{22,33,34} Pd(PPh₃)₄ is a source of palladium(0). In solution, Pd(PPh₃)₄ undergoes rapid dissociation of a triphenylphosphine ligand to give Pd(PPh₃)₃ **68**.⁵⁶ The rate law for oxidative addition (1) shows that the rate is proportional to [Pd⁰] and [ArX] and inversely proportional to [PPh₃]. The inverse dependence of the rate of oxidative addition on [PPh₃] is evidence that Pd⁰(PPh₃)₃ **68** undergoes further ligand dissociation to give the catalytically active species Pd⁰(PPh₃)₂.^{37, 57}

$$\frac{d[\text{Pd}^0]}{dt} = \frac{d[\text{ArX}]}{dt} = -k \frac{[\text{Pd}^0][\text{Ar}]}{[\text{PPh}_3]} \quad (1)$$

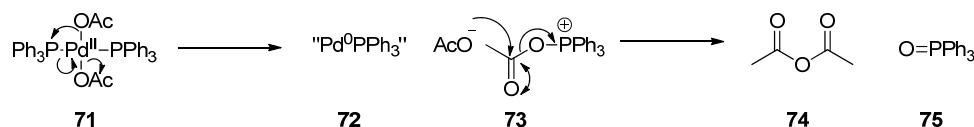
Suzuki-Miyaura coupling reactions are not restricted to the use of Pd(PPh₃)₄ as the catalyst. Table 4 shows sources of palladium used in Suzuki-Miyaura reactions with their costs. A key consideration for scaling up Suzuki-Miyaura reactions is the cost of the palladium source, so if cheaper sources of palladium, such as palladium(II)

acetate, palladium(II) chloride or palladium on carbon can be used, costs will be significantly reduced.

Table 4: Palladium sources used in Suzuki-Miyaura reactions and their associated costs.⁵⁸

Palladium source	Price in US \$ per mol Pd
Pd(PPh ₃) ₄	18900
PdCl ₂ (dppf)	19300
Pd(OAc) ₂	6800
PdCl ₂	5100
Pd ₂ (dba) ₃	12900
10% w/w Pd-C (50% water wet)	2

Palladium(0) can be generated *in situ* by reduction of palladium(II) salts, such as palladium(II) acetate, or palladium(II) chloride. Palladium(II) acetate is used in combination with a phosphine ligand. Jutand *et al.* have shown palladium(II) acetate and triphenyl phosphine combine in solution to form the complex Pd^{II}(OAc)₂(PPh₃)₂ **71**.⁵⁹ This study showed “Pd⁰PPh₃” **72** and triphenylphosphine oxide **75** generated by an intramolecular reaction of Pd^{II}(OAc)₂(PPh₃)₂ **71** (Scheme 17).



Scheme 17: Reactions of palladium complex 71.

The monoligated “Pd⁰PPh₃” **72** formed is not stable and probably exists as a dimeric species [Pd⁰₂(PPh₃)₂(OAc)_xS_y]^{x-} (where S is solvent). The study showed the low ligated palladium(0) species **72** could be trapped by phenyl iodide, or stabilised by the addition of excess triphenylphosphine ligands.

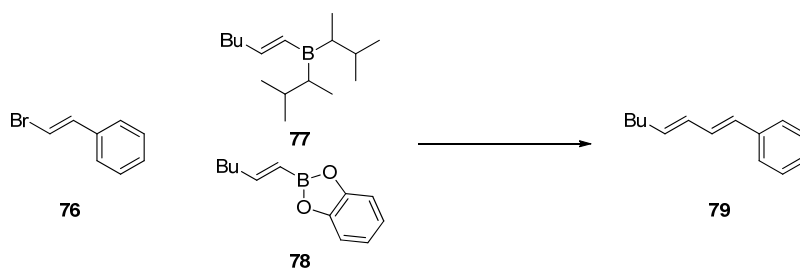
Another source of palladium(0) for Suzuki-Miyaura couplings is Pd(dba)₂ and phosphine ligands. Pd(dba)₂ is more stable during storage than Pd(PPh₃)₄, as Pd(dba)₂ is not as sensitive to oxygen, so it was thought it could be used as a more convenient source of palladium(0). It was also thought using Pd(dba)₂ forming a species such as Pd(PR₃)₄ would not be necessary, enabling the use of phosphine ligands in limited supply following a lengthy synthesis. However it was observed that, rather than the rate of reaction being comparable to when Pd(PPh₃)₄ was used,

the rate of reaction was slower using Pd(dba)₂ and 2PPh₃. Jutand *et al.* investigated these two systems and demonstrated the same species of the active catalyst, “Pd⁰(PPh₃)₂” was present, but when generated from Pd(dba)₂ and triphenylphosphine, the concentration of “Pd⁰(PPh₃)₂” was much lower.⁶⁰ The lower concentration of “Pd⁰(PPh₃)₂” when using Pd(dba)₂/PPh₃ is due to dibenzylideneacetone being a better ligand for palladium(0) than triphenylphosphine.

1.5.6 Boronic Coupling Partners

Early studies carried out by Miyaura and Suzuki into alkenyl-alkenyl cross couplings compared catecholboronate esters with alkylboranes.^{33,34} The investigation showed better yields using catecholboronate esters **78** when compared with alkylboranes **77** (Table 5).

Table 5: Comparison of Suzuki-Miyaura reaction using organoboranes and boronate esters.^a

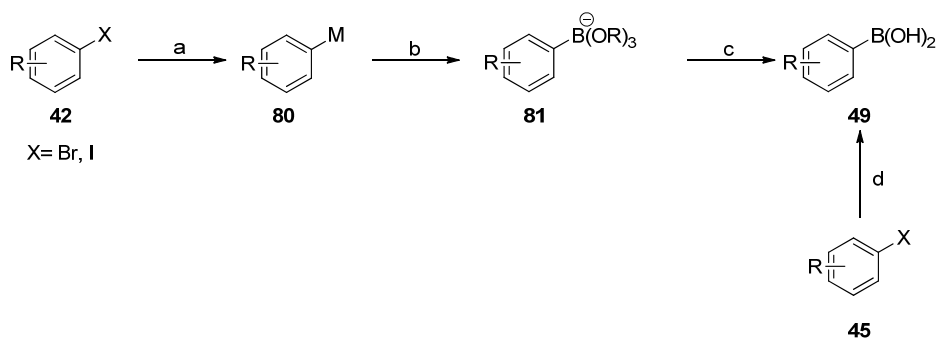


Entry	Organoboron	Solvent	Temperature °C	Base	Catalyst mol %	Yield %
1	77	THF	65	NaOH	3	59
2	78	Benzene	80	NaOEt	1	80

^a Conditions: Aryl halide **76** (1.0 eq), organoboron (1.1 eq), base (2.2 eq), Pd(PPh₃)₄, 2 hours.

Alkylboranes such as **77** are readily oxidized, so it is important to ensure the system is completely degassed in order to obtain good yields. In addition, organoboranes can be decomposed *via* dehydroboration and protodeboronation.⁶¹

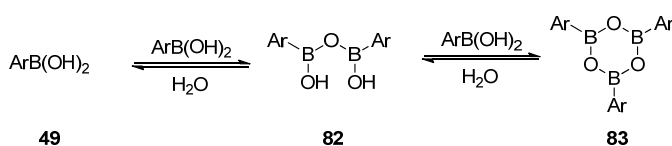
Use of boronic acids in aryl-aryl cross couplings was first reported by Suzuki and Miyaura (Scheme 10).²² Boronic acids are air/moisture stable and widely available. Boronic acids **49** are easy to prepare from aryl halides **42** either *via* preparation of an organolithium⁶²/organomagnesium **80**^{63,64} followed by quenching with B(OMe)₃/B(OⁱPr)₃, or palladium catalysis with bisboronic acid (Scheme 18).^{65,66}



Conditions: a) Aryl bromide **42**, organolithium or organomagnesium; b) B(OR)_3 ; c) H_3O^+ ; d) Aryl halide **45**, Pd^0 , bisboronic acid.

Scheme 18: Synthesis of boronic acids.

Boronic acids exist as a mixture of monomeric **49**, dimeric **82** and cyclic trimeric **83** species (Scheme 19).



Scheme 19: Formation of boronic acid oligomers.

Formation of oligomers of the boronic acid can impede progress of the Suzuki-Miyaura coupling reaction. Usually this is overcome by the aqueous conditions used in these reactions, which enables the dimeric **82** and trimeric species **83** to be converted to the reactive monomeric species **49**. Use of boronic esters **84**, trifluoroborate salts **85** and MIDA boronates **86**, also enable a monomeric boronic acid species to be dosed into a reaction mixture (Figure 11).

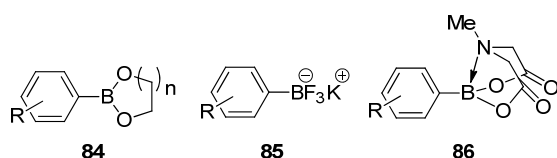
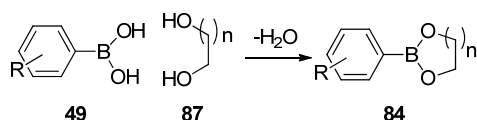


Figure 11: Protected boronic acids.

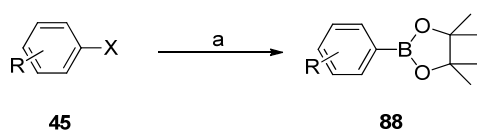
Introduction of a boronic acid into a synthetic sequence is usually in the step prior to the Suzuki-Miyaura reaction, due to the incompatibility of boronic acids with many reagents. Boronic acids are typically used in Suzuki couplings without further synthetic manipulation. Use of boronic esters **84**, trifluoroborate salts **85** and MIDA boronates **86** (Figure 11) allow the boronic acid group to be masked, protecting this group through a synthesis.

A variety of boronic esters have been used in Suzuki-Miyaura couplings. In principle, any 1,2 diol, or 1,3 diol could be used to prepare a boronic ester **84** from a boronic acid **49** under dehydrating reaction conditions (Scheme 20).



Scheme 20: Preparation of boronate esters from boronic acids and diols.

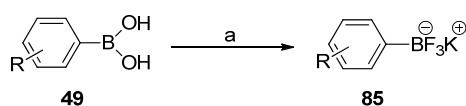
Pinacol boronate esters **88** can also be prepared using Miyaura borylation, where aryl halides **45** are reacted with bis-pinacolatoboron using palladium catalysis (Scheme 21).^{67,68}



Conditions: a) Aryl halide **45** (1.0eq), bis-pinacolatoboron (1.1 eq), potassium acetate (3.0 eq), Pd(dppf)Cl₂ (3 mol%), DMSO, 80 °C.

Scheme 21: Miyaura borylation.

Potassium trifluoroborate salts **85** have recently come to prominence as boron species for Suzuki-Miyaura couplings. Like boronate esters **84** and **88** and MIDA boronates **86**, potassium trifluoroborate salts **85** are convenient for dosing a monomeric species into cross coupling reactions. Potassium trifluoroborate salts **85** also are isolated as free flowing crystalline powders⁶⁹ which is a significant advantage over their boronic acid and boronate ester counterparts, which are frequently difficult to handle.⁷⁰



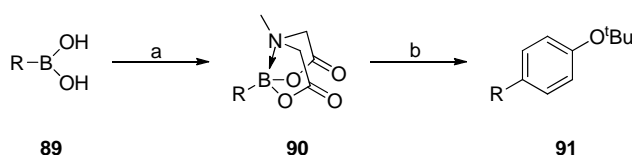
Conditions: a) Aryl boronic acid **49**, aqueous KHF₂, methanol

Scheme 22: Formation of potassium trifluoroborate salts from boronic acids.

Potassium trifluoroborate salts **85** are easily prepared from boronic acids **49** and potassium bifluoride⁷¹ (Scheme 22), however the reaction mixture tends to etch glassware. Lloyd-Jones has shown using potassium fluoride and L-tartaric acid instead of potassium bifluoride, potassium trifluoroborate salts **85** can be prepared conveniently without etching glassware.⁷²

Potassium trifluoroborate salts **85** can be used directly in Suzuki-Miyaura couplings. It has been shown the trifluoroborate anion undergoes hydrolysis under the reaction conditions, and it is the boronic acid **49** which undergoes transmetalation.^{69,73,74} Although use of potassium trifluoroborate salts **85** offer advantages in Suzuki-Miyaura cross couplings, a fundamental disadvantage is the generation of fluoride in the waste streams, which will become an important consideration if the cross coupling is to be carried out on kilogram scale.

Use of MIDA boronates **90** allow the boronic acid group to be protected, to enable manipulation through a synthesis (Scheme 23).⁷⁵



Conditions: a) Boronic acid **89** (1.0 eq), N-methyliminodiacetic acid (1.0-1.5 eq), DMSO, toluene, Dean-Stark, 2-18 hours; b) 1-*tert*-butoxy-4-chlorobenzene (1.0 eq), MIDA boronate **90** (1.2 eq), Pd(OAc)₂ (5 mol%), SPhos (10 mol%), K₃PO₄ (7.5 eq), 1,4-dioxane, water, 60 °C, 6 hours.

Scheme 23: Formation of MIDA boronates and subsequent Suzuki-Miyaura reaction.

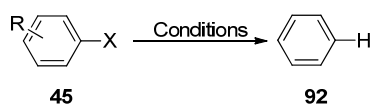
Under mild basic conditions of the Suzuki-Miyaura reaction, the MIDA boronate **90** is hydrolysed to the boronic acid **89** enabling cross coupling (Scheme 23). A wide variety of functional group transformations can be carried out in the presence of a MIDA boronate group, enabling boron to be incorporated into a synthetic sequence several steps before the boron species undergoes cross coupling.⁷⁶ 2-Heterocyclic, vinylic and cyclopropylboronic acids can be unstable during storage and under Suzuki-coupling conditions. Forming MIDA boronates can allow storage in air.⁷⁵ The Suzuki-Miyaura reaction conditions can be manipulated in order to facilitate slow release of the active boronic acid species, enabling competing protodeborylation to be minimised for unstable boronic acids.

1.5.7 Side reactions observed during Suzuki-Miyaura couplings

Several side reactions are known to occur during Suzuki-Miyaura couplings, which cause the formation of impurities in the reaction. Avoiding impurity formation is important during scale-up of reactions in the pharmaceutical industry, to ensure high quality drug substance is prepared for patients.

1.5.7.1 Protodehalogenation

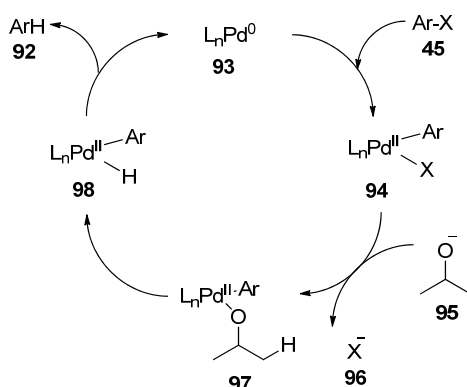
Aryl halide substrates **45** can undergo protodehalogenation during cross coupling reactions (Scheme 24).



Scheme 24: Protodehalogenation.

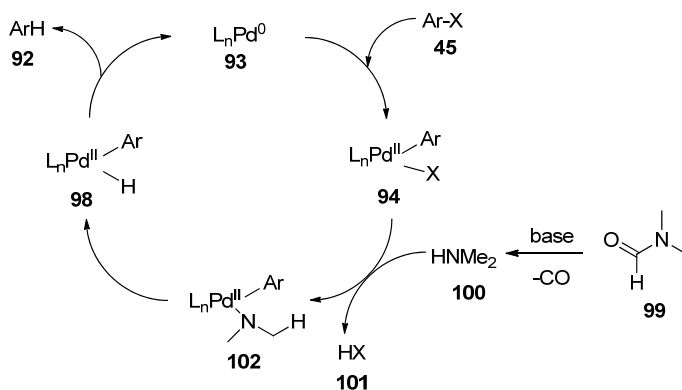
Protodehalogenation occurs after the aryl halide has undergone oxidative addition to Pd^0L_n **93** (Scheme 25). Reaction solvents are a potential source of hydride, which can coordinate to palladium after oxidative addition has taken place.

Alcohols are used as solvents for Suzuki-Miyaura couplings. Under the basic conditions used during Suzuki-Miyaura couplings, alkoxides **95** can be formed (Scheme 25). The alkoxide **95** can displace the halogen in the oxidative addition product **94**. After displacement by alkoxide, beta hydride elimination from **97** followed by reductive elimination of **98** gives the protodehalogenated product **92**.⁷⁷



Scheme 25: Protodehalogenation with alcohols.

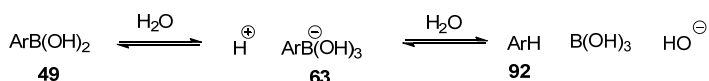
Protodehalogenation can also occur when DMF **99** is used as a solvent (Scheme 26). Dimethylamine **100** (produced by reaction of DMF **99** with base eliminating carbon monoxide) reacts with the oxidative addition product **94** in a similar manner to the alkoxide **95** in Scheme 25. Subsequent beta hydride elimination and reductive elimination gives the protodehalogenated product **92**.⁷⁸



Scheme 26: Protodehalogenation with DMF.

1.5.7.2 Protodeboronation

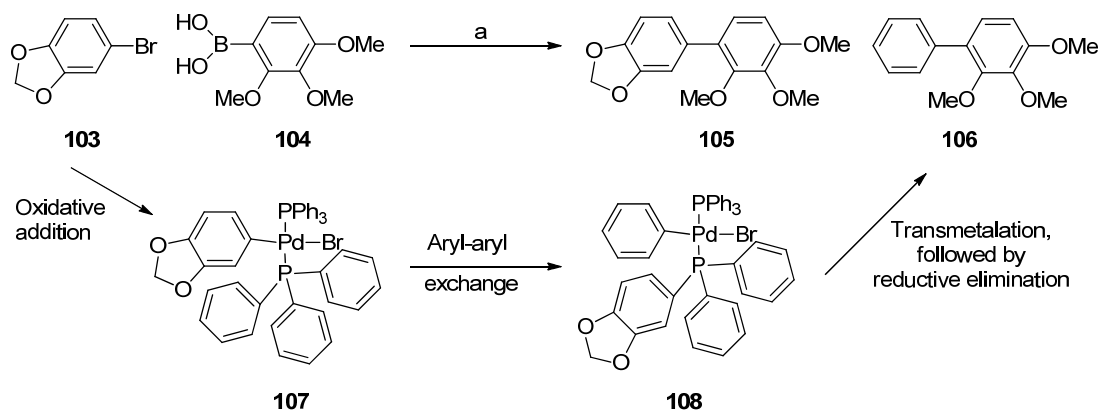
Protodeboronation can occur under the basic aqueous conditions used in the Suzuki coupling⁷⁹ (Scheme 27). Under basic aqueous conditions, boronic acids **49** readily form boronate anions **63**, which can undergo electrophilic aromatic substitution with water, to give the arene **92**. This transformation is favoured at positions on the aryl ring which can be stabilised by electron donating groups or heteroatoms.



Scheme 27: Protodeboronation.

1.5.7.3 Exchange of aryl groups on ligands

It has been observed in the palladium complexes formed in oxidative addition **107**, the aryl group coordinated to palladium can exchange with the aryl groups on the phosphine ligand to give intermediates such as **108**, which undergo transmetalation and reductive elimination to give an impurity **106** (Scheme 28).^{80 81} The aryl bromide **103** is particularly susceptible as it is substituted with two electron-donating groups.



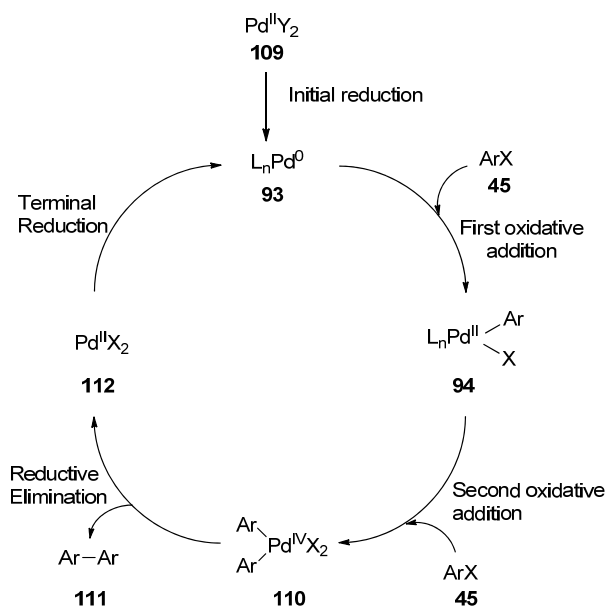
Conditions: a) Na_2CO_3 , $\text{Pd}(\text{PPh}_3)_4$, DME/ethanol, water.

Scheme 28: Exchange of aryl group from ligand.

In the reaction to form **105** from the cross coupling of **103** and **104**, reducing the loading of tetrakis(triphenylphosphine)palladium from 3 mol% to 1 mol % reduced the levels of aryl-aryl exchange impurity **106** from 29% to 11%. Exchanging triphenylphosphine for tri(*o*-tolyl)phosphine, a bulkier ligand, also suppressed formation of **106**. Use of phosphines can be avoided by using nickel complexes instead of palladium and phosphine ligands to catalyze Suzuki-Miyaura couplings.⁸²

1.5.7.4 Homocoupling

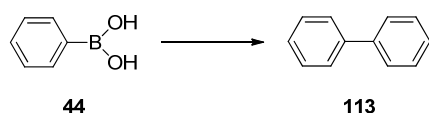
The Ullman reaction can be thought of as the inspiration for the development of aryl-aryl cross couplings, however it is also a potential side reaction in a Suzuki-Miyaura cross coupling. In the absence of the arylboronic acid, the palladium(0) species **93** can undergo two successive oxidative additions, giving the unstable palladium(IV) complex **110**, which quickly undergoes reductive elimination to give the homocoupled product **111** (Scheme 29).^{83 84 85}



Scheme 29: Homocoupling of aryl halides.

Homocoupling of arylboronic acids has been observed during Suzuki-Miyaura reactions. This process has been studied by Moreno-Mañas *et al.*, who showed the presence of oxygen accelerates the homo-coupling of arylboronic acids (Table 6).⁸⁶ The reaction rate for the homo-coupled aryl boronic acid product **113** was observed to increase when the reaction was carried out under air (entry 2) instead of nitrogen (entry 1). A further increase in reaction rate was observed when the reaction was carried out under an oxygen atmosphere (entry 3).

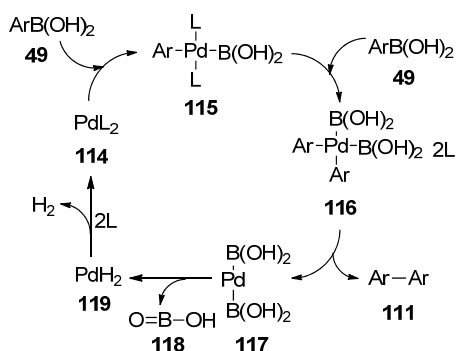
Table 6: Influence of atmosphere on homocoupling of phenylboronic acid **44.**^a



Atmosphere	% yield 113 at given time
Nitrogen	23 at 5 hours
Air	64 at 5 hours
Oxygen	66 at 2.6 hours

^a Conditions: Phenylboronic acid **44** (1.0 eq), Pd(PPh₃)₄ (2 mol%), toluene, rt.

Moreno-Mañas proposed a mechanism for the homo-coupling of aryl boronic acids (Scheme 30). Oxygen present in the reaction mixture can oxidize the intermediate palladium hydride species **119**, which will regenerate the palladium catalyst **114**.

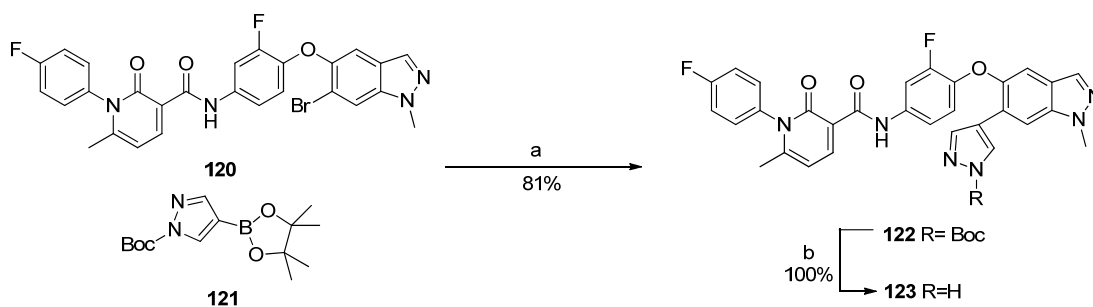


Scheme 30: Homocoupling of aryl boronic acids.

1.5.8 Palladium Removal

A consideration for scaling up the Suzuki-Miyaura reaction is the separation of the palladium catalyst from the desired product. This is particularly relevant in the pharmaceutical industry, where the specification for palladium in the drug substance requires palladium to be reduced to ppm levels.⁸⁷ A variety of methods are used to ensure the drug substance meets the specification and a selection of examples will be described in this Section.

Palladium scavenger resins are solid-supported reagents, which can complex palladium. Solutions of drug substance are added to the palladium scavenger resin and after the palladium has bound to the solid-supported reagent, the scavenger resin is removed by filtration. A team from Eli Lilly has used thiol functionalised silica gel to separate palladium from an intermediate **122** required to prepare a MET kinase inhibitor **123** investigated for the treatment of cancer (Scheme 31).⁸⁸



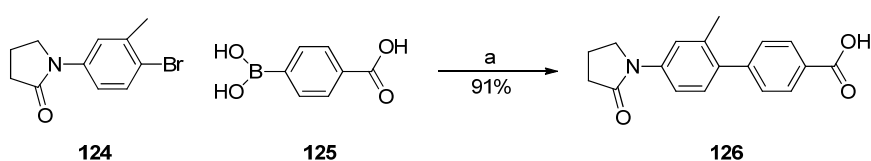
Conditions: a) i. Aryl bromide **120** (1.0 eq), Boronate ester **121** (1.24 eq), K_3PO_4 (2.1 eq), Boc_2O (0.26 eq), [1,1'-bis(di-*tert*-butylphosphino)]ferrocene palladium(II) dichloride (1.5 mol%), THF, water, 45 °C, 70 minutes; ii. Thiol-functionalised silica gel (0.16 wt); b) Biaryl **122** (1.0 eq), DBU (1.21 eq), ethanol, reflux, 9 hours.

Scheme 31: Preparation of MET kinase inhibitor 123.

Using thiol functionalised silica gel, 25 Kg intermediate **122** containing 14 ppm Pd was prepared. Palladium scavenger resins offer a convenient method for reducing the

palladium content in drug substance required for testing in early clinical trials, where around 1-50 Kg drug substance is required for testing. Using palladium scavenger resins during this phase of development enables fast delivery of drug substance. As the quantities of drug substance increase, palladium scavenger resins are no longer suitable for preparation of drug substance, as palladium scavenger resins are expensive and result in a significant amount of waste.

The palladium catalyst used in a Suzuki-Miyaura reaction can have a significant impact on the palladium level in the biaryl product. 6.3 Kg biphenyl acid **126** was prepared containing <6 ppm palladium, when Pd/C was used to catalyse the reaction.⁸⁹



Conditions: a) Aryl bromide **124** (1.0 eq), arylboronic acid **125** (1.06 eq), Na₂CO₃ (1.9 eq) Pd/C (1.2 mol%), methanol, water, reflux, 5 hours.

Scheme 32: Suzuki-Miyaura reaction catalysed by Pd/C.

Using Pd(PPh₃)₄, biphenyl acid **126** was prepared containing 40-80 ppm palladium. Exchanging Pd(PPh₃)₄ for heterogeneous Pd/C enabled the palladium content of the isolated product **126** to be reduced, as the catalyst could be removed by filtration through Celite at the end of the reaction.

Palladium can be separated from drug substance, through an aqueous work-up with *N*-acetyl-*L*-cysteine **127** and *L*-cysteine **128** (Figure 12).^{90,91} Palladium chelates to *N*-acetyl-*L*-cysteine **127**, or *L*-cysteine **128** to form water soluble palladium complexes, which are either extracted to the aqueous phase, or left in the mother liquors following crystallisation.

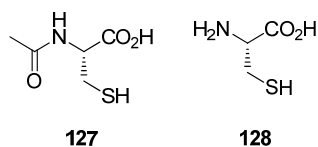
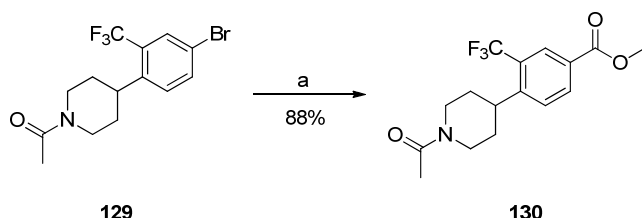


Figure 12: *N*-acetyl-*L*-cysteine **127 and *L*-cysteine **128**.**

Recently, *N*-acetyl-*L*-cysteine **127** has been used to remove palladium from product **130** formed by the carbonylation of aryl bromide **129** (Scheme 33).⁹²

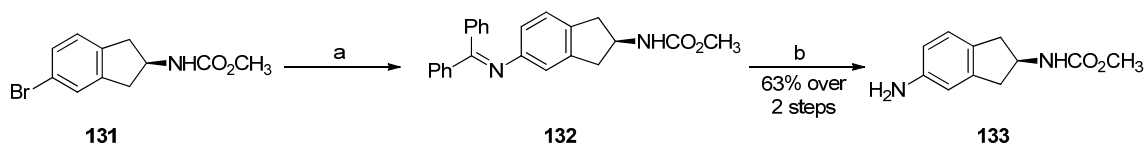


Conditions: a) i. Aryl bromide **129** (1.0 eq), CO (100 psi), TEA (2.0 eq), Pd(OAc)₂ (0.2 mol%), DPPP (0.22 mol%), methanol, 90 °C, 20 hours; ii. NMP, *N*-acetyl-*L*-cysteine **127**, water, 60 °C.

Scheme 33: Palladium catalysed carbonylation of 129.

Following reaction completion and distillation to replace methanol with NMP, *N*-acetyl-*L*-cysteine **127** followed by water was charged to the NMP solution of **130**. Following crystallisation, **130** was isolated containing 4.1 ppm Pd.

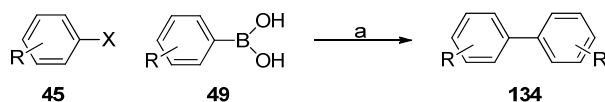
Palladium can be removed from the products of palladium catalysed reactions by treatment with activated carbon. A team from Novartis has used activated carbon to reduce the palladium content of **133** to <1 ppm Pd, following synthesis *via* palladium catalysed amination (Scheme 34).⁹³



Conditions: a) Benzophenone imine, Pd₂(dba)₃, BINAP, NaOMe, toluene; b) i. 6N HCl; ii. NaOH; iii. 100% wt carbon (PICA P1400), methanol, 63-67 °C, 5 hours.

Scheme 34: Removal of palladium using activated carbon.

Operating palladium catalysed reaction in continuous flow reactions rather than batch reactions may offer reduced palladium content in the isolated products, as the palladium catalyst is immobilised. This has been demonstrated with the Suzuki-Miyaura reaction using a *SiliaCat* DPP Pd catalyst on a sol-gel support to prepare biaryl products **134** containing 1-5 mg palladium per kilogram of product (Scheme 35).⁹⁴



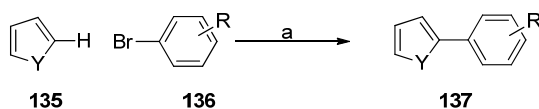
Conditions: a) Aryl halide **45** (1.0 eq), arylboronic acid **49** (1.01-1.25 eq), potassium carbonate (1.1-1.5 eq), *SiliaCat* DPP Pd (0.25 mmol/g), THF and ethanol/ DMF and methanol, water.

Scheme 35: Suzuki-Miyaura reaction in flow.

1.5.9 The future of aryl-aryl cross coupling reactions

C-H activation offers an exciting opportunity for aryl-aryl cross coupling methodology. Instead of an organometallic partner, such as an organoborane, it has

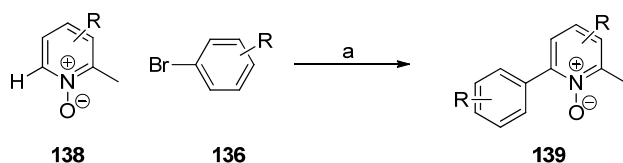
been shown an aryl halide can be reacted directly with an activated C-H bond. Development of this methodology enables syntheses of biaryl compounds to become more efficient, because synthetic transformations to prepare the organometallic partner do not need to be carried out. C-H activation processes are also sustainable as stoichiometric metallic waste is not generated. Fagnou's group has shown that many heterocycles have C-H bonds which are sufficiently activated to undergo cross coupling with aryl bromides (Scheme 36).⁹⁵



Conditions: a) Aryl bromide **136** (1.0 eq), heterocycle **135** (1.0 eq), pivalic acid (0.3 eq), potassium carbonate (1.5 eq), Pd(OAc)₂ (2 mol%), PCy₃·HBF₄ (4 mol%), DMA, 100 °C.

Scheme 36: Direct arylation of heterocycles.

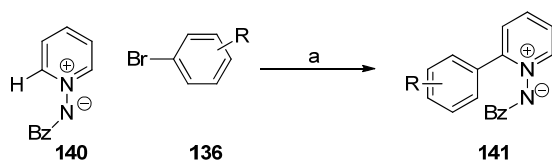
Fagnou's group have also shown using similar conditions, cross coupled products can be obtained from an excess of benzene.⁹⁶ Fagnou *et al.* have also shown biaryl products can be obtained through the palladium catalysed reaction of an aryl bromide with pyridine *N*-oxide (Scheme 37).⁹⁷



Conditions: a) Aryl bromide **136** (1.0 eq), pyridine *N*-oxide **138** (2 eq), potassium carbonate (1.5 eq), Pd(OAc)₂ (5 mol%), P^tBu₃·HBF₄ (6 mol%), toluene, 110 °C, overnight.

Scheme 37: Direct arylation of pyridine *N*-oxides.

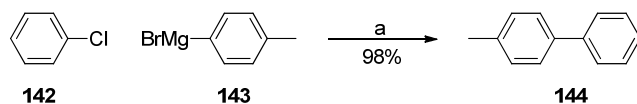
The 2-position on **138** is activated by the *N*-oxide, which enables the reaction to deliver product **139** selectively. Similarly, Charette's group has also shown the 2-position on pyridine can be activated by formation of the *N*-iminopyridinium ylide **140** to give biaryl products **141** (Scheme 38).⁹⁸



Conditions: a) Aryl halide **136** (1.0 eq), *N*-iminopyridinium ylide **140** (1.5 eq), potassium carbonate (3.0 eq), Pd(OAc)₂ (5 mol%), P^tBu₃ (15 mol%), toluene, 3 Å molecular sieves 125 °C, 16-20 hours.

Scheme 38: Direct arylation of *N*-iminopyridinium ylide.

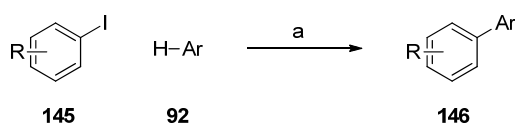
Palladium has proved to be a versatile catalyst for many reactions including cross coupling. However, palladium is expensive and toxic, so more abundant transition metals have been investigated for use in cross coupling reactions.^{99,100} Of particular interest is catalysis using iron, as it is readily available and significantly less toxic. Nakamura has published a method for aryl-aryl cross coupling using iron catalysis (Scheme 39).¹⁰¹



Conditions: a) Phenyl chloride **142** (1.0 eq), *p*-tolylmagnesium bromide **143** (1.2 eq), FeF₃·3H₂O (6 mol%), SIPr·HCl (9 mol%), ethylmagnesium bromide (0.18 eq), THF, 60 °C, 24 hours.

Scheme 39: Aryl-aryl cross coupling using iron catalysis.

In Nakamura's method, a Grignard reagent is used as the organometallic coupling partner instead of an aryl boronic acid. As aryl boronic acids are prepared from organomagnesiums,^{63,64} Nakamura's method offers an opportunity to remove a synthetic step as well as the advantages of iron catalysis. Charette's group have also demonstrated direct arylation using iron catalysis, in addition to direct arylation using palladium (Scheme 40).¹⁰²



Conditions: a) Aryl iodide **145** (1.0 eq), arene **92** (100 eq), potassium *t*-butoxide (2.0 eq) Fe(OAc)₂ (5 mol%), bathophenanthroline (10 mol%), 80 °C, 20 hours.

Scheme 40: Direct arylation using iron catalysis.

1.5.10 Conclusions

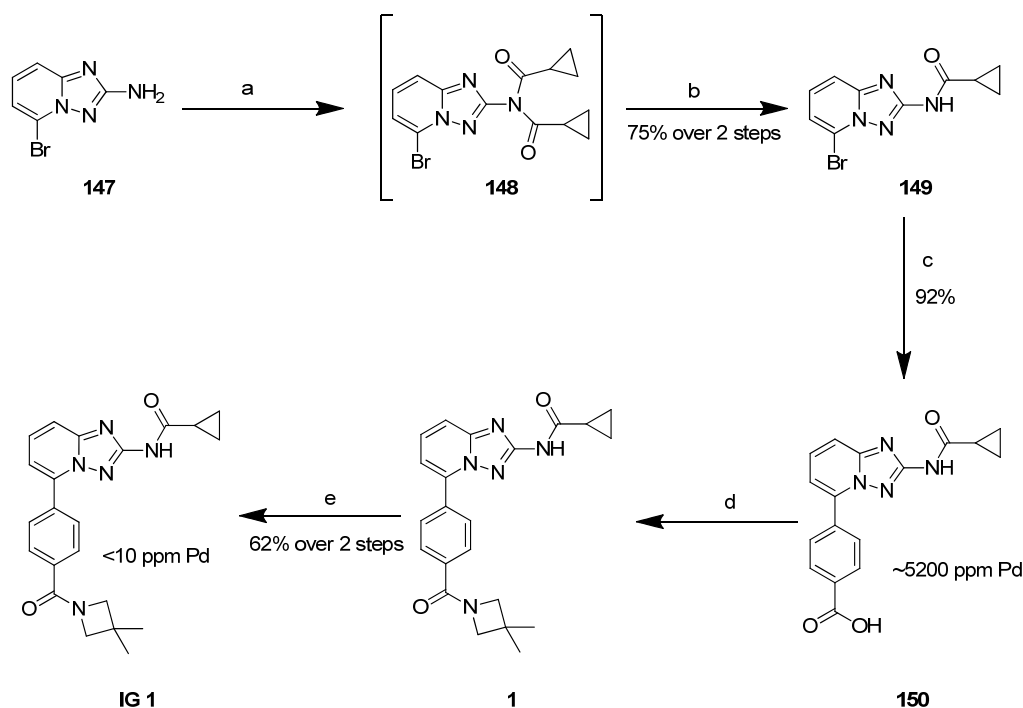
The development of cross coupling methodology has enabled access to biaryl structures which are biologically important. The most popular of the cross coupling methodologies is the Suzuki-Miyaura reaction, due to the stability of the organometallic coupling partner and the relatively benign by-products formed. The Suzuki-Miyaura coupling has been successfully scaled up to hundreds of kilograms, to deliver high quality drug substance. Further development of the aryl-aryl cross couplings to eliminate organometallic cross coupling partners through C-H activation, or to catalyse these reaction using less toxic and cheaper metals such as iron, will deliver more sustainable processes in the future.

**2 Development of a New Route to Drug Substance for the
Treatment of Systemic Lupus Erythematosus**

2.1 Introduction

2.1.1 Medicinal Chemistry Route (Route A)

1 is a selective JAK1⁷ inhibitor, which has been developed in partnership between GSK and Galapagos for the treatment of SLE.¹ Early toxicological studies and Phase I clinical trials were supplied by **1** prepared using the medicinal chemistry route, which is known as Route A (Scheme 41).¹⁰³



Conditions: Stage 1 a) Cyclopropylcarbonyl chloride, NEt_3 , acetone, b) 7N NH_3 in MeOH (75%); Stage 2 c) 4-boronobenzoic acid, $\text{Pd}(\text{dppf})\text{Cl}_2$, KOH, 1:1 dioxane/water (92%); Stage 3 d) i. EDC, HOBT, CH_2Cl_2 , ii. 3,3-dimethylazetidinium hydrochloride, diisopropylethylamine, e) i. Quadrasil MP, CH_2Cl_2 , ii. Quadrapure TU (62%).

Scheme 41: Route A preparation of **1**.

Aminotriazole **147**¹⁰⁴ is treated with cyclopropylcarbonyl chloride and triethylamine to give the bis-acylated intermediate **148**, which is followed by *trans*-amination using ammonia to give the desired mono-acylated product **149** in 75% yield. The monoacylated product **149** was coupled to 4-boronobenzoic acid under Suzuki-Miyaura conditions to give **150**, which was isolated containing ~5200ppm Pd in 92% yield. In Stage 3, the activation of carboxylic acid **150** was carried out using 1-ethyl-3-(3-dimethylaminopropyl)carbodiimide (EDC) and 1-hydroxybenzotriazole

(HOBt). 3,3-Dimethylazetidene hydrochloride and Hünig's base were added to the activated **150**, to give **1**. The reaction was followed by an aqueous work-up, which was necessary for the removal of HOBt, but tended to form emulsions. The desired product **1** was treated with two palladium scavengers, Quadrasil MP and Quadrapure TU, in order to remove palladium to <10 ppm, as required for molecules tested in clinical trials.⁸⁷ 6 Kg of **1** was prepared in 43% overall yield using the medicinal chemistry route outlined in Scheme 41 in June 2011 at Novasep, an external contract research organisation.

2.1.2 Improvements Made to the Route A

A further campaign was to be carried out in our pilot plant facilities, to manufacture 25 Kg of **1**. Removal of palladium was an area of concern for scaling up the route to **1**, since for every 10 Kg input of **1** into the scavenging process 4 Kg of each palladium scavenger was required. Other methods of palladium removal required investigation, as the larger quantities of palladium scavengers required to prepare 25 Kg of **1**, would be difficult to source. Loose activated carbon powder is convenient for laboratory purification of compounds as it is easily removed by filtration.⁸⁷ However, it is disfavoured for scaling up into pilot plant equipment because fine powder is difficult to remove from the reactor vessels and filtration times can be long. Our pilot plants prefer to use activated carbon which is immobilised inside a cartridge and then a solution of the target molecule is pumped through the cartridge (Figure 13).

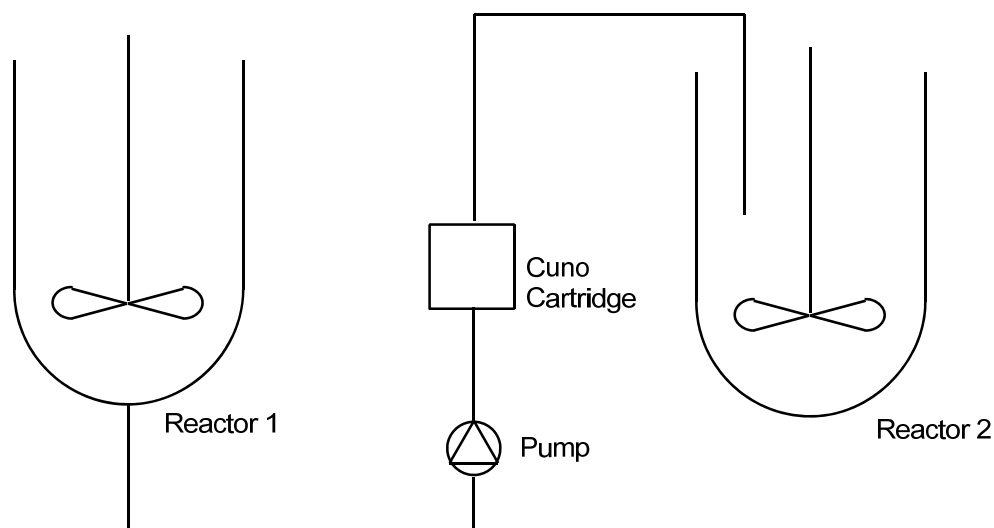
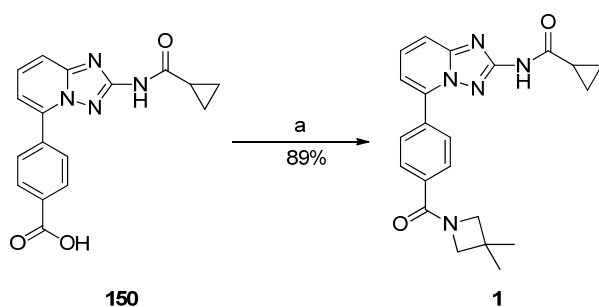


Figure 13: Cuno cartridge set up with pilot plant reactors.

The temperature of the solution, the flow rate and type of carbon used can be optimized in order to improve palladium removal. There are several companies which provide equipment and cartridges for this.^{87,93,105} In our pilot plants and manufacturing facilities, the cartridges are provided by Cuno. A process was developed where a DMSO solution of **150** was passed through a Cuno cartridge and then crystallised by addition of water to give **150** containing 1500-2000 ppm Pd. This was a significant reduction compared to the carboxylic acid **150** prepared using the Novasep process which contained ~5200 ppm Pd. Preparation of **150** containing 1500-2000 ppm Pd enabled less palladium to enter the Stage 3 process, which would improve the process when scaled up into the pilot plant.

For the scale-up of Stage 3 at GSK, use of HOBt was a concern as HOBt is known to be explosive¹⁰⁶ and was difficult to remove through aqueous work-up. Use of EDC without HOBt showed incomplete activation of **150**. In order to find a replacement for HOBt in Stage 3, a screen of amide coupling reagents was carried out. This identified 1,1'-carbonyldiimidazole (CDI) as the most suitable reagent for the activation of **150** and the subsequent amide coupling (Scheme 42).



Conditions: a) i. CDI (1.6 eq), CH₂Cl₂, 20 °C, 15 minutes, ii. 3,3-dimethylazetidine hydrochloride (1.54 eq), 20 °C, 15 minutes.

Scheme 42: Activation of 150 with CDI, to prepare 1.

It was observed that after replacing EDC and HOBt with CDI, emulsions still tended to form in the aqueous work-up which followed the reaction. Closer inspection of these emulsions, revealed black particulates were present in the emulsion. As these black particulates were likely to be palladium, the quenched reaction mixture was filtered through Celite. Good separation of the two phases was observed in the filtrate. ICP-AES analysis revealed the palladium concentration in the product **1**, had been reduced from ~260 ppm to 61 ppm after the filtration through Celite. Using the Cuno purified intermediate **150** in the newly developed CDI process generated **1**,

with 15-50 ppm Pd. Subsequent treatment with 0.2 wt of the palladium scavenger Quadrasil MP, followed by a solvent swap into ethyl acetate gave intermediate grade (IG) **1** with under 10 ppm Pd. After Route A was optimized at GSK, the campaign delivered IG **1** with the overall yield increased from 43% to 58%. A further recrystallisation (discussed in section 2.1.3) of **1** was carried out, to prepare the desired more thermodynamically stable polymorph of **1** (API **1**) for drug product formulation.

2.1.3 Controlling the Polymorph of **1**

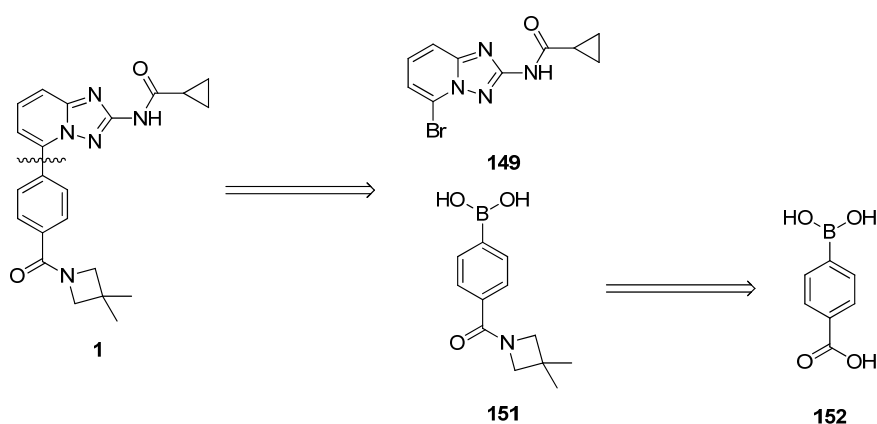
Polymorphism is where a solid compound can exist as more than 1 crystalline form, or polymorph. Polymorphs are chemically identical, but the crystal packing in polymorphs is different.¹⁰⁷ Physical properties dependent on the lattice energy of the crystal, such as melting point and solubility, will vary for different polymorphs. Differences in solubility can impact the ability to formulate the drug substance, or the bioavailability of the drug substance. For this reason, regulatory authorities require pharmaceutical companies to search for the different polymorphs of a drug substance and to select a single polymorph for use in formulation.

A process must be designed in order to control the formation of the polymorph produced. This process is usually a separate recrystallisation step carried out after the final step of the synthesis. In our laboratories, the drug substance prepared in the final step of the synthesis is designated intermediate grade (IG) and the recrystallised drug substance is known as the active pharmaceutical ingredient (API). Control of the output of the recrystallisation is obtained by seeding a solution of the product with the desired polymorph.¹⁰⁸

There are 2 known polymorphs of **1**, which are known as Form I and Form II. Form II is the most thermodynamically stable polymorph of **1**, therefore Form II is used in formulations. A recrystallisation process to generate Form II (API **1**) has been developed using 4:1 IMS/water to dissolve **1**. The solution of **1** is then seeded with API **1** and the solution is cooled to enable crystal growth to give API **1**. To date, **1** prepared from the final bond forming step has always been Form I and as this is not the desired polymorph for formulation, this is known as IG **1**.

2.1.4 Objectives for Route B

A second campaign was scheduled to prepare 125 Kg of API **1** in the pilot plant over June-September 2012. This campaign presented an opportunity to investigate the preparation of IG **1** from a different route without having an impact on pivotal clinical studies. Preparing the API from a different route could give rise to a different impurity profile, so based on this the optimal synthetic route should be used to supply API for the pivotal clinical trials. Accordingly, the 125 Kg campaign was the last opportunity for a change in the synthetic route of **1**, without having an impact on these clinical trials. A more convergent Route B was proposed, which is shown in Scheme 43.



Scheme 43: Retrosynthetic analysis of 1 using route B.

The route B disconnection focuses on bringing fragments **149** and **151** together using a Suzuki-Miyaura coupling in the final bond formation, enabling a convergent route to **1**. This approach would introduce a palladium catalyst in the final chemical step, therefore, ensuring IG **1** from Route B was prepared with acceptable palladium levels would be a key deliverable for Route B. Route A could be thought of as advantageous over Route B, as palladium removal could be carried out before the final synthetic step. In practice however, the product of the Route A Suzuki-Miyaura coupling **150** (Scheme 41), was highly insoluble making purification difficult, so significant quantities of palladium were taken into final synthetic step of Route A.

Convergent routes can offer the advantages of improving the overall yield and reducing lead times to prepare the target molecule. Route A (Scheme 41) consisted of three synthetic stages and two palladium purification stages to prepare IG **1**. In effect, the palladium removal steps considerably lengthen the synthetic route. The

aryl bromide **149** required for Route B was also required in Route A, so the first stage of chemistry for Route B would be in common with Route A. Activation of the carboxylic acid **152** had already been demonstrated using thionyl chloride.^{109,110} In order for Route B to be endorsed for the second campaign, IG **1** would need to be prepared in greater than 60% overall yield. Recrystallisation of IG **1** prepared from Route B would need to give API **1** with no single organic impurity greater than 0.06% and palladium content below 10 ppm. The requirement for low levels of impurities is driven by **1** being administered to patients at a relatively high dose of 400 mg twice daily.¹¹¹

2.1.5 Reaction Optimisation using Design of Experiments

Chemical reactions require optimisation for a number of reasons. One of the key considerations for scale up of a reaction, is to provide an efficient synthesis of intermediates and target molecules. To enable this, reactions may require optimisation to improve yields and purity.

For a given reaction, there are likely to be several variables (such as time, temperature, etc.) which it is felt should be investigated in order to optimise a reaction. The reaction could be examined by investigating a single variable at several values. This variable is then set at the optimum value investigated and the process is then repeated with the next variable. This method is exemplified in Figure 14, where 3 variables x , y and z are represented as different axes and the cube formed by the axes is the potential area for operating the reaction. Each red dot in Figure 14 represents an experiment carried out. This method of optimisation is sometimes referred to as OVAT (One Variable At a Time).

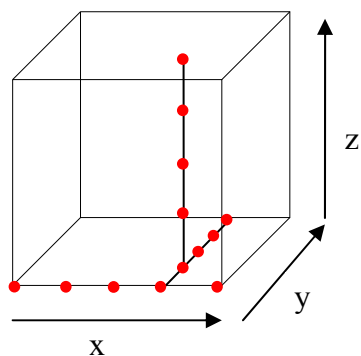


Figure 14: 3-Dimensional representation of OVAT optimization.

Figure 14 shows using the OVAT method of optimisation, potential areas where the reaction could be operated are not investigated. Using the OVAT method, it is assumed the variables are independent of each other. This assumption could lead to the optimum reaction conditions being missed as there are likely to be interactions between variables. For this reason, it would be advisable to investigate multiple variables simultaneously, which is known as a design of experiments (DoE). There are various methods of DoE which can be used to optimise reactions. In this section, an introduction is provided for the methods of experimental design which are to be discussed in later chapters of this thesis.

Factorial design is a DoE method, where each variable, or factor is investigated at 2 or more levels. In a 2-level factorial design, each variable is investigated at 2 levels, designated a 'high' or 'low' value. For r variables, this will require 2^r individual experiments to be run. This is illustrated in Figure 15 with 3 factors x , y and z .

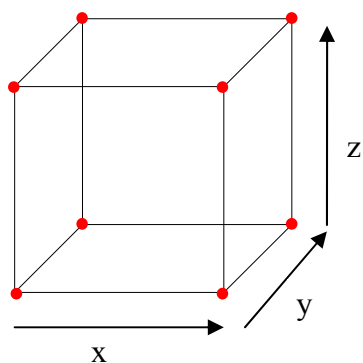


Figure 15: 3-Dimensional representation of a 2-level factorial design.

Comparison of Figure 14 with Figure 15 shows the potential area for operating the reaction is explored more thoroughly, using the 2-level factorial design.

Factorial designs exponentially increase the number of experimental runs required as the number of variables increases, which means carrying out a factorial design can quickly become extremely resource intensive. A factorial design can be fractionated, to reduce the number of experiments to be run. For example, to investigate 3 variables as a factorial design, would require 8 experiments. This could be reduced by half to 4 experiments (as shown in Figure 16) to give a half fraction factorial design.

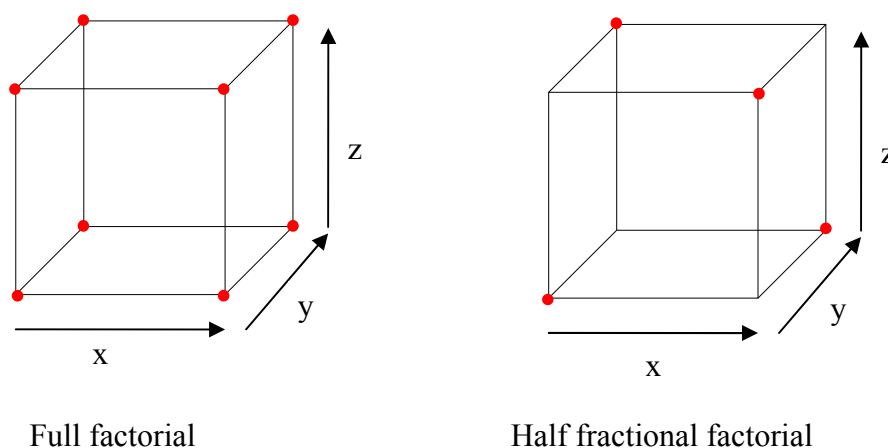


Figure 16: Comparison of full factorial design with half fractional factorial design.

When the number of variables to be studied exceeds three, it becomes difficult to visualise how to select the experiments to be studied in order to carry out the fractionated factorial design. For this reason, an experimental design will usually be planned using statistical software. The software used in our laboratories is Design Expert.¹¹² Experimental designs can be further fractionated to give quarter or eighth fractional factorial designs depending on how much resource is available to run the experimental design.

A limitation with studying the parameters at their high and low settings is there will be no understanding of how the variable affects the outcome between the high and low setting of the variable, i.e. is there a linear relationship between the outcome and the variable, or is the response curved as the variable is changed from low to high? To understand if the relationship is linear, an extra experiment is run, where all the variables are at the mid-point of their range. This experiment is known as a centre point experiment. The centre point experiment is as a minimum run in duplicate to determine how reproducible the experimental data is.

Once all the experiments in a DoE screen have been run, the data is examined to determine which variables have an effect on the desired outcome. For a particular variable, several runs will have been carried out at the 'high' and 'low' settings of the variable. A model will be formed for the output of the experiment, based on the averages of the output value at the 'high' and 'low' settings of the variable. If the model is statistically significant against the background noise of variation between the experimental runs, the variable is a significant factor in determining an effect on the output value.

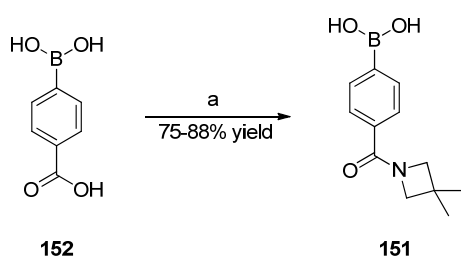
2.2 Results & Discussion

2.2.1 Development of Route B Stage 2

A key requirement of a new route of synthesis of a drug substance is the ability to deliver API to the clinical specification. For this reason, preparation of API **1** from Route B as soon as possible would enable an understanding of the impurity profile. Any impurities in API **1** above the clinical specification would require identification. Once impurities are identified, their route of formation can be determined and the new route can be optimised to minimise their formation. For this reason, it was

important to quickly have access to both Route B Suzuki-Miyaura coupling partners. A supply of aryl bromide **149** was already established from the Route A synthesis, so the focus of laboratory investigations was to prepare boronic acid **151** quickly.

Boronic acid **152** was shown to be activated CDI enabling an amide coupling with 3,3-dimethylazetididine hydrochloride to be carried out. A scalable process was developed in 2-methyltetrahydrofuran, using CDI to carry out the activation, leading to **151** in 75-88% yield (Scheme 44). The process was successfully demonstrated using a 300 g input of **152**.



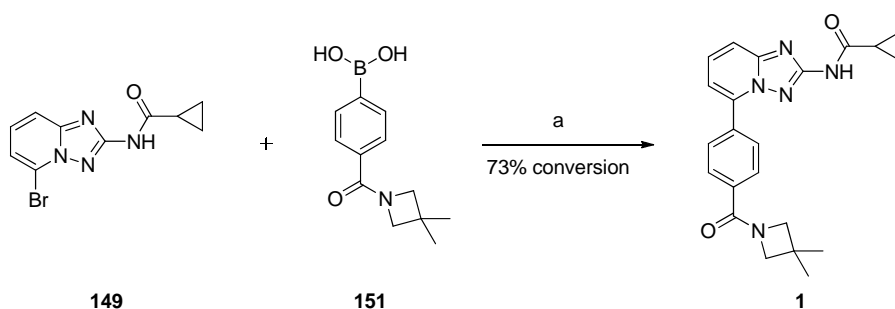
Conditions: a) i. CDI, DMSO, 2-methyltetrahydrofuran, 20-25 °C, 30 minutes; ii. 3,3-dimethylazetididine hydrochloride, 20-25 °C, 1 hour.

Scheme 44: Route B stage 2 process developed for pilot plant.

2-Methyltetrahydrofuran was chosen as a solvent for this transformation, because it is immiscible with water which enables an aqueous work-up. 2-Methyltetrahydrofuran is also a sustainable solvent as it is derived from biomass.¹¹³

2.2.2 Identification of Reaction Conditions for Route B Stage 3

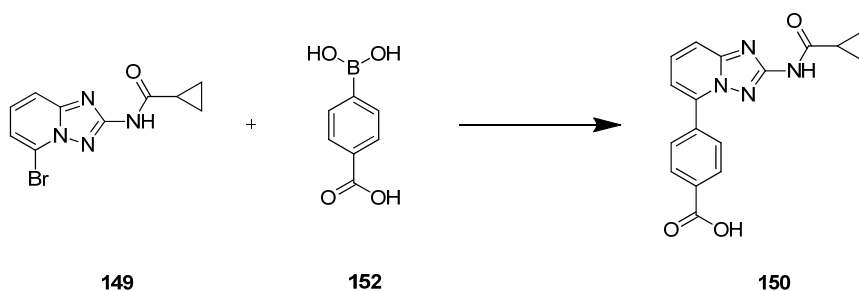
Having access to both of the final stage coupling partners, attention was turned to the final stage Suzuki-Miyaura coupling. Using the Suzuki-Miyaura conditions from Route A to prepare **150**, 73% conversion to **1** was observed (Scheme 45). The rate of the reaction to prepare **1** was slower than in the preparation of carboxylic acid **150** in Route A. In the Route A campaign, the Suzuki-Miyaura coupling was complete in 6 hours. For the Route B Suzuki-Miyaura coupling, HPLC analysis showed, after an overnight reaction, conversion to **1** was not complete with both starting materials **149** and **151** remaining. This showed optimisation of the reaction conditions would be required in order for Route B to be considered as a realistic alternative to Route A.



Conditions: a) Aryl bromide **149** (1 eq), boronic acid **151** (1.15 eq), KOH (1 eq), Pd(dppf)Cl₂ (5 mol%), 1:1 dioxane/water, reflux, overnight.

Scheme 45: Route B Suzuki-Miyaura coupling using route A conditions.

Selecting alternative reaction conditions for the Suzuki-Miyaura coupling gave an opportunity to remove 1,4-dioxane from the synthesis of **1**. 1,4-Dioxane is not suitable for manufacturing scale, due to its carcinogenic properties.¹¹⁴ Using different catalysts and ligands may also enable the product to be isolated containing less palladium. With these issues in mind, alternative solvents, catalysts, ligands and bases had been screened for the Route A Suzuki-Miyaura coupling reaction (Table 7). Using a standard DoE screen was not possible as the variables to be investigated had discrete levels rather than numerical values. A d-optimal screen allows several variables with discrete levels, such as solvents and bases, to be investigated.¹¹⁵ Design Expert 7 software was used to plan a d-optimal screen to look at five catalyst/ligand combinations, five solvents and five bases in 61 unique combinations, instead of the total possible 125 combinations. The Design Expert 7 software reduces 125 possible combinations of variables to 61 combinations using the same principles, which enables a full factorial DoE to be reduced to a fractional factorial design (Figure 16).

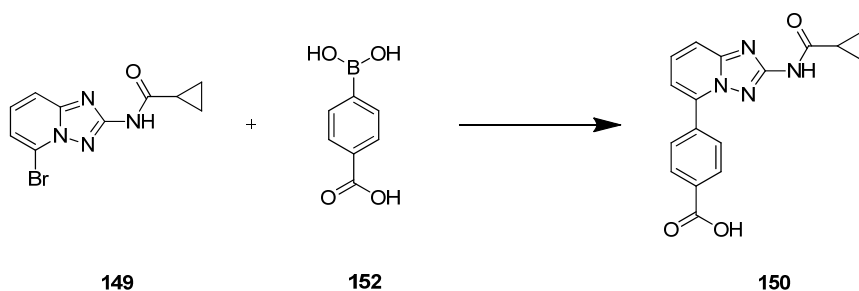
Table 7: Variables investigated in d-optimal screen for route A Suzuki-Miyaura coupling.^a

Catalyst/ligand combination	Solvents	Bases
Pd(PPh ₃) ₄	Dichloromethane	NaOH
PdCl ₂ , PPh ₃	THF	K ₃ PO ₄
Pd(OAc) ₂ , PPh ₃	Toluene	KHCO ₃
Pd ₂ (dba) ₃ , DavePhos	Methanol	Na ₂ CO ₃
Pd-C	Ethanol	KOH

^a Conditions: Aryl bromide **149** (1 eq), boronic acid **152** (1.15 eq), base (2.1 eq), 1:1 solvent/water, palladium source (5 mol%), phosphine (0-10 mol%), μ wave, 15 minutes.

Four homogeneous catalysts were selected for investigation, which included palladium(II) sources Pd(OAc)₂ and PdCl₂ and pre-formed palladium(0) sources Pd(PPh₃)₄ and Pd₂(dba)₃. Two different ligands PPh₃ and DavePhos were examined with the preformed Pd⁰ sources. In addition to the homogeneous catalysts, heterogeneous catalyst Pd-C was investigated. Pd-C could provide significant benefit as it would be removed easily from the reaction mixture by filtration, reducing the need for separate palladium removal processes. Another objective of the screen was to investigate alternative solvents to 1,4-dioxane. Tetrahydrofuran was selected as an alternative polar aprotic solvent, which was structurally similar to 1,4-dioxane. The remaining solvents examined included non-polar solvents toluene and dichloromethane and polar protic solvents methanol and ethanol. A range of bases with different strengths were also investigated.

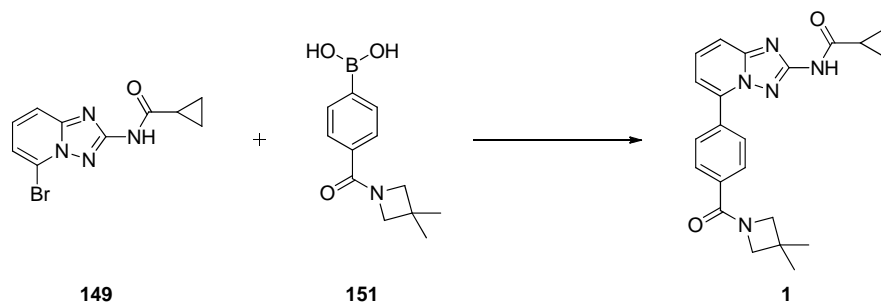
The screen identified palladium(II) acetate and triphenylphosphine as an alternative catalyst/ligand system (see Appendix 6.1). Table 8 shows the alternative bases and solvents identified in the d-optimal screen for Route A.

Table 8: Alternative bases and solvents identified for the Suzuki-Miyaura coupling in Route A.^a

Entry	Bases	Solvent	Boronic acid 152 % PAR ^b	Aryl bromide 149 % PAR ^b	Coupled product 150 % PAR ^b
1	KHCO ₃	Methanol	<1	1	90
2	NaOH	Methanol	<1	<1	87
3	KOH	Ethanol	<1	5	82
4	Na ₂ CO ₃	Methanol	<1	2	78
5	NaOH	Ethanol	2	<1	78
6	KHCO ₃	Ethanol	<1	9	76

^a Conditions: Aryl bromide **149** (1 eq), boronic acid **152** (1.15 eq), base (2.1 eq), 1:1 solvent/water, palladium(II) acetate (5 mol%), PPh₃ (10 mol%), μ wave, 15 minutes; ^b Determined by HPLC.

Table 8 shows using palladium(II) acetate and triphenylphosphine, there were several combinations of solvent and base which could give good conversion to the Route A Suzuki-Miyaura coupling product **150**, with potassium bicarbonate and methanol (entry 1), giving the highest conversion (90%). The conditions in Table 8 were evaluated for the Suzuki-Miyaura coupling in Route B (Table 9), which identified sodium carbonate and potassium bicarbonate as the most suitable bases for obtaining a clean reaction profile. The highest conversion to **1** (88%) was obtained using the combination Na₂CO₃/methanol (Table 9, entry 1) at reflux overnight.

Table 9: Suzuki-Miyaura coupling conditions investigated in Route B.^a

Entry	Solvent	Base	Boronic acid 151 % PAR ^b	Aryl bromide 149 % PAR ^b	Product 1 % PAR ^b
1	Methanol	Na ₂ CO ₃	3	1	88
2	Methanol	KHCO ₃	11	6	77
3	Ethanol	Na ₂ CO ₃	21	8	50
4	Ethanol	KHCO ₃	5	3	83

^a Conditions: Aryl bromide **149** (1 eq), boronic acid **151** (1.15 eq), base (1 eq), 1:1 solvent/water, palladium(II) acetate (5 mol%), PPh₃ (10 mol%), reflux, overnight; ^b Determined by HPLC.

2.2.3 Optimisation of Sodium Carbonate/Methanol Reaction Conditions

Having identified methanol as the optimum solvent and sodium carbonate as the optimal base for the Stage 3 coupling, a selection of 6 reaction variables (Table 10) were chosen for further investigation using a quarter fractional factorial DoE.

Table 10: Reaction variables evaluated in DoE screen.

Variable ^a	Range Investigated
Palladium(II) acetate mol%	1-5
Triphenylphosphine relative to palladium(II) acetate	1-3
Na ₂ CO ₃ equivalents	1.0-1.5
% v/v water in methanol	40-60
Boronic acid 151 equivalents	1.00-1.15
Total solvent volumes	8-16

^a Charges are relative to aryl bromide **149** unless stated.

The input variables and the output responses used to construct the model are given in section 4.2 (page 122). Figure 17 shows the half-normal plot for conversion to **1** obtained after analysis of the HPLC data from the DoE screen. The half-normal plot shows conversion to **1** is favoured when the equivalents triphenylphosphine relative to palladium(II) acetate, palladium(II) acetate and % v/v water in methanol are low. Reducing these variables is also shown to reduce levels of starting materials **149** and **151** in the reaction mixture.

Design-Expert® Software
Logit(1)

▲ Error from replicates

Shapiro-Wilk test

W-value = 0.992

p-value = 0.999

A: Mol% Pd

B: Base Eq.

C: % Water

D: Boronic Acid Eq.

E: Ligand Eq. relative to Pd

F: Total Solvent Volumes

■ Positive Effects

■ Negative Effects

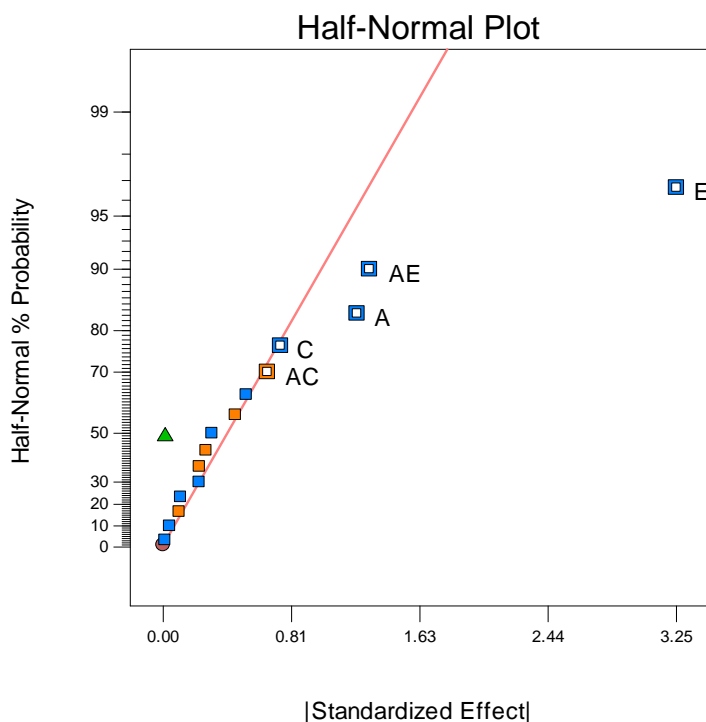


Figure 17: Half-normal plot for 1.

Figure 17 also shows there are 2-factor interactions involving the equivalents triphenylphosphine relative to palladium(II) acetate with both palladium(II) acetate and % *v/v* water in methanol (shown in more detail in Figure 18 and Figure 19). The equivalents of triphenylphosphine relative to palladium(II) acetate dominates the 2-factor interaction between triphenylphosphine relative to palladium(II) acetate and palladium(II) acetate, as the equivalents of triphenylphosphine are low, the conversion to **1** is similar at across the range of the palladium(II) acetate loading (Figure 18).

Design-Expert® Software
Original Scale
1

● Design Points

■ E- 1.000
▲ E+ 3.000

X1 = A: Mol% Pd

X2 = E: Ligand Eq. relative to Pd

Actual Factors

B: Base Eq. = 1.25

C: % Water = 50.00

D: Boronic Acid Eq. = 1.08

F: Total Solvent Volumes = 12.00

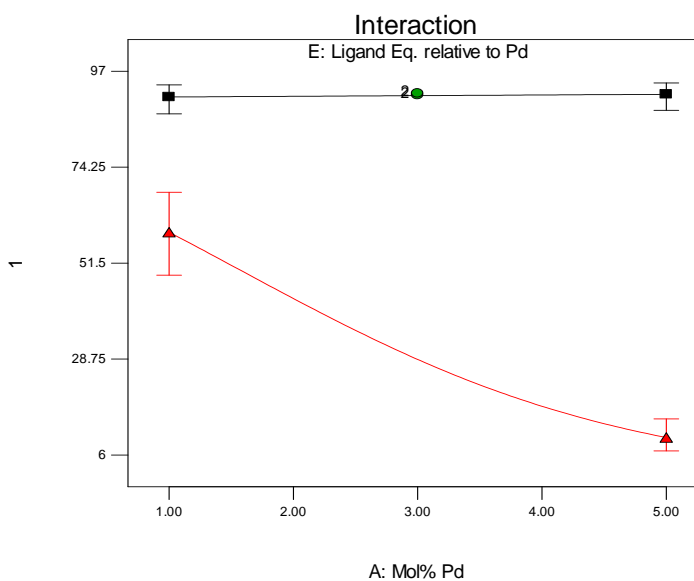


Figure 18: 2-factor interaction between equivalents of triphenylphosphine relative to palladium(II) acetate and palladium(II) acetate mol%.

The 2-factor interaction of palladium(II) acetate loading and % v/v water in methanol shows at high loadings of palladium(II) acetate, the amount of water has a negligible effect on the conversion to **1** (Figure 19). However, at low loadings of palladium acetate, the conversion to **1** is significantly increased when the amount of water is low.

Design-Expert® Software
Original Scale
1

- Design Points
- C- 40.000
- ▲ C+ 60.000

X1 = A: Mol% Pd
X2 = C: % Water

Actual Factors

B: Base Eq. = 1.25
D: Boronic Acid Eq. = 1.08
E: Ligand Eq. relative to Pd = 2.00
F: Total Solvent Volumes = 12.00

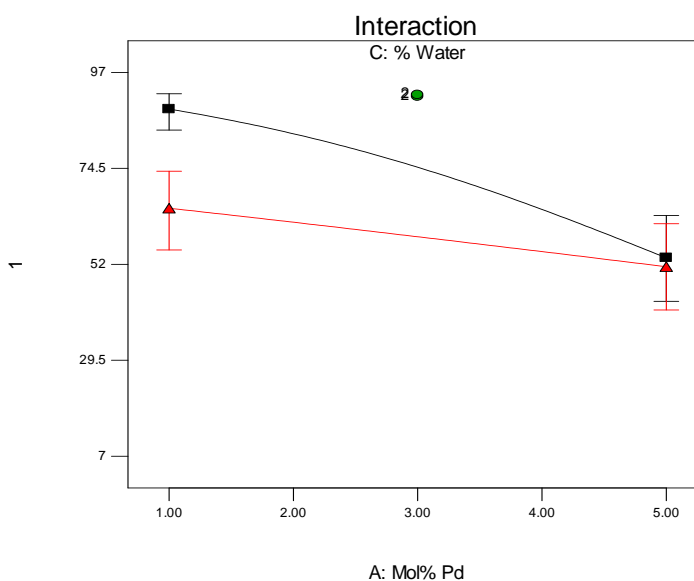
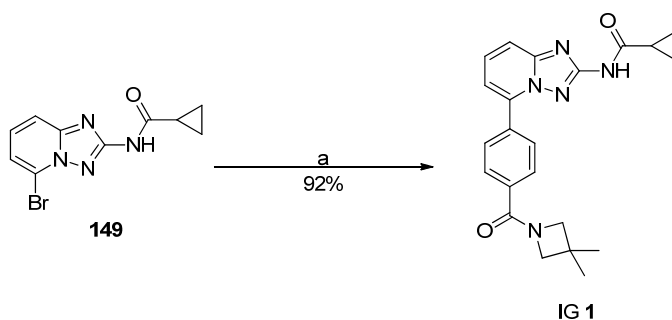


Figure 19: 2-factor interaction palladium(II) acetate mol% and % v/v water in methanol.

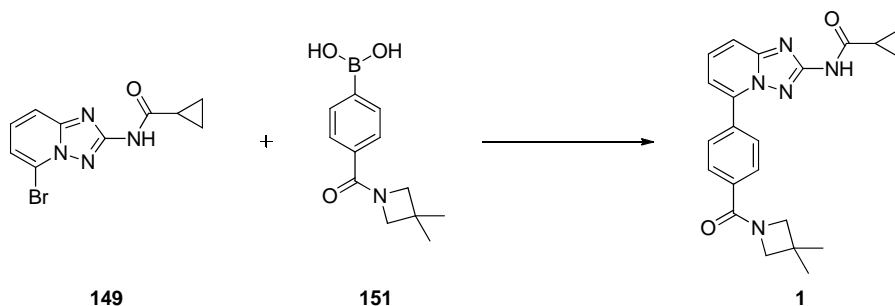
The results of the DoE screen showed the conversion to **1** was favoured when the equivalents triphenylphosphine relative to palladium(II) acetate, palladium(II) acetate and % v/v water in methanol are fixed to the lower values. As the remaining variables do not have significant influence on the conversion to **1**, it was decided to fix these variables to their lower values to minimize waste. As a result of the DoE screen, all the variables were set to the lower values on the ranges investigated (Scheme 46).



Conditions: a) Aryl bromide **149** (1 eq), boronic acid **151** (1 eq), Na₂CO₃ (1 eq), 40% v/v aqueous methanol (8 vol), palladium(II) acetate (1 mol%), PPh₃ (1 mol%), reflux, 4.5 hours.

Scheme 46: Reaction conditions identified by DoE screen to prepare 1.

Using the conditions in Scheme 46, clean conversion to **1** was observed, enabling IG **1** to be isolated in 92% yield, containing ~2800 ppm Pd. Further investigations were carried out to determine if the palladium(II) acetate loading could be reduced further (Table 11).

Table 11: Further investigations following DoE Screen.^a

Conditions	% v/v water	Solvent volumes (vol)	PPh ₃ (mol %)	Pd(OAc) ₂ (mol %)	Temp. (°C)	Yield (%)	Pd (ppm) ^b	Product 1 % PAR ^c
1 ^d	40	8	1	1	65	92	2850	99.9
2 ^e	20	8	0.5	0.5	70	92	545	99.7
3	40	16	0.25	0.25	70	83	263	99.8
4	40	16	0.1	0.1	70	72	NE	94.5 ^f

^a Conditions: Aryl bromide **149** (1 eq), boronic acid **151** (1 eq), Na₂CO₃ (1 eq), methanol, palladium(II) acetate, PPh₃. ^b Determined by ICP-AES. ^c Determined by HPLC (Method C). ^d Solids washed with 50% v/v aqueous methanol (15 volumes). ^e After the reaction mixture had cooled to room temperature, 40% aqueous methanol (15 vol) was added. ^f Determined by HPLC (Method A).

During the reaction, the suspension of **1** obtained was very thick, making stirring and transferring out of the vessel during isolation difficult for scaling up into plant vessels (Table 11, entries 1 and 2). Increasing the solvent to 16 volumes, provided a stirrable slurry which could be transferred easily out of the vessel (entries 3 and 4). In order to minimise the amount of palladium which would need to be removed from the isolated **1**, further experiments were carried out to investigate reducing the palladium loading. This demonstrated good conversion with 0.25 mol% palladium acetate without an adverse effect on reaction rate or product purity (entry 3). Using catalyst loadings below 0.25 mol% in the reaction was shown to increase the amount of impurities formed (entry 4).

Using the optimised conditions, with 0.25 mol% palladium acetate in 16 volumes of aqueous methanol, IG **1** was isolated by filtration in 83% yield, containing ~260 ppm Pd (Table 11, entry 3). This result shows Route B has a significant benefit over Route A, which required 2 mol% palladium catalyst, resulting in the Suzuki-Miyaura product **150** containing ~5200 ppm Pd. Decreasing the catalyst loading from 1 mol% to 0.25 mol% in the Route B coupling, reduced the concentration of palladium in isolated IG **1** from ~2800 ppm Pd to ~260 ppm Pd (entry 1 and entry 3), however the

specification set for Pd was <10 ppm Pd, so the process to prepare IG **1** required further development to decrease the Pd content of the isolated solid.

2.2.4 Investigation of Palladium Removal Methods

Having established IG **1** could be isolated containing ~260 ppm Pd, using 0.25 mol% palladium(II) acetate, palladium removal methods were investigated. **1** (prepared using 0.25 mol% Pd catalyst loading) was dissolved in dichloromethane and various palladium scavenging reagents were added to the solution obtained (summarised in Table 12). In addition to Cuno R55S powder, several other reagents (shown in Figure 20) were added to the dichloromethane solution of **1**, as they were expected to chelate with palladium to enable removal.

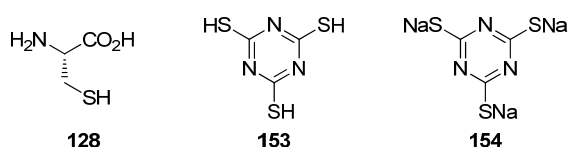
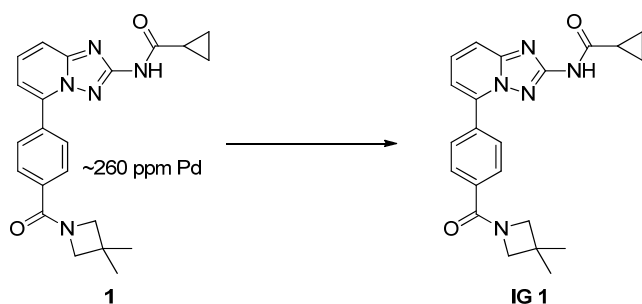


Figure 20: Palladium scavenging reagents investigated for **1 generated from Na₂CO₃/methanol conditions.**

L-Cysteine **128** has been successfully demonstrated to remove palladium from organic phases during an aqueous work-up.^{90,91} Trimercaptotriazine **153** has been shown to be successful at removing palladium by forming insoluble complexes which are removed by filtration.¹¹⁶ The trisodium salt of trimercaptotriazine **154** was also selected as it is water soluble and it may form a water soluble complex with palladium.⁹⁰

Table 12: Palladium levels in IG 1 after dissolution in dichloromethane and treatment with additives.^a

Entry	Additive	Pd content of IG 1 ^b (ppm)
1	CUNO R55S powder	67
2	NaTMT 154	77
3	<i>L</i> -cysteine 128	29
4	TMT 153	150

^a **1** was dissolved in dichloromethane and treated with additive; ^b Isolated by evaporation to dryness.

Although IG **1** was isolated by evaporation to dryness, which would not be acceptable for further scale-up, it was known from the Route A Stage 3 process, IG **1** could be precipitated from a dichloromethane solution by addition of ethyl acetate. With careful control of both the addition of ethyl acetate and removal of dichloromethane, by a constant volume distillation, it was known this isolation could reduce the palladium content in IG **1**, therefore it was expected the palladium content values shown in Table 12 could be reduced further. Although the methods of palladium removal in Table 12 showed a significant reduction compared with the input (~260 ppm Pd), these methods of palladium removal would mean a separate processing stage was required. In effect, this would lengthen the synthetic route and the benefit of the convergent route would be reduced.

Addition of a palladium scavenging reagent into the reaction mixture following complete conversion to **1**, would be a more efficient process to operate in a manufacturing plant. Palladium scavenging reagents were chosen based on their solubility in the reaction solvent 40% v/v aqueous methanol, so TMT **153** was not included in this screen. *N*-Acetyl-*L*-cysteine **127** (Figure 21) has also been shown to remove palladium from reaction product by forming water soluble palladium complexes^{90,92} and was therefore examined in this second screen.

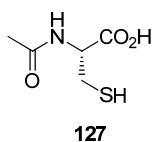
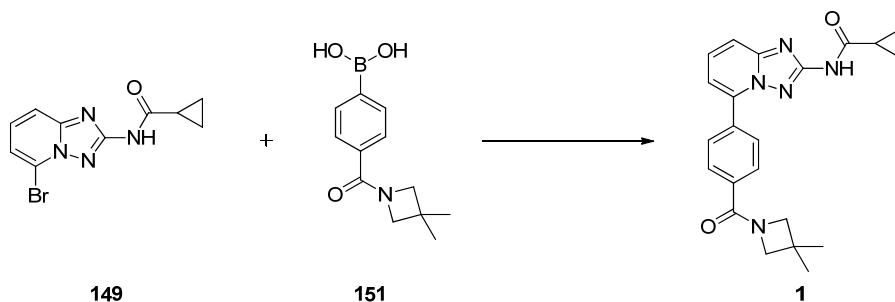


Figure 21: N-Acetyl-L-cysteine 127.

Table 13 shows the palladium content of IG **1** after palladium scavenging reagents had been added to the reaction mixture which had reached complete conversion.

Table 13: Palladium levels in IG 1 after addition of palladium scavenger reagent post reaction completion.^a



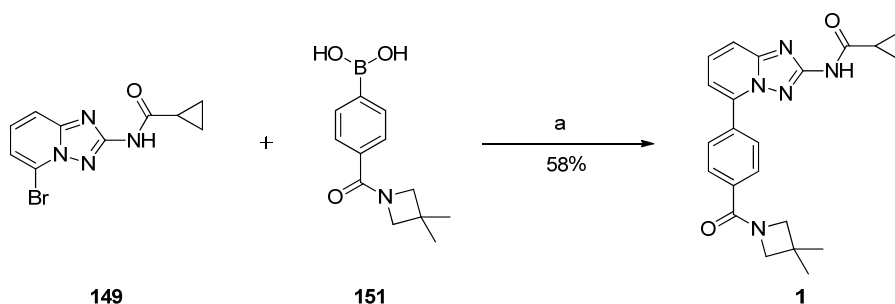
Conditions	Additive	Pd content of IG 1 ^b (ppm)
1	NaTMT 154	489
2	<i>N</i> -Acetyl- <i>L</i> -cysteine 127	103
3	<i>L</i> -cysteine 128	135

^a Conditions: Aryl bromide **149** (1 eq), boronic acid **151** (1 eq), base (1 eq), 40% *v/v* aqueous methanol, palladium(II) acetate (0.25 mol%), PPh₃ (0.25 mol%), followed by addition of additive after complete conversion to **1**; ^b Isolated by filtration.

Table 13 shows addition of *L*-cysteine **128** and *N*-acetyl-*L*-cysteine **127** to the reaction mixture after completion reduces the palladium content of isolated **1**, however, Table 13 shows higher levels of palladium in **1** than found previously (Table 12). It was observed at the end of the Suzuki-Miyaura coupling, **1** began to precipitate once the reaction was complete, as it was not soluble in the reaction solvent, 40% *v/v* aqueous methanol. This could lead to incorporation of palladium species into the crystal lattice of **1**, preventing exposure to the palladium scavenging reagents added after the reaction was complete. It was proposed that dissolving **1** in dichloromethane before addition of palladium scavenging reagents, would enable more palladium to be exposed to the scavenging reagent resulting in a more efficient palladium removal. However, this was not investigated further as examination of additional solvents showed promising alternatives.

2.2.5 Development of Stage 3 *n*-Butanol Reaction Conditions

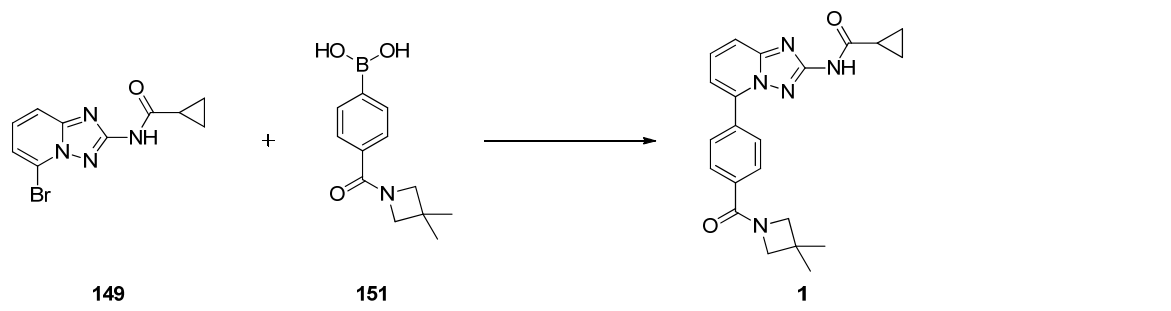
To enable IG **1** to be prepared *via* Route B and meet the specification for palladium, an alternative reaction solvent to methanol could also prove beneficial, to enable **1** to remain in solution at the end of the reaction. It was postulated, *n*-butanol could be a suitable reaction solvent, as it would allow higher temperatures to be accessed than with methanol. Although **1** showed low solubility in *n*-butanol at room temperature, no investigation into higher temperatures had been carried out. Additionally, *n*-butanol is not miscible with water, which could enable an aqueous work-up to improve the purity of the isolated product. Using *n*-butanol as a solvent, good conversion to **1** was observed (Scheme 47). At the end of the reaction, **1** was shown to be soluble in *n*-butanol and precipitated palladium black particles were observed. After filtration through Celite to remove precipitated palladium, **1** crystallised from the reaction solvent, to give IG **1** with 25 ppm Pd in 58% yield. Although lower yielding, this alternative solvent showed promise, so was investigated further.



Conditions: a) Aryl bromide **149** (1 eq), boronic acid **151** (1 eq), Na₂CO₃ (1 eq), *n*-butanol (9.6 vol), water (6.4 vol), palladium(II) acetate (0.25 mol%), PPh₃ (0.25 mol%), reflux, 19 h.

Scheme 47: Route B Stage 3 using *n*-Butanol.

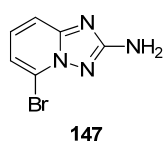
Using catalysts immobilized on solid supports can enable products to be isolated which meet the low specifications required for heavy metals.¹¹⁷ Dithiopalladium modified silicas have been reported to be used to this effect¹¹⁸ in Suzuki-Miyaura couplings and were evaluated for the Stage 3 process, as shown in Table 14.

Table 14: Comparison of supported palladium reagents in Suzuki-Miyaura coupling.^a


Entry	Pd(OAc) ₂ source ^b	Time (h)	Hydrolysed aryl bromide 147 % PAR ^c	Aryl bromide 149 % PAR ^c	Boronic acid 151 % PAR ^c	Hydrolysed product 157 % PAR ^c	Product 1 % PAR ^c	Pd content ^d (ppm)
1	A	19			0.3	3.9	94.9	26
2	B	18	39.8	24.0	20.3	1.5	9.3	Not isolated
3	C	23	0.9		0.13	12.0	85.1	29
4	D	18	0.6	0.8	0.3	2.9	92.6	86

^a Conditions: Aryl bromide **149** (1 eq), boronic acid **151** (1.15 eq), Na₂CO₃ (1 eq), 40% v/v aqueous *n*-butanol (16 vol), palladium(II) acetate source (0.25 mol% Pd), PPh₃ (0.25 mol%); ^b A = palladium(II) acetate, B = palladium acetate 2-mercaptoethyl ethyl sulfide silica, C = palladium acetate 3-mercaptoethyl ethyl sulfide silica, D = palladium acetate ethanoate ethyl sulfide silica; ^c Determined by HPLC (Method A); ^d Isolated by filtration, Pd content determined by ICP-AES.

All the supported palladium acetate reagents were shown to give slower conversions to **1** (entries 2–4) compared with using unsupported palladium acetate (entry 1). For palladium acetate 2-mercaptoethyl ethyl sulfide silica (entry 2), the rate of the desired Suzuki-Miyaura coupling was significantly slower than the rate of hydrolysis of **149**, which led to the major product of the reaction being aminotriazole **147** (Figure 22).

**Figure 22: Aminotriazole 147.**

Intermediate grade **1**, prepared using the other supported palladium acetate reagents (entries 3 and 4) showed similar or higher Pd content compared with using palladium(II) acetate (entry 1), suggesting leaching of the palladium catalyst into the reaction mixture was occurring.¹¹⁹ Overall, the supported palladium(II) acetate reagents examined did not offer any benefit over using palladium(II) acetate.

In Stage 3 of Route B, the filtration of the organic phase through Celite had successfully removed insoluble palladium. The palladium content remaining in the isolated solid would therefore originate from soluble palladium species present at the end of the reaction. Two methods were proposed for removing soluble palladium species: either treatment with activated carbon or the addition of chelating agents, which would enable removal of palladium through aqueous work-up.

In addition to the palladium scavenging reagents investigated previously, sodium diethyldithiocarbamate trihydrate **155** and sodium dimethyldithiocarbamate hydrate **156** were investigated (Figure 23). Analytical scientists elsewhere in our laboratories were investigating the palladium complexes formed with **155** and **156**, in order to quantify palladium by HPLC analysis. As the palladium complexes formed would need to be water soluble in order to carry out the HPLC analysis, these reagents were included in the aqueous work-up investigation.

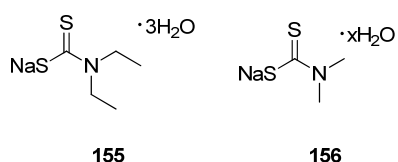
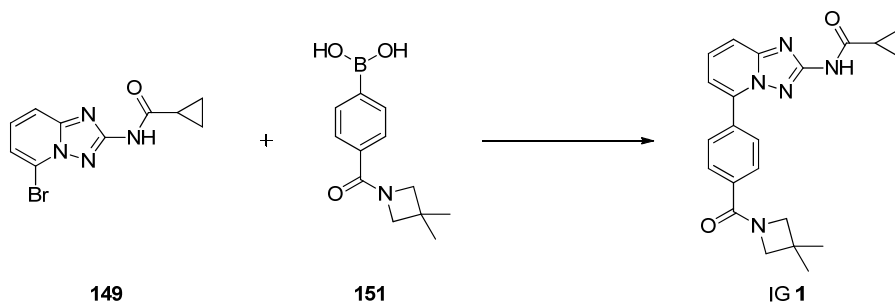


Figure 23: Additional palladium scavenging reagents.

Table 15 summarises the palladium removal reagents investigated and the palladium content of IG 1 after isolation.

Table 15: Screening of Palladium Removal Reagents.^a

Entry	Scavenging reagent	Pd content ^d (ppm)
1	Loose Cuno R55S Powder ^b	16
2	Sodium diethyldithiocarbamate trihydrate 155 ^c	24
3	<i>N</i> -Acetyl- <i>L</i> -cysteine 127 ^c	10
4	Trithiocyanuric acid, trisodium salt monohydrate 154 ^c	50
5	<i>L</i> -Cysteine 128 ^c	69
6	Sodium dimethyldithiocarbamate hydrate 156 ^c	519

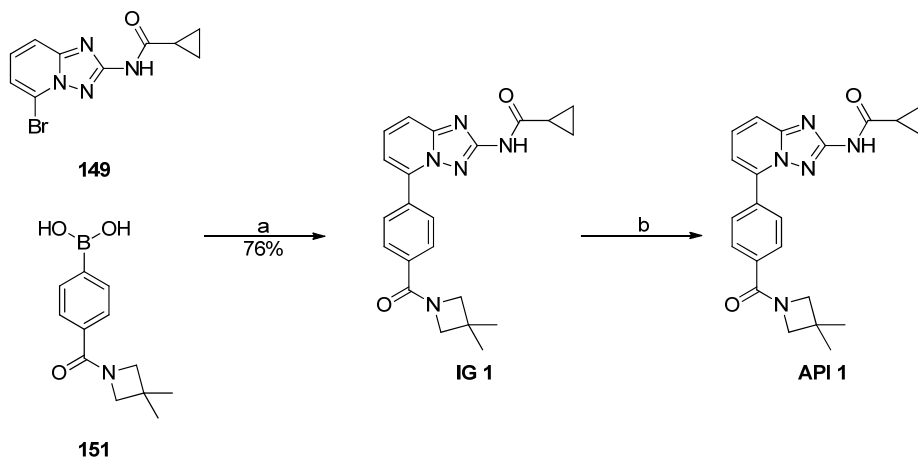
^a Conditions: Aryl bromide **149** (1 eq), boronic acid **151** (1.15 eq), Na₂CO₃ (1 eq), *n*-butanol (9.6 vol), water (6.4 vol), palladium(II) acetate (0.25 mol%), PPh₃ (0.25 mol%) followed by addition of scavenging reagent to organic phase; ^b Organic solution of **1** heated with reagent overnight at 50 °C, followed by filtration through Celite; ^c Organic solution heated with reagent and water overnight at 50 °C; ^d Isolated by filtration, Pd content determined by ICP-AES.

Comparison of the isolated solids (Table 15) showed treatment with *N*-acetyl-*L*-cysteine **127** enabled intermediate grade **1** to be isolated with 10 ppm Pd (entry 3). This demonstrated Route B could offer a significant advantage over Route A, as extra processing steps would not be required to remove palladium.

2.2.6 Scale-up of Sodium Carbonate/*n*-Butanol Process

Having identified *N*-acetyl-*L*-cysteine **127** as the most effective reagent for removing palladium, the reaction conditions were scaled-up into a controlled laboratory reactor (CLR), which is a minaturised version of a plant vessel. The work-up process was slightly modified compared with the smaller scale experiment. In order to keep the product in solution during the *N*-acetyl-*L*-cysteine wash, the biphasic mixture was held at 82 °C. After removing the aqueous phase, a water wash was carried out, followed by an atmospheric distillation to azeotropically dry the solution, which reduced the solubility of **1**. Intermediate grade **1** was isolated in 76% yield containing 13 ppm Pd. IG **1** was recrystallised in Stage 4 to give API **1**, which contained one impurity above the specification limit of 0.06% area (Table 16).

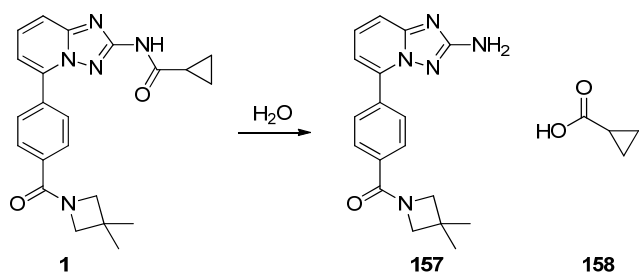
Table 16: Comparison of IG 1 (prepared in 250 mL CLR) and API 1.



		IG 1 % PAR	API 1 % PAR
HPLC	RRT		
		0.46	ND
		0.56	ND
		0.87	0.09
		1.00	99.23
		1.04	0.05
		1.23	0.03
		1.27	0.05
	1.34	0.04	0.04
ICP-AES (ppm)	Element		
	Na	1	ND
	Pd	13	2

Conditions: a) i. **149** (1 eq), **151** (1 eq), Na₂CO₃ (1 eq), *n*-butanol (9.6 vol), water (6.4 vol), palladium(II) acetate (0.25 mol%), PPh₃ (0.25 mol%), reflux, 5 hours, ii. *N*-acetyl-*L*-cysteine **127** (2.5 mol%), water (6.4 vol), 82 °C, overnight; b) IMS (8 vol), water (2 vol).

The impurity with RRT 0.87 was identified by LC-MS to be **157**, which is a hydrolysis product of **1** (Scheme 48).

Scheme 48: Hydrolysis of **1** to give impurity **157**.

HPLC time course analysis was carried out during the scaled-up reaction, to monitor the rate of the reaction and formation of impurities (Figure 24).

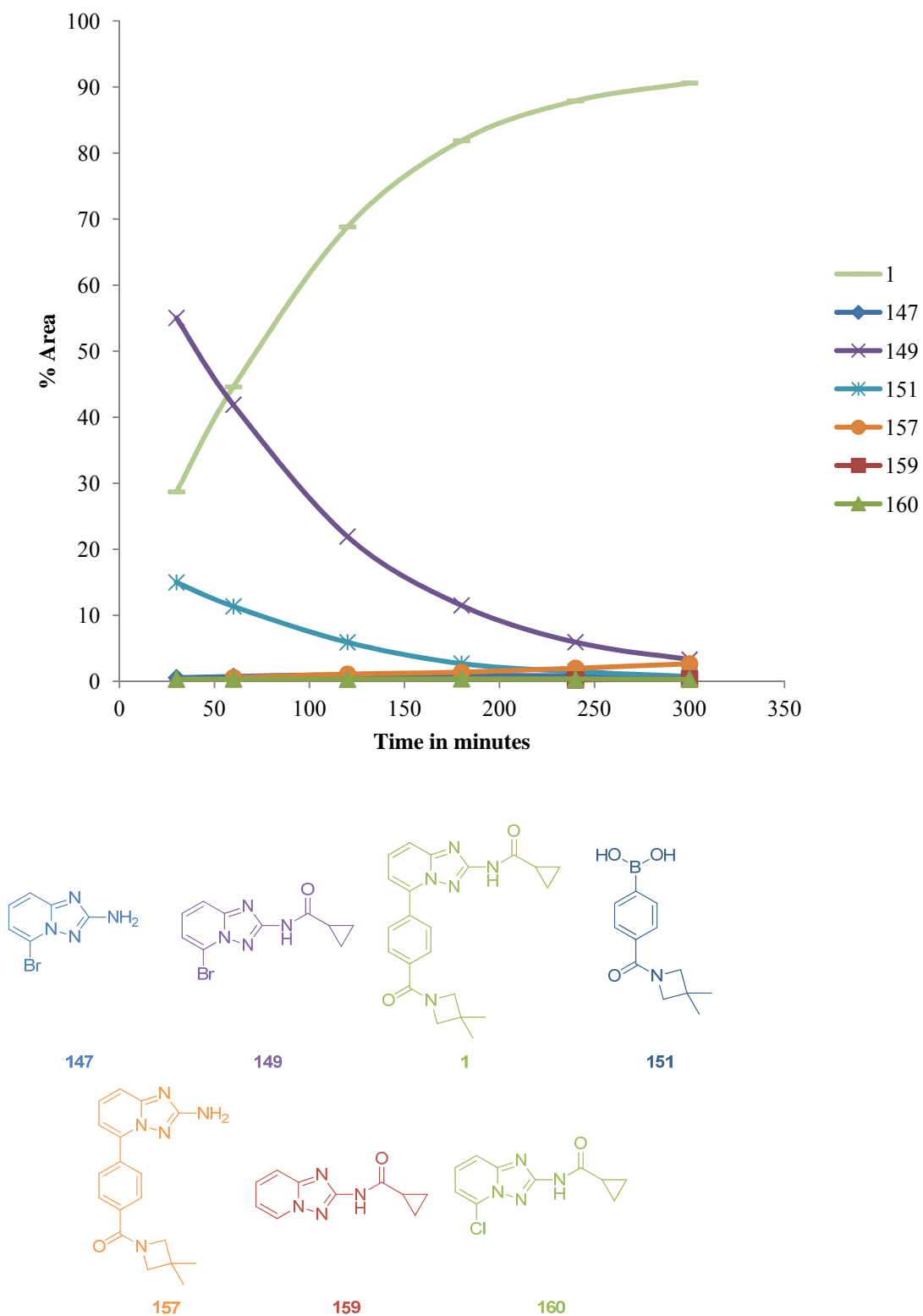


Figure 24: HPLC time course analysis of Suzuki-Miyaura coupling using sodium carbonate.

Figure 24 shows the rate of formation of the hydrolysis impurity **157**, which increases with the formation of the desired product **1**. The rate of formation of **157** is shown in greater detail in Figure 25.

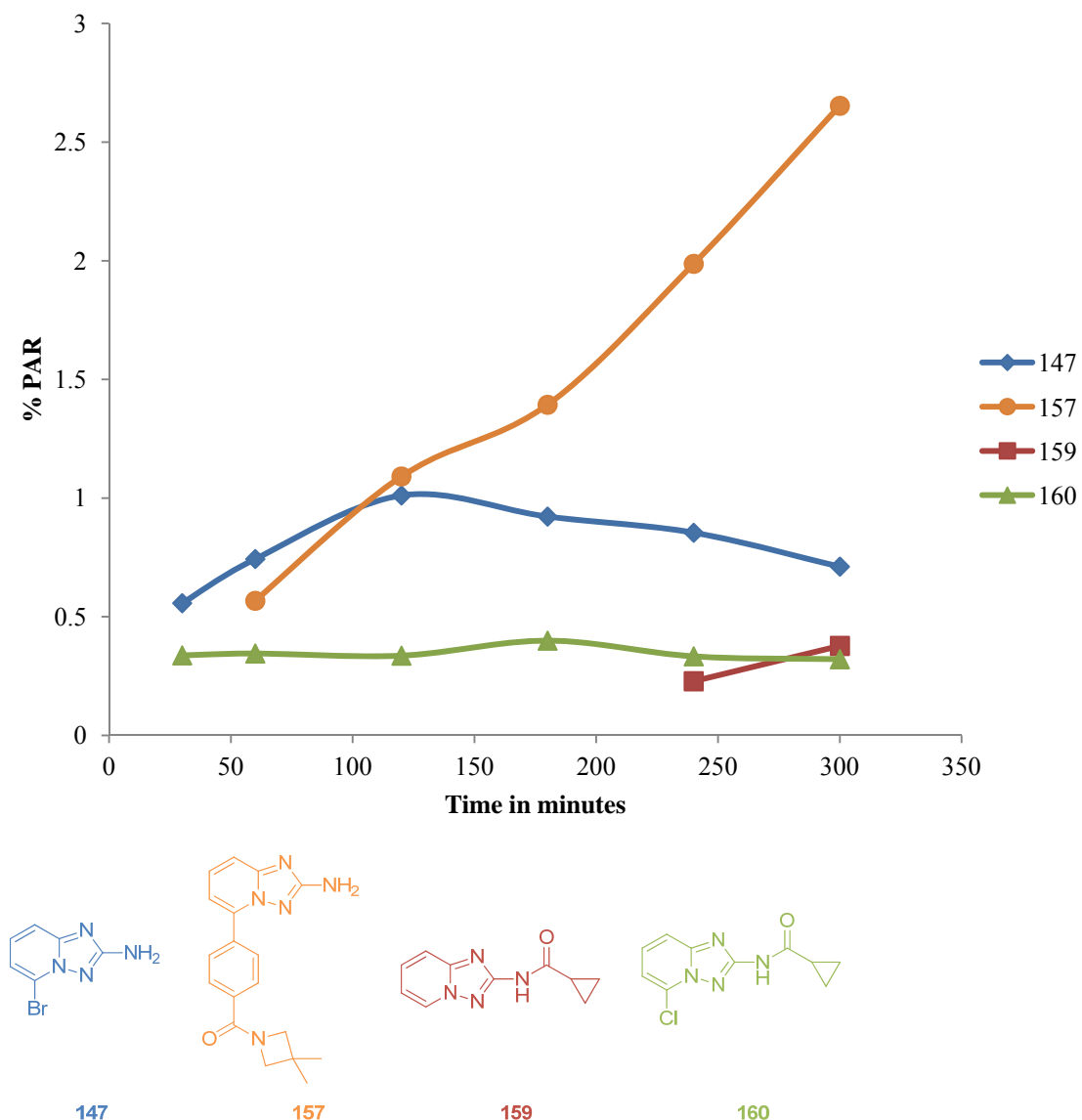
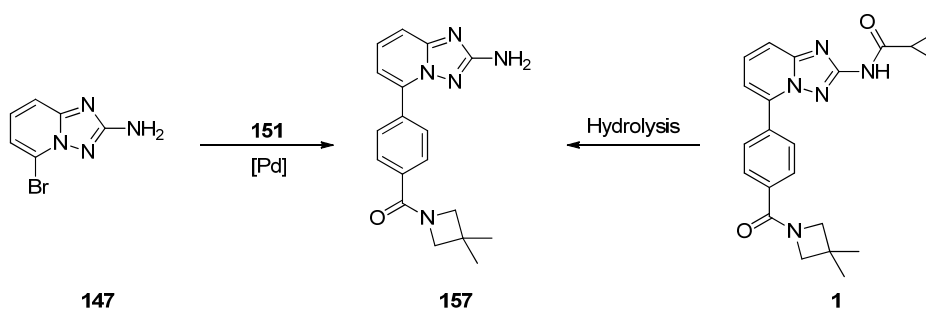


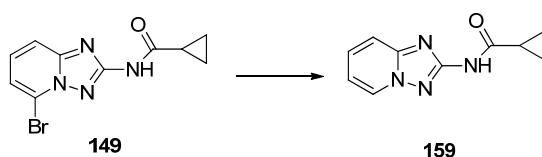
Figure 25: HPLC time course analysis of impurities formed during the Suzuki-Miyaura coupling using sodium carbonate.

Figure 25 shows hydrolysis of the product **1** and hydrolysis of the aryl bromide **149** was occurring in the reaction mixture to give impurities **157** and **147** respectively. The level of **147** was shown to increase initially and then decrease, suggesting **147** was undergoing the Suzuki-Miyaura coupling to give **157**. The rate of formation of **157** increases slightly, as the rate of formation of **147** decreases, suggesting these 2 pathways are contributing to the formation of **157** (Scheme 49).



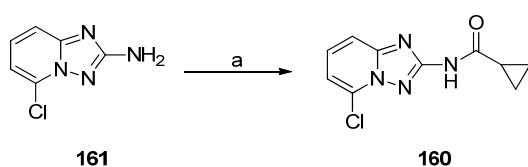
Scheme 49: Pathways to the formation of 157.

Figure 25 shows there are other impurities formed in the reaction mixture, which are not observed in isolated batches of IG **1**, as these are purged during the crystallisation of **1** from *n*-butanol. Impurity **159** (Scheme 50) was identified as the product formed when aryl bromide **149** is proto-dehalogenated.



Scheme 50: Proto-dehalogenation of aryl bromide 149 to give impurity 159.

Impurity **160** is the chloro-analogue of **149**, which is formed from **161** being present in **147**, the Stage 1 starting material. Under the Stage 1 reaction conditions, **160** is formed from **161**. In the Stage 3 Suzuki-Miyaura coupling, the level of **160** remains constant through the reaction, suggesting the rate of oxidative addition of **149** is faster than **160**.



Conditions: a) i. Cyclopropylcarbonyl chloride, NEt_3 , acetone, ii. 7N NH_3 in MeOH.

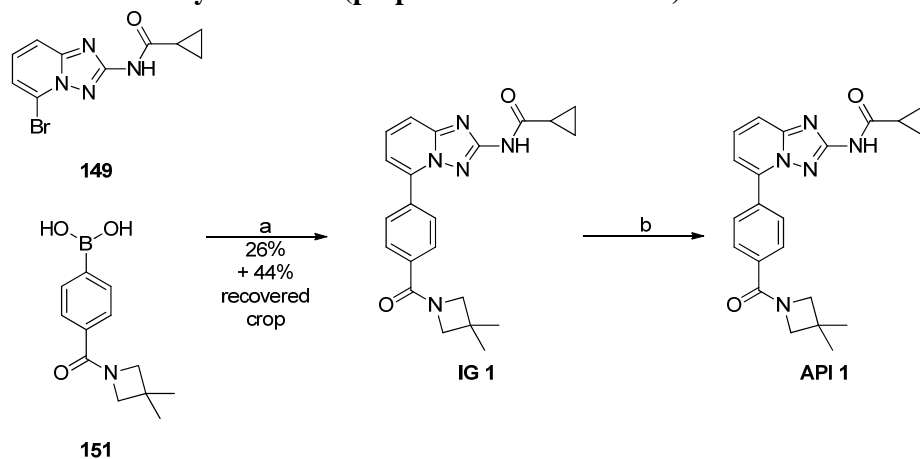
Scheme 51: Formation of 160.

Figure 25 shows at the end of the reaction, desamido **157** was present in solution at a level of 2.65%. Following the aqueous work-up and crystallisation, **157** was reduced to 0.44% in isolated IG **1**. As stage 4 recrystallisation of **1** did not sufficiently purge **157** in order to meet the API specification, the formation of **157** in the coupling reaction needed to be minimised.

As the Stage 3 reaction conditions were biphasic, it was decided to look at the effect of improving mixing in Stage 3. The Stage 3 reaction conditions required overnight

reflux in order to reach completion. It was proposed that improving the mixing in the reaction may enable a faster Suzuki-Miyaura coupling, whilst reducing exposure of **149** and **1** to the basic conditions. A single flight anchor impeller had been used in 250 mL scale reaction, which was expected to give inferior mixing compared with the equipment in the pilot plant.¹²⁰ The Stage 3 reaction was repeated in a 500 mL CLR fitted with a double flight impeller which was more representative of pilot plant equipment, but this was shown to have no effect on increasing the rate of the formation of **1**.

At the end of the reaction, sulfuric acid washes were investigated to see if **157** could be removed by washing into the aqueous phase. HPLC analysis showed washing the organic phase with sulfuric acid reduced **157** from 3.1% to 2.7%, which was not sufficient for reducing the levels of **157** to an acceptable level in isolated **1**. The isolated IG **1** obtained from this reaction contained a higher level of **157**, **149** and other impurities (shown in Table 17) compared with the experiment carried out at 250 mL scale (shown in Table 16).

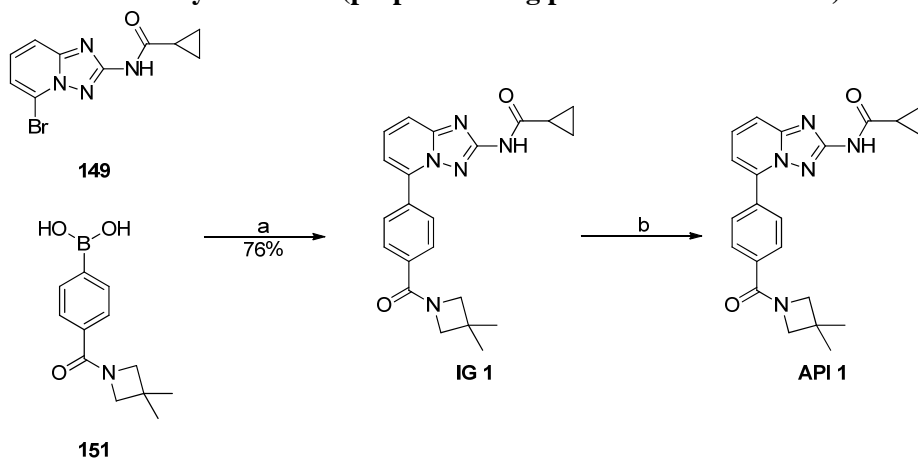
Table 17: Analysis of IG 1 (prepared in 500 mL CLR) and API 1.

		IG 1	API 1
HPLC (% PAR)	HPLC RRT		
		0.45	ND
		0.55 (149)	ND
		0.87 (157)	0.11
		1.00 (1)	99.68
		1.04	ND
		1.23	ND
		1.27	0.07
		1.34	0.07
	1.35	0.10	
ICP-AES (ppm)	Element		
	Na	2	<1
	Pd	8	2

Conditions: a) i. **149** (1 eq), **151** (1 eq), Na₂CO₃ (1 eq), n-butanol (9.6 vol), water (6.4 vol), palladium(II) acetate (0.25 mol%), PPh₃ (0.25 mol%), reflux, 5 hours, ii. 1N H₂SO₄ (9.6 vol), iii. *N*-acetyl-*L*-cysteine **127** (2.5 mol%), water (6.4 vol) 78 °C, 75 minutes; (b) IMS (8 vol), water (2 vol).

2.2.7 Development of Stage 3 Process using Potassium Bicarbonate

In order to reduce the rate of hydrolysis of **1**, Stage 3 was carried out using the weaker base potassium bicarbonate instead of sodium carbonate. The rate of formation of **1** was similar to that observed using sodium carbonate, but the levels of **157** in the reaction mixture were reduced to 0.5%, compared with 2.6-2.9% using sodium carbonate. After isolation, intermediate grade **1** was obtained with 0.12-0.18% **157**, which was shown to be reduced to under the specification limit after the Stage 4 recrystallisation.

Table 18: Analysis of IG 1 (prepared using potassium bicarbonate) and API 1.

	IG 1	API 1
	RRT	
	0.45	ND
	0.56	ND
	0.87 (157)	0.04
HPLC (% PAR)	1.00 (1)	99.81
	1.04	0.02
	1.23	ND
	1.24	ND
	1.27	0.05
	1.34	0.07
	Element	
ICP-AES (ppm)	Pd	10

Conditions: a) **149** (1 eq), **151** (1 eq), KHCO_3 (1 eq), n-butanol (9.6 vol), water (6.4 vol), palladium(II) acetate (0.25 mol%), PPh_3 (0.25 mol%), reflux 5 hours; ii. *N*-acetyl-*L*-cysteine **127** (3.0 mol%), water (4 vol) 84 °C, 2 hours; b) IMS (8 vol), water (2 vol).

The reaction mixture was held overnight at reflux, which resulted in a small increase of **157** from 0.53% to 0.71%. This increase in **157** was significantly lower than 2.6-2.9% **157**, observed using sodium carbonate and demonstrated using potassium bicarbonate, would result in a more robust Stage 3 process.

2.2.8 Identification of Late Running Impurities

Table 18 shows an impurity at RRT 1.34 at 0.07% PAR in isolated API **1**, which is above the specification limit of 0.06%. In addition, Table 17 shows further compounds, RRT 1.27 and RRT 1.35 which were at a level of 0.07% in API **1**. Without knowledge of the structure of these three impurities, it could not be guaranteed the impurities would not increase on scale-up. In addition, HPLC analysis showed the Stage 4 recrystallisation did not reduce these impurities significantly, which increased the need for identification of these impurities, in order to understand their formation. To do this, the project specific HPLC method was set up on an

LC-MS instrument, in order to obtain a mass ion for these impurities. The proposed structures are shown in Figure 26.

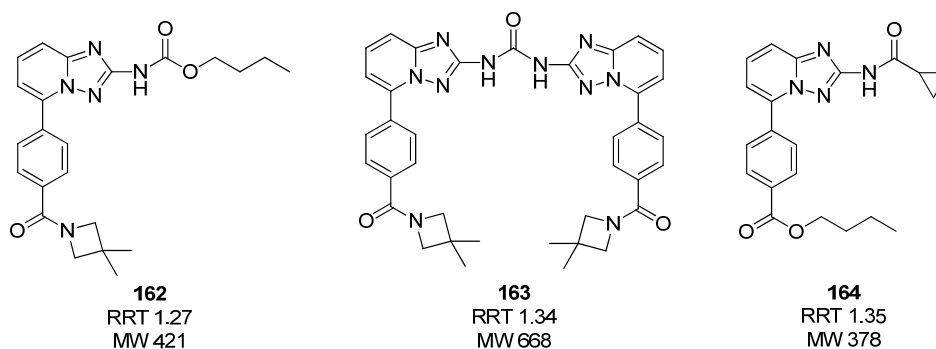
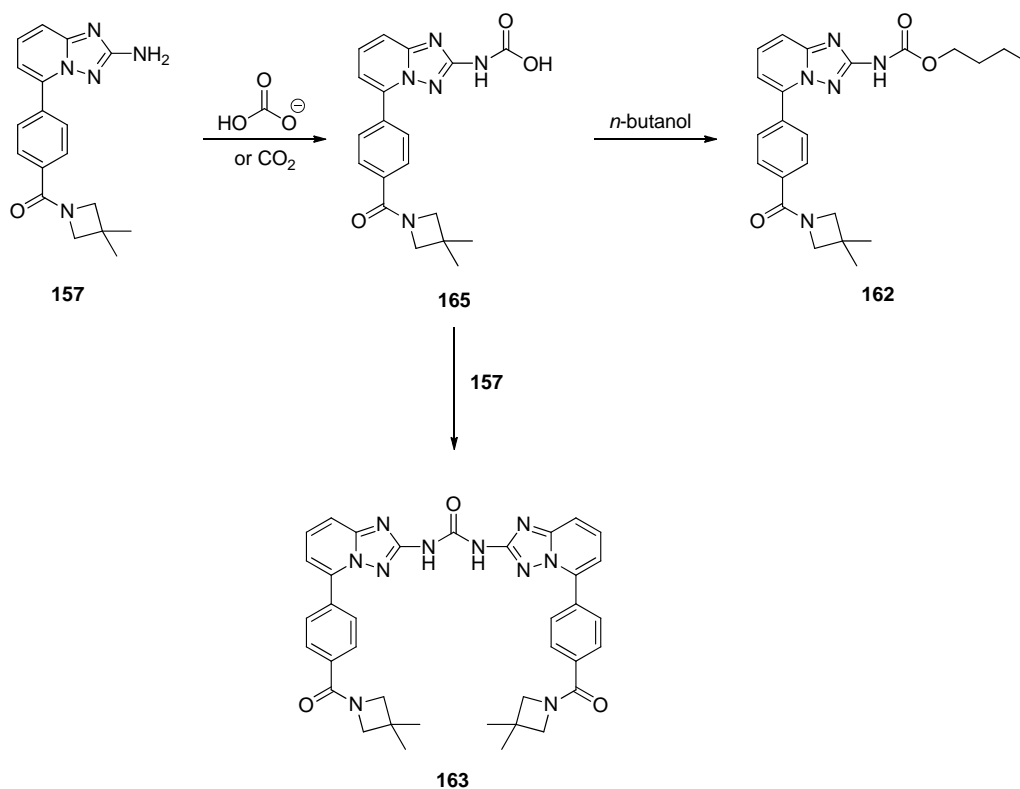


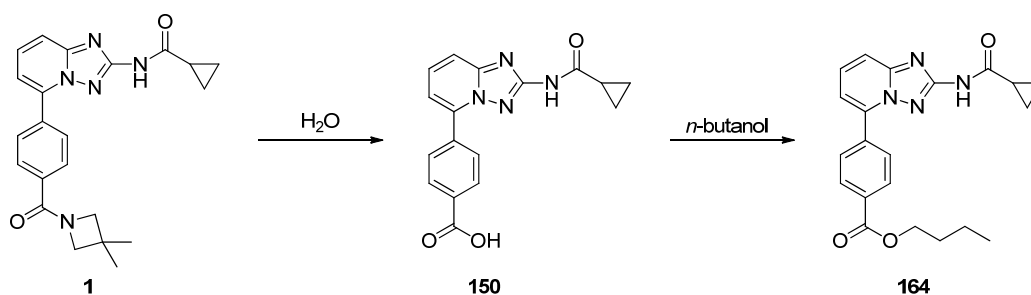
Figure 26: Structures of late running impurities proposed through LC-MS analysis.

The LC-MS analysis had shown, that two of the impurities **162** and **163**, were formed by reaction of **157** with bicarbonate anions or dissolved carbon dioxide, followed by either reaction with *n*-butanol or further reaction with **157** (Scheme 52).



Scheme 52: Proposed formation of 162 and 163.

The structure of impurity **164**, showed solvolysis was occurring at the second amide bond, but given the low levels of **164** compared with **157**, hydrolysis of this amide bond was occurring to a lesser extent (Scheme 53).



Scheme 53: Proposed formation of 164.

Identifying the structures of the late running impurities and the high levels of **157** in the isolated product had shown side reactions involving hydrolysis of product and starting materials needed to be controlled in order to give the correct quality of API **1**.

2.2.9 Optimisation of Potassium Bicarbonate Reaction Conditions with DoE

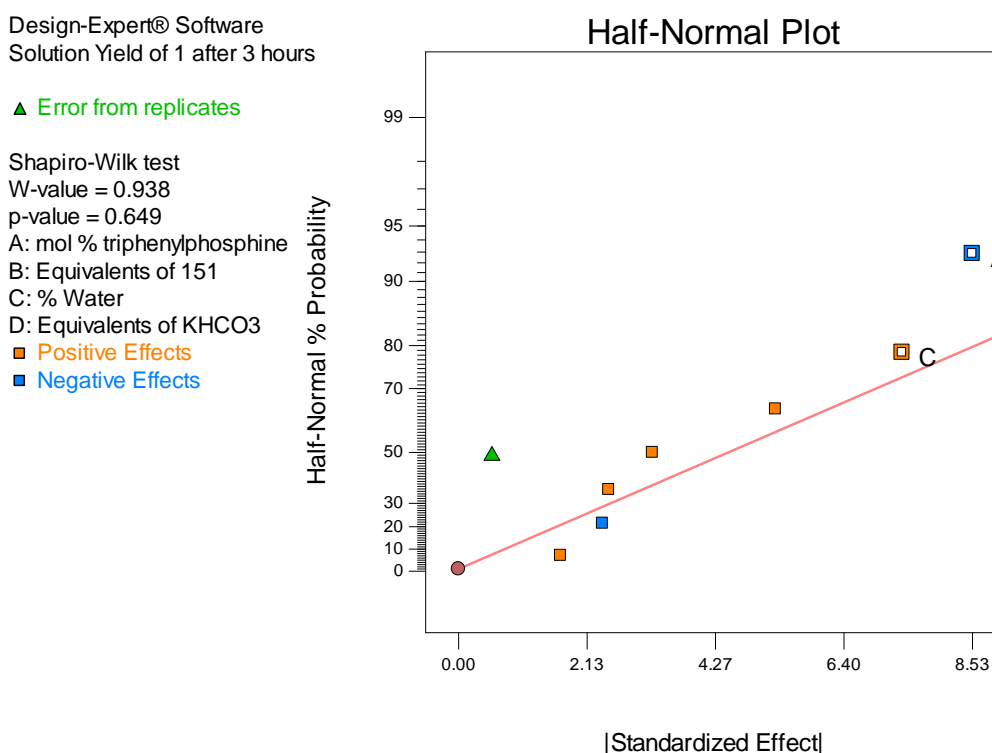
After repeating the potassium bicarbonate/aqueous *n*-butanol reaction conditions, it was becoming apparent that several hydrolysis pathways were affecting the isolated purity of **1**. Water and base are known to have critical roles in the Suzuki-Miyaura coupling and are also known to promote hydrolysis of amides, so understanding the effect of changing these variables in the reaction would be key to optimisation of the process to prepare IG **1**. The potassium bicarbonate/aqueous *n*-butanol Suzuki-Miyaura reaction needed to be carried out overnight at reflux in order to consume **1**. The prolonged reaction time increased exposure of the starting materials and the desired product to basic aqueous conditions promoting impurity formation. Varying the levels of water and potassium bicarbonate could potentially affect impurity formation. Understanding the effect of varying the boronic acid **151** and the ligand triphenylphosphine on the reaction rate may also enable the reaction time to be reduced.

In order to minimise impurity levels, a total of four variables were to be investigated, to determine their impact on the conversion to **1**, consumption of starting materials **149** and **151** and formation of impurities. The four variables (shown in Table 19) were explored in a half fraction factorial design. The half fractional factorial design contained ten experiments, including 2 centre points.

Table 19: Ranges of variables investigated in DoE Screen.

Variable	Range investigated
Mol% Triphenylphosphine	0.25–0.75
Equivalents of 151	1.0–1.1
% v/v Water	20–60
Equivalents of Potassium Bicarbonate	0.97–1.1

The input variables and the output responses used to construct the model are given in section 4.2 (page 132). The model showed the variable having the largest effect on maximising desired product **1** and minimising starting materials **149** and **151**, was the equivalents of triphenylphosphine relative to palladium(II) acetate (Figure 27).

**Figure 27: Half-normal plot for solution yield of 1 after 3 hours.**

The solution yield of **1** was maximised when the equivalents of triphenylphosphine to palladium(II) acetate were low. This is shown in more detail in Figure 28 where, as the equivalents of triphenylphosphine were increased, the solution yield of desired product **1** decreased. The centre points (red dots in Figure 28) lie above the line plotted, indicating the presence of curvature in the response. This curvature is such that at 0.50 mol% triphenylphosphine (centre points), the solution yield of **1** is

similar to solution yield of **1** obtained when there is 0.25 mol% triphenylphosphine. The curvature in the response could be further investigated and modelled using a response surface design.¹²¹

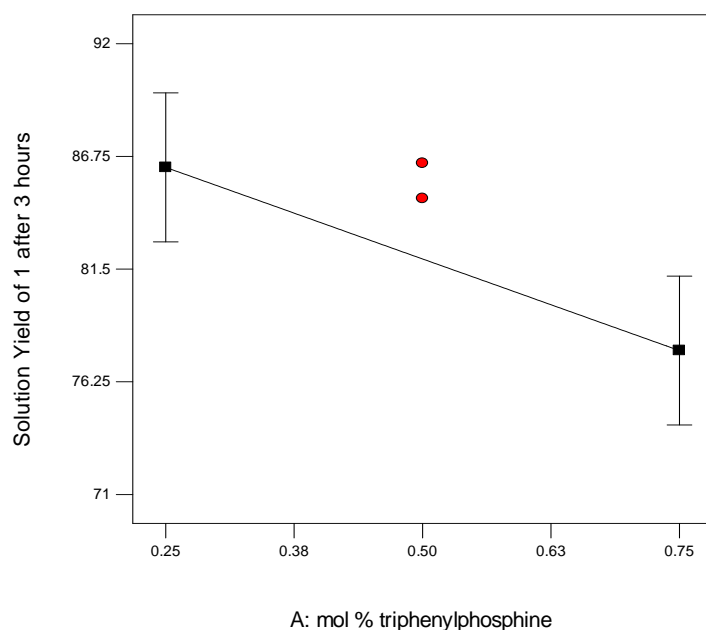


Figure 28: Effect of varying triphenylphosphine equivalents on solution yield of 1.

As expected, the opposite trend was observed for starting materials **149** and **151**. The starting materials **149** and **151** are minimised, when the equivalents of triphenylphosphine are low. The relationship between solution yield of **149** and **151** and equivalents of triphenylphosphine are also affected by curvature (shown in Figure 29 for solution yield of **149**).

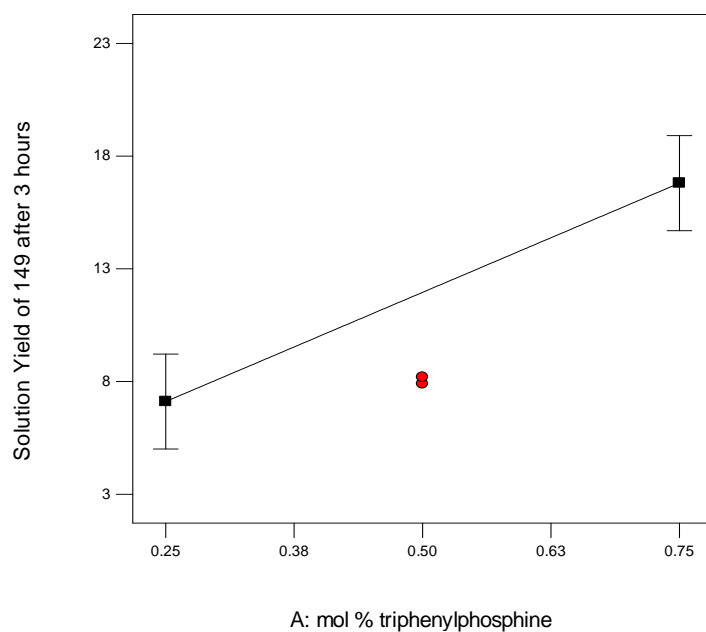


Figure 29: Effect of varying triphenylphosphine equivalents on solution yield of 149.

The solution yield of **1** was also maximised when the equivalents of boronic acid **151**, potassium bicarbonate and the % *v/v* water were increased. The impact of these variables was not as great as the impact of the equivalents of triphenylphosphine. Curvature was also seen in these models, so the centre point values are close to the values obtained at the ‘high’ input for the variable. This is exemplified in Figure 30 with % *v/v* water.

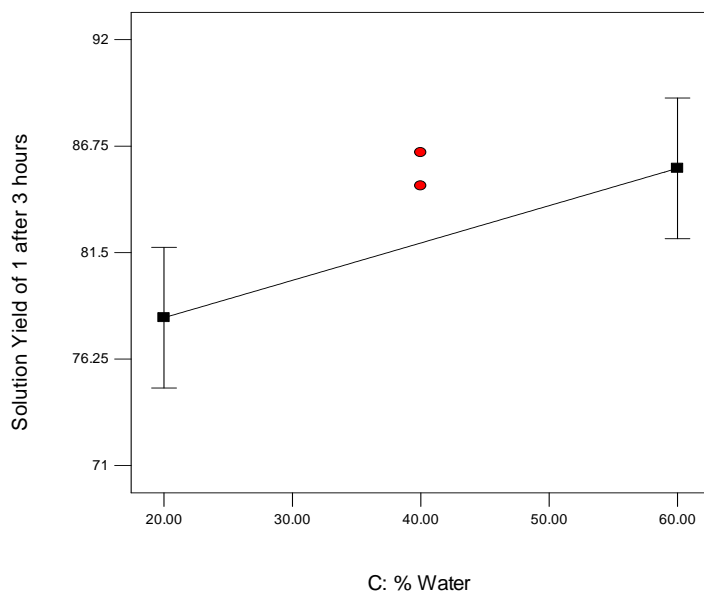


Figure 30: Effect of % v/v water on solution yield of 1.

The solution yields of **149** and **151** were also minimised when the equivalents of **151**, potassium bicarbonate and the % v/v water were increased. These variables had a similar non-linear impact on the solution yield of **1**, with curvature present in the model.

Design Expert 7¹¹² was used to analyse the formation of the impurities formed in the reaction mixture. The range of the individual impurity levels over 10 runs were very low, typically between 0-0.15%, making it difficult for the main effects to be observed over the noise from the centrepoints in the model. The range of individual impurity levels was narrow compared to range of solution yields observed for **1** in the 10 experiments, which was 72-92% solution yield after 3 hours (Figure 31).

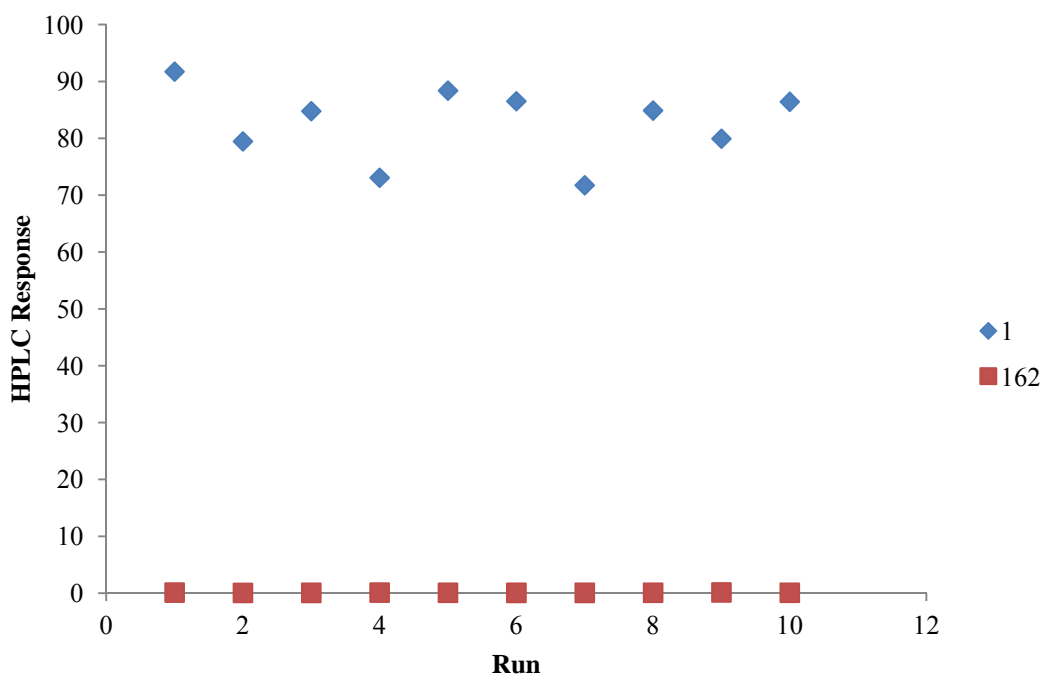
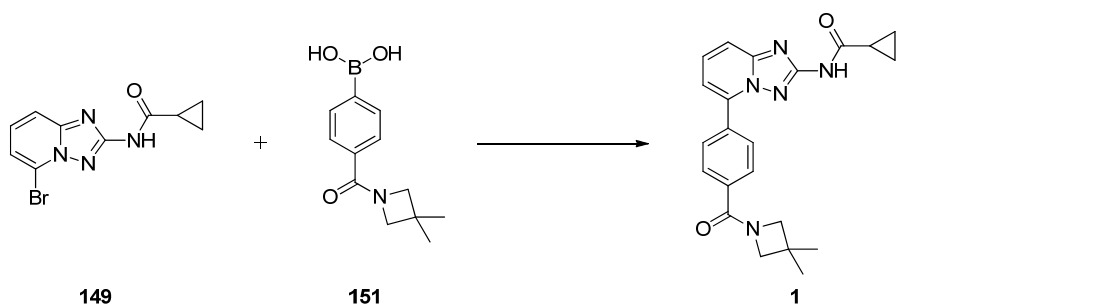


Figure 31: HPLC response of 1 and 162 in the DoE screen.

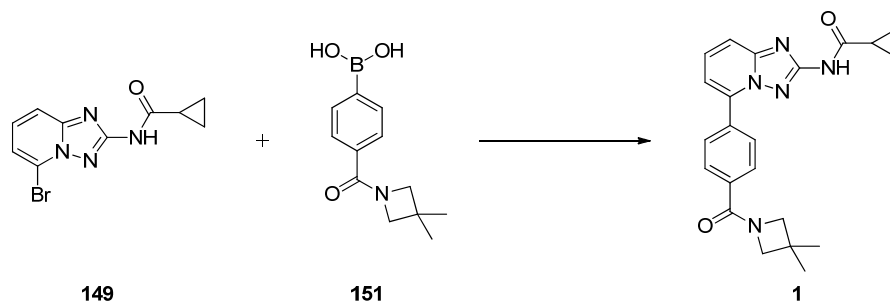
Understanding the effects of the parameters studied on the solution yields of the Suzuki-Miyaura coupling partners and the desired product **1** enabled new reaction conditions to be proposed. There were 2 sets of reaction conditions proposed from the DoE screen (B and C) and these are shown in Table 20 with the original reaction conditions (A).

Table 20: Original reaction conditions (A) and proposed reaction conditions (B and C) from DoE screen.^a

Parameter	Reaction Conditions		
	A	B	C
Mol% Triphenylphosphine	0.25	0.25	0.25
Equivalents of 151	1	1.05	1.10
% v/v Water	40	40	60
Equivalents of potassium bicarbonate	1	1.04	1.10

^a Conditions: **149** (1 eq), palladium(II) acetate (0.25 mol%), *n*-butanol, reflux.

The screen had shown the variable with the largest effect on the consumption of starting materials and formation of the desired product was the equivalents of ligand relative to catalyst, so this parameter was set at its lowest value when proposing new reaction conditions ‘B’ and ‘C’. It was also shown that the remaining parameters maximised the formation of product when set at their highest value. To run the Suzuki-Miyaura coupling with the higher equivalents of potassium bicarbonate and the higher % v/v water, could give rise to higher quantities of hydrolysis impurities, which needed to be avoided. Also, running the Suzuki-Miyaura coupling with a higher excess of the boronic acid **151** would increase the cost of the final API. With all of these parameters, there was significant curvature. Although this could be modelled with further experiments, due to time constraints, it was decided to directly test reaction conditions ‘B’ and ‘C’, where ‘B’ contained the remaining parameters at their centrepoint values and ‘C’ contained the remaining parameters at their upper ranges. A comparison of the HPLC reaction profiles for reactions ‘A’, ‘B’ and ‘C’ is shown in Table 21.

Table 21: Comparison of reaction conditions 'A', 'B' and 'C'.

Reaction Conditions	Time h	Aryl Bromide 149 % PAR ^d	Boronic Acid 151 % PAR ^d	Hydrolysis Impurity 157 % PAR ^d	Product 1 % PAR ^d
A ^a	21	2.3	0.2	0.7	96.0
B ^b	2.5	2.8	1.9	0.2	94.6
C ^c	2.5	ND	2.6	0.4	96.5

^a Conditions: **149** (1 eq), **151** (1 eq), KHCO₃ (1 eq), palladium(II) acetate (0.25 mol%), PPh₃ (0.25 mol%), 40% v/v aqueous *n*-butanol (16 vol), reflux;^b Conditions: **149** (1 eq), **151** (1.05 eq), KHCO₃ (1.04 eq), palladium(II) acetate (0.25 mol%), PPh₃ (0.25 mol%), 40% v/v aqueous *n*-butanol (16 vol), reflux;^c Conditions: **149** (1 eq), **151** (1.10 eq), KHCO₃ (1.10 eq), palladium(II) acetate (0.25 mol%), PPh₃ (0.25 mol%), 60% v/v aqueous *n*-butanol (16 vol), reflux;^d determined by HPLC (Method A).

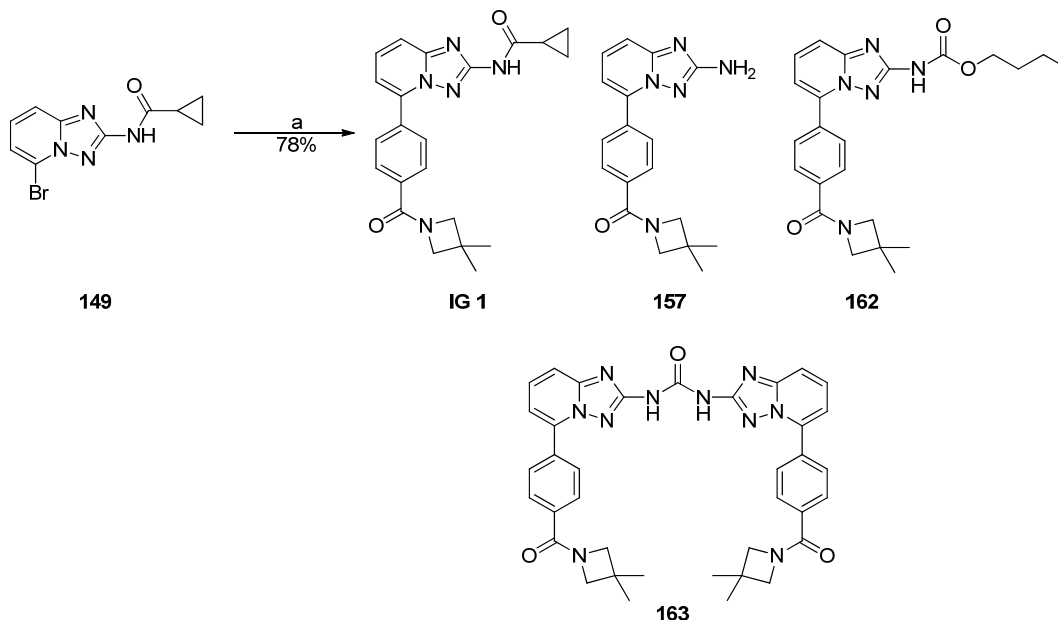
Comparison of the HPLC reaction profiles in Table 21 shows the rate of the Suzuki-Miyaura coupling reaction has increased when using reaction conditions 'B' and 'C'. In order for the reaction to be considered complete, it was decided that aryl bromide **149** should be under 3% by HPLC, as it was known that this quantity of **149** would be purged to acceptable levels after work-up. Using reaction conditions 'A', this could only be achieved after an overnight hold at reflux, but using reaction conditions 'B' and 'C' this was achieved after 2.5 hours. The difference in the HPLC profiles for 'B' and 'C' was small, but there appeared to be no advantage to using higher equivalents of potassium bicarbonate and boronic acid **151**. It was decided to use reaction conditions 'B' for the pilot plant scale up of the Suzuki-Miyaura coupling, as using reduced quantities of **151** and potassium bicarbonate would reduce the overall cost of API **1**. Later experiments carried out using reaction conditions 'B' showed the aryl bromide **149** was reduced further if the reaction time was extended to 4 hours with no significant changes in purity of the product **1**.

2.2.10 Optimisation of Reaction Work-up to Control Impurities

The DoE screen had shown the late running impurities **162** and **163** had not formed during the reaction. Impurity **164** was shown to form in the DoE reaction mixtures initially, but this decreased over time. Since the reaction conditions did not give rise

to the formation of these late running impurities, the work-up was investigated in order to determine at which point the impurities were formed. Table 22 shows a summary of HPLC analysis carried out during the work-up of the reaction mixture.

Table 22: HPLC analysis carried out during work-up.^a



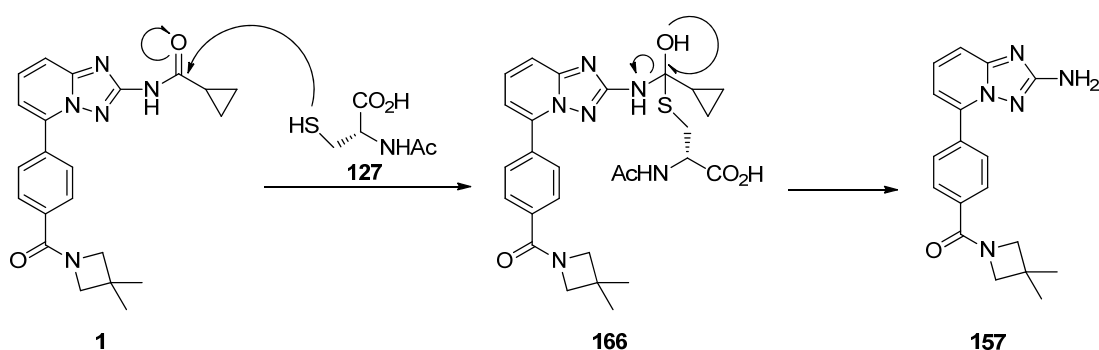
Step	157 % PAR ^b	162 % PAR ^b	163 % PAR ^b
End of reaction	0.23	0.09	-
After <i>N</i> -acetyl- <i>L</i> -cysteine wash	3.54	-	-
After holding filtered organic phase overnight at reflux	4.01	-	0.06
Isolated Solid	0.31	-	0.09

^a Conditions: (a) **149** (1 eq), **151** (1.05 eq), KHCO₃ (1.04 eq), n-butanol (9.6 vol), water (6.4 vol), palladium(II) acetate (0.25 mol%), PPh₃ (0.25 mol%); ^b determined by HPLC (Method C).

Although **162** was shown to decrease during the work-up, it was not present in the isolated solid. Table 22 shows the level of impurity **163** increases significantly when the organic phase obtained at the end of the aqueous work-up is heated overnight at reflux (93-94 °C). In this experiment, the organic phase was held at reflux overnight, in order to mimic the effect of scaling up the distillation. Distillation times increase on scale-up and the prolonged hold at high temperature can cause impurities to form. In this case, the atmospheric distillation would require the temperature of the contents to reach 116-118 °C for a prolonged period. As holding the organic phase at 93-94 °C had shown an increase in impurity **163**, it was proposed to carry out the distillation under vacuum in order to lower the temperature of the organic phase.

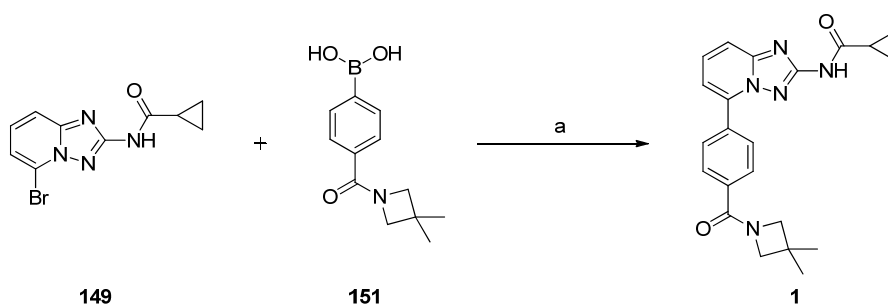
After exchanging the atmospheric distillation for a vacuum distillation in the Stage 3 process, all batches of IG **1** were isolated without impurity **163** present.

Project specific HPLC analysis before and after the *N*-acetyl-*L*-cysteine wash showed an increase of impurity **157** from 0.2% to 3.5%, demonstrating hydrolysis could be catalysed by *N*-acetyl-*L*-cysteine **127** in the biphasic mixture. There are 2 possible mechanisms for the hydrolysis of the amide bond by *N*-acetyl-*L*-cysteine **127**. Firstly, there is a carboxylic acid present in *N*-acetyl-*L*-cysteine **127**, which could provide protons which catalyse the hydrolysis of the cyclopropylamide. Secondly, the thiol in *N*-acetyl-*L*-cysteine **127** could act as a nucleophile which could lead to hydrolysis of the amide bond (Scheme 54).



Scheme 54: Proposed mechanism for the formation of 157.

The *N*-acetyl-*L*-cysteine wash and subsequent phase separation was carried out at 90 °C. It was postulated, the *N*-acetyl-*L*-cysteine wash could cause less hydrolysis to **157**, if it was carried out at a lower temperature. A lower temperature of 60 °C was investigated as carrying out the phase separations at this temperature in the pilot plant would make the process safer to operate. HPLC analysis before and after the overnight *N*-acetyl-*L*-cysteine wash at 60 °C showed **157** increased from 0.09% to 0.32%. After isolation, IG **1** contained 0.09% **157**, a substantially more acceptable result than observed previously.

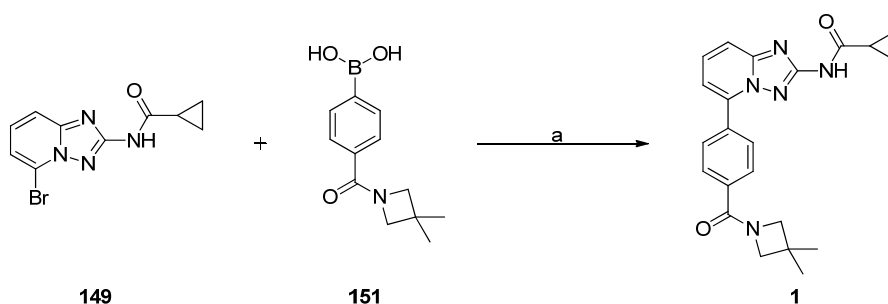


Conditions: a) **149** (1 eq), **151** (1.05 eq), KHCO_3 (1.04 eq), *n*-butanol (9.6 vol), water (6.4 vol), palladium(II) acetate (0.25 mol%), PPh_3 (0.25 mol%)

Scheme 55: Optimised reaction conditions for Stage 3.

Although carrying out the *N*-acetyl-*L*-cysteine wash at 60 °C instead of 90 °C had shown a significant reduction in hydrolysed impurity **157**, the product isolated subsequently contained 70-90 ppm Pd. Increasing the temperature of the *N*-acetyl-*L*-cysteine wash to 70 °C, enabled **1** to be isolated containing 8 ppm Pd and 0.18% **157**, as outlined in Scheme 56.

The yield of the final stage Suzuki-Miyaura coupling was typically 74-78%. Investigations into sources of yield loss, showed the desired product may have been held up on the Celite pad which the organic phase was filtered through to remove palladium black particles prior to isolation. Doubling the volume of *n*-butanol used to wash the Celite pad was shown to increase the yield to 85-89%, but inductively coupled plasma-atomic emission spectroscopy (ICP-AES) analysis of the isolated product revealed 25 ppm Pd. If the desired product **1** was allowed to crystallise out of solution after the reaction was complete, subsequent *N*-acetyl-*L*-cysteine treatment was not as effective with isolated IG **1** containing 46 ppm Pd. In an experiment, where both the product was allowed to crystallise out before the *N*-acetyl-*L*-cysteine treatment was carried out and the Celite pad was washed with an increased amount of *n*-butanol, the isolated solid contained 86 ppm Pd. These observations highlighted the Stage 3 process which was about to be run in the pilot plant delivered IG **1** containing variable levels of palladium. The Stage 4 recrystallisation of IG **1** was shown to purge all the levels of palladium observed in IG **1**, enabling API **1** to meet the clinical specification of <10 ppm Pd, giving the project team confidence in the finalised Stage 3 process (Scheme 56).



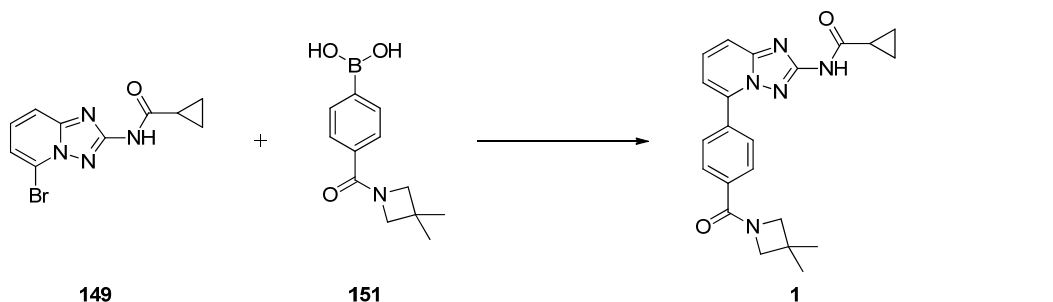
Conditions: a) i. **149** (1 eq), **151** (1.05 eq), KHCO_3 (1.04 eq), *n*-butanol (9.6 vol), water (6.4 vol), palladium(II) acetate (0.25 mol%), PPh_3 (0.25 mol%), reflux, 4 hours ii. *N*-acetyl-*L*-cysteine **127** (0.1 eq), water (6.4 vol), 70 °C, 13-21 hours, iii. Water (6.4 vol), 70 °C, 1 hour; followed by filtration through Celite, vacuum distillation and collection of IG **1** by filtration.

Scheme 56: Finalised reaction and work-up conditions for the pilot plant preparation of IG 1.

2.2.11 Transfer of Route B Suzuki-Miyaura Coupling to Pilot Plant

After these investigations, confidence in the Route B Suzuki-Miyaura coupling was established and the process was transferred to the pilot plant facility, where a total of five batches of IG **1** would be produced. The knowledge of the Suzuki-Miyaura process was transferred to the pilot plant team using a document known as the ‘Working Directions’ (see Appendix 6.2.1, page 174). Using this document, a process chemist and process engineer author the batch record, which is used by the technicians carry out the reaction and isolate the product in the pilot plant facility.

A phased delivery of 3,3-dimethylazetidine hydrochloride, meant two batches of **1** would be prepared using an input of around 26 Kg **149**, and approximately four weeks later, three larger batches of **1** would be prepared, using an input of around 46 Kg **149**. Table 23 shows the yield and purity of the first batch prepared in the pilot plant.

Table 23: Pilot Plant Batch Data for Batch 1 of IG 1. ^a

Batch	Input of 149	Yield	Pd (ppm) ^b	1% PAR ^c	157% PAR ^c
1	26.4 Kg	85.0%	60-130	99.8	0.12

^a Conditions: **149** (1 eq), **151** (1.05 eq), KHCO₃ (1.04 eq), n-butanol (9.6 vol), water (6.4 vol), palladium(II) acetate (0.25 mol%), PPh₃ (0.25 mol%), reflux, 4 hours; ^b determined by ICP-AES; ^c determined by HPLC (Method C).

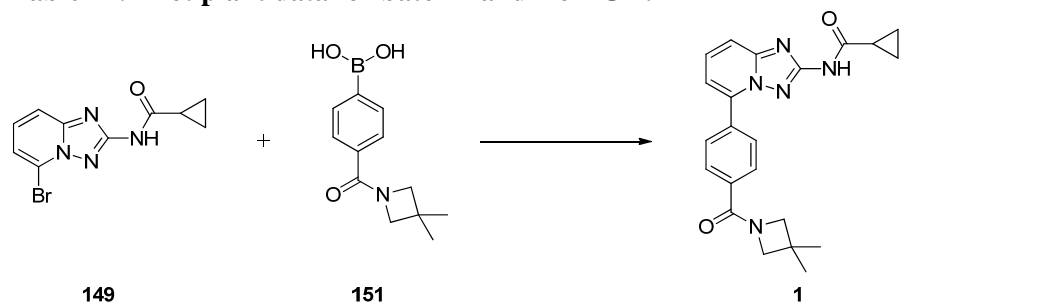
The yield and HPLC purity obtained for the first batch was consistent with yields and purities observed in the laboratory. The palladium level in the first batch was not consistent with levels in IG **1** which had been isolated in the laboratory. IG **1** from the first pilot plant batch was heterogeneous and contained orange lumps. ICP-AES analysis of the isolated solid was repeated and this showed variation from 60 ppm Pd to 130 ppm Pd. The variation of the palladium levels was caused by the heterogeneous nature of isolated **1**. ICP-AES analysis of the first batch showed **1** was contaminated with calcium as well as palladium. Further ICP-AES analysis of all the starting materials and reagents showed no calcium was present, so Celite was thought to be the most likely source of the calcium contamination.

Pilot plant batch 1 of **1** was recrystallised in the laboratory using the Stage 4 process and API **1** was obtained with <10 ppm Pd. Although this result gave the team confidence the Stage 4 process could tolerate an higher level of Pd in IG **1**, it was decided the Stage 3 pilot plant process should be changed in order to prepare IG **1** with lower palladium content.

Previous laboratory experiments had shown variable amounts of palladium in IG **1** (Section 2.2.10). Two laboratory experiments had been carried out where the filtration through Celite was exchanged for a filtration through a Cuno R55S cartridge. Both these experiments had yielded IG **1**, which was a homogeneous solid containing under 10 ppm Pd. For the second pilot plant batch of IG **1** the filtration through the Cuno R55S cartridge was used instead of the Celite filtration in order to

reduce the risk of API **1** not meeting the specification for palladium. Scaling up the Cuno process in the second batch using a 26.8 Kg input of **149** gave IG **1**, which was isolated as a white homogeneous solid containing 4 ppm Pd (Table 24).

Table 24: Pilot plant data for batch 1 and 2 of IG 1.^a



Batch	Input of 149	Yield	Pd (ppm) ^b	1% PAR ^c	157% PAR ^c
1	26.4 Kg	85.0%	60-130	99.8	0.12
2	26.8 Kg	86.3%	4	99.8	0.12

^a Conditions: (a) **149** (1 eq), **151** (1.05 eq), KHCO₃ (1.04 eq), *n*-butanol (9.6 vol), water (6.4 vol), palladium(II) acetate (0.25 mol%), PPh₃ (0.25 mol%), reflux, 4 hours; ^b determined by ICP-AES; ^c determined by HPLC (Method C).

In the laboratory it had been difficult to determine the benefit given to the process by carrying out the Cuno filtration, as ICP-AES analysis before and after the Cuno filtration had shown the reduction of palladium in solution was negligible. During the pilot plant preparation of batch 2, 1 L samples were taken of the organic phase pre and post Cuno filtration. On receiving these samples in the laboratory after they had been allowed to cool slightly, it could be observed there was a small quantity of aqueous phase at the bottom of both samples. Table 25 shows the concentration in solution of various elements determined by ICP-AES analysis.

Table 25: ICP-AES analysis of solutions pre and post Cuno filtration in batch 2.^a

	B	Ca	K	Pd
Organic Phase Pre Cuno	767	3	107	37
Organic Phase Post Cuno	287	2	11	30
Aqueous Phase Pre Cuno	1491	2	2206	140
Aqueous Phase Post Cuno	625	2	296	41

^a Elemental content (ppm) by ICP-AES.

ICP-AES analysis showed a negligible difference in palladium content between the organic phase pre and post Cuno filtration, which was consistent with data generated in the laboratory. Interestingly, ICP-AES analysis of the aqueous phase pre and post Cuno filtration showed a significant difference in the level of palladium. This

showed there was a clear benefit of the Cuno filtration, where the activated carbon was responsible for lowering palladium levels as well as removing palladium black particles. The ICP-AES analysis also showed there was water soluble palladium present prior to the filtration and suggested more water washes may be necessary, particularly if a Celite filtration was to be reinvestigated at a later date.

Table 25 also shows during the production of the second pilot plant batch of IG 1, calcium was not detected in the ICP-AES analysis pre and post Cuno filtration, so the source of the calcium contamination in the first pilot plant batch of IG 1 had not been identified. After the pilot plant campaign, laboratory experiments were carried out to determine if calcium had been leached into the organic phase from the Celite used to remove palladium black particles. Firstly, stirring Celite in fresh aqueous *n*-butanol at 70 °C was investigated and this showed by ICP-AES analysis of the supernatant liquid showed calcium was not present. In a second experiment, the organic phase obtained after the aqueous work-up was stirred with Celite at 70-80 °C and after 90 minutes, ICP-AES analysis showed ~200 ppm calcium was present in the organic phase. Therefore it is not appropriate to filter the organic phase through Celite on scale, as the time elapsed between filtering the organic phase and washing the Celite pad with *n*-butanol enables leaching of calcium from the Celite bed, which contaminates the batch of IG 1. During the pilot plant preparation of IG 1, the Celite bed had been in contact with a portion of the organic phase for around 90 minutes between the filtration of the organic phase and the filtration of the *n*-butanol wash, so it is expected the calcium contamination of pilot plant batch 1 occurred at this point in the process.

Recrystallising pilot plant batches 1 and 2 of IG 1 (Stage 4) in the laboratory showed API 1 obtained contained under 10 ppm Pd and all individual impurities by HPLC were under 0.06%. A decision was taken to mix the first two batches of IG 1 and submit these to two Stage 4 recrystalliations in pilot plant. The output of the first batch of API 1, was a heterogeneous solid, with bands of orange material observed in the white filter cake as shown in Figure 32.



Figure 32: Filter cake of API 1 obtained in pilot plant.

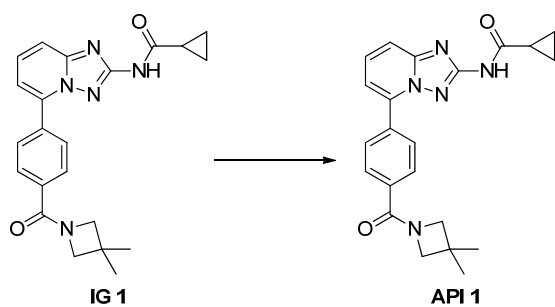
The heterogeneous nature of the filter cake makes this batch of API grade **1** unsuitable for micronisation and formulation. ICP-AES analysis of the bulk of the cake showed 25 ppm Ca and 38 ppm Pd, whereas ICP-AES analysis of the orange particles from the top of the cake showed 97 ppm Ca and 157 ppm Pd. Comparison of HPLC analysis of the solids from the top of the cake and the bulk of the cake, showed no significant difference in impurity profile, indicating the orange colour was probably originating from a palladium species.

The remainder of the second batch of IG **1** containing 4 ppm Pd was successfully recrystallised *via* the Stage 4 process in the pilot plant, which suggested the failure of the first API recrystallisation was attributed to the high level of palladium in the first IG **1** batch. In the laboratory user tests of pilot plant IG **1**, the solution of **1** in 4:1 IMS/water was clarified through a polypropylene filter cartridge, which was shown to remove some colour from the solution. The clarification in the pilot plant was carried out using a different filter and no failure of the filter cartridge was observed. A brown solid was observed to have deposited on the outside of the filter cartridge and microscopy revealed the brown solid was an oil rather than crystalline. The filter cartridges used in plant are designed to remove solid particulates, in order to prevent contamination in API batches and for this project it was assumed the palladium species present in IG batches of **1** were discrete particles, making their removal in the

clarification in the Stage 4 process predictable on scale-up. Discovering the palladium species remaining in the IG batches was an oil meant the likely cause of failure had been identified, as the filter cartridges used in plant were not designed to remove this type of material. An experiment was carried out in the laboratory, which reproduced the pilot plant Stage 4 process and showed the orange material was not produced. However, carrying out the Stage 4 recrystallisation without a clarification produced orange solids in the isolated API grade **1**. This demonstrated scaling up the clarification was not predictable.

Understanding palladium was the main contaminant in the coloured material obtained in the API batch enabled a purification process to be developed. The likely source of the palladium contamination was from the first IG batch which had been filtered through Celite. Cuno filtration had enabled the second IG batch to be prepared with low palladium content (4 ppm) and the second IG batch was successfully recrystallised *via* Stage 4 in the pilot plant. For these reasons, a process was developed where the failed API batch and the remainder of the first IG batch were dissolved in aqueous *n*-butanol and was passed through a Cuno cartridge. The filtrate obtained was azeotropically dried under vacuum to enable **1** to be isolated by filtration. In the laboratory this process was demonstrated to give **1** containing <1 ppm Pd in 95% yield. The process was scaled up successfully in the pilot plant giving similar results to the laboratory experiment. The reworked batch was successfully recrystallised in the Stage 4 process.

Table 26: Batch data for pilot plant batches of API 1.^a



Batch of API 1	Input of IG 1	Yield	Pd (ppm)% PAR ^b	1% PAR ^c
1	16.95 Kg	82.1%	<1	100.0
2	35.00 Kg	83.9%	ND	99.9

^a Conditions: 4:1 IMS/Water; ^b determined by ICP-AES; ^c determined by HPLC (Method C).

With the first 2 batches of API grade **1** successfully prepared, the preparation of the remaining 3 IG batches of **1** was carried out in Stevenage pilot plant using a Cuno filtration. Table 27 shows the pilot plant batch data for the later batches of IG **1** prepared.

Table 27: Batch data for pilot plant batches 3-5.^a

Batch	Input of 149	Yield	Pd (ppm) ^b	1% PAR ^c	157% PAR ^c
3	46.7 Kg	73.7%	1	99.87	0.13
4	45.7 Kg	92.0%	2	99.84	0.16
5	46.5 Kg	64.2%	2	99.83	0.15
Heel		27.2%	2	99.84	0.14
Average Yield from Schenk		85.6%			

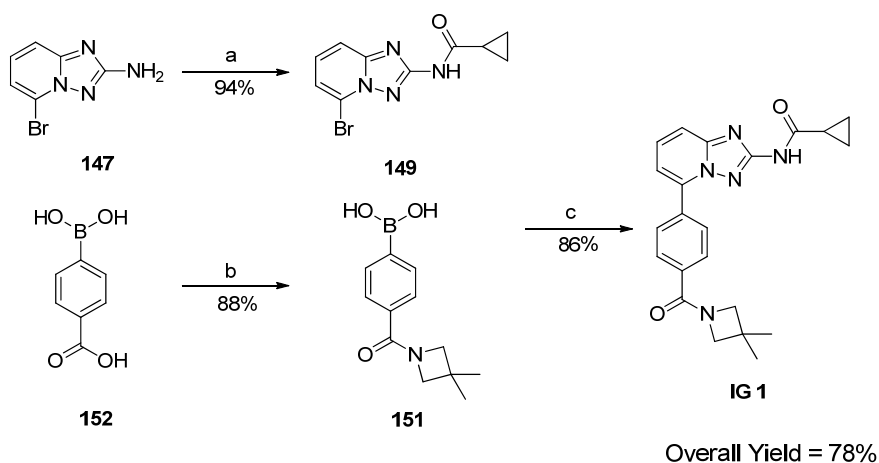
^a Conditions: a) **149** (1 eq), **151** (1.05 eq), KHCO₃ (1.04 eq), *n*-butanol (9.6 vol), water (6.4 vol), palladium(II) acetate (0.25 mol%), PPh₃ (0.25 mol%); ^b determined by ICP-AES; ^c determined by HPLC (Method C).

ICP-AES and HPLC analysis showed the IG batches of **1** were of the required quality for Stage 4. There was variation in the yield, which was due to the Schenk oven used for filtration and drying of the batches. The Schenk oven was used for the later three batches, due to their larger size compared with the first two batches. A large amount of the dried product can be held up in the Schenk after removing the majority of the batch. The held up material is referred to as the ‘heel’ and it is left in place and recovered in the following batch. At the end of processing the stage, the ‘heel’ remaining in the Schenk is recovered using an antisolvent of the product to generate a suspension which is filtered in a pan filter and dried in a separate oven. The average yield is calculated by taking the sum of all the output material (IG **1**) and dividing by the total input of aryl bromide **149**. The average yield from the Schenk for the three batches is similar to the yield obtained for the smaller two batches isolated from the pan filter. Overall using the Cuno filtration in the final stage Route B Suzuki-Miyaura coupling gave consistent yields and product quality.

2.3 Conclusions

A new route has been demonstrated to give IG **1** using processes which have been scaled up in our pilot plant facilities (Scheme 57). Boronic acid **152** was activated with CDI in 2-methyltetrahydrofuran, followed by addition of 3,3-dimethylazetidinium hydrochloride to prepare **151** in 88% yield using a 35 Kg input of **152**. The final stage Suzuki-Miyaura coupling conditions were optimised in order to prepare API **1** with all organic impurities below 0.06%. Introduction of *N*-acetyl-*L*-cysteine **127** in the aqueous work-up, followed by Cuno filtration enabled IG **1** to be isolated with palladium content under 10 ppm.

The final stage Suzuki-Miyaura coupling was carried out on 45 Kg scale to prepare 3 batches of IG **1** in consistent yield (86%) and quality (Table 27). The overall yield of IG **1** from Route B was 78%, which was a significant improvement from Route A where the overall yield is 60%.



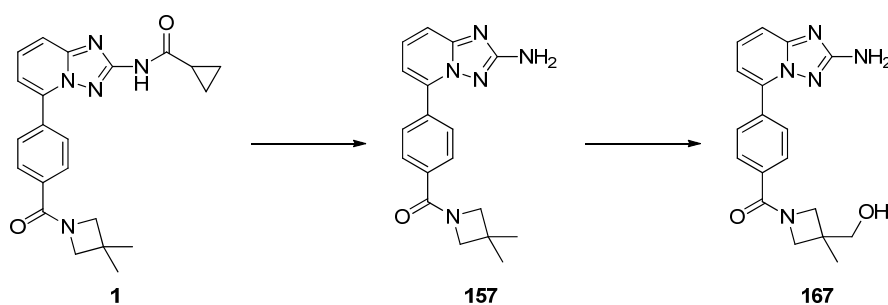
Conditions: Stage 1 a) i. Cyclopropylcarbonyl chloride, NEt_3 , acetone; ii) 7N NH_3 in MeOH (94%); Stage 2 b) i. CDI, DMSO, 2-methyltetrahydrofuran; ii. 3,3-dimethylazetidinium hydrochloride (88%); Stage 3 c) i. KHCO_3 , *n*-butanol, water, palladium(II) acetate, PPh_3 ; ii. *N*-acetyl-*L*-cysteine **127** (86%).
Scheme 57: Route B to IG 1.

The improvement in overall yield by exchanging linear Route A for convergent Route B gives a reduction in the cost of drug substance **1** from £4850/Kg to £3870/Kg. The reduction in the cost of drug substance will bring savings during the drug development process and ultimately to the patient, once the drug is approved.

3 Synthesis of Metabolites

3.1 Introduction

Metabolism of drug substances is an important area to be investigated during the development of a medicine. Drug substances undergo metabolism in the body to enable elimination and this is usually by forming a more polar product than the parent drug substance to allow the metabolite to be excreted. Drug substance **1** is hydrolysed in humans to give the primary metabolite **157** and the commercially available cyclopropane carboxylic acid **158** (Scheme 58). Metabolite **157** undergoes hydroxylation to give secondary metabolite **167**.



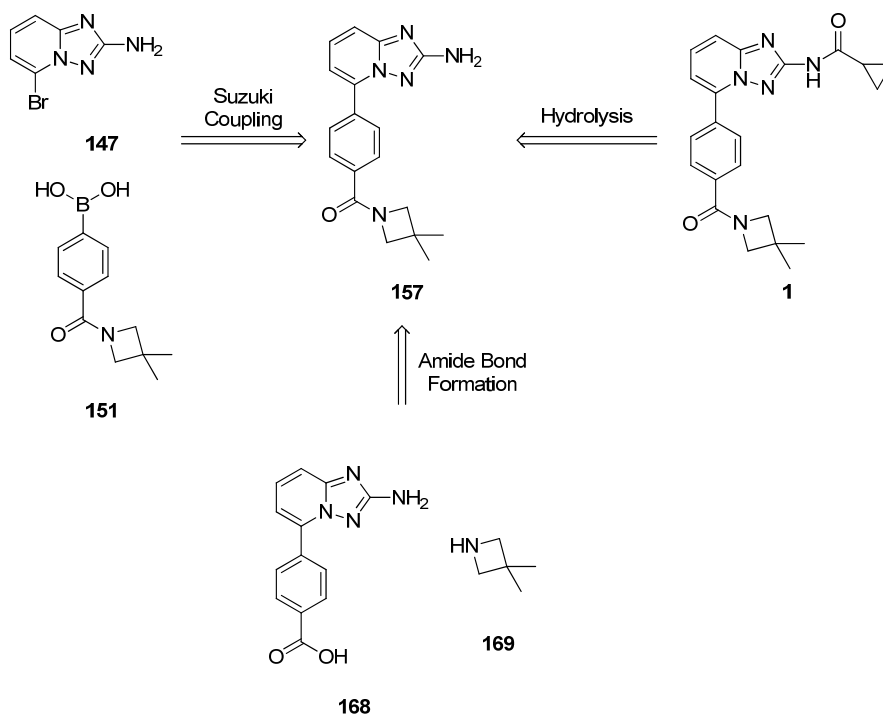
Scheme 58: Metabolism of drug substance 1 to give metabolites 157 and 167.

During the development of drug substance **1** into a medicine, it became necessary to synthesise metabolites **157** and **167** for safety testing and for use as analytical markers. Study of metabolites is required to quantify the rate of metabolism of the parent drug substance in the body. It is also important to investigate the toxicity of any metabolite in humans as this will impact the safety of dosing the parent drug substance.

3.2 Synthesis of Metabolite 157

3.2.1 Retrosynthetic Analysis of 157

There are several potential synthetic pathways for the synthesis of metabolite **157** and these are summarised in Scheme 59.

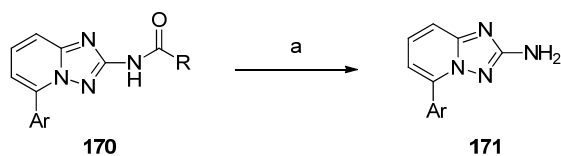


Scheme 59: Retrosynthetic analysis of **157**.

Choice of synthetic strategy is dependent on the use of the desired compound. As the initial use of **157** was for an Ames test¹, the synthetic route must enable high purity, as previous experience within our laboratories had shown low levels of impurities could cause false positive results. Preparation of metabolite **157** by a final stage Suzuki-Miyaura coupling was disfavoured as it would require purification to remove palladium. Another strategy for the synthesis of **157** was to form an amide bond from carboxylic acid **168** and azetidine **169**. This synthesis could potentially involve extra protection/deprotection steps to prevent the carboxylic acid in **168** self-condensing with the aniline nitrogen. Hydrolysis of drug substance **1** could potentially provide the desired product in a single step and in high purity. This route was particularly attractive, because **1** was available in gram quantities of high purity from the pilot plant synthesis.

Hydrolysis of compounds similar to **1** had been reported previously (Scheme 60).^{122,123} These compounds contain a single amide bond and hydrolysis takes place under acidic aqueous conditions.

¹ An Ames test is a biological assay which is used to determine the potential for a compound to be mutagenic



where R = cyclopropyl, or Me

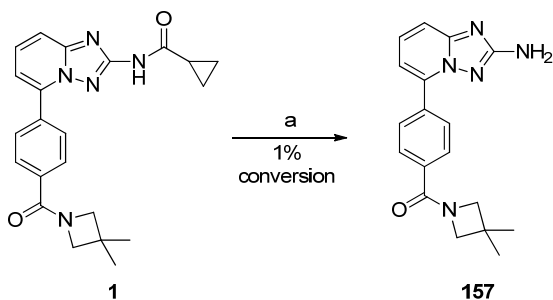
Conditions: a) HCl, aqueous 1,4-dioxane, rt-110 °C, 2-18 hours.

Scheme 60: Hydrolysis of compounds similar to 1.

Based on this precedent, we elected to examine the preparation of **157** through hydrolysis of **1**.

3.2.2 Synthesis of 157

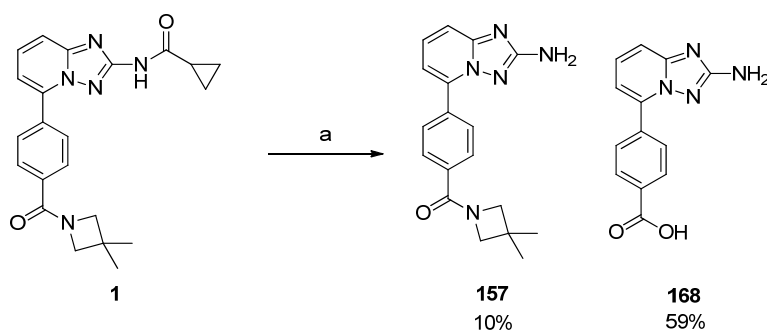
As hydrolysis of amide bonds will occur under acidic and basic aqueous conditions, both methods were investigated in parallel. Under basic aqueous conditions, 1% conversion to the desired metabolite **157** was observed after overnight reaction at 50 °C (Scheme 61).



Conditions: (a) 50% w/w aqueous KOH (3 eq), THF, 50 °C, overnight.

Scheme 61: Hydrolysis of drug substance 1 to give 157.

A faster rate of reaction would be obtained by increasing the temperature of the reaction, so the higher boiling solvent 1,4-dioxane was examined. Increasing the temperature of the reaction to 90-95 °C, showed 69% conversion of drug substance, but the major product of the reaction was **168**, obtained by hydrolysis of both amide bonds (Scheme 62).

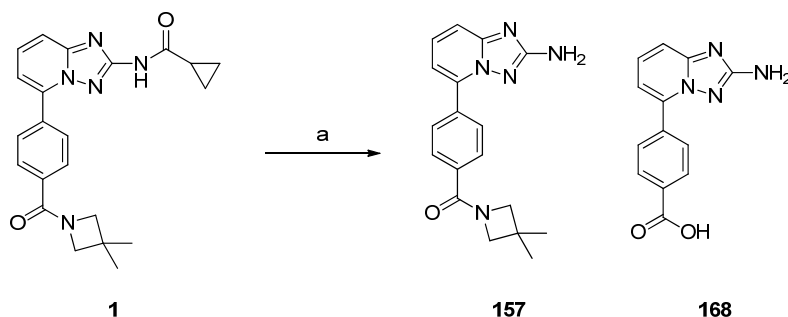


Conditions: (a) 50%w/w aqueous KOH (3 eq), 1,4-dioxane, water, 90-95 °C, 30 minutes.

Scheme 62: Hydrolysis of drug substance 1 to give 157 and 168.

Comparison of these two experiments showed hydrolysis of drug substance **1** to prepare **157** was possible, but in order to achieve a higher rate of reaction whilst maintaining selectivity, further investigation was required (Table 28). In addition to 1,4-dioxane, cyclopentyl methyl ether was examined, because of its high boiling point and similar properties to ethereal solvents. Sodium hydroxide and lithium hydroxide were examined in addition to potassium hydroxide to determine if varying the cation had a beneficial effect on the transformation.

Table 28: Investigation into basic hydrolysis of drug substance 1.^a



Entry	Solvent	Base	168% PAR^b	Metabolite 157% PAR^b	Drug Substance 1% PAR^b
1	CPME	KOH	8.5	9.0	81.8
2	CPME	NaOH	3.7	3.4	92.3
3	CPME	LiOH	13.3	7.6	75.0
4	1,4-Dioxane	KOH	45.3	22.7	7.9
5	1,4-Dioxane	NaOH	40.7	19.5	11.7
6	1,4-Dioxane	LiOH	3.3	3.8	91.1

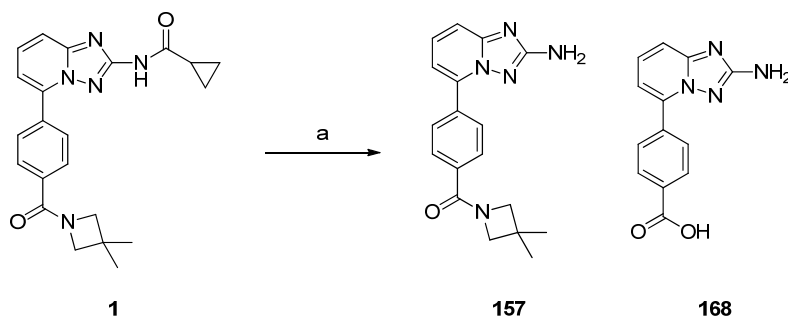
^a Conditions: 1:1 Solvent/water, base (2 eq), 45 °C, overnight; ^b determined by HPLC (Method B).

Table 28 shows hydrolysis of **1** occurred readily in 1,4-dioxane using either potassium hydroxide or sodium hydroxide (entries 4 and 5). In all reaction mixtures using CPME and lithium hydroxide/1,4-dioxane (entries 1, 2, 3 and 6), undissolved solids were observed, indicating the solubility of **1** was important to obtain

hydrolysis in a reasonable timeframe. Table 28 shows conversion to the desired product **157** could not be achieved in a reasonable time scale without significant formation of the bis-hydrolysis product **168**, so it was decided not to investigate the basic hydrolysis of drug substance **1** further.

Acid catalysed hydrolysis of **1** showed more promising results than basic conditions (Table 29).

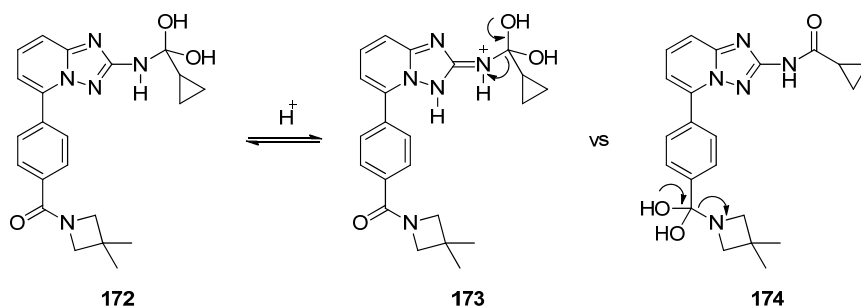
Table 29: Investigation into acidic hydrolysis of drug substance 1.^a



Entry	Acid	168 % PAR ^b	Metabolite 157 % PAR ^b	Drug Substance 1 % PAR ^b
1	2M HCl (aq)	4.7	48.0	38.5
2	Acetic Acid	-	-	99.9
3	1M H ₂ SO ₄ (aq)	0.6	28.0	69.8

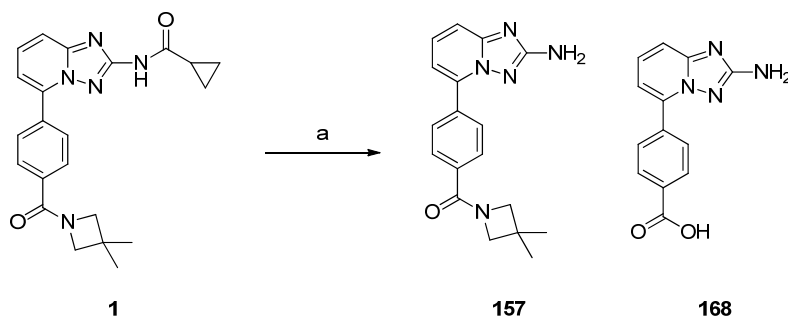
^aConditions: Tetrahydrofuran, Acid (1.2 eq), 53 °C, overnight; ^b determined by HPLC.

Using acetic acid (entry 2), hydrolysis of either amide bond did not occur. Using hydrochloric acid and sulfuric acid (entries 1 and 3) conversion to the desired product **157** was observed with significantly less bis-hydrolysed product **168** than was observed using basic reaction conditions (Table 28). The aniline is in close proximity to basic nitrogens which can be protonated under acidic conditions, enabling an intermediate such as **173** to form (Scheme 63). The aniline in **173** is a better leaving group than the azetidine in **174**, providing an explanation why the cyclopropylamide is hydrolysed more readily under acidic aqueous conditions.



Scheme 63: Alternative intermediates in the hydrolysis of 1.

Table 29 shows conversion to metabolite **157** was faster using hydrochloric acid (entry 1), but hydrolysis was less selective using the stronger acid. Using sulfuric acid (entry 3), the purity profile of the reaction mixture was cleaner, so sulfuric acid was chosen for scaling up the reaction.



Conditions: a) 1:1 THF/water, H₂SO₄ (2 eq), reflux, 64 h.

Scheme 64: Acid catalysed hydrolysis of 1 to give metabolite 157.

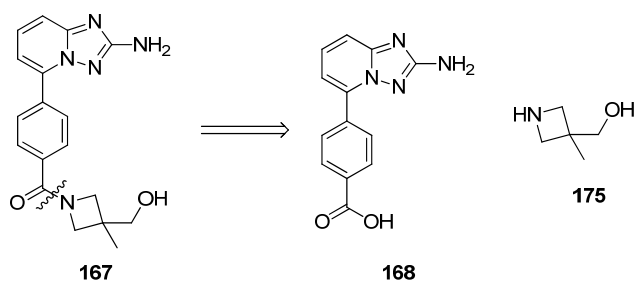
Complete conversion of drug substance **1** was observed when the reaction time was extended to 64 hours. Conversion to the bis-hydrolysed impurity **168** was observed (20% PAR) but this impurity precipitated on cooling of the reaction mixture, enabling removal of **168** by filtration. Neutralisation of the filtrate induced precipitation of the desired product **157** in 72% yield and 99.7% PAR purity, making **157** available for an Ames test.

3.3 Synthesis of Metabolite 167

3.3.1 Retrosynthetic Strategy for Metabolite 167

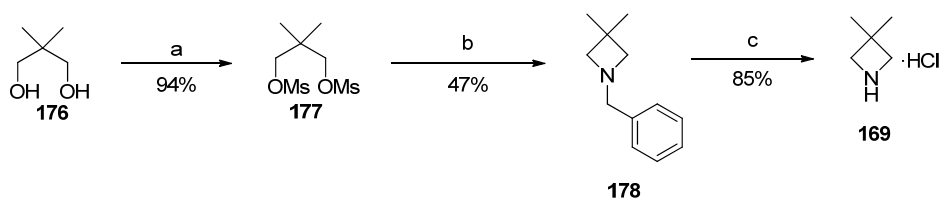
Metabolite **167** was required as an analytical marker to confirm the structure of the metabolite. The structure had been proposed by LC-MS data obtained during dosing to humans. 500 mg metabolite **167** was required with a minimum purity of 97% with no single impurity greater than 1%. The retrosynthetic analysis for metabolite **167**

focussed on forming the amide bond from carboxylic acid **168** and amine **175** (Scheme 65).



Scheme 65: Retrosynthetic analysis of metabolite 167.

A supply of **168** had been obtained during the synthesis of metabolite **157** (section 3.2.2). By contrast, however azetidine **175** was novel and required further retrosynthesis. As a starting point, the synthesis of azetidine **169**¹²⁴ (used to prepare drug substance **1**) was considered.

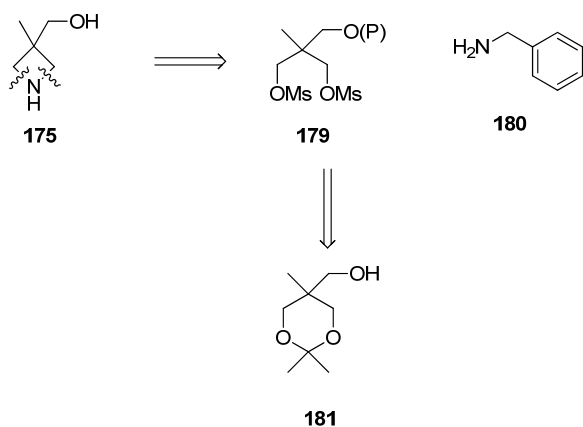


Conditions: a) Methanesulfonyl chloride (2.04 eq), triethylamine (2.09 eq), THF, 10 °C, 1 h; b) Benzylamine (6.1 eq), 33% aqueous NaOH (1.5 eq), 90 °C, 6–7 days; c) i. Pd-C, H₂, methanol, 55 °C, 10 h, ii. HCl (1.01 eq).

Scheme 66: Synthesis of azetidine 169.

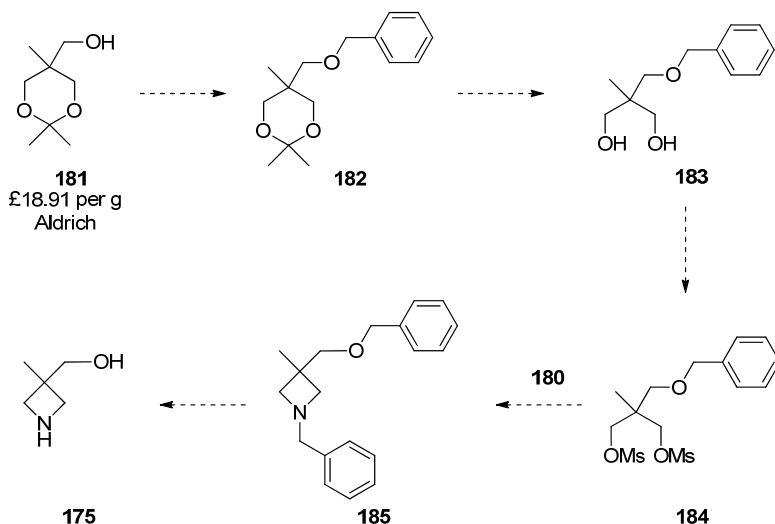
The two hydroxyl groups in **176** were activated as the bis-mesylate **177**. Displacement of both mesylates in **177** by one molecule of benzylamine gave the benzyl protected azetidine product **178**. The benzyl group in **178** was cleaved under hydrogenation conditions to give azetidine **169** as the hydrochloride salt in an overall yield of 37.5%.

Scheme 67 shows the disconnection required for **175** to be prepared adopting the same strategy used to be prepare azetidine **169**.



Scheme 67: Retrosynthetic strategy for azetidine 175.

The azetidine ring in **175** would be formed by displacement of the mesylates in **179** by benzylamine **180**. It was envisaged bis-mesylate **179** could be prepared easily from readily available **181**. The proposed synthesis of **175** from **181**, is shown in Scheme 68.

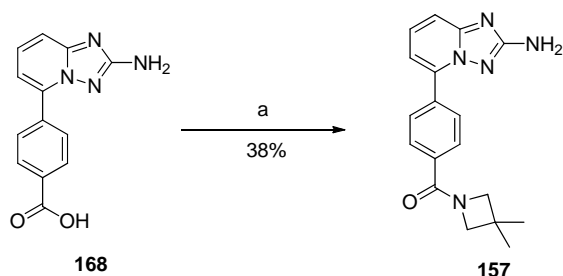


Scheme 68: Proposed synthesis of azetidine 175.

The primary alcohol in **181** would be protected by the formation of the benzyl ether **182**, which would undergo hydrolysis of the acetonide group to reveal diol **183**. The diol **183** would be activated using methanesulfonyl chloride to form bis-mesylate **184**. Addition of benzylamine to bis-mesylate **184** would enable access to the benzyl protected azetidine **185**. Hydrogenation of **185** would cleave both benzyl groups to give desired azetidine **175**.

3.3.2 Testing the Endgame strategy

With a stock of **168** available from the synthesis of **157**, a model reaction was carried out to test the final amide bond forming step in the synthesis. The model reaction would help to determine whether the aniline in **168** would react with the activated acid species, or form a urea with CDI.



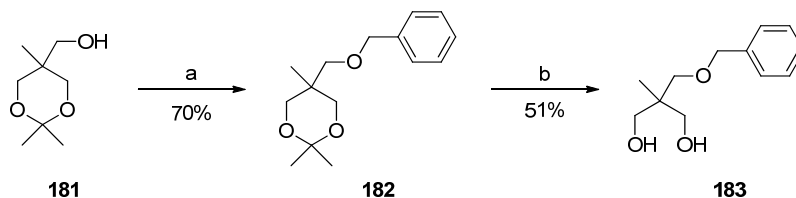
Conditions: a) i. CDI (2.4 eq), dichloromethane, DMSO, 20 °C, 4.5 h; ii. 3,3-dimethylazetidine hydrochloride (1.2 eq), 20 °C, overnight.

Scheme 69: Preparation of **157** from **168**.

Carrying out the above reaction gave the desired product **157** in 38% yield. The aniline in **168**, was shown not to react with the activated imidazolide or with CDI directly, so there would be no need for protection of the aniline.

3.3.3 Route 1 to Azetidine **175**

Reaction conditions for the first two steps in route 1 had been published (Scheme 70).¹²⁵ Repeating the literature conditions showed 63% conversion to product **182** after 90 minutes increasing to 79% conversion after 20 hours. It was also observed that some starting material **181** remained unreacted and benzyl chloride was converted to benzyl alcohol under the reaction conditions, so it was hypothesised the conversion to **182** could be improved either through addition of excess benzyl chloride or by using a more active alkylation agent.

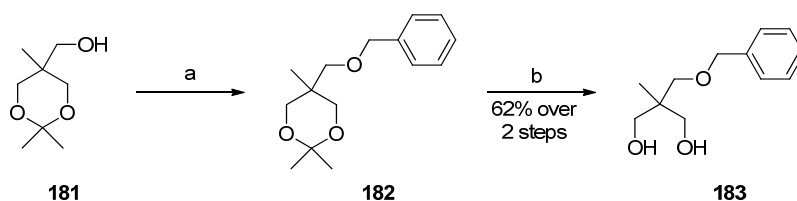


Conditions: a) NaOH (1.6 eq), Bu₄NHSO₄ (0.04 eq), benzyl chloride (1.15 eq), THF, reflux, 20 h; b) conc. HCl, methanol, reflux, 17 h.

Scheme 70: Preparation of **183** from **181**, using benzyl chloride to prepare **182**.¹²⁵

As benzyl bromide is a better electrophile than benzyl chloride, it was proposed this should give better conversion to the desired product. It was also proposed phase

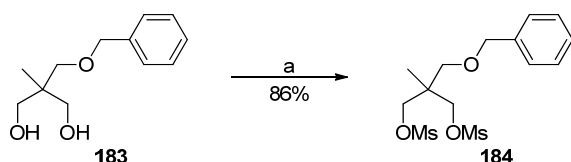
transfer conditions should also be beneficial for this transformation, as they could prevent conversion of the alkylating agent to benzyl alcohol. The rate of the desired alkylation reaction was improved significantly by the addition of 38% aqueous sodium hydroxide solution as demonstrated in a similar transformation by Darensbourg *et al.*¹²⁶ Use of concentrated sodium hydroxide solution enabled conversion to the desired product to increase to 96%. During the isolation of **182**, the acetonide group was observed to be partially removed to reveal the diol **183**. The conversion to diol **183** was completed by addition of aqueous hydrochloric acid to obtain the diol in 62% overall yield from dioxane **181**.



Conditions: a) BnBr (3.9 eq), TBAB (0.25 eq), 38% aqueous NaOH (7.0 eq), PhMe, reflux followed by 20 °C, 5 days; b) 2M HCl, methanol, 20 °C, 1 h.

Scheme 71: Preparation of 183, following formation of 182 under phase transfer conditions.

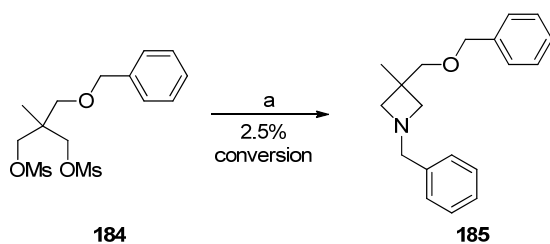
The diol **183** was doubly activated with methanesulfonyl chloride to give bis-mesylate **184** in quantitative yield (Scheme 72) using identical reaction conditions used to prepare the bis-mesylate **177** from 3,3-dimethylpropanediol **176**.



Conditions: a) NEt₃ (2.1 eq), MsCl (2.04 eq), THF, 0-10 °C, 30 minutes.

Scheme 72: Formation of bis-mesylate 184 from diol 183.

Preparation of the azetidine ring in **185** by addition of benzylamine to bis-mesylate **184** (Scheme 73) encountered several difficulties. The reaction appeared to be hampered by the formation of an insoluble solid which prevented good mixing.



Conditions: a) Benzylamine **180** (13.4 eq), 38% aqueous NaOH (1 eq), 90 °C, 3 days

Scheme 73: Preparation of 185 from bis-mesyate 184.

The desired product **185** was observed to have formed by LC-MS analysis, which showed **185** was present at a level of 2.5%. Figure 33 shows the structure of two significant impurities which were identified by LC-MS and ¹H NMR analysis.

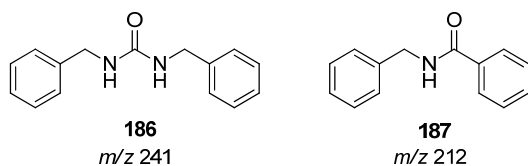
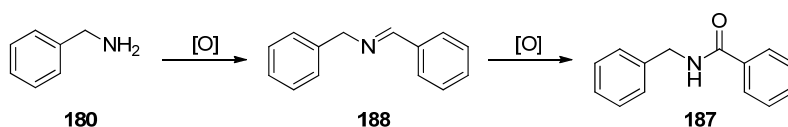


Figure 33: Impurities arising from benzylamine 180.

Symmetrical ureas such as impurity **186** have been shown to form under basic conditions in the presence of carbon dioxide.¹²⁷ Scheme 74 shows the proposed route of formation of impurity **187**.



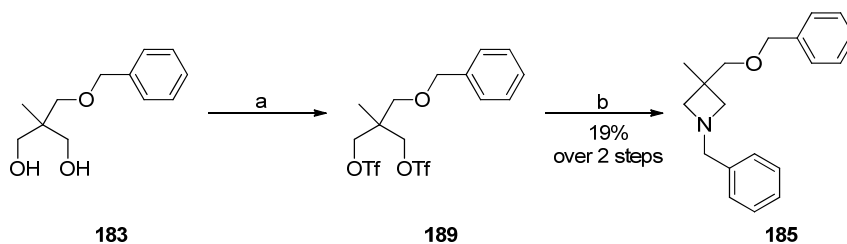
Scheme 74: Formation of 187.

Benzylamine can undergo oxidative homo-coupling to form the imine **188** when heated in water in the presence of oxygen.¹²⁸ It has also been shown imine **188** can be oxidised to form amide **187**.^{129,130}

Identification of impurities **186** and **187** had shown the presence of air in the reaction was likely to be detrimental to the progress of the desired transformation. Impurities **186** and **187** were minimised by vacuum/nitrogen purging of the flask prior to heating the reaction mixture. Once these impurities were controlled, HPLC analysis showed 15% conversion to the desired product **185** with two major impurities, one at a level of 45% and another at a level of 16%. The nature of these impurities could not be identified quickly using the standard methods available. As the desired

transformation to prepare **185** was proving difficult, it was therefore decided to examine alternative leaving groups to improve the reaction.

To circumvent this problem, the bis-triflate **189** was investigated instead of the bis-mesylate, as the triflate is a more activated electrophile compared with mesylate. The formation of the bis-triflate **189** followed by azetidine ring formation had been investigated in the literature by Hillier.¹³¹

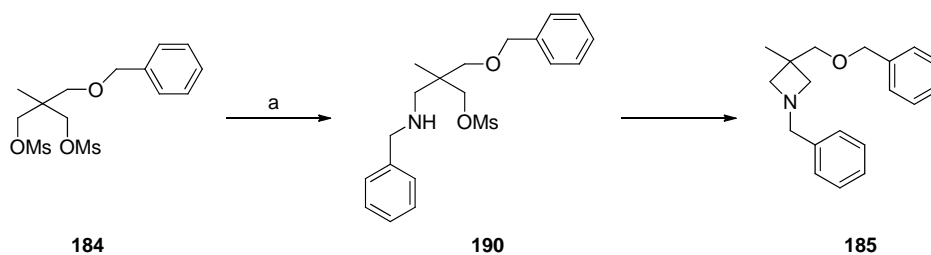


Conditions: a) Triflic anhydride (2.1 eq), DIPEA (2.5 eq), acetonitrile, -20 °C, 10 min; b) DIPEA (2.5 eq), benzylamine (0.95 eq), 70-75 °C, overnight.

Scheme 75: Preparation of 185 via bis-triflate 189.

These transformations were repeated in order to prepare azetidine **185** (Scheme 75). Analysis of the reaction mixture showed the desired product **185** had formed in addition to several impurities. Purification of the crude product by mass directed autopreparation (MDAP) showed the overall yield of these transformations was 19%. With this low yield, it had become clear using the reaction of benzylamine with a bis-electrophile to form an azetidine ring was potentially unviable for formation of sufficient quantities of metabolite **167** on time for the DMPK studies.

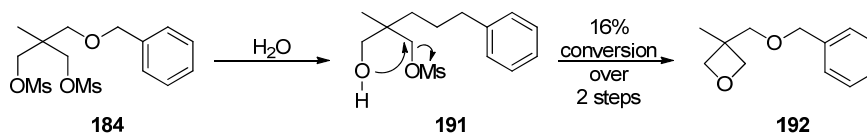
The bis-mesylate **184** and the bis-triflate **189** are both hindered electrophiles, as the neopentyl position of the leaving group makes nucleophilic substitution difficult. S_N2 reactions are slow at this position, because the steric bulk of the neopentyl group makes approach by the nucleophile difficult. Substitution via an S_N1 pathway is also not favoured because loss of leaving group would result in an unstable primary cation. Evidence for the neopentyl effect in the reactions carried out to form **185** from **184** or **189** is reinforced by the observation that an intermediate such as **190** is not observed during the reaction (Scheme 76). This suggests the difficulty in forming the azetidine may be due to the rate determining step being displacement of the electrophile by benzylamine, since **190** is not observed.



Conditions: a) Benzylamine (13.4 eq), 38% aqueous NaOH (1 eq), 90 °C, 3 days

Scheme 76: Proposed route of formation of 185 from 184.

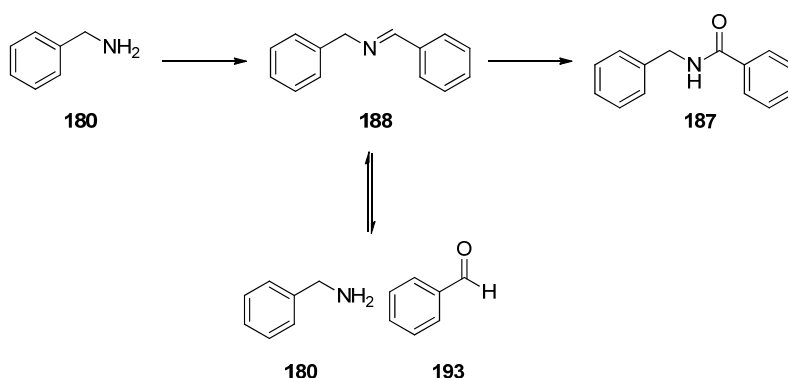
During the formation of **185** from benzylamine and bis-mesylate **184**, two major impurities were observed by HPLC. The first impurity at a level of 16% was later identified using high resolution mass spectrometry (HRMS), to be the oxetane impurity **192** (Scheme 77). The oxetane **192** could have been formed by displacement of a single mesylate in **184** by water, to give an alcohol **191** which could displace the remaining mesylate to form the oxetane **192**.



Scheme 77: Formation of oxetane impurity 192.

Using positive electrospray ionisation in the mass spectrometer makes identification of oxetane **192** difficult, as there are no suitable basic groups to be protonated during ionisation. Oxetane **192** could only be identified using a weak signal in the HRMS.

The second larger impurity at a level of 45% was later identified as benzaldehyde **193** by comparison of HPLC retention times with an authentic sample. Scheme 78 shows benzaldehyde **193** is formed from the hydrolysis of the imine **188**, which could have been formed by oxidative coupling of benzylamine.

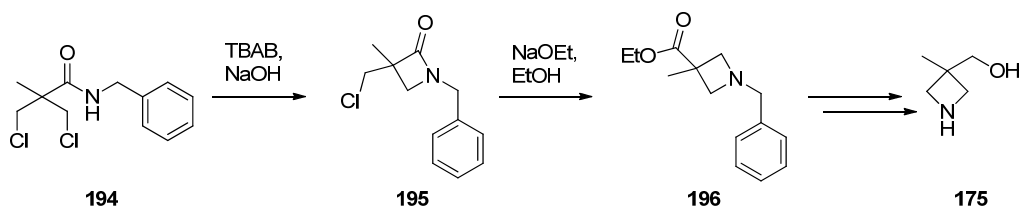


Scheme 78: Impurities arising from benzylamine 180.

It was also found the reaction mixtures contained imine **188**, despite the vacuum/nitrogen purging of the reaction vessel prior to heating the reaction mixture. With the deadline for the preparation of metabolite **167** fast approaching, a number of issues had to be considered to determine if the route for preparation of **175** was appropriate for delivering **167** on time. Although some conversion to desired product was observed, the reaction was taking several days and purification was necessary. In addition, the synthetic route to **175** was decreasing the molecular weight from the starting material to the desired product. These factors were beginning to suggest a significant scale-up would be required to deliver enough **175** for the preparation of target molecule **167**. Due to the short timelines available, it was thought sensible to investigate an alternative route to **175** in parallel to investigating purification of the crude **185** formed from intermediates **184**, or **189**.

3.3.4 Route 2 to Azetidine 175

With significant concerns over the ability of Route 1 to provide **175**, new ideas to form an azetidine ring were considered. Bartholomew and Stocks published an intriguing rearrangement for azetidine synthesis, which was considered to be a potential alternative route to **175**.¹³²

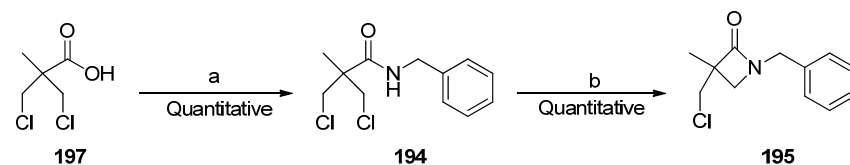


Scheme 79: Proposed Route 2 to 175.

After forming the azetidine **196**, the ester could be reduced to a primary alcohol, followed by hydrogenolysis to give azetidine **175**. This alternative route should overcome the neopentyl effect, as the nitrogen nucleophile is brought into close proximity to the chloride leaving groups, *via* the formation of an amide bond instead of alkylation. The nitrogen is able to be a more effective nucleophile as it is tethered close to the desired site of reaction, rendering this key bond formation intermolecular.

The route to prepare **195** is shown in Scheme 80. Dichloropivalic acid **197** is readily available and was easily converted to the acid chloride using thionyl chloride.¹³² The

acid chloride was reacted with benzylamine to give **194** in quantitative yield. Phase transfer conditions were used to convert **194** to the lactam **195**, also in quantitative yield.

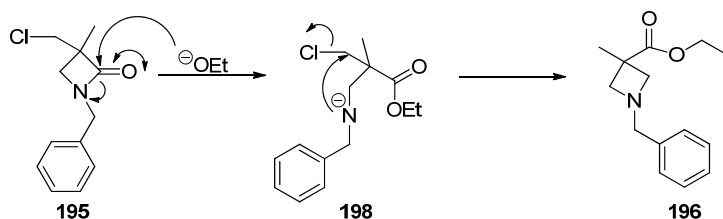


£1.06 per g
Aldrich

Conditions: a) i. Thionyl chloride (1.2 eq), DIPEA (1.2 eq), dichloromethane, 0 °C, 2 hours; ii. Benzylamine (1.2 eq), DIPEA (1.2 eq), 0 °C, 4 hours; b) TBAB (0.1 eq), aqueous sodium hydroxide (10 eq), dichloromethane, room temperature, 45 min.

Scheme 80: Route to lactam 195.

With a convenient route to the lactam **195** established, the ethoxide mediated rearrangement of the lactam was investigated. Scheme 81 shows the proposed mechanism by which the desired product **196** could be formed from lactam **195**



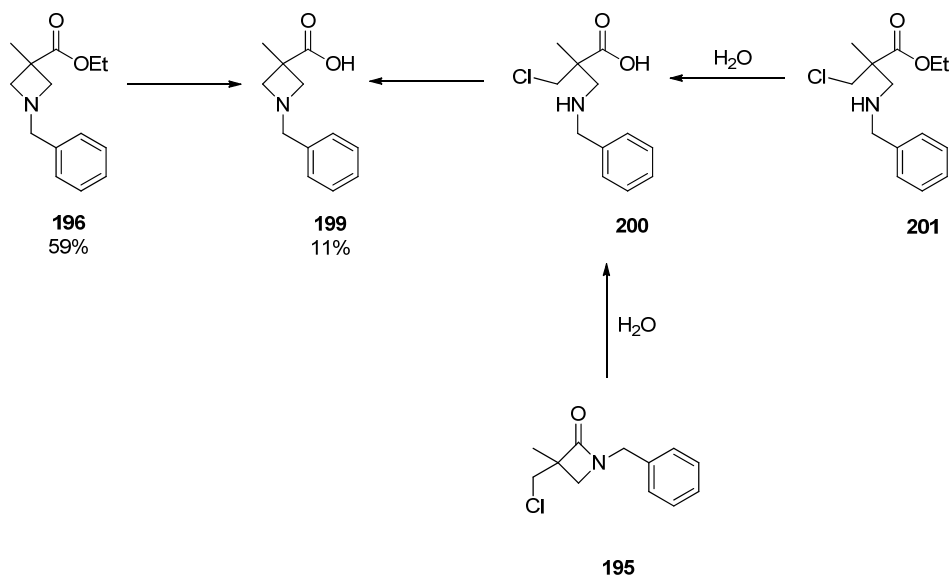
Scheme 81: Rearrangement of 195 to give 196.

This method of forming the azetidine ring avoids the neopentyl effect encountered using the bis-electrophiles **184** and **189**. Formation of the amide bond in **194** from benzylamine and dichloropivalic acid, brings the nitrogen in close proximity to the chloride leaving groups and enables S_N2 reaction under phase transfer conditions to give **195** (Scheme 80). Amide bonds are usually stable to nucleophilic substitution, but the lactam in **195**, is a strained ring system which is susceptible to nucleophilic attack by ethoxide (Scheme 81). Once the lactam ring has been opened, the nitrogen is able to displace the chloride in a second intramolecular S_N2 reaction to form the desired azetidine **196**. The displacement of the chloride in **198**, is irreversible leading to conversion to the desired product **196**.

Formation of the azetidine **196** from **195**, encountered some side reactions. HPLC analysis of the reaction mixture showed 59% conversion to desired product **196** after complete consumption of the starting material **195**. HPLC analysis also showed

several impurities had formed over the course of the reaction. From LC-MS analysis, tentative structures could be assigned to these impurities.

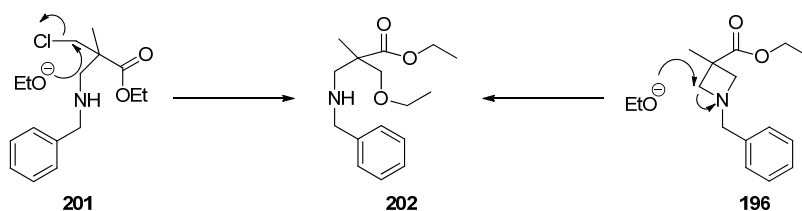
LC-MS data suggested 11% conversion to the impurity **199** had occurred during the reaction. **199** is formed by hydrolysis of the ester in either the product **196** or the intermediate **201**. **199** could also be formed by water opening the lactam in **195**.



Scheme 82: Proposed routes for the formation of impurity 199.

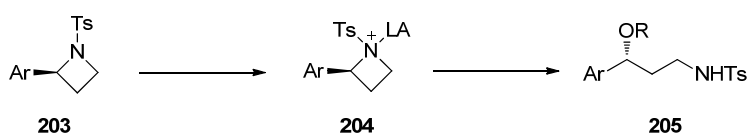
Aqueous conditions are required in order to form impurity **199**. The amount of **199** was not reduced by the use of anhydrous ethanol, indicating another source of water was responsible for the formation of this impurity. Fortunately, the impurity **199** was removed in the aqueous work-up following the reaction.

LC-MS data also suggested 19% conversion to impurity **202**. The potential routes of formation of **202** are outlined in Scheme 83. **201** is an observed intermediate in the reaction. The chloride present in **201** could be displaced by ethoxide to give **202**. Alternatively, **202** could be formed by ethoxide opening of the azetidine ring in the desired product **196**.



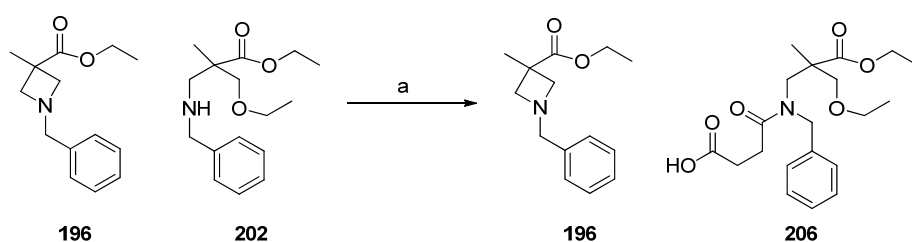
Scheme 83: Proposed routes for the formation of impurity 202.

Monitoring of the reaction mixture showed impurity **202** formed at the same rate as the product **196**, so a method of minimising the formation of this impurity was not immediately obvious. Ring opening of azetidines such as **196**, is known to be mediated by Lewis acids (Scheme 84).¹³³ In the azetidine **203**, the lone pair of nitrogen is accepted by the Lewis acid, enabling the ring to be opened regioselectively and stereospecifically by nucleophilic attack of an alcohol. Rearrangement of **195** to prepare **196** is carried out under basic conditions, so the nitrogen in **196** will remain neutral as there is no acceptor for the nitrogen lone pair. It is more plausible for the impurity **202** to be formed by the displacement of chloride in **201** as this is a better leaving group.



Scheme 84: Ring opening of azetidines mediated by Lewis acids.

After the aqueous work-up, ¹H NMR analysis showed the crude product contained 26% w/w impurity **202** and 74% w/w desired product **196**. Column chromatography did not offer a suitable separation to purify the desired product. Succinic anhydride had been used by another project within our laboratories to remove a secondary amine from a tertiary amine after aqueous work-up.¹³⁴ Reaction of the secondary amine **202** with succinic anhydride, forms the adduct **206**, containing a carboxylic acid (Scheme 85). The carboxylic acid enables the adduct to be extracted into a basic aqueous phase, leaving the desired tertiary amine product in the organic phase.



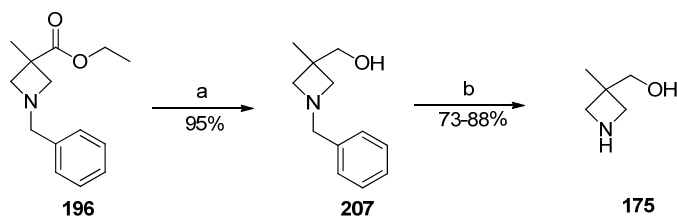
Conditions: a) Succinic anhydride (1.2 eq), pyridine (1.1 eq), PhMe, 70-80 °C, 15 min.

Scheme 85: Reaction of 196 and 202 with succinic anhydride.

Treatment of a mixture of **196** and **202** with succinic anhydride was shown to successfully derivitise the secondary amine impurity **202** to **206**. The derivitised impurity **206** was removed from the organic phase using a caustic wash. After an

acid/base extraction the desired tertiary amine product **196** was obtained in 45% yield from **195** in 96% purity.

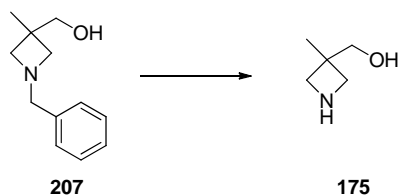
In order to prepare **175** from **196**, reduction of the ester and hydrogenolysis of the benzyl group was required.



Reagents: a) LiAlH_4 , (2.1 eq), THF, 20 °C, 45 min; b) H_2 , Pd-C (various), methanol, acetic acid (0-1.1 eq), 55 °C.

Scheme 86: Route to prepare 175 from 196.

Reduction of the ester was carried out using lithium aluminium hydride in tetrahydrofuran.¹³⁵ The primary alcohol product **207** was obtained in 95% yield and 96% purity. Reaction conditions were screened for the deprotection of **207** to reveal azetidine **175**. Table 30 shows the four catalysts that were investigated for this transformation in the presence and absence of acetic acid. Catalyst manufacturer Evonik¹³⁶ recommends the palladium hydroxide catalyst E5 for *N*-debenzylations. The remaining three Pd-C catalysts were chosen as these catalysts were shown to enable the *N*-debenzylation of *N*-benzyl-3,3-dimethylazetidine **178** to give 3,3-dimethylazetidine **169**. All four catalysts were tested with and without acetic acid, as the rate of *N*-debenzylation of *N*-benzyl-3,3-dimethylazetidine **178** was significantly increased when acetic acid was added to the reaction mixtures.

Table 30: Investigation of reaction conditions for the preparation of 175.^a

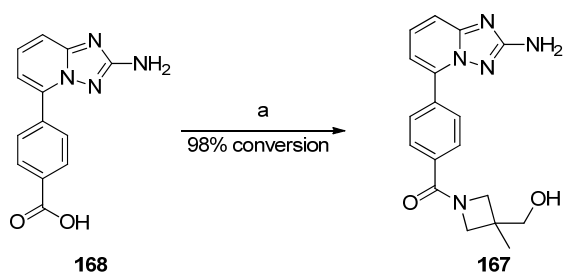
Entry	Catalyst	Acetic Acid (eq)	Purity Profile ^b
1	Evonik Degussa E 101 NO/W Pd-C	0	Highest purity observed for freebase isolated
2	Evonik Degussa E 101 NO/W Pd-C	1.1	Baseline impurities observed
3	Evonik Degussa E5 (Pd(OH) ₂)	0	Baseline impurities observed
4	Evonik Degussa E5 (Pd(OH) ₂)	1.1	Product recovered from Celite pad contained significant impurities
5	Johnson Matthey, Type 394 Pd-C	0	Baseline impurities observed
6	Johnson Matthey, Type 394 Pd-C	1.1	Baseline impurities observed
7	BASF CP M/UR 00034 Pd-C	0	Baseline impurities
8	BASF CP M/UR 00034 Pd-C	1.1	Highest purity observed for acetic acid salt of product

^a Conditions: H₂, catalyst, acetic acid, methanol, 55 °C overnight. ^b Determined by ¹H NMR spectroscopy.

Entries 1 and 8 showed the cleanest ¹H NMR purity profiles for the freebase **175** and acetic acid salt of **175**. In addition, the acetic acid salt of **175** obtained (entry 8) was isolated as a solid. Although good conversion to the desired product **175** was obtained with other reaction conditions investigated, the conditions in entry 8 were the only conditions which yielded **175** as a solid. Preparation of **175** as a solid was considered advantageous, as it could potentially be purified through crystallisation and filtration. The conditions in entry 8 were scaled up using 5.8 g input giving key azetidine **175** as the acetic acid salt in 90% yield.

3.3.5 End game

With the synthesis of **168** and **175** complete, the final stage coupling to prepare metabolite **167** could be carried out (Scheme 87). CDI was selected as the amide coupling activation reagent, as it had been demonstrated to activate carboxylic acid **168** in a model reaction (section 3.3.2)



Conditions: a) i. CDI (2.1 eq), dichloromethane, DMSO, rt, 45 minutes; ii. **175** (1.2 eq), rt, 15 minutes.

Scheme 87: Formation of Metabolite 167.

Carboxylic acid **168** was activated using CDI and **175** was added to the activated imidiazolide of **168**. This resulted in the preparation of the desired product metabolite **167**, however there were 2 impurities present at greater than 1% by HPLC. Figure 34 shows the proposed structures for these impurities based on LC-MS data.

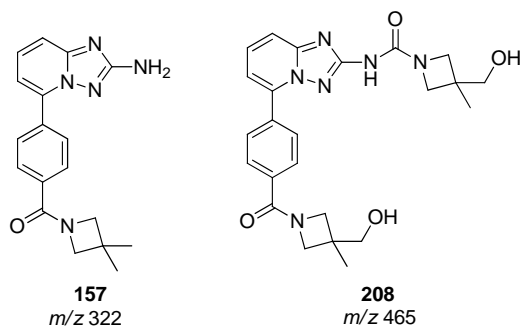
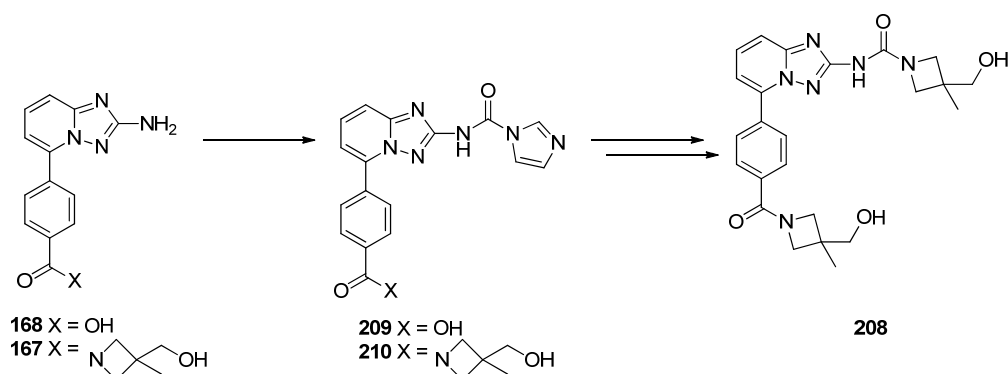


Figure 34: Impurities formed during preparation of metabolite 167.

Impurity **157** is an impurity present in carboxylic acid **168**. Impurity **208** is formed during the reaction to prepare metabolite **167**. Reaction of CDI with the aniline nitrogen in either the starting material **168** or product **167**, will form imidazole *N*-carboxamide **209** or **210**, which can react with azetidine **175**, to give impurity **208** (Scheme 88).¹³⁷



Scheme 88: Proposed routes of formation of 69.

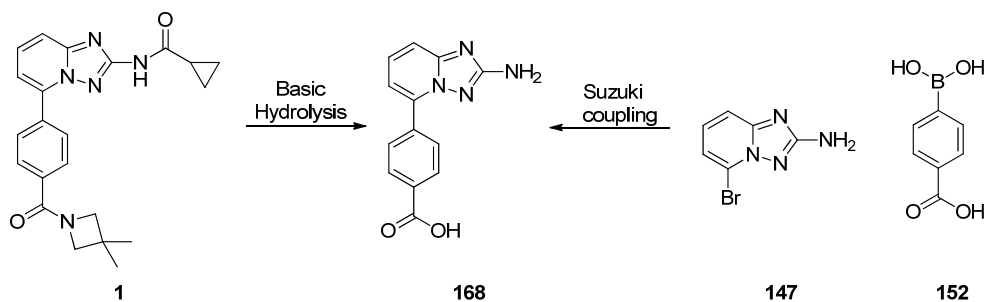
During the preparation of metabolite **167** it was observed that 2 equivalents of CDI were necessary in order to activate carboxylic acid **168**. Initially, this was thought to be due to use of poor quality CDI¹³⁸ or water present from solvents, but when high quality CDI and anhydrous solvents were used in the activation, 2 equivalents of CDI were still required for the reaction. With evidence for the formation of impurity **208** it seems likely both the carboxylic acid and the aniline in **168** underwent reaction with CDI.

At the end of the reaction, water was added and **167** was taken into the aqueous phase due to the use of DMSO as a reaction solvent. **167** was extracted from the aqueous phase using solid phase extraction in 47% yield (2.47 g). It is expected further material could have been recovered from the aqueous phase using the solid phase extraction technique, but with limited time available to provide 500 mg of **167**, it was decided to proceed with purification of 2.47 g **167** recovered from the aqueous phase. Impurities **157** and **208** were removed from the product using column chromatography. In order to provide **167** in the required purity, 2 purifications by column chromatography were necessary, providing **167** in 18% yield.

3.3.6 Improvements to the Synthesis of Metabolite 167

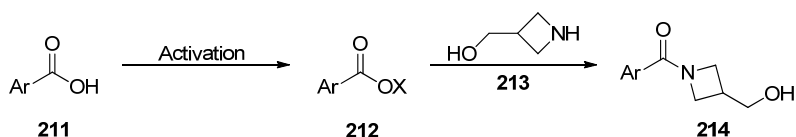
With the identity of the impurities formed during the synthesis of metabolite **167** established, it is possible to suggest modifications to the synthesis of **167** to improve efficiency. In order to minimise levels of **157**, **168** would need to be prepared in higher purity. Due to the zwitterionic nature of **168**, it is highly insoluble making purification difficult by column chromatography or acid/base extractive aqueous work-up. A dedicated synthesis of **168** either by basic hydrolysis of drug substance **1** (see section 3.2.2) or by Suzuki-Miyaura coupling of aminotriazole **147** and

4-carboxyphenylboronic acid **152** may enable **168** to be prepared in higher purity without the presence of **157** (Scheme 89).



Scheme 89: Potential alternative routes to 168.

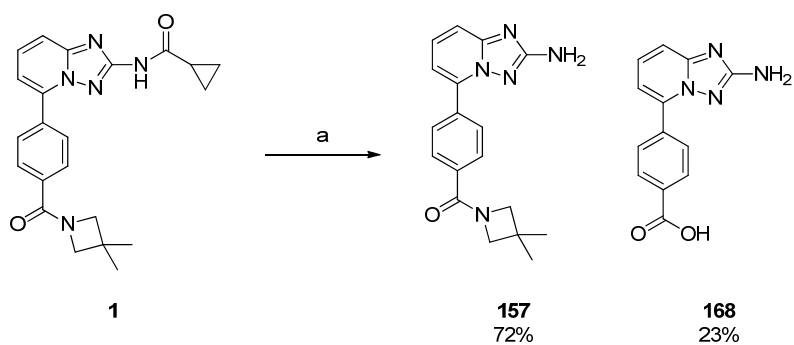
Formation of impurity **208** during the synthesis of metabolite **167**, could be reduced by using an alternative reagent to form an activated carboxylic acid to react with azetidine **175**. Various reagents including EDC/HOBt¹³⁹ and BOP¹⁴⁰ have been shown to activate carboxylic acids and form amide bonds with azetidine **213**, which is similar to **175** (Scheme 90).



Scheme 90: Example of amide coupling with azetidine similar to 175.

3.4 Conclusions

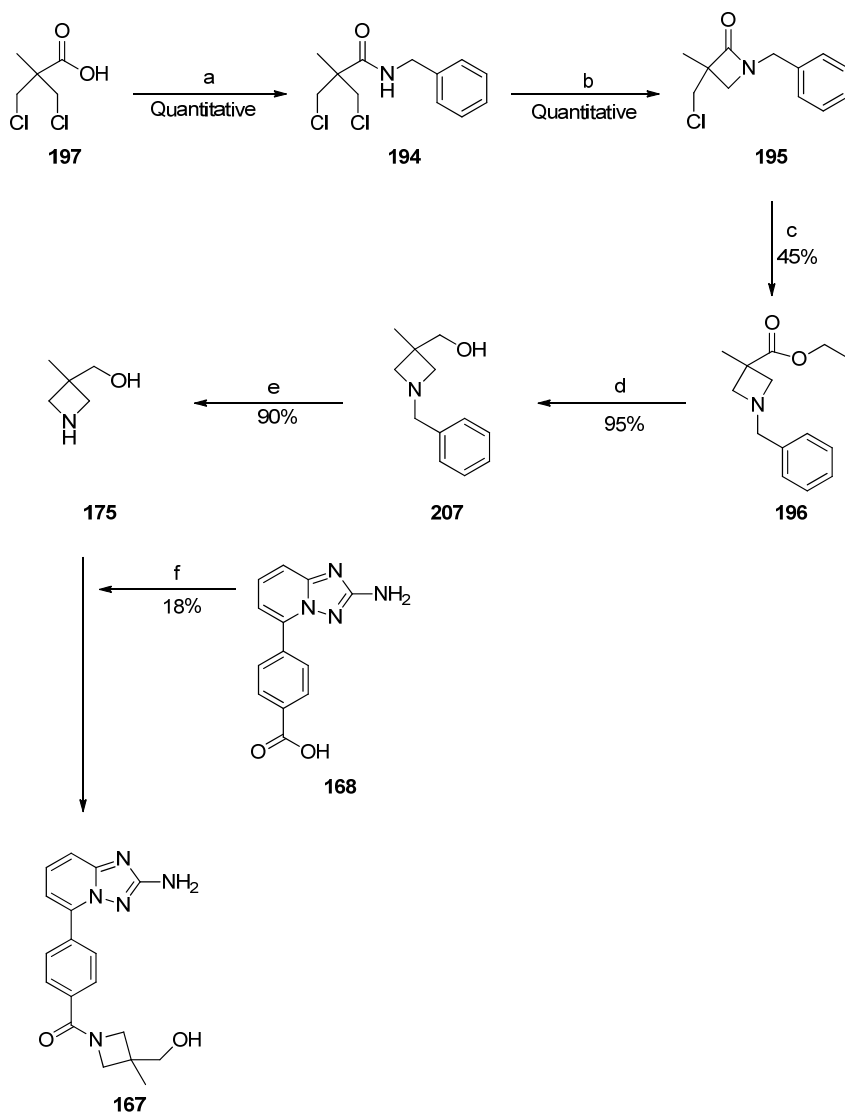
Acid and base catalysed hydrolysis of drug substance **1** has been investigated in order to prepare metabolite **157**. Hydrolysis of **1** using sulfuric acid enabled **157** to be prepared in high purity for Ames testing. The synthesis of **157** also yielded a supply of carboxylic acid **168**, which was required for the synthesis of metabolite **167**. Using this method, **157** was prepared in 72% yield and 99.6% purity (Scheme 91). The synthesis of **157** will be scaled up by a third party to prepare 50 g **157** for animal studies.



Conditions: a) 1:1 THF/water, H₂SO₄ (2 eq), reflux, 64 h;

Scheme 91: Synthesis of Metabolite 157.

Two routes were investigated to prepare novel azetidine **175** required for the synthesis of metabolite **167**. The route used to prepare azetidine **175** offers an interesting alternative to the current route of synthesis of azetidine **169** which is a key starting material for the drug substance **1**. Metabolite **167** has been prepared *via* a 7 step synthesis in 7% overall yield and 99.6% purity (Scheme 92), for use as an analytical marker in safety assessment studies. The synthesis of metabolite **167** is also to be outsourced to a third party to prepare 50 g for animal studies.



Conditions: a) i. Thionyl chloride (1.2 eq), DIPEA (1.2 eq), dichloromethane, 0 °C, 2 hours; ii. Benzylamine (1.2 eq), DIPEA (1.2 eq), 0 °C, 4 hours; b) TBAB (0.1 eq), aqueous sodium hydroxide (10 eq), dichloromethane, 45 min; c) i. NaOEt (2.7 eq), EtOH, reflux 5 hours; ii. Succinic anhydride (1.2 eq), pyridine (1.1 eq), PhMe, 70-80 °C, 15 min; d) LiAlH₄, (2.1 eq), THF, 20 °C, 45 min; e) H₂, Pd-C, methanol, acetic acid (1.1 eq), 55 °C, 100 min; f) a) i. CDI (2.1 eq), dichloromethane, DMSO, rt, 45 minutes; ii. **175** (1.2 eq), rt, 15 minutes.

Scheme 92: Synthetic Route to 167.

4 Experimental

4.1 General Experimental Details

All solvents and reagents used were standard laboratory grade unless stated, and were employed without further purification.

All experiments were carried out under an atmosphere of nitrogen gas unless otherwise stated.

NMR data were obtained on a Bruker DPX 400 or Bruker AV 400 spectrometer, operating at 400.2 MHz for ^1H spectra and 100.63 MHz for ^{13}C spectra. Chemical shifts in ^1H and ^{13}C spectra are reported on the δ scale relative to tetramethylsilane (TMS). ^{13}C spectra were proton decoupled. All NMR data were obtained at 299 K in d_6 -DMSO unless otherwise stated.

HPLC data were obtained on a number of different methods as detailed below:

Method A

Column details	Phenomenex Luna C18(2), 50 x 2.0 mm, 3 μm		
Column Temperature	40 $^\circ\text{C}$		
Mobile Phase A	0.05% v/v Trifluoroacetic acid in water		
Mobile Phase B	0.05% v/v Trifluoroacetic acid in acetonitrile		
Flow rate	1 mL/min		
Gradient Profile	Time / min	% A	% B
	0	100	0
	8	5	95
	8.01	100	0
	11	100	0
Detector Wavelength	UV at 232 nm (unless otherwise stated)		
Injection volume	1 μL		
Sample diluent	Methanol		

Method B

Column details	Agilent Zorbax SB-C18, 50 x 3.0 mm, 1.8 μ m		
Column Temperature	60 °C		
Mobile Phase A	0.05% v/v Trifluoroacetic acid in water		
Mobile Phase B	0.05% v/v Trifluoroacetic acid in acetonitrile		
Flow rate	1.5 mL/min		
Gradient Profile	Time / min	% A	% B
	0	100	0
	2.5	5	95
	2.7	5	95
	2.71	100	0
	3.3	100	0
Detector Wavelength	UV at 232 nm (unless otherwise stated)		
Injection volume	1 μ L		
Sample diluent	Methanol		

Method C

Column details	X-Bridge C18 (150-4.6 mm, 3.5 μ m)		
Column Temperature	40 °C		
Mobile Phase A	10 Mm ammonium acetate in water (adjusted to pH 5.5 with acetic acid)		
Mobile Phase B	Methanol		
Flow rate	1 mL/min		
Gradient Profile	Time / min	% A	% B
	0	85	15
	10	50	50
	15	45	55
	25	5	95
	25.1	85	15
	30	85	15
Detector Wavelength	UV at 232 nm (unless otherwise stated)		
Injection volume	10 μ L		
Sample diluent	Methanol		

LCMS data were obtained using HPLC Method A coupled to a mass spectrometer, which used positive electrospray ionisation with a quadrupole detector.

GSK CONFIDENTIAL

High resolution mass spectrometry data were obtained using HPLC Method A coupled to a Thermo-Finnigan Orbitrap Fourier-transform mass spectrometer running in positive electrospray ionisation mode.

Melting points were obtained using a Stuart SMP40 melting point apparatus

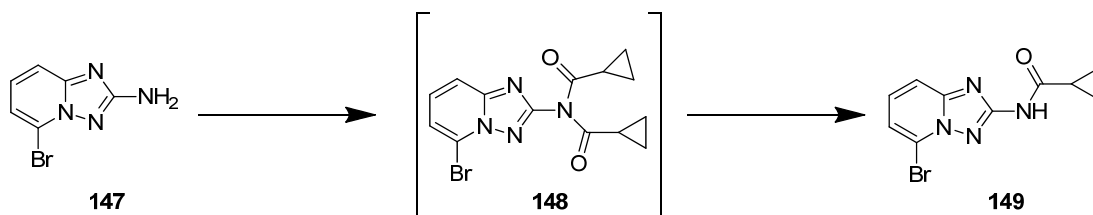
Infra red (IR) spectra were obtained on a Perkin Elmer Spectrum One instrument with a diamond attenuated total reflection accessory. Only data for main functional groups and strong peaks are reported.

ICP-AES data was obtained on a Varian 730-ES, gathering counts for palladium, sodium, potassium, boron and calcium at 340.458, 589.592, 766.491, 249.772 and 317.933 nm, respectively. Certified ICP standards were prepared at 0.1 and 1.0 µg/mL and with a blank measurement generated a calibration curve for the samples; a system suitability standard is run at the end to determine instrument drift is within acceptable tolerances. Samples are typically dissolved in 2 % v/v HCl in dimethylsulfoxide at 10 mg/mL.

Chromatography was carried out using a Biotage SP4 instrument, with pre-packed silica columns. Details of solvent system, column size, silica type, flow rate and column loading are provided for individual examples.

4.2 Experimental Details for Chapter 2

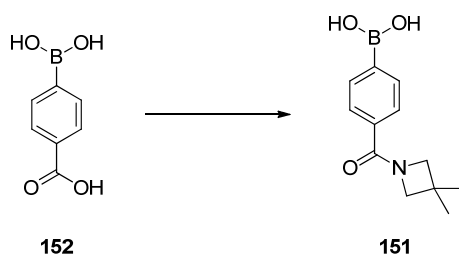
Preparation of *N*-(5-bromo-[1,2,4]triazolo[1,5-*a*]pyridin-2-yl)cyclopropanecarboxamide **149**



Anhydrous triethylamine (7.25 mL, 52.0 mmol) was added to a stirred suspension of 5-bromo-[1,2,4]triazolo[1,5-*a*]pyridin-2-amine **147** (5.00 g, 23.5 mmol) in acetone (25 mL) and the suspension was cooled in an ice bath. A solution of cyclopropanecarbonyl chloride (4.6 mL, 50.6 mmol) in acetone (5 mL), was added to the suspension over 20-25 minutes. After 2 hours, TEA (0.98 mL, 7.0 mmol) was added to the reaction mixture. The reaction mixture was cooled in an ice bath and cyclopropanecarbonyl chloride (0.64 mL, 7.0 mmol) was added. The reaction was left to stir at room temperature. After HPLC analysis showed the reaction was complete, 7N ammonia in methanol (9 mL, 63.0 mmol) was charged to the reaction vessel and the reaction mixture was left to stir at room temperature. After HPLC analysis showed the reaction was complete, the suspension was concentrated to ~25 mL at atmospheric pressure and then was allowed to cool to room temperature. The suspension was filtered and washed with water (10 mL). The damp solid was charged to a round bottom flask and water (20 mL) was added to give a suspension, which was stirred for 30 minutes. The suspension was filtered and washed with water (20 mL) followed by acetone (2 x 20 mL), to give an off-white solid which was placed in the vacuum oven and removed after several days to give *N*-(5-bromo-[1,2,4]triazolo[1,5-*a*]pyridin-2-yl)cyclopropanecarboxamide **149** (4.99 g, 76%) as off-white needles. ¹H NMR (400 MHz, DMSO-*d*₆) δ ppm 11.19 (s, 1 H), 7.70 (dd, *J* = 8.8, 0.8 Hz, 1 H), 7.55 (dd, *J* = 8.8, 7.6 Hz, 1 H), 7.48 (dd, *J* = 7.6, 0.8 Hz, 1 H), 2.04 (br. s., 1 H), 0.78-0.94 (m, 4 H); ¹³C NMR (101 MHz, DMSO-*d*₆) δ ppm 171.4 (s), 157.8 (s), 150.2 (s), 130.9 (d), 117.6 (d), 116.9 (s), 113.6 (d), 13.9 (d), 7.9 (t); IR

(neat) 3137, 3100, 2997, 2959, 2905, 1671, 1627, 1563, 1532, 1511 cm^{-1} ; HRMS found m/z 281.0033 $[\text{M}+\text{H}]^+$, calcd for $\text{C}_{10}\text{H}_{10}^{79}\text{BrN}_4\text{O}$ 281.0033; mp 200-202 $^{\circ}\text{C}$.

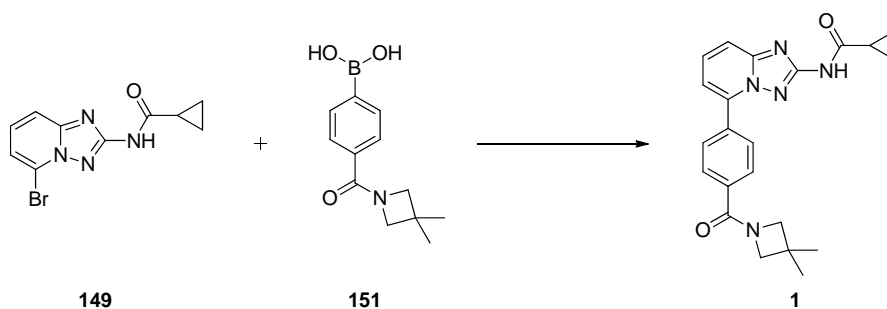
Preparation of (4-(3,3-dimethylazetididine-1-carbonyl)phenyl)boronic acid **151**



2-methyltetrahydrofuran (225mL) was added to 4-boronobenzoic acid **152** (14.65 g, 88 mmol) in a round bottom flask. The contents were heated to reflux and over 5 hours, the volume of the reaction mixture was reduced to 150 mL. The reaction mixture was allowed to cool to room temperature and DMSO (15 mL) was added to the reaction vessel to give a solution, which was stirred overnight. The following morning, CDI (26.86 g, 166 mmol) was charged in portions over 24 hours until HPLC analysis showed the reaction was complete. 3,3-dimethylazetididine hydrochloride (13.19 g, 108 mmol) was charged to the reaction mixture. The following morning, 2M HCl solution (150 mL) was added maintaining contents temperature 15-25 $^{\circ}\text{C}$. The aqueous layer was washed twice with 2-methyltetrahydrofuran (75 mL). The organic layers were combined and washed with water (75 mL). After 3 days, the organic layer was concentrated to 120 mL under atmospheric pressure. Isopropyl acetate (150 mL) was added to reaction flask and the contents were concentrated to 120 mL under atmospheric pressure. The contents were allowed to cool to 40-45 $^{\circ}\text{C}$ and the solution was seeded with (4-(3,3-dimethylazetididine-1-carbonyl)phenyl)boronic acid **151** (15mg). After seeding, the contents were left to stir at room temperature overnight. The suspension was cooled in an ice bath for 2.5 hours. The suspension was filtered and the solids were washed with isopropyl acetate (30 mL). The damp solid was dried overnight in a vacuum oven at 40 $^{\circ}\text{C}$ to give (4-(3,3-dimethylazetididine-1-carbonyl)phenyl)boronic acid **151** (17.78g, 86%) as white laths. ^1H NMR (400 MHz, $\text{DMSO}-d_6$) δ ppm 8.17 (s, 2 H) 7.83 (d, $J = 8.0$ Hz, 2 H) 7.57 (d, $J = 8.0$ Hz, 2 H) 3.96 (s, 2 H) 3.72 (s, 2 H) 1.24 (s, 6 H); ^{13}C NMR (101 MHz, $\text{DMSO}-d_6$) δ ppm 169.1 (s) 133.9 (d) 126.6 (d) 64.8 (t)

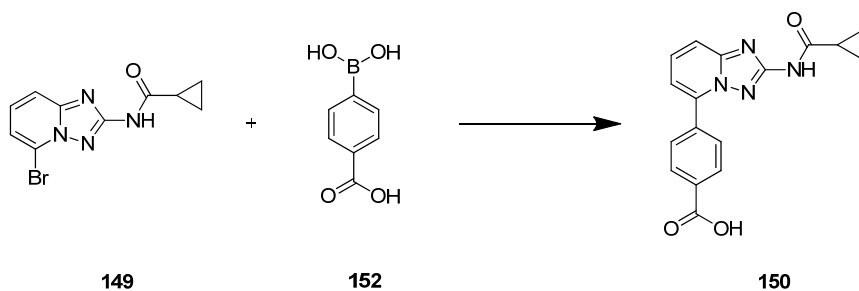
60.5 (t) 31.0 (s) 26.6 (q); IR (neat) 3287, 1599, 1547, 1508 cm^{-1} ; HRMS found m/z 234.1296 $[\text{M}+\text{H}]^+$, calcd for $\text{C}_{12}\text{H}_{17}\text{BNO}_3$ 234.1296; mp 148-150 $^{\circ}\text{C}$.

Preparation of *N*-(5-(4-(3,3-dimethylazetid-1-yl)cyclopropanecarboxamido)phenyl)-[1,2,4]triazolo[1,5-*a*]pyridin-2-yl)cyclopropanecarboxamide **1** using Route A Suzuki-Miyaura Coupling Conditions



N-(5-bromo-[1,2,4]triazolo[1,5-*a*]pyridin-2-yl)cyclopropanecarboxamide **149** (0.50 g, 1.78 mmol), (4-(3,3-dimethylazetid-1-yl)cyclopropanecarboxamido)phenylboronic acid **151** (0.477 g, 2.05 mmol) and $\text{PdCl}_2(\text{dppf})$ (6.5 mg, 89 μmol) were suspended in 1,4-dioxane (5 mL). Potassium hydroxide (0.10 g, 1.78 mmol) was dissolved in distilled water (5 mL) and added to the suspended reagents. The suspension was stirred at reflux overnight. The following morning, HPLC analysis (Method B) of the reaction mixture showed 73% PAR **1**, 13% PAR **151** and 9% PAR **149**.

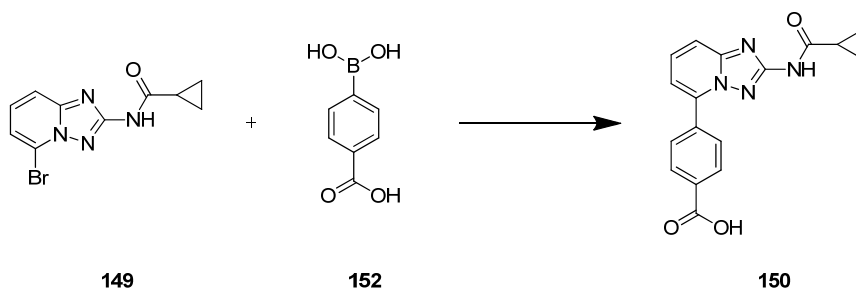
Preparation of 4-(2-(cyclopropanecarboxamido)-[1,2,4]triazolo[1,5-*a*]pyridin-5-yl)benzoic acid **150** in Route A – Screen of palladium/ligand combinations, solvents and bases



N-(5-bromo-[1,2,4]triazolo[1,5-*a*]pyridin-2-yl)cyclopropanecarboxamide **149** (0.10 g, 0.36 mmol), 4-boronobenzoic acid **152** (0.068 g, 0.41 mmol), palladium source *a* (18 μmol) and ligand *b* (36 μmol) were suspended in solvent *d* (0.5 mL). A solution of

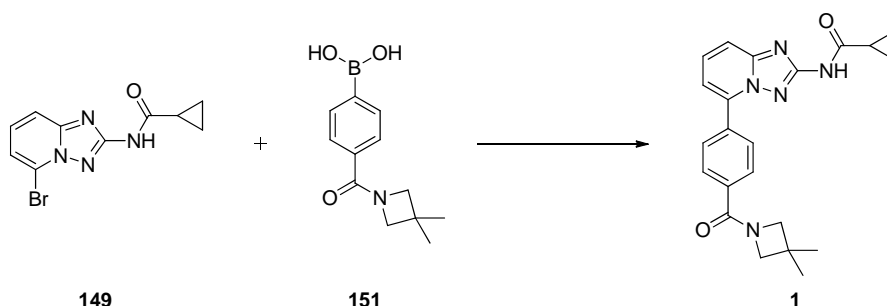
base *c* (0.75 mmol) in water (0.5 mL) was added and the reaction mixture was microwaved on high absorption for 15 mins. The reaction mixture was sampled for HPLC analysis (Method B). Full details of palladium source, ligands, solvents and bases can be found in (Appendix 6.1, page 170).

Preparation of 4-(2-(cyclopropanecarboxamido)-[1,2,4]triazolo[1,5-*a*]pyridin-5-yl)benzoic acid **150** in Route A



N-(5-bromo-[1,2,4]triazolo[1,5-*a*]pyridin-2-yl)cyclopropanecarboxamide **149** (32.75 Kg, 116.5 mol), 4-boronobenzoic acid **152** (22.23 Kg, 134.0 mol), PdCl₂(dppf) acetone adduct (1.83 Kg, 2.3 mol), and 50% *w/w* potassium hydroxide (26.20 Kg, 233.0 mol) were suspended in 1,4-dioxane (164 L) and water (151 L). The suspension was heated at reflux for 16 hours. Water (151 L) was added and the solution concentrated to 295 L. Water (164 L) was added and the solution was concentrated to 295 L. At the end of the distillation, the mixture was cooled to 55 °C and ethanol (164 L) added. The mixture was acidified to pH 2 by addition of conc. HCl (13 L) over 30 minutes and stirred at 55 °C for 1.5 hours. The suspension was cooled to 25 °C, filtered and washed with 2:1 water/ethanol (131 L), water (2 x 98 L) and acetone (131 L). The brown solid was dried in a vacuum oven at 50 °C to give 4-(2-(cyclopropanecarboxamido)-[1,2,4]triazolo[1,5-*a*]pyridin-5-yl)benzoic acid **150** (36.95 Kg, 98%). ¹H NMR (400 MHz, DMSO-*d*₆) δ ppm 13.17 (br. s, 1 H), 11.04 (s, 1 H), 7.97-8.30 (m, 4 H), 7.63-7.85 (m, 2 H), 7.21-7.50 (m, 1 H), 2.03 (br. s, 1 H), 0.63-0.98 (m, 4 H); ¹³C NMR (101 MHz, DMSO-*d*₆) δ ppm 171.3 (s), 166.8 (s), 158.2 (s), 150.3 (s), 138.5 (s), 135.9 (s), 131.8 (s), 130.3 (d), 129.23 (d), 129.21 (d), 114.3 (d), 114.2 (d), 13.9 (d), 7.7 (t); IR (neat) 3265, 3173, 3095, 3016, 1683, 1625, 1554, 1523 cm⁻¹; HRMS found *m/z* 323.1142 [M+H]⁺, calcd for C₁₇H₁₅N₄O₃ 323.1139; mp 284 °C (dec.).

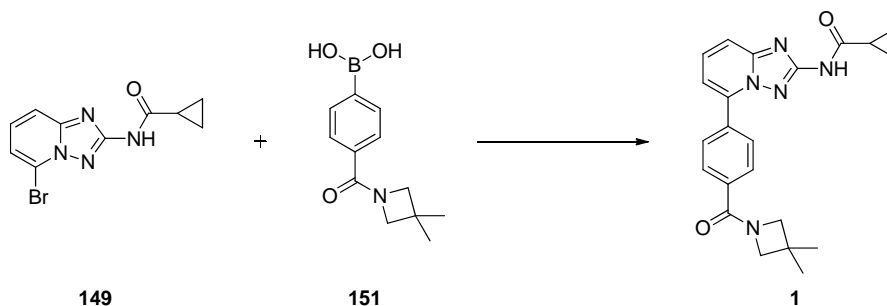
Preparation of *N*-(5-(4-(3,3-dimethylazetidide-1-carbonyl)phenyl)-[1,2,4]triazolo[1,5-*a*]pyridin-2-yl)cyclopropanecarboxamide **1** in Route B – Screen of Solvents and Bases



N-(5-bromo-[1,2,4]triazolo[1,5-*a*]pyridin-2-yl)cyclopropanecarboxamide **149** (0.50 g, 1.78 mmol), (4-(3,3-dimethylazetidide-1-carbonyl)phenyl)boronic acid **151** (0.477 g, 2.05 mmol), palladium(II) acetate (20 mg, 89 μ mol) and triphenylphosphine (47 mg, 178 μ mol) were suspended in solvent *a* (5 mL). Base *b* (1.78 mmol) was dissolved in distilled water (5 mL) and added to the suspended reagents. The suspension was heated at reflux overnight and the following morning HPLC analysis (Method B, 3:1 methanol/water as diluent) was carried out.

Entry	Solvent <i>a</i>	Base <i>b</i>	Boronic acid 151 % PAR	Aryl bromide 149 % PAR	Product 1 %PAR
1	Methanol	Na ₂ CO ₃	3	1	88
2	Methanol	KHCO ₃	11	6	77
3	Ethanol	Na ₂ CO ₃	21	8	50
4	Ethanol	KHCO ₃	5	3	83

Preparation of *N*-(5-(4-(3,3-dimethylazetidide-1-carbonyl)phenyl)-[1,2,4]triazolo[1,5-*a*]pyridin-2-yl)cyclopropanecarboxamide **1** using methanol/sodium carbonate - DoE Screen



GSK CONFIDENTIAL

To a mixture of *N*-(5-bromo-[1,2,4]triazolo[1,5-*a*]pyridin-2-yl)cyclopropanecarboxamide **149** (*a*, 1 eq), (4-(3,3-dimethylazetidide-1-carbonyl)phenyl)boronic acid **151** (*b*), sodium carbonate (*c*), palladium(II) acetate (*d*), and triphenylphosphine (*e*) was added aqueous methanol (*f*, *g*). The reaction mixture was heated to reflux. After 16 hours, the reaction mixture was sampled for HPLC analysis (Method B, 3:1 methanol/water as diluent).

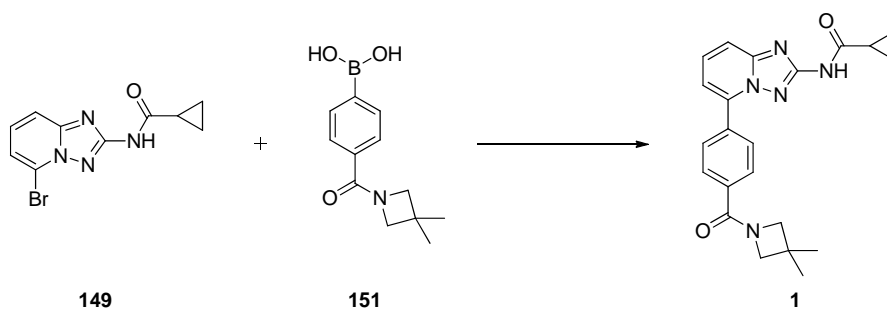
Run	Mass of 149 (g) <i>a</i>	Equivalents of Boronic Acid 151 <i>b</i>	Equivalents of Na ₂ CO ₃ <i>c</i>	Mol% Pd(OAc) ₂ <i>d</i>	PPh ₃ Equivalents relative to Pd(OAc) ₂ <i>e</i>	% v/v Water <i>f</i>	Total Solvent Volumes <i>g</i>
1	1.00	1	1	1	1	40	8
2	1.00	1	1	5	3	40	8
3	0.50	1	1.5	1	3	40	16
4	0.50	1	1.5	5	1	40	16
5	0.50	1	1	1	3	60	16
6	0.50	1	1	5	1	60	16
7	1.00	1	1.5	1	1	60	8
8	1.00	1	1.5	5	3	60	8
9	0.50	1.15	1	1	1	40	16
10	0.50	1.15	1	5	3	40	16
11	1.00	1.15	1.5	1	3	40	8
12	1.00	1.15	1.5	5	1	40	8
13	1.00	1.15	1	1	3	60	8
14	1.00	1.15	1	5	1	60	8
15	0.50	1.15	1.5	1	1	60	16
16	0.50	1.15	1.5	5	3	60	16
17	0.67	1.075	1.25	3	2	50	12
18	0.67	1.075	1.25	3	2	50	12

Variable Setting

Low
Centre Point
High

Run	% PAR by HPLC after 16 hours		
	149	151	1
1	0.3	0.3	96.6
2	62.7	21.5	10.1
3	15.4	4.8	72.7
4	5.2	1.4	85.3
5	54.3	19.2	25.0
6	1.3	0.7	92.1
7	16.1	5.3	74.9
8	63.2	21.9	7.9
9	0	5.3	91.4
10	54.1	21.3	14.6
11	7.2	7.9	80.8
12	0	0.9	94.1
13	30.5	13.3	52.7
14	0.4	3.3	92.7
15	0	5.8	91.7
16	61.2	23.5	9.1
17	0	2.9	91.3
18	0	3.8	91.7

Preparation of *N*-(5-(4-(3,3-dimethylazetidide-1-carbonyl)phenyl)-[1,2,4]triazolo[1,5-*a*]pyridin-2-yl)cyclopropanecarboxamide **1** in Route B –
Optimisation of Methanol/Na₂CO₃ Reaction Conditions



N-(5-bromo-[1,2,4]triazolo[1,5-*a*]pyridin-2-yl)cyclopropanecarboxamide **149** (1 eq) was suspended in aqueous methanol (*a*, *b*) and to this suspension, was added (4-(3,3-dimethylazetidide-1-carbonyl)phenyl)boronic acid **151** (1 eq), triphenylphosphine (*c*), palladium(II) acetate (*d*), and sodium carbonate (1 eq). The reaction mixture was stirred at temperature (*e*). After analysis by HPLC showed conversion to **1** was complete, the reaction mixture was allowed to cool to room temperature. The suspension was filtered and washed with aqueous methanol (*f*, *g*). The filtered solid was dried under vacuum at 40 °C, to give *N*-(5-(4-(3,3-dimethylazetidide-1-carbonyl)phenyl)-[1,2,4]triazolo[1,5-*a*]pyridin-2-yl)cyclopropanecarboxamide **1** (*h*), which was submitted for HPLC analysis (Method C, unless otherwise stated) and ICP-AES analysis.

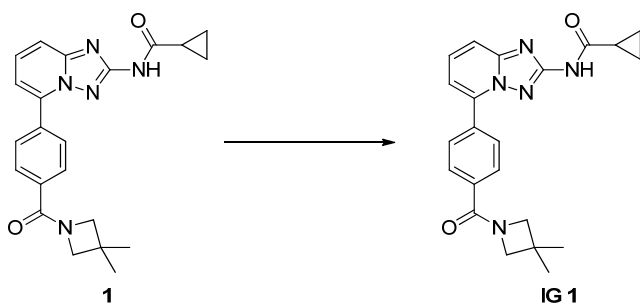
Conditions	% v/v	Solvent	PPh ₃	Pd(OAc) ₂	Temp.	% v/v	Solvent	Yield
	water	volumes				water	volumes	
	<i>a</i>	(vol)	<i>c</i>	<i>d</i>	(°C)	<i>f</i>	(vol)	<i>h</i>
1	40	8	1	1	65	50	15	92
2 ^a	20	8	0.5	0.5	70	40	10	92
3	40	16	0.25	0.25	70	40	6.5	83
4	40	16	0.1	0.1	70	33	4	72

^a after the reaction mixture had cooled to room temperature, 40% aqueous methanol (15 vol) was added.

Conditions	HPLC (% PAR)				ICP-AES (ppm)	
	1	157	RRT	RRT	Pd	Na
1	99.9	ND	1.03	1.35	2850	NE
2	99.7	0.20	0.07	0.07	545	35
3	99.8	0.12	0.07	0.06	263	188
4	94.5 ^a	N/A	N/A	N/A	NE	NE

^a Determined by Method A

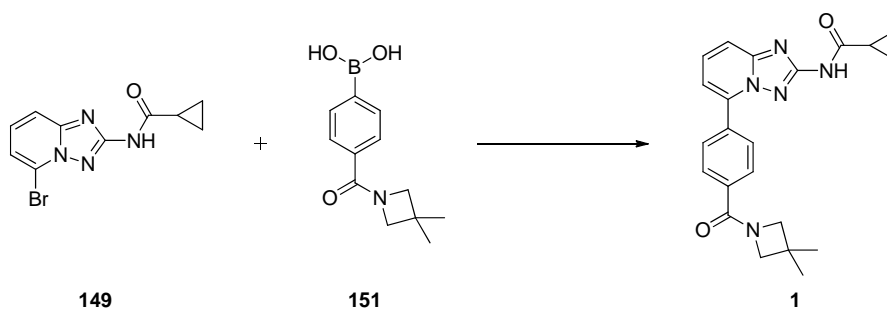
Purification of *N*-(5-(4-(3,3-dimethylazetidide-1-carbonyl)phenyl)-[1,2,4]triazolo[1,5-*a*]pyridin-2-yl)cyclopropanecarboxamide **1** in Route B Using Dichloromethane



Dichloromethane (8 mL) was added to *N*-(5-(4-(3,3-dimethylazetidide-1-carbonyl)phenyl)-[1,2,4]triazolo[1,5-*a*]pyridin-2-yl)cyclopropanecarboxamide **1** (0.80 g, 2.05 mmol) and a clear orange solution was obtained. To this solution, an additive *a*, was added and the mixture was heated to reflux. After 20 hours at reflux, the contents were allowed to cool to room temperature. The additive was removed (*b*) and the dichloromethane solution was evaporated to give **1** as a solid (*c*). ICP-AES analysis of the evaporated solid was carried out.

Entry	Additive <i>a</i>	Additive removal method <i>b</i>	Yield <i>c</i>	ICP-AES (ppm)	
				Na	Pd
1	Cuno R55S powder (0.20 g, 0.25 wt)	Filtered through Celite	95%	N/A	67
2	NaTMT monohydrate (0.20 g, 0.82 mmol)	Filtered through Celite	31%	171	77
3	<i>L</i> -cysteine (0.20 g, 1.65 mmol)	Filtered followed by evaporation, residue redissolved in CH ₂ Cl ₂ and washed with 0.5M HCl solution (8 mL, 10 vol) and 0.5M NaOH solution (8 mL, 10 vol)	91%	26	29
4	TMT (0.20 g, 1.13 mmol)	Filtered through Celite	0.82 g (crude yield)	13	150

Preparation of *N*-(5-(4-(3,3-dimethylazetidide-1-carbonyl)phenyl)-[1,2,4]triazolo[1,5-*a*]pyridin-2-yl)cyclopropanecarboxamide **1** in Route B using Methanol/Na₂CO₃ and Subsequent Screen of Additives to Remove Palladium

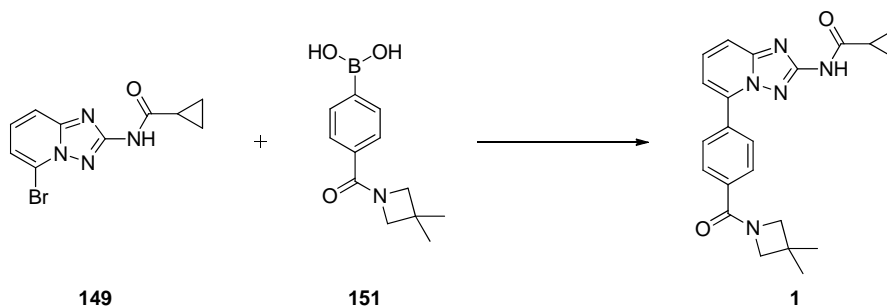


N-(5-bromo-[1,2,4]triazolo[1,5-*a*]pyridin-2-yl)cyclopropanecarboxamide **149** (0.50 g, 1.78 mmol), (4-(3,3-dimethylazetidide-1-carbonyl)phenyl)boronic acid **151** (0.46 g, 1.78 mmol), triphenylphosphine (1.2 mg, 5 μmol), sodium carbonate (0.19 g, 1.79 mmol), palladium(II) acetate (1.0 mg, 4 μmol) and 40% *v/v* aqueous methanol (8 mL) were charged to an Integrity 10 tube. The tube was evacuated and purged with nitrogen 3 times and the contents were heated using external temperature 70 °C overnight. After analysis by HPLC showed conversion to **1** was complete, additive (*a*) was added to the reaction mixture, which was heated using an external temperature of 70 °C for time (*b*). The contents were cooled to 20 °C at a rate of 0.5 °C per minute and stirred at 20 °C until the following morning. The suspension was filtered and washed with 40% *v/v* aqueous methanol (4 mL) to give *N*-(5-(4-(3,3-dimethylazetidide-1-carbonyl)phenyl)-[1,2,4]triazolo[1,5-*a*]pyridin-2-yl)cyclopropanecarboxamide **1** as a beige solid, which was placed in a vacuum oven

at 50 °C. The following morning, **1** (*c*) was removed from the vacuum oven and submitted for ICP-AES analysis.

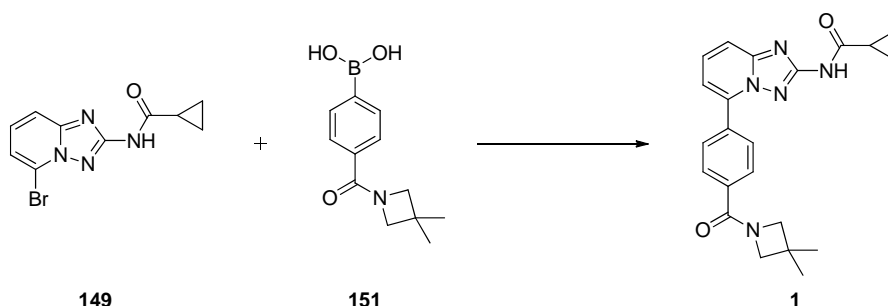
Entry	Additive <i>a</i>	Time <i>b</i>	Yield <i>c</i>	ICP-AES (ppm)	
				Pd	Na
1	NaTMT (125 mg, 514 μmol)	5.5 h	76%	489	49
2	<i>N</i> -acetyl- <i>L</i> -cysteine (100 mg, 613 μmol)	4 h	66%	103	86
3	<i>L</i> -cysteine (100 mg, 825 μmol)	4 h	72%	135	36

Preparation of *N*-(5-(4-(3,3-dimethylazetidone-1-carbonyl)phenyl)-[1,2,4]triazolo[1,5-*a*]pyridin-2-yl)cyclopropanecarboxamide **1** in *n*-Butanol



N-(5-bromo-[1,2,4]triazolo[1,5-*a*]pyridin-2-yl)cyclopropanecarboxamide **149** (5.00 g, 17.79 mmol), (4-(3,3-dimethylazetidone-1-carbonyl)phenyl)boronic acid **151** (4.35 g, 17.79 mmol), triphenylphosphine (12 mg, 44 μmol), sodium carbonate (1.89 g, 17.83 mmol), *n*-butanol (48 mL) and water (32 mL) were charged to a 100 mL flask (equipped with overhead stirrer) containing palladium(II) acetate (10 mg, 45 μmol), which was heated to reflux. After 19 hours, HPLC analysis (Method A) showed the reaction was complete (94.9% **1**, 3.9% **157** and 0.3% **151**). The contents were allowed to cool to room temperature and the aqueous phase was discarded. The organic phase was filtered through Celite. The filtrate was heated to 80 °C and allowed to cool to room temperature. The following morning, the suspension was filtered and washed with TBME (20 mL), give *N*-(5-(4-(3,3-dimethylazetidone-1-carbonyl)phenyl)-[1,2,4]triazolo[1,5-*a*]pyridin-2-yl)cyclopropanecarboxamide **1** (4.04 g, 58% yield) as white needles. ICP-AES: Pd 25 ppm, Na 39 ppm.

Preparation of *N*-(5-(4-(3,3-dimethylazetidide-1-carbonyl)phenyl)-[1,2,4]triazolo[1,5-*a*]pyridin-2-yl)cyclopropanecarboxamide **1** in Route B using *n*-butanol/Na₂CO₃ and supported palladium acetate

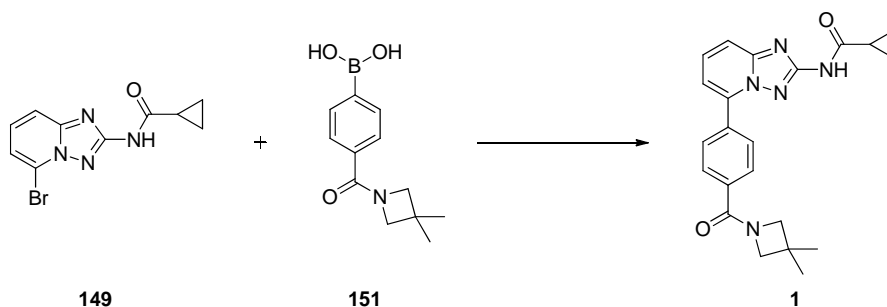


N-(5-bromo-[1,2,4]triazolo[1,5-*a*]pyridin-2-yl)cyclopropanecarboxamide **149** (3.00 g, 10.67 mmol), (4-(3,3-dimethylazetidide-1-carbonyl)phenyl)boronic acid **151** (2.61 g, 10.67 mmol), triphenylphosphine (7.0 mg, 0.027 mmol), sodium carbonate (1.131 g, 10.67 mmol), palladium(II) acetate source *a* (0.027 mmol), *n*-butanol (29 mL) and water (19 mL) were charged to an Easymax flask. The contents were stirred and the jacket temperature was set to 105°C. After *b* hours, the organic phase was sampled for HPLC analysis (Method A). The reaction mixture was filtered and the solids were washed with *n*-butanol (6 mL). The aqueous phase of the filtrate was discarded. The organic phase adjusted to 60-62 °C and seeded with *N*-(5-(4-(3,3-dimethylazetidide-1-carbonyl)phenyl)-[1,2,4]triazolo[1,5-*a*]pyridin-2-yl)cyclopropanecarboxamide IG **1** (20 mg). The mixture was cooled to 5 °C over 2 hours and continued stirring at 5 °C over the next two days. The cooled suspension was filtered and the solids were washed twice with TBME (6 mL). The solids were dried in a vacuum oven at 50 °C to give *N*-(5-(4-(3,3-dimethylazetidide-1-carbonyl)phenyl)-[1,2,4]triazolo[1,5-*a*]pyridin-2-yl)cyclopropanecarboxamide IG **1**.

Entry	Pd(OAc) ₂ source	Time (h)
	<i>a</i>	<i>b</i>
1	palladium acetate 2-mercaptoethyl ethyl sulfide silica	18
2	palladium acetate 3-mercaptoethyl ethyl sulfide silica	23
3	palladium acetate ethanoate ethyl sulfide silica	18

Entry	HPLC (Method A)					ICP-AES
	Hydrolysed aryl bromide 147% PAR	Aryl bromide 149% PAR	Boronic acid 151 % PAR	Hydrolysed product 157 % PAR	Product 1 % PAR	Pd content ^d (ppm)
1	39.8	24.0	20.3	1.5	9.3	Not isolated
2	0.9		0.13	12.0	85.1	29
3	0.6	0.8	0.3	2.9	92.6	86

Preparation of *N*-(5-(4-(3,3-dimethylazetidide-1-carbonyl)phenyl)-[1,2,4]triazolo[1,5-*a*]pyridin-2-yl)cyclopropanecarboxamide **1** in Route B using *n*-butanol/Na₂CO₃ and Subsequent Screen of Additives to Remove Palladium

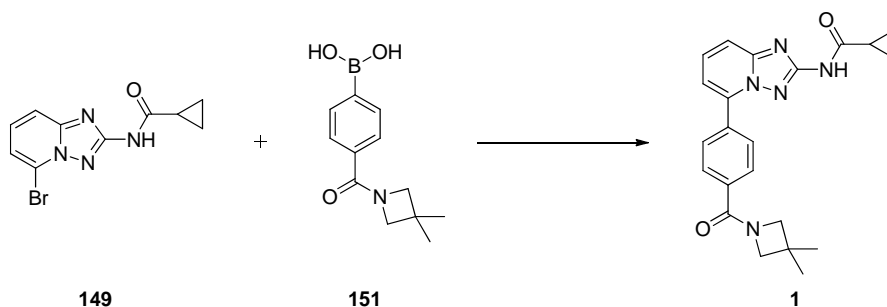


N-(5-bromo-[1,2,4]triazolo[1,5-*a*]pyridin-2-yl)cyclopropanecarboxamide **149** (5.00 g, 17.79 mmol), (4-(3,3-dimethylazetidide-1-carbonyl)phenyl)boronic acid **151** (4.35 g, 17.79 mmol), triphenylphosphine (12 mg, 44 μmol), sodium carbonate (1.89 g, 17.83 mmol), *n*-butanol (48 mL) and water (32 mL) were charged to a 100 mL flask (equipped with overhead stirrer) containing palladium(II) acetate (10 mg, 45 μmol), which was heated to reflux. After analysis by HPLC showed conversion to **1** was complete, the aqueous phase was discarded and the organic phase was split into six 10 mL portions. To each portion, a palladium scavenging reagent (0.167 g) and water (*b*) was added. The mixtures were heated at 50 °C overnight. The following morning, the mixtures were allowed to cool to room temperature. After stirring for 1 hour at room temperature, the suspensions were filtered and washed with TBME (3 mL). The isolated solids were placed in a vacuum oven at 50°C overnight to give *N*-(5-(4-(3,3-dimethylazetidide-1-carbonyl)phenyl)-[1,2,4]triazolo[1,5-*a*]pyridin-2-yl)cyclopropanecarboxamide **1**, which were analysed using ICP-AES.

Entry	Palladium scavenging reagent <i>a</i>	Water (mL) <i>b</i>	Pd content (ppm)
1	Loose Cuno R55S Powder ^a	0	16
2	Sodium diethyldithiocarbamate trihydrate	5	24
3	<i>N</i> -Acetyl- <i>L</i> -cysteine	5	10
4	Trithiocyanuric acid, trisodium salt monohydrate	5	50
5	<i>L</i> -Cysteine	5	69
6	Sodium dimethyldithiocarbamate hydrate	5	519

^a After heating overnight at 50 °C, solution filtered through Celite and filtrate seeded with **1**.

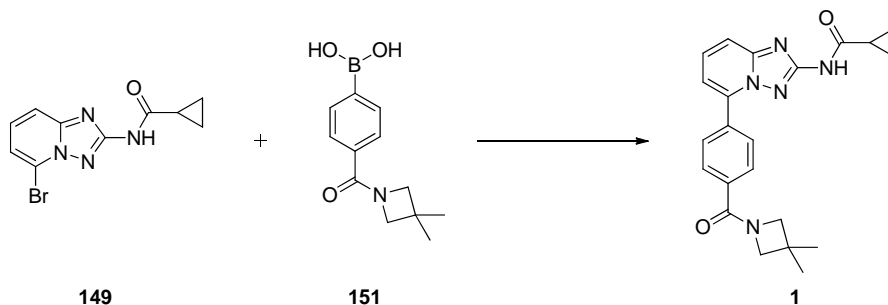
Preparation of *N*-(5-(4-(3,3-dimethylazetidene-1-carbonyl)phenyl)-[1,2,4]triazolo[1,5-*a*]pyridin-2-yl)cyclopropanecarboxamide **1** using Sodium Carbonate and *n*-Butanol in a 250 mL CLR



N-(5-bromo-[1,2,4]triazolo[1,5-*a*]pyridin-2-yl)cyclopropanecarboxamide **149** (13.00 g, 46.2 mmol), (4-(3,3-dimethylazetidene-1-carbonyl)phenyl)boronic acid **151** (11.16 g, 46.2 mmol), triphenylphosphine (0.030 g, 0.12 mmol), palladium(II) acetate (0.026 g, 0.12 mmol), sodium carbonate (4.90 g, 46.2 mmol), *n*-butanol (125 mL) and water (83 mL) were charged to a 250 mL CLR equipped with a single flight impeller. The contents were heated to reflux. After 5 hours, HPLC analysis (Method A) showed conversion to **1** was complete (90.6% **1**, 2.7% **157**, 3.3 % **149** and 0.7% **151**). The contents temperature was adjusted to 82 °C and the aqueous phase was discarded. *N*-Acetyl-*L*-cysteine (0.19 g, 1.2 mmol) followed by water (83 mL) were charged to the CLR and heated at 82 °C overnight. The following morning, the aqueous phase was discarded and the organic phase was washed with water (50 mL). The aqueous phase was discarded and the organic phase distilled at atmospheric pressure to ~5.8 vol. *n*-Butanol (75 mL) was added and the contents were distilled at atmospheric pressure to ~75 mL. The suspension was cooled to 20 °C and stirred at 20 °C for a further hour. The suspension was filtered and washed with TBME (20 mL). The damp solid was placed in a vacuum oven at 50 °C, to give

N-(5-(4-(3,3-dimethylazetidide-1-carbonyl)phenyl)-[1,2,4]triazolo[1,5-*a*]pyridin-2-yl)cyclopropanecarboxamide **1** (13.62 g, 76%), as white needles. ¹H NMR (400 MHz, DMSO-*d*₆) δ ppm 11.04 (br. s, 1 H), 8.10 (d, *J* = 8.6 Hz, 2 H), 7.81 (d, *J* = 8.6 Hz, 2 H), 7.68-7.78 (m, 2 H), 7.34-7.39 (m, 1 H), 4.06 (s, 2 H), 3.79 (s, 2 H), 2.05 (br. s, 1 H), 1.28 (s, 6 H), 0.84 (d, *J* = 6.1 Hz, 4 H); ¹³C NMR (101 MHz, DMSO-*d*₆) δ ppm 171.3 (s), 168.3 (s), 158.2 (s), 150.3 (s), 138.7 (s), 134.4 (s), 134.0 (s), 130.3 (d), 129.0 (d), 127.7 (d), 114.1 (d), 114.0 (d), 64.8 (t), 60.6 (t), 31.1 (s), 26.6 (q), 13.9 (d), 7.7 (t); IR (neat) 3252, 3147, 3088, 3023, 2950, 2912, 2871, 1680, 1625, 1553, 1522, 1507 cm⁻¹; HRMS found *m/z* 390.1920 [M+H]⁺, calcd for C₂₂H₂₄N₅O₂ 390.1925; mp 235-237 °C; HPLC (Method C): 99.2% PAR **1**, 0.11% PAR RRT 0.56, 0.44% PAR **157**; ICP-AES Na 1 ppm, Pd 13 ppm.

Preparation of *N*-(5-(4-(3,3-dimethylazetidide-1-carbonyl)phenyl)-[1,2,4]triazolo[1,5-*a*]pyridin-2-yl)cyclopropanecarboxamide **1** using Sodium Carbonate and *n*-Butanol in a 500mL CLR

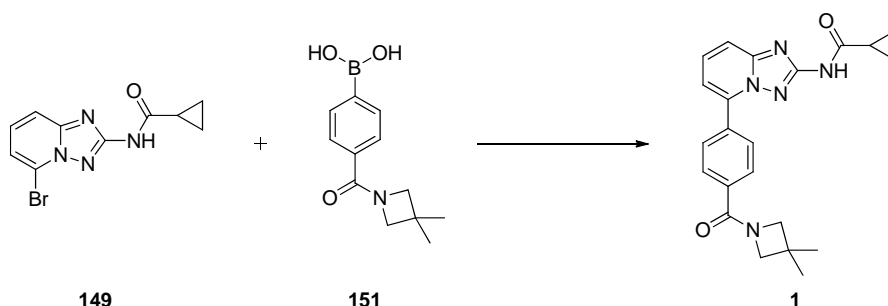


N-(5-bromo-[1,2,4]triazolo[1,5-*a*]pyridin-2-yl)cyclopropanecarboxamide **149** (26.00 g, 92 mmol), (4-(3,3-dimethylazetidide-1-carbonyl)phenyl)boronic acid **151** (22.32 g, 92 mmol), triphenylphosphine (0.061 g, 0.231 mmol), palladium(II) acetate (0.052 g, 0.231 mmol), sodium carbonate (9.80 g, 92 mmol), *n*-butanol (250 mL) and water (166 mL) were charged to a 500 mL CLR equipped with a double flight impeller. The contents were heated to reflux. After HPLC analysis (Method A) showed conversion to **1** was complete (88.9% **1**, 2.9% **157**, 4.4 % **149** and 0.9% **151**), the contents temperature was adjusted to 82 °C and the aqueous phase was discarded. The organic phase was washed with water (166 mL) and left to stand at room temperature for 3 days. Water (30 mL) was added and the contents were heated using a jacket temperature of 80 °C to ensure all solids dissolved. The organic phase

was washed with 1N H₂SO₄ solution (250 mL) and water (166 mL). The organic phase was filtered through Celite (52 g, 2 wt, pre-wetted with *n*-butanol) and washed with *n*-butanol (99 mL). The filtrate was charged back to the CLR. *N*-Acetyl-*L*-cysteine (0.377 g, 2.312 mmol), followed by water (166 mL) was charged to the CLR and the biphasic mixture was stirred for 75 minutes. The aqueous phase was discarded and the organic phase was filtered through Celite (52 g, 2 wt, pre-wetted with *n*-butanol) and washed with *n*-butanol (130 mL). The filtrate was charged to a cleaned CLR and was concentrated at atmospheric pressure to 130 mL. *n*-Butanol (130 mL) was charged to the CLR and the contents were concentrated to 130 mL at atmospheric pressure. The suspension was allowed to cool to room temperature overnight. The following morning, the suspension was filtered and washed with *n*-butanol (2 x 26 mL) washes not transferred through CLR), to give an off-white solid, which was dried in a vacuum oven at 50 °C to give *N*-(5-(4-(3,3-dimethylazetidine-1-carbonyl)phenyl)-[1,2,4]triazolo[1,5-*a*]pyridin-2-yl)cyclopropanecarboxamide **1** (9.47 g, 26%) as off-white needles. ¹H NMR (400 MHz, DMSO-*d*₆) δ ppm 11.05 (br. s, 1 H), 8.10 (d, *J* = 8.6 Hz, 2 H), 7.81 (d, *J* = 8.6 Hz, 2 H), 7.69-7.78 (m, 2 H), 7.33-7.38 (m, 1 H), 4.05 (s, 2 H), 3.79 (s, 2 H), 2.05 (br. s, 1 H), 1.28 (s, 6 H), 0.79-0.91 (m, 4 H), spectroscopic data consistent with authentic sample; HPLC (Method C) 98.5% PAR **1**, 0.86% PAR **157**, 0.15% PAR **149**, 0.13% PAR RRT 0.45, 0.10% PAR **164**, 0.10% PAR **163**, 0.08% PAR **162**; ICP-AES, 8ppm Pd.

A second crop of **1** (27.80 g, 57.2% w/w **1**, 44% yield) was recovered by dissolving the solids remaining in the CLR in dichloromethane and followed by evaporation.

Preparation of *N*-(5-(4-(3,3-dimethylazetidide-1-carbonyl)phenyl)-[1,2,4]triazolo[1,5-*a*]pyridin-2-yl)cyclopropanecarboxamide **1** in Route B Stage 3
DoE Screen



N-(5-bromo-[1,2,4]triazolo[1,5-*a*]pyridin-2-yl)cyclopropanecarboxamide **149** (6.25 g, 22.2 mmol), (4-(3,3-dimethylazetidide-1-carbonyl)phenyl)boronic acid **151** (*a*), triphenylphosphine (*b*), palladium(II) acetate (12 mg, 0.056 mmol), potassium bicarbonate (*c*), 1,3,5-trimethoxybenzene (~0.65 g, accurately weighed), and water (*d*) were added to a 250 mL Flexylab vessel equipped with an overhead stirrer. *n*-Butanol was added in order to bring the total solvent volume to 100 mL. The vessel was placed under nitrogen. The contents were heated to reflux and sampled after 3, 5, 7 and 23 hours. HPLC calibration curves (Method A) had been run for **149**, **151** and **1**, enabling the solution yield of these components to be calculated using the mass of 1,3,5-trimethoxybenzene in the reaction vessel.

Run	Equivalents of 151 <i>a</i>	mol% PPh ₃ <i>b</i>	Equivalents of KHCO ₃ <i>c</i>	Volumes of Water <i>d</i>
1	1.1	0.25	0.97	9.6
2	1	0.75	0.97	9.6
3	1.05	0.50	1.035	6.4
4	1	0.75	1.1	3.2
5	1.1	0.25	1.1	3.2
6	1.1	0.75	1.1	9.6
7	1.1	0.75	0.97	3.2
8	1	0.25	1.1	9.6
9	1	0.25	0.97	3.2
10	1.05	0.50	1.035	6.4

Variable Setting
Low
Centre Point
High

GSK CONFIDENTIAL

Solution Yield after 3 hours

Run	149	151	1
1	3.2	8.7	91.7
2	15.6	11.6	79.5
3	7.9	9.3	84.8
4	22.7	17.6	73.1
5	4.4	9.5	88.4
6	8.7	12.5	86.5
7	20.2	21.7	71.8
8	8.0	4.8	84.9
9	12.7	9.1	79.9
10	8.2	8.7	86.4

Solution Yield after 5 hours

Run	149	151	1
1	2.2	7.5	91.8
2	9.5	6.5	85.9
3	2.3	4.7	91.0
4	12.3	9.3	80.4
5	ND	5.7	93.0
6	0.8	6.7	93.8
7	13.6	17.1	80.2
8	3.3	1.0	91.0
9	6.7	4.3	87.1
10	2.9	4.5	90.4

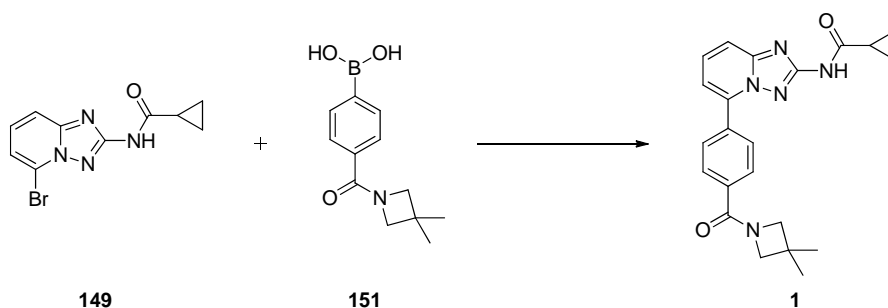
Solution Yield after 7 hours

Run	149	151	1
1	1.9	7.4	90.3
2	7.3	4.7	86.8
3	0.4	3.1	92.5
4	8.7	6.4	84.0
5	ND	5.6	93.9
6	ND	5.5	95.2
7	10.6	14.6	82.3
8	2.3	0.2	92.3
9	4.8	3.2	86.9
10	0.8	2.8	93.0

Solution Yield after 23 hours

Run	149	151	1
1	1.3	7.2	89.2
2	4.0	2.0	88.1
3	ND	2.2	93.1
4	2.7	1.4	89.0
5	ND	4.8	94.0
6	ND	5.3	92.4
7	5.0	10.0	87.2
8	1.9	ND	91.5
9	2.7	1.2	87.2
10	ND	0.7	92.4

Preparation of *N*-(5-(4-(3,3-dimethylazetidide-1-carbonyl)phenyl)-[1,2,4]triazolo[1,5-*a*]pyridin-2-yl)cyclopropanecarboxamide **1** in Route B – Comparison of Reaction conditions A, B and C

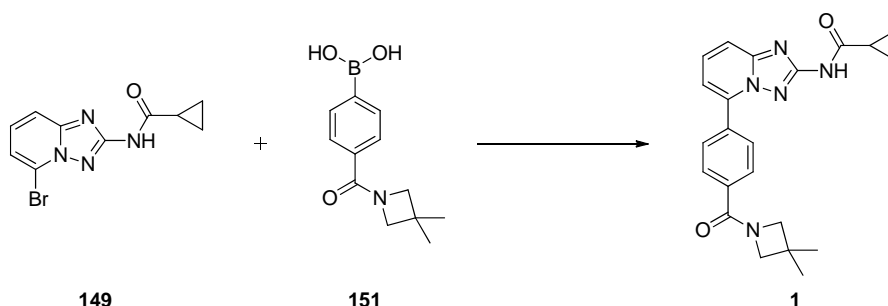


N-(5-bromo-[1,2,4]triazolo[1,5-*a*]pyridin-2-yl)cyclopropanecarboxamide **149** (1 eq, 1 wt), (4-(3,3-dimethylazetidide-1-carbonyl)phenyl)boronic acid **151** (*a*), palladium acetate (0.25 mol%), triphenylphosphine (0.25 mol%), potassium bicarbonate (*b*), *n*-butanol (*c*) and water (*d*) were charged to a 250 mL CLR and the contents were heated to reflux. The reaction mixture was monitored by HPLC analysis (Method A) until complete.

Conditions	Boronic Acid 151 (eq) <i>a</i>	KHCO ₃ (eq) <i>b</i>	<i>n</i> -Butanol (vol) <i>c</i>	Water (vol) <i>d</i>
A	1	1	9.6	6.4
B	1.05	1.04	9.6	6.4
C	1.10	1.10	6.4	9.4

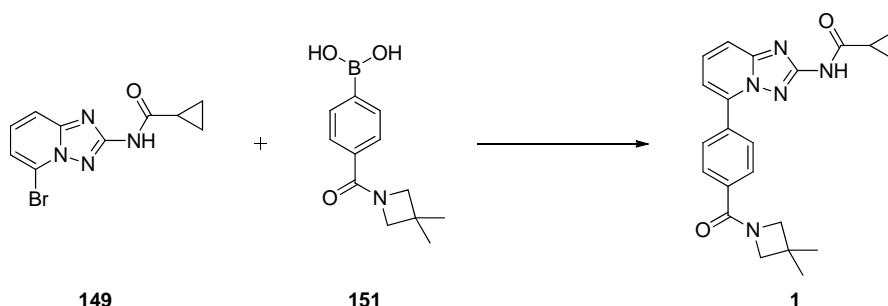
Conditions	Time h	HPLC Analysis (Method A)			
		Aryl Bromide 149 % PAR	Boronic Acid 151 % PAR	Hydrolysis Impurity 157 % PAR	Product 1 % PAR
A	6	3.9	0.8	0.5	93.9
A	21	2.3	0.2	0.7	96.0
B	2.5	2.8	1.9	0.2	94.6
C	2.5	ND	2.6	0.4	96.5

Preparation of *N*-(5-(4-(3,3-dimethylazetidide-1-carbonyl)phenyl)-[1,2,4]triazolo[1,5-*a*]pyridin-2-yl)cyclopropanecarboxamide **1** in Route B using Celite filtration



A mixture of *N*-(5-bromo-[1,2,4]triazolo[1,5-*a*]pyridin-2-yl)cyclopropanecarboxamide **149** (144.0 g, 512 mmol), (4-(3,3-dimethylazetidide-1-carbonyl)phenyl)boronic acid **151** (128.0 g, 538 mmol), palladium acetate (0.288 g, 1.3 mmol), triphenylphosphine (0.336 g, 1.3 mmol), potassium bicarbonate (53.3 g, 533 mmol), *n*-butanol (1382 mL) and water (922 mL) was heated to reflux with stirring. After HPLC analysis showed the reaction was complete, the biphasic mixture was cooled to 70 °C and the phases were allowed to separate. The aqueous phase was discarded and *N*-acetyl-*L*-cysteine (8.36 g, 51.2 mmol), followed by water (922 mL) were added to the organic phase. The biphasic mixture was stirred overnight at 67 °C. The following morning, the phases were allowed to separate and the aqueous phase was discarded. The organic phase was washed with water (922 mL). The organic phase was distilled under reduced pressure to approximately 1150 mL. *n*-Butanol (720 mL) was added to the organic phase and the mixture was distilled under reduced pressure to 1150 mL. The suspension was cooled to 20 °C and filtered and washed with *n*-butanol (2 x 288 mL). The off-white solid was placed in a vacuum oven at 50 °C overnight to give *N*-(5-(4-(3,3-dimethylazetidide-1-carbonyl)phenyl)-[1,2,4]triazolo[1,5-*a*]pyridin-2-yl)cyclopropanecarboxamide IG **1** (181.3 g, 91%) as off-white needles. ¹H NMR (400 MHz, DMSO-*d*₆) δ ppm 11.05 (s, 1 H), 8.10 (d, *J* = 8.4 Hz, 2 H), 7.81 (d, *J* = 8.4 Hz, 2 H), 7.71-7.77 (m, 2 H), 7.32-7.40 (m, 1 H), 4.06 (s, 2 H), 3.79 (s, 2 H), 2.05 (br. s, 1 H), 1.28 (s, 6 H), 0.77-0.92 (m, 4 H), spectroscopic data consistent with authentic sample; HPLC (Method C) 99.7% PAR **1**, 0.23% PAR **157**; ICP-AES Pd 29ppm.

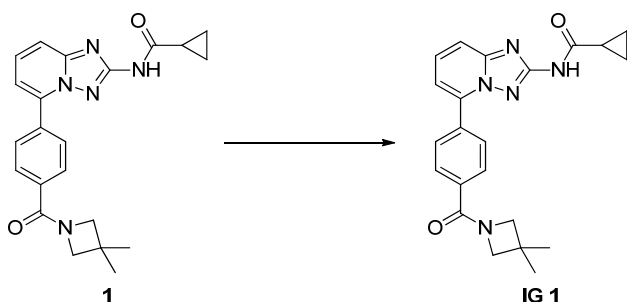
Preparation of *N*-(5-(4-(3,3-dimethylazetidide-1-carbonyl)phenyl)-[1,2,4]triazolo[1,5-*a*]pyridin-2-yl)cyclopropanecarboxamide **1** in Route B using Cuno Filtration



N-(5-bromo-[1,2,4]triazolo[1,5-*a*]pyridin-2-yl)cyclopropanecarboxamide **149** (30.00 g, 107 mmol), (4-(3,3-dimethylazetidide-1-carbonyl)phenyl)boronic acid **151** (26.20 g, 112 mmol) palladium(II) acetate (0.06 g, 267 μ mol), triphenylphosphine (0.07 g, 267 μ mol), potassium bicarbonate (11.11 g, 111 mmol), *n*-butanol (288 mL) and water (192 mL) were charged to a 500 mL CLR and the contents were heated to reflux. After HPLC analysis had shown the reaction was complete, the temperature of the mixture was adjusted to 70 °C. The aqueous phase was discarded and *N*-acetyl-*L*-cysteine (1.74 g, 10.67 mmol) followed by water (192 mL) were charged to the CLR. The biphasic mixture was stirred overnight at 70 °C. The following morning the aqueous phase was discarded and water (192 mL) was charged to the CLR. After stirring at 70 °C for 5 hours, the aqueous phase was discarded. The organic phase was passed through an R55S 90 mm Cuno disc (pre-heated in a vacuum oven and wetted with hot *n*-butanol) into a clean CLR. The Cuno disc was washed with *n*-butanol (200 mL). The combined Cuno filtrates were concentrated under reduced pressure until the contents volume reached ~240 mL. *n*-Butanol (70 mL) was charged and the contents were concentrated under reduced pressure until the contents volume reached ~180 mL. *n*-Butanol (60 mL) was charged to wash in product encrusted on the vessel walls. The suspension was held for 2 hours at 50 °C and the suspension was cooled to 20 °C. After reaching 20 °C, the suspension continued to stir overnight and the following morning, the suspension was filtered and washed with *n*-butanol (2 x 60 mL). The white solid was placed in the vacuum oven at 50 °C to give *N*-(5-(4-(3,3-dimethylazetidide-1-carbonyl)phenyl)-[1,2,4]triazolo[1,5-

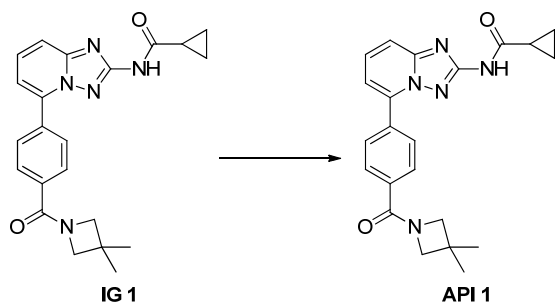
a]pyridin-2-yl)cyclopropanecarboxamide **IG 1** (37.62 g, 91%) as white needles. HPLC (Method C) 99.7% PAR **1**, 0.20% PAR **157**, HPLC data consistent with authentic sample; ICP-AES Pd 3 ppm.

Cuno purification of *N*-(5-(4-(3,3-dimethylazetidide-1-carbonyl)phenyl)-[1,2,4]triazolo[1,5-*a*]pyridin-2-yl)cyclopropanecarboxamide **IG 1**



N-(5-(4-(3,3-dimethylazetidide-1-carbonyl)phenyl)-[1,2,4]triazolo[1,5-*a*]pyridin-2-yl)cyclopropanecarboxamide **1** (50.00 g, 128 mmol), *n*-butanol (378 mL) and water (72 mL) were charged to a 1 L CLR and the contents were heated until a hazy orange solution was obtained. The solution was passed through a 90mm R55S Cuno disc (pre-heated in an oven and pre-wetted with hot *n*-butanol) to give a clear colourless solution which was transferred into a clean 500 mL CLR. *n*-Butanol (200 mL) and water (38 mL) were passed through the Cuno disc and were transferred to the clean 500 mL CLR. The contents were concentrated at reduced pressure until a volume of 320mL (6.4vol) was achieved. *n*-Butanol (250 mL) was charged to the CLR and the contents were concentrated at reduced pressure until a volume of 220 mL was obtained. *n*-Butanol (100mL) added to CLR and the contents were cooled to 50 °C, stirred for 2 hours at 50 °C for two hours and then cooled to 20 °C. The suspension was stopped from stirring and was left standing at room temperature for 3 days. The suspension was stirred for around 1 hour and then was filtered and washed with *n*-butanol (2 x 72 mL) to give a white solid which was placed in a vacuum oven at 50 °C to give *N*-(5-(4-(3,3-dimethylazetidide-1-carbonyl)phenyl)-[1,2,4]triazolo[1,5-*a*]pyridin-2-yl)cyclopropanecarboxamide **IG 1** (44.59 g, 89%) as white needles. HPLC: 100% PAR **1**, all impurities under 0.05% PAR, spectroscopic data consistent with authentic sample; ICP-AES Pd <1 ppm.

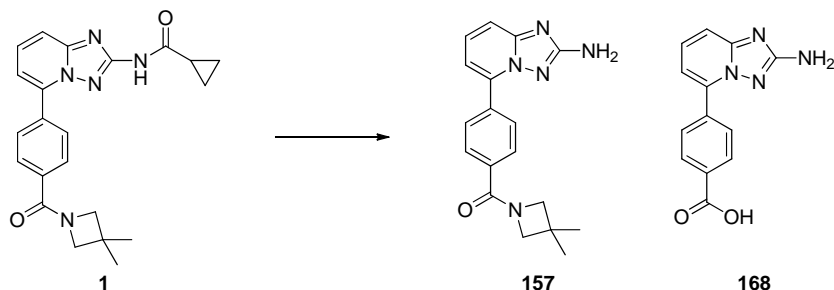
Preparation of *N*-(5-(4-(3,3-dimethylazetidide-1-carbonyl)phenyl)-[1,2,4]triazolo[1,5-*a*]pyridin-2-yl)cyclopropanecarboxamide API 1



N-(5-(4-(3,3-dimethylazetidide-1-carbonyl)phenyl)-[1,2,4]triazolo[1,5-*a*]pyridin-2-yl)cyclopropanecarboxamide **IG 1** (50.00 g, 128 mmol), IMS (360 mL) and water (90 mL) were charged to a 1 L CLR and the contents were heated until a clear solution was obtained. The solution was clarified through a Domnick Hunter 5.0 micron filter into a clean pre-heated CLR. The Domnick Hunter filter was washed with 4:1 IMS/water (50 mL). Once a solution was obtained, the contents temperature was adjusted to 60 °C. **API 1** (0.25 g, 642 μmol), followed by water (2 mL) was added to the solution. The contents were aged at 60 °C for 1 hour and then cooled to 5 °C. After 2 hours at 5 °C, the suspension was filtered and washed with 4:1 IMS/water (2 x 85 mL). The white solid was dried in a vacuum oven at 50 °C to give *N*-(5-(4-(3,3-dimethylazetidide-1-carbonyl)phenyl)-[1,2,4]triazolo[1,5-*a*]pyridin-2-yl)cyclopropanecarboxamide **API 1** (40.57 g, 81%) as white prisms. ¹H NMR (400 MHz, DMSO-*d*₆) δ ppm 11.04 (br. s, 1 H) 8.09 (d, *J* = 8.4 Hz, 2 H) 7.80 (d, *J* = 8.4 Hz, 2 H) 7.67 -7.76 (m, 2 H) 7.29-7.40 (m, 1 H) 4.04 (s, 2 H) 3.77 (s, 2 H) 2.03 (br. s, 1 H) 1.27 (s, 6 H); ¹³C NMR (101 MHz, DMSO-*d*₆) δ ppm 171.3 (s), 168.3 (s), 158.2 (s), 150.3 (s), 138.7 (s), 134.4 (s), 134.0 (s), 130.3 (d) 129.0 (d) 127.7 (d), 114.1 (d) 114.0 (d), 64.8 (t), 60.6 (t), 31.1 (s) 26.6 (q), 13.9 (d), 7.7 (t) ; IR (neat) 3217, 3084, 2957, 2877, 1710, 1610, 1550 cm⁻¹; HRMS found *m/z* 390.1920 [M+H]⁺, calcd for C₂₂H₂₄N₅O₂ 390.1925; mp 240-242 °C; HPLC: 99.9% **PAR 1**, all impurities under 0.05% **PAR**, HPLC data consistent with authentic sample.

4.3 Experimental Details for Chapter 3

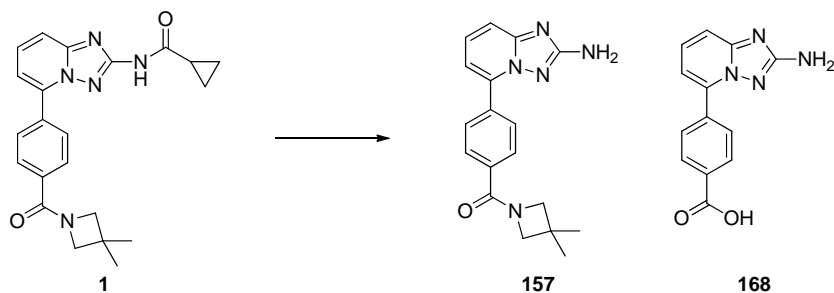
Preparation of (4-(2-amino-[1,2,4]triazolo[1,5-*a*]pyridin-5-yl)phenyl)(3,3-dimethylazetididin-1-yl)methanone **157** from *N*-(5-(4-(3,3-dimethylazetididine-1-carbonyl)phenyl)-[1,2,4]triazolo[1,5-*a*]pyridin-2-yl)cyclopropanecarboxamide **1**



To a reaction vial, was added *N*-(5-(4-(3,3-dimethylazetididine-1-carbonyl)phenyl)-[1,2,4]triazolo[1,5-*a*]pyridin-2-yl)cyclopropanecarboxamide **1** (0.20 g, 514 μ mol), solvent *a*, 50% aqueous potassium hydroxide solution (3 eq) and water (*b*). The contents were stirred and heated at temperature *c* for time *d*. The reaction mixtures were sampled for HPLC analysis (Method B UV detector at 220 nm).

Entry	Solvent <i>a</i>	Water (mL) <i>b</i>	Temperature (°C) <i>c</i>	Time <i>d</i>	HPLC Analysis		
					168 % PAR	Metabolite 157 % PAR	Drug Substance 1 % PAR
1	THF (2 mL)	0	50	Overnight	ND	1.0	99.0
2	1,4-Dioxane (1 mL)	1	90-95	30 min	59.1	10.2	26.9

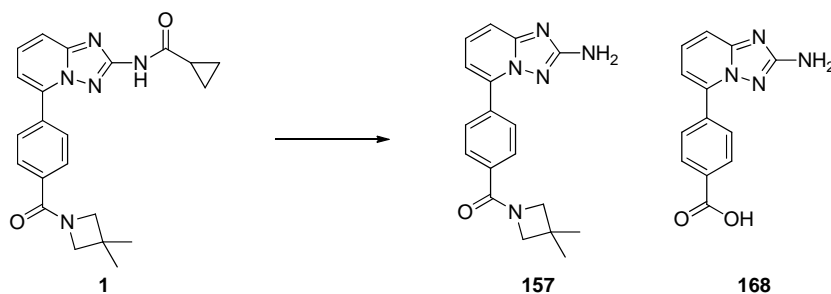
Preparation of (4-(2-amino-[1,2,4]triazolo[1,5-*a*]pyridin-5-yl)phenyl)(3,3-dimethylazetididin-1-yl)methanone **157** from *N*-(5-(4-(3,3-dimethylazetididine-1-carbonyl)phenyl)-[1,2,4]triazolo[1,5-*a*]pyridin-2-yl)cyclopropanecarboxamide **1**



To a reaction vial, was added *N*-(5-(4-(3,3-dimethylazetididine-1-carbonyl)phenyl)-[1,2,4]triazolo[1,5-*a*]pyridin-2-yl)cyclopropanecarboxamide **1** (0.20 g, 514 μmol), solvent *a* (1 mL), base *b* (2 eq) and water (1 mL). The contents were stirred and heated at 45 °C overnight. The reaction mixtures were sampled for HPLC analysis (Method B UV detector at 230 nm).

Entry	Solvent <i>a</i>	Base <i>b</i>	168% PAR	Metabolite 157% PAR	Drug Substance 1% PAR
1	CPME	KOH	8.5	9.0	81.8
2	CPME	NaOH	3.7	3.4	92.3
3	CPME	LiOH	13.3	7.6	75.0
4	1,4-Dioxane	KOH	45.3	22.7	7.9
5	1,4-Dioxane	NaOH	40.7	19.5	11.7
6	1,4-Dioxane	LiOH	3.3	3.8	91.1

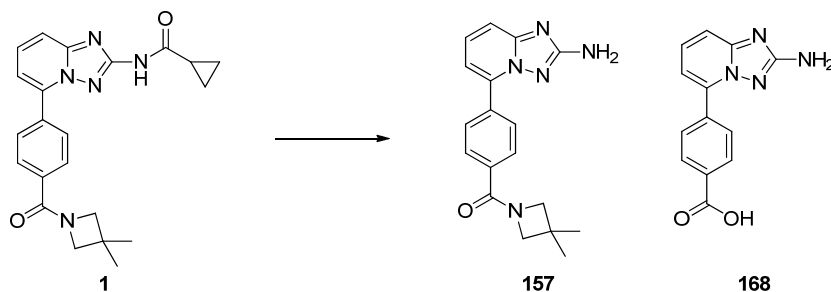
Preparation of (4-(2-amino-[1,2,4]triazolo[1,5-*a*]pyridin-5-yl)phenyl)(3,3-dimethylazetididin-1-yl)methanone **157** from *N*-(5-(4-(3,3-dimethylazetididine-1-carbonyl)phenyl)-[1,2,4]triazolo[1,5-*a*]pyridin-2-yl)cyclopropanecarboxamide **1**



To a reaction vial, was added **1** (0.20 g, 514 μmol), tetrahydrofuran (2 mL) and acid *a* (1.2 eq). The contents were stirred and heated at 53 °C overnight. The reaction mixtures were sampled for HPLC analysis (Method B, UV detector at 220 nm).

Entry	Acid	168% PAR	Metabolite 157% PAR	Drug Substance 1% PAR
1	2M HCl (aq)	4.7	48.0	38.5
2	Acetic Acid	-	-	99.9
3	1M H ₂ SO ₄ (aq)	0.6	28.0	69.8

Preparation of 4-(2-amino-[1,2,4]triazolo[1,5-*a*]pyridin-5-yl)benzoic acid **168** and (4-(2-amino-[1,2,4]triazolo[1,5-*a*]pyridin-5-yl)phenyl)(3,3-dimethylazetid-1-yl)methanone **157** from *N*-(5-(4-(3,3-dimethylazetid-1-yl)phenyl)-[1,2,4]triazolo[1,5-*a*]pyridin-2-yl)cyclopropanecarboxamide **1**

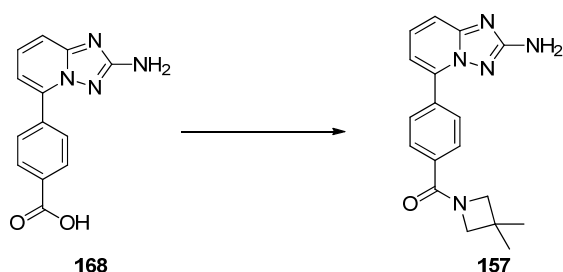


Tetrahydrofuran (THF) (300 mL) was added to *N*-(5-(4-(3,3-dimethylazetid-1-yl)phenyl)-[1,2,4]triazolo[1,5-*a*]pyridin-2-yl)cyclopropanecarboxamide **1**, (30.00 g, 77 mmol) and the suspension was stirred under nitrogen. Water (200 mL) was added to the suspension. Sulfuric acid (8.2 mL, 154 mmol) was added dropwise. Water (100 mL) was added and the reaction mixture was heated to reflux for 64 hours. The reaction mixture was allowed to cool to room temperature and stirred for a further 24 hours. The suspension was filtered and washed with tetrahydrofuran (60 mL) to give a white solid, which was dried in a vacuum oven set at 50 °C to give 4-(2-amino-[1,2,4]triazolo[1,5-*a*]pyridin-5-yl)benzoic acid **168** as a white powder (4.50 g, 23%). ¹H NMR (400 MHz, DMSO-*d*₆) δ ppm 8.02-8.18 (m, 4 H), 7.80 (dd, *J* = 8.4, 7.6 Hz, 1 H), 7.60 (dd, *J* = 8.4, 0.8 Hz, 1 H), 7.38 (dd, *J* = 7.6, 0.8 Hz, 1 H); ¹³C (100 MHz, DMSO-*d*₆) δ ppm 166.8 (s), 161.1 (s), 147.5 (s), 138.4 (s), 135.6 (s), 131.9 (d), 131.8 (d), 129.4 (d), 128.2 (d), 114.9 (d), 110.8 (d); IR (neat) 3176, 1720, 1672, 1573, 1529, 1504 cm⁻¹; HRMS found *m/z* 255.0874 [M+H]⁺, calcd for C₁₃H₁₀N₄O₂ 255.0877; mp 297-299 °C (dec.).

2-methyltetrahydrofuran (200 mL) and water (200 mL) were added to the filtrate. The pH of the aqueous phase was adjusted from pH 1.5 to pH 6.9 with 40% w/v aqueous potassium carbonate solution (79 mL). The neutralised suspension was left to stir overnight at room temperature. The suspension was filtered and washed with 2-methyltetrahydrofuran (100 mL) to give a white solid, which was dried in a vacuum oven at 50 °C to give (4-(2-amino-[1,2,4]triazolo[1,5-*a*]pyridin-5-

yl)phenyl)(3,3-dimethylazetididin-1-yl)methanone **157** as a white powder (17.88 g, 72%). ^1H NMR (400 MHz, $\text{DMSO-}d_6$) δ ppm 8.04 (d, $J = 8.4$ Hz, 2 H), 7.78 (d, $J = 8.3$ Hz, 2 H), 7.53 (dd, $J = 8.8, 7.6$ Hz, 1 H), 7.41 (dd, $J = 8.8, 1.2$ Hz, 1 H), 7.07 (dd, $J = 7.6, 1.2$ Hz, 1 H), 6.06 (s, 2 H), 4.03 (s, 2 H), 3.78 (s, 2 H), 1.26 (s, 6 H); ^{13}C (100 MHz, $\text{DMSO-}d_6$) δ ppm 168.4 (s), 165.8 (s), 151.3 (s), 137.7 (s), 134.7 (s), 134.1 (s), 129.0 (d), 128.8 (d), 127.6 (d), 111.9 (d), 64.9 (t), 60.59 (t), 31.05 (s), 28.53 (q); IR (neat) 3347, 1626, 1553, 1515 cm^{-1} ; HRMS found m/z 321.1580 $[\text{M}+\text{H}]^+$, calcd for $\text{C}_{18}\text{H}_{19}\text{N}_5\text{O}$ 321.1584; mp. 212-214 $^\circ\text{C}$.

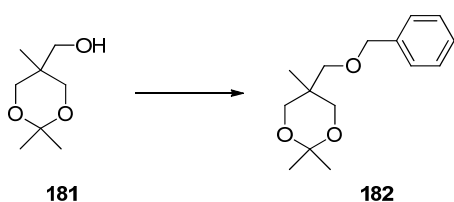
Preparation of (4-(2-amino-[1,2,4]triazolo[1,5-a]pyridin-5-yl)phenyl)(3,3-dimethylazetididin-1-yl)methanone **157** from -(2-amino-[1,2,4]triazolo[1,5-a]pyridin-5-yl)benzoic acid **168**



Dichloromethane (2 mL) was added to 4-(2-amino-[1,2,4]triazolo[1,5-a]pyridin-5-yl)benzoic acid **168** (0.200 g, 790 μmol) to give a white suspension which was stirred. CDI (0.15 g, 940 μmol) was added and the solids were washed in with dichloromethane (2 mL). After 2 hours 15 minutes, DMSO (2 mL) was added to the reaction mixture. After a further 40 minutes, CDI (0.15 g, 940 μmol) was added to the reaction mixture. After stirring for 90 minutes, HPLC analysis showed activation of **168** was complete. 3,3-dimethylazetididine hydrochloride (0.12 g, 940 μmol) was dissolved in dichloromethane (2 mL) and the solution was added to the reaction mixture. The reaction mixture was held at room temperature overnight. The following morning, water (6 mL) was added to the reaction mixture. The aqueous phase was discarded and ethyl acetate (12 mL) was added dropwise to the organic phase. After stirring for several hours at room temperature, the suspension was filtered and washed with ethyl acetate (10 mL) to give a white solid, which was dried in air overnight to give (4-(2-amino-[1,2,4]triazolo[1,5-a]pyridin-5-

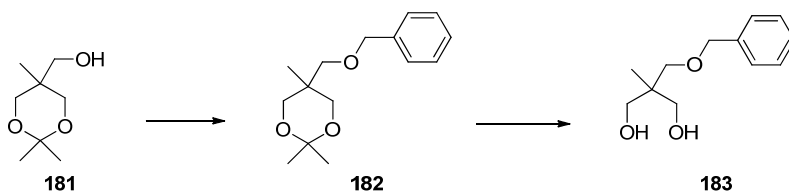
yl)phenyl)(3,3-dimethylazetidin-1-yl)methanone **157** as a white powder (0.097 g, 38%). ^1H NMR (400 MHz, $\text{DMSO-}d_6$) δ ppm 8.04 (d, $J = 8.3$ Hz, 2 H), 7.78 (d, $J = 8.3$ Hz, 2 H), 7.55 (dd, $J = 8.8, 7.2$ Hz, 1 H), 7.41 (dd, $J = 8.8, 1.2$ Hz, 1 H), 7.09 (dd, $J = 7.2, 1.2$ Hz, 1 H), 6.04 (s, 2 H), 4.04 (s, 2 H), 3.78 (s, 2 H), 1.27 (s, 6 H); ^{13}C (100 MHz, $\text{DMSO-}d_6$) δ ppm 168.4 (s), 165.7 (s), 151.3 (s), 137.7 (s), 134.7 (s), 134.0 (s), 129.1 (d), 127.6 (d), 111.9 (d), 111.8 (d), 64.9 (t), 60.8 (t), 31.1 (s), 26.5 (q), spectroscopic data consistent with authentic sample; HPLC (Method A) 100% PAR **157**.

Preparation of 5-((benzyloxy)methyl)-2,2,5-trimethyl-1,3-dioxane **182**



Ground sodium hydroxide (0.197 g, 4.94 mmol) and tetrabutylammonium hydrogen sulfate (0.403 g, 1.187 mmol) were added to a stirred solution of (2,2,5-trimethyl-1,3-dioxan-5-yl)methanol **181** (0.507 g, 3.16 mmol) in THF (5 mL) under nitrogen. Benzyl chloride (0.423 mL, 3.64 mmol) was added and the reaction mixture was heated to reflux. After 90 minutes, ^1H NMR analysis showed 63 mol% **182** and 37 mol% **181**. After 20 hours, ^1H NMR analysis showed 79% mol% **182** and 21 mol% **181**.

Preparation of 2-((benzyloxy)methyl)-2-methylpropane-1,3-diol **183**

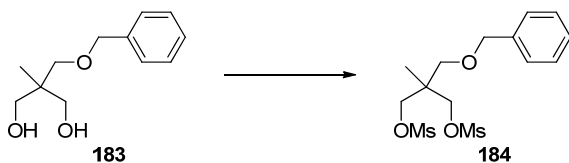


5-Hydroxymethyl-2,2,5-trimethyl-1,3-dioxane **181** (1.00 g, 6.2 mmol) and benzyl bromide (0.9 mL, 7.5 mmol) was dissolved in toluene (10 mL) and TBAB (0.302 g, 940 μmol) was added followed by 2M sodium hydroxide solution (10 mL, 20.0 mmol). The mixture was stirred and heated to reflux. After 2.5 hours, an aliquot of benzyl bromide (1.0 mL, 8.4 mmol) was added. The reaction mixture was heated at

reflux for a further 2 hours and then was allowed to cool to room temperature overnight. The aqueous phase was removed and the organic phase was returned to the reaction flask. 38% sodium hydroxide solution was added (2.5 mL, 23.8 mmol), together with fresh TBAB (0.20 g, 620 μ mol) and benzyl bromide (1.0 mL, 8.4 mmol) and mixture stirred vigorously at ambient temperature for 5 days. The aqueous phase was removed and the organic phase was washed with water (10 mL) and 80% aqueous methanol (4 x 5 mL). The solvent was removed under vacuum to give 5-((benzyloxy)methyl)-2,2,5-trimethyl-1,3-dioxane **182** as a pale yellow oil (mass not obtained). ^1H NMR (400 MHz, CDCl_3) δ ppm 7.11-7.48 (m, 5 H), 4.54 (s, 2 H), 3.74 (d, $J = 11.94$ Hz, 2 H), 3.56 (d, $J = 11.94$ Hz, 2 H), 3.47 (s, 2 H), 1.43 (s, 3 H), 1.38 (s, 3 H), 0.90 (s, 3 H); IR (solution) 2941, 2865, 1717 cm^{-1} .

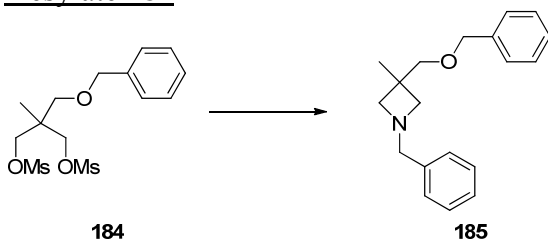
The pale yellow oil was diluted with water (50 mL) and was heated to reflux under Dean and Stark conditions for 2 hours to remove benzyl bromide. The following morning, the mixture was distilled at atmospheric pressure. The residue was diluted with water (20 mL) extracted with toluene (2 x 15 mL) and the combined organic phases were dried over sodium sulfate. The solvent was removed under vacuum to give a pale yellow oil (1.77 g). The oil was dissolved in methanol (15 mL), 2M HCl (10 mL) was added and the mixture was stirred at ambient for 1 h. The mixture was further diluted with water (20 mL) and the biphasic mixture was washed with n-heptane (2 x 10 mL). The organic phase was discarded. The aqueous phase was washed with 2-methyltetrahydrofuran (2 x 15 mL) using a small quantity of TBME to aid the separations (5 to 10 mL for each extraction). The combined organic phases were dried and the solvent was removed under vacuum to afford 2-((benzyloxy)methyl)-2-methylpropane-1,3-diol **183** as a colourless oil (0.81 g, 62%), which solidified on standing. ^1H NMR (400 MHz, CDCl_3) δ ppm 7.27-7.40 (m, 5 H), 4.52 (s, 2 H), 3.67-3.78 (m, 2 H), 3.55-3.64 (m, 2 H), 3.47 (s, 2 H), 2.36 (s, 2 H), 0.83 (s, 3 H); ^{13}C (100 MHz, CDCl_3) δ ppm 137.9 (s), 128.5 (d), 127.9 (d), 127.6 (d), 75.7 (t), 73.7 (t), 68.1 (t) 40.9 (s), 17.2 (q); IR (neat) 3274, 2956, 2936, 2875 cm^{-1} ; HRMS found m/z 211.1328 $[\text{M}+\text{H}]^+$, calcd for $\text{C}_{12}\text{H}_{19}\text{O}_3$ 211.1329; mp. 44-46 $^\circ\text{C}$.

Preparation of 2-((benzyloxy)methyl)-2-methylpropane-1,3-diyl dimethanesulfonate **184**



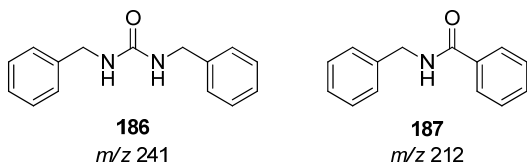
Triethylamine (0.28 mL, 2.0 mmol) and THF (1 mL) were added to 2-((benzyloxy)methyl)-2-methylpropane-1,3-diol **183** (0.20 g, 0.95 mmol) and the mixture was cooled in a ice/water bath for around 30 minutes. Methanesulfonyl chloride (0.15 mL, 1.9 mmol) was charged (CAUTION: Highly exothermic reaction). After 2 hours, the reaction mixture was partitioned between dichloromethane (5 mL) and water (5 mL). The aqueous phase was discarded. The organic phase was evaporated to give 2-((benzyloxy)methyl)-2-methylpropane-1,3-diyl dimethanesulfonate **184** as an orange oil (0.30 g, 86%). ^1H NMR (400 MHz, CDCl_3) δ ppm 7.22 - 7.41 (m, 5 H), 4.50 (s, 2 H), 4.16 (d, $J = 9.6$ Hz, 2 H), 4.13 (d, $J = 9.6$ Hz, 2 H), 3.37 (s, 2 H), 2.99 (s, 6 H), 1.10 (s, 3 H); ^{13}C (100 MHz, CDCl_3) δ ppm 137.6 (s), 128.5 (d), 127.9 (d), 127.7 (d), 73.5 (t), 71.0 (t), 70.7 (t), 40.0 (s), 37.1 (q), 16.7 (q); IR (neat) 3040, 2940, 2867 cm^{-1} ; HRMS found m/z 367.0883 $[\text{M}+\text{H}]^+$, calcd for $\text{C}_{14}\text{H}_{23}\text{O}_7\text{S}_2$ 367.0880.

Preparation of 1-benzyl-3-((benzyloxy)methyl)-3-methylazetidene **185** from bis-mesylate **184**

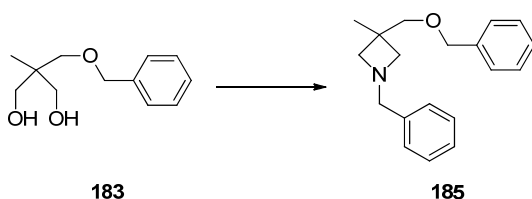


Benzylamine (1 mL, 9.16 mmol) was added to 2-((benzyloxy)methyl)-2-methylpropane-1,3-diyl dimethanesulfonate **184** (0.25g) and the mixture was stirred to give a solution. 8M Sodium hydroxide (0.085 mL, 0.682 mmol) was added to the reaction vessel and the contents were heated in a DrySyn bath set at 90°C. After 3 days, the reaction mixture was sampled for LC-MS analysis, which showed 2.5% **185**. The following day, the reaction mixture was stopped from heating. Once cooled

to room temperature, the reaction mixture was partitioned between benzylamine (2 mL) and water (4 mL) and the phases were left to separate overnight. The lower phase was washed with cyclohexane (10 mL). The aqueous phase was sampled for LC-MS analysis which showed 46 and other impurities. Using ^1H NMR and HRMS, the following structures for the impurities were proposed to be **186** and **187**.

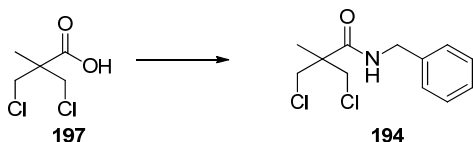


Preparation of 1-benzyl-3-((benzyloxy)methyl)-3-methylazetididine **185** from diol **183**



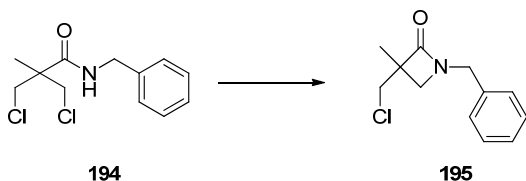
2-((Benzyloxy)methyl)-2-methylpropane-1,3-diol **183** (0.21 g, 1.0 mmol) was stirred in dry acetonitrile (10 mL) at -20 °C. Triflic anhydride (0.355 mL, 2.1 mmol) was added over 10 minutes followed by DIPEA (0.437 mL, 2.5 mmol). The solution was stirred for 10 minutes at -20 to -30 °C and then further DIPEA (0.437 mL, 2.5 mmol) was added. Benzylamine (0.104 mL, 0.95 mmol) was added and the dark solution heated at 70 - 75 °C overnight.

The reaction mixture was concentrated to give a dark solid which was dissolved in dichloromethane (10 mL) and the solution washed with water (2 x 10 mL). The organic solution was dried over magnesium sulphate and concentrated to give a dark brown oil (0.70 g). The brown oil (0.20 g) was purified by MDAP to give 1-benzyl-3-((benzyloxy)methyl)-3-methylazetididine **185** as a clear oil (15 mg, 19%). ^1H NMR (400 MHz, CDCl_3) δ ppm 7.13-7.50 (m, 10 H), 4.57 (s, 2 H), 3.76 (s, 2 H), 3.43 (s, 2 H), 3.36 (d, $J = 8.1$ Hz, 2 H), 3.17 (d, $J = 8.1$ Hz, 2 H), 1.29 (s, 3 H); ^{13}C (100 MHz, CDCl_3) δ ppm 138.4 (s), 130.9 (s), 128.8 (d), 128.5 (d), 128.4 (d), 127.7 (d), 127.6 (d), 127.5 (d), 75.8 (t), 73.4 (t), 62.0 (t), 61.7 (t), 35.4 (s), 22.6 (q).

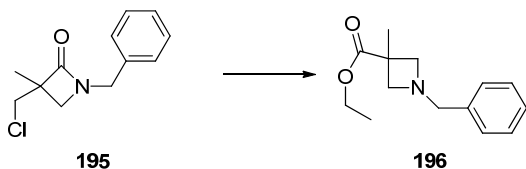
Preparation of *N*-benzyl-3-chloro-2-(chloromethyl)-2-methylpropanamide **194**

A solution of dichloropivalic acid **197** (20.00 g, 117 mmol) in dichloromethane (60 mL) was added to a solution of thionyl chloride (10.0 mL, 137 mmol) in dichloromethane (80 mL) cooled in an ice bath under nitrogen. DIPEA (24.5 mL, 140 mmol) in dichloromethane (20 mL) was added to the cooled reaction mixture dropwise, followed by dichloromethane (10 mL). After 2 hours, benzylamine (15.0 mL, 137 mmol) was added dropwise to the cooled reaction vessel, followed by DIPEA (24.5 mL, 140 mmol). After 4 hours, the reaction mixture was cooled in an ice bath and water (200 mL) was added dropwise to the reaction mixture. The biphasic mixture was stirred for around 60 minutes and then was left to stand at room temperature overnight.

The following morning, the aqueous phase was washed with dichloromethane (50 mL). The organic phases were combined and washed with 0.5M NaOH solution (200 mL). The aqueous phase was washed with dichloromethane (50 mL). The organic phases were combined and washed with 0.5M HCl solution (200 mL). The aqueous phase was washed with dichloromethane (50 mL). The combined organic phase was evaporated to give *N*-benzyl-3-chloro-2-(chloromethyl)-2-methylpropanamide **194** as a brown amorphous solid (31.52g, crude). The product was used without further purification. ¹H NMR (400 MHz, CDCl₃) δ ppm 7.20-7.37 (m, 5 H), 6.41 (br. s, 1 H), 4.45 (d, *J* = 5.6 Hz, 2 H), 3.79 (d, *J* = 11.2 Hz, 2 H), 3.69 (d, *J* = 11.2 Hz, 2 H), 1.39 (s, 3 H); ¹³C (100 MHz, CDCl₃) δ ppm 171.7 (s), 137.7 (s), 128.78 (d), 128.75 (d), 127.6 (d), 49.3 (s), 48.8 (t), 43.9 (t), 19.2 (q); IR (neat) 3321, 3088, 2981, 2928, 1655, 1629, 1549 cm⁻¹; HRMS found *m/z* 260.0599 [M+H]⁺, calcd for C₁₂H₁₆³⁵Cl₂NO, 260.0604; mp. 60-63 °C.

Preparation of 1-benzyl-3-(chloromethyl)-3-methylazetidin-2-one **195**

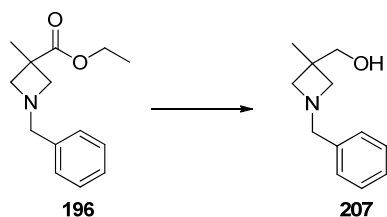
Dichloromethane (300 mL) was added to tetrabutylammonium bromide (3.73 g, 11.6 mmol) and the solution was added to *N*-benzyl-3-chloro-2-(chloromethyl)-2-methylpropanamide **194** (31.26 g, 116 mmol), to give a dark brown solution, which was stirred. Sodium hydroxide (145 mL, 1158 mmol) was added to the reaction mixture. After 1 hour 45 minutes, water (300 mL) was added to the reaction flask and the phases were allowed to separate. The aqueous phase was washed with dichloromethane (50 mL). The organic phases were combined and washed with water (300 mL). The aqueous phase was washed with dichloromethane (50 mL). The combined organic phase was washed with water (300 mL). The aqueous phase was washed with dichloromethane (50 mL) and the combined organic phase was evaporated to give 1-benzyl-3-(chloromethyl)-3-methylazetidin-2-one **195** as a brown liquid (28.09g, crude). The product was used without further purification. ^1H NMR (400 MHz, CDCl_3) δ ppm 7.19-7.40 (m, 5 H), 4.41 (d, $J = 15.2$ Hz, 1 H), 4.37 (d, $J = 15.2$ Hz, 1 H), 3.72 (d, $J = 11.2$ Hz, 1 H), 3.59 (d, $J = 11.6$ Hz, 1 H), 3.26 (d, $J = 5.7$ Hz, 1 H), 2.91 (d, $J = 5.8$ Hz, 1 H), 1.41 (s, 3 H); ^{13}C (100 MHz, CDCl_3) δ ppm 169.69 (s), 135.33 (s) 128.87 (d) 128.19 (d) 127.85 (d) 55.97 (s) 50.27 (t) 46.91 (t) 45.84 (t) 17.62 (q); IR (neat) 2966, 1741, 1604 cm^{-1} ; HRMS found m/z 224.0836 $[\text{M}+\text{H}]^+$, calcd for $\text{C}_{12}\text{H}_{15}^{35}\text{ClNO}$, 224.0837.

Preparation of ethyl 1-benzyl-3-methylazetidine-3-carboxylate **196**

Ethanol (150 mL) was added to 1-benzyl-3-(chloromethyl)-3-methylazetidin-2-one **195** (27.83 g, 115 mmol) and the brown solution was added to a 3 neck 500 mL reaction flask containing sodium ethoxide (17.17 g, 252 mmol) and ethanol (80 mL).

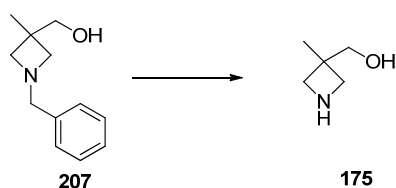
The solution was washed in with ethanol (110 mL) and the contents were heated to reflux. After 4 hours 15 minutes, sodium ethoxide (4.29 g, 63.0 mmol) was added to the reaction mixture. The solids were washed in with ethanol (30 mL). After 1 hour, the reaction mixture was allowed to cool and was evaporated. Chloroform (200 mL), followed by water (200 mL) was added to the residue. The aqueous phase was washed with chloroform (200 mL). The organic phases were combined and evaporated to give a brown liquid (34.03 g). The brown liquid was loaded on to a 375 g Biotage KP NH column and the column was eluted with 12% v/v EtOAc in heptane over 1 column volume, 12% v/v EtOAc in heptane increasing to 34% v/v EtOAc in heptane over 2.5 column volumes. 16 fractions of 120 mL were collected. Fractions containing the desired product were combined and evaporated to give an orange liquid (18.73 g).

The orange liquid was transferred to a round bottom flask containing succinic anhydride (2.11 g, 21.1 mmol). The orange liquid was washed in with toluene (54 mL) and pyridine (1.6 mL, 19.8 mmol) was added. The reaction mixture was heated at 70–80 °C for 15 minutes. The reaction mixture was cooled to room temperature. 0.5M sodium hydroxide solution (54 mL) was added to the reaction mixture. The aqueous phase was washed with toluene (18 mL). The toluene back extraction was washed with 0.5M sodium hydroxide solution (18 mL). The organic phases were combined and washed with 0.5M HCl solution twice (80 mL, followed by 50 mL). The acidic aqueous phases were combined and 50% wt sodium hydroxide aqueous solution (3 mL) and toluene (120 mL) was added to the aqueous phase. The organic phase was retained. 50% wt sodium hydroxide solution (3 mL) and toluene (90 mL) were added to the aqueous phase. The organic phases were combined and evaporated to give ethyl 1-benzyl-3-methylazetidone-3-carboxylate **196** as a yellow liquid (13.29 g, 45%). ¹H NMR (400 MHz, CDCl₃) δ ppm 7.18-7.33 (m, 5 H), 4.15 (q, *J* = 7.1 Hz, 2 H), 3.61 (s, 2 H), 3.47 (d, *J* = 7.6 Hz, 2 H), 3.13 (d, *J* = 7.8 Hz, 2 H), 1.53 (s, 3 H), 1.25 (t, *J* = 7.1 Hz, 3 H); ¹³C (100 MHz, CDCl₃) δ ppm 175.7 (s), 138.1 (s), 128.4 (d), 128.3 (d), 127.0 (d), 63.2 (t), 62.9 (t), 60.7 (t), 39.9 (s), 22.6 (q), 14.2 (q); IR (neat) 3035, 2976, 2932, 2829, 1729 cm⁻¹; HRMS found *m/z* 234.1487 [M+H]⁺, calcd for C₁₄H₂₀O₂N, 234.1489.

Preparation of (1-benzyl-3-methylazetididin-3-yl)methanol **207**

Lithium aluminium hydride (104 mL, 104 mmol) was added to a 3 neck round bottom flask under nitrogen and was washed in with tetrahydrofuran (20 mL). The solution was stirred and to it was added a solution of ethyl 1-benzyl-3-methylazetididine-3-carboxylate **196** (12.98 g, 50.6 mmol) in tetrahydrofuran (70 mL) over 25 minutes, keeping the contents temperature below 30 °C. The solution was washed in with tetrahydrofuran (20 mL). After 45 minutes, 1:1 THF/water (30 mL) was added to the reaction mixture over 1 hour 45 minutes keeping the contents temperature under 30 °C. The contents of the reaction flask were filtered and the solids were washed with 1:1 THF/water (70 mL). The filtrate was partitioned between dichloromethane and water. The aqueous phase was washed with dichloromethane. The organic phases were combined and evaporated to give (1-benzyl-3-methylazetididin-3-yl)methanol **207** as a clear colourless liquid (7.79 g, 72%). ¹H NMR (400 MHz, CDCl₃) δ ppm 7.08-7.51 (m, 5 H), 3.84 (br. s, 1 H), 3.47-3.68 (m, 4 H), 3.28 (d, *J* = 7.3 Hz, 2 H), 2.89 (d, *J* = 7.3 Hz, 2 H), 1.13 (s, 3 H); ¹³C (100 MHz, CDCl₃) δ ppm 138.0 (s) 128.4 (d) 128.3 (d) 127.0 (d) 69.1 (t) 63.1 (t) 62.7 (t) 36.9 (s) 22.0 (q); IR (neat) 3089, 3062, 3029, 2948, 2925, 2823, 1606, 1587 cm⁻¹; HRMS found *m/z* 192.1382 [M+H]⁺, calcd for C₁₂H₁₇NO 192.1383.

Further (1-benzyl-3-methylazetididin-3-yl)methanol **207** was recovered by washing the filtered solids with 1:1 tetrahydrofuran/water, extracting into dichloromethane and concentration to give a yellow oil (2.53 g, 23%).

Preparation of (3-methylazetididin-3-yl)methanol **175** - screen of reaction conditions

GSK CONFIDENTIAL

Reaction vessels were loaded with (1-benzyl-3-methylazetid-3-yl)methanol **207** (0.20 g) and methanol (3 mL). Catalyst *a* and acetic acid *b* was added to each of the vessels. The reaction vessels were placed under 3 bar H₂ and heated at 55 °C. After 15 hours 30 minutes, the reaction mixtures were allowed to cool. Each reaction mixture was filtered through a pad of Celite, which was washed with methanol. The filtrate was evaporated to give (3-methylazetid-3-yl)methanol **175**.

Entry	Catalyst <i>a</i>	Acetic Acid <i>b</i>	Yield	Impurity Level by ¹ H NMR
1	Evonik Degussa E 101 NO/W	0 μL	0.19 g (Crude)	Highest purity observed for freebase isolated
2	Evonik Degussa E 101 NO/W	60 μL	88%	Baseline impurities observed
3	Evonik Degussa E5 (Pd(OH) ₂)	0 μL	0.11 g (Crude)	Baseline impurities observed
4	Evonik Degussa E5 (Pd(OH) ₂)	60 μL	30% - product lost to Celite pad	Product recovered from Celite pad contained significant impurities
5	Johnson Matthey, Type 394	0 μL	0.16 g (Crude)	Baseline impurities observed
6	Johnson Matthey, Type 394	60 μL	73%	Baseline impurities observed
7	BASF CP M/UR 00034	0 μL	0.13 g (Crude)	Baseline impurities
8	BASF CP M/UR 00034	60 μL	87%	Highest purity observed for acetic acid salt of product

Entry 1: ¹H NMR (400 MHz, CDCl₃) δ ppm 3.59 (s, 2 H), 3.48 (d, *J* = 8.3 Hz, 2 H), 3.34 (d, *J* = 8.3 Hz, 2 H), 1.22 (s, 3 H).

Entry 2: ¹H NMR (400 MHz, CDCl₃) δ ppm 4.02 (d, *J* = 10.5 Hz, 2 H), 3.68 (d, *J* = 10.5 Hz, 2 H), 3.51 (s, 2 H), 1.99 (s, 3 H), 1.23 (s, 3 H).

Entry 3: ¹H NMR (400 MHz, CDCl₃) δ ppm 3.60 (s, 2 H), 3.50 (d, *J* = 8.3 Hz, 2 H), 3.35 (d, *J* = 8.3 Hz, 2 H), 1.22 (s, 3 H).

Entry 4: ¹H NMR (400 MHz, CDCl₃) δ ppm 3.95 (d, *J* = 10.5 Hz, 2 H), 3.73 (d, *J* = 10.5 Hz, 2 H), 3.52 (s, 2 H), 2.04 (s, 3 H), 1.26 (s, 3 H).

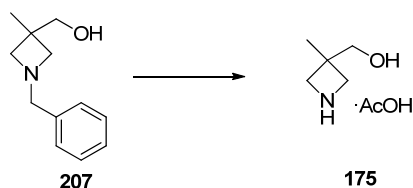
Entry 5: ¹H NMR (400 MHz, CDCl₃) δ ppm 3.60 (s, 2 H), 3.48 (d, *J* = 8.3 Hz, 2 H), 3.34 (d, *J* = 8.3 Hz, 2 H), 1.22 (s, 3 H).

Entry 6: ^1H NMR (400 MHz, CDCl_3) δ ppm 4.03 (d, $J = 10.5$ Hz, 2 H), 3.69 (d, $J = 10.5$ Hz, 2 H), 3.50 (s, 2 H), 1.99 (s, 3 H), 1.23 (s, 3 H).

Entry 7: ^1H NMR (400 MHz, CDCl_3) δ ppm 3.62 (s, 2 H), 3.49 (d, $J = 8.1$ Hz, 2 H), 3.36 (d, $J = 8.1$ Hz, 2 H), 1.22 (s, 3 H).

Entry 8: ^1H NMR (400 MHz, CDCl_3) δ ppm 4.03 (d, $J = 10.5$ Hz, 2 H), 3.68 (d, $J = 10.5$ Hz, 2 H), 3.49 (s, 2 H), 1.97 (s, 3 H), 1.24 (s, 3 H).

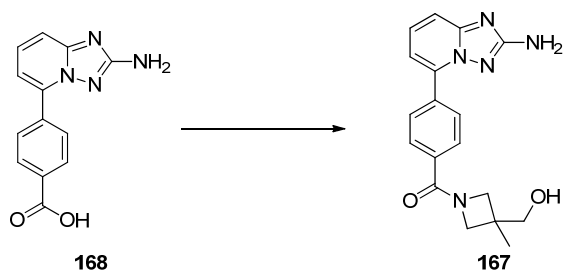
Preparation of acetic acid salt of (3-methylazetid-3-yl)methanol **175**



A hydrogenation vessel was loaded with 10% palladium on carbon (2.33 g), methanol (88 mL), (1-benzyl-3-methylazetid-3-yl)methanol **207** (5.83 g, 27.7 mmol) and acetic acid (1.75 mL, 30.6 mmol). H_2 at 3 bar was applied to the vessel. The reaction vessel was heated using a Buchi bath set at 55-60 °C. After 1 hour 40 minutes, the vessel was allowed to cool.

The cooled reaction mixture was filtered through a pad of Celite. The Celite pad was washed with methanol (300 mL). The filtrates were combined and evaporated to give a yellow oil, which began to crystallise on standing. Toluene (30 mL) was added and solids were observed, but these did not look sufficiently crystalline for filtration. The mixture was evaporated to give the acetic acid salt of (3-methylazetid-3-yl)methanol **175** as an off-white foam (4.91 g, 90%). ^1H NMR (400 MHz, CDCl_3) δ ppm 4.05 (d, $J = 10.5$ Hz, 2 H), 3.68 (d, $J = 10.5$ Hz, 2 H), 3.50 (s, 2 H), 1.98 (s, 3 H), 1.23 (s, 3 H); ^{13}C (100 MHz, CDCl_3) δ ppm 178.5 (s), 66.1 (t), 52.5 (t), 39.55 (s), 23.8 (q), 21.3 (q); IR (neat) 3177, 2964, 2902, 2654, 2467, 1628, 1552 cm^{-1} ; HRMS found m/z 102.0914 $[\text{M}+\text{H}]^+$, calcd for $\text{C}_5\text{H}_{12}\text{NO}$ 102.0913; Product deliquesced before melting point could be obtained.

Preparation of (4-(2-amino-[1,2,4]triazolo[1,5-a]pyridin-5-yl)phenyl)(3-(hydroxymethyl)-3-methylazetidin-1-yl)methanone **167**



Dichloromethane (20 mL) was added to 4-(2-amino-[1,2,4]triazolo[1,5-a]pyridin-5-yl)benzoic acid **168** (4.00 g, 15.7 mmol) and the white suspension was stirred under nitrogen. CDI (3.06 g, 18.9 mmol) (was added and the solids were washed in with dichloromethane (10 mL). DMSO (4 mL) was added to the reaction mixture. After 70 minutes, CDI (2.32 g, 14.3 mmol) was added to the reaction mixture and the solids were washed in with dichloromethane (5 mL). After 50 minutes, (3-methylazetidin-3-yl)methanol **175** (3.71 g, 18.9 mmol) was charged as a solid to the reaction vessel. The solids were washed in with dichloromethane (10 mL), followed by DMSO (2 mL) followed by dichloromethane (5 mL). After 20 minutes, water (40 mL) was added to the reaction vessel and the biphasic mixture was transferred to a separating funnel. The biphasic mixture was washed in with dichloromethane (10 mL) and water (10 mL). The organic phase was evaporated to give **167**, as a clear oil (0.46 g). HPLC analysis (Method A) showed 73% **167**.

The aqueous phase was filtered under gravity through an Oasis HLB 35cc (6 g) LP extraction cartridge (pre-wetted with 100 mL methanol, followed by 100 mL water). The Oasis cartridge was eluted under vacuum with water (50 mL) The Oasis cartridge was eluted under vacuum with methanol (2 x 50 mL). The methanol fractions were evaporated to give a clear straw-coloured oil (2.47 g). The oil was adsorbed onto silica which was loaded onto a 375 g KP-NH Biotage column (pre-wetted with 2.4% v/v methanol in dichloromethane). The column was eluted with 2.4% v/v methanol in dichloromethane over 1 column volume, followed by 2.4% v/v methanol in dichloromethane increasing to 11.2% v/v methanol in dichloromethane over 5 column volumes. 26 fractions of 120 mL were collected. Fractions of similar purity were combined to give batches of **167**.

Fractions 9, 10, 11, 12, 13, 16 and 17 were combined and evaporated to give a white foam (~0.50 g). Methanol was added to the foam and a suspension was obtained. Toluene (30 mL) was added slowly to the suspension. The suspension was filtered to give a white powder, which was dried in a vacuum oven at 40 °C, to give (4-(2-amino-[1,2,4]triazolo[1,5-*a*]pyridin-5-yl)phenyl)(3-(hydroxymethyl)-3-methylazetidin-1-yl)methanone **167** (0.15 g, 2.8%); spectroscopic data was consistent with authentic sample. The filtrate was evaporated to give a white foam, which was dried in the vacuum oven at 40 °C, to give (4-(2-amino-[1,2,4]triazolo[1,5-*a*]pyridin-5-yl)phenyl)(3-(hydroxymethyl)-3-methylazetidin-1-yl)methanone **167** (0.16 g, 3.0%). ¹H NMR (400 MHz, DMSO-*d*₆) δ ppm 7.95-8.10 (m, 2 H), 7.71-7.87 (m, 2 H), 7.53 (dd, *J* = 8.7, 7.6 Hz, 1 H), 7.40 (dd, *J* = 8.8, 1.3 Hz, 1 H), 7.07 (dd, *J* = 7.6, 1.3 Hz, 1 H), 4.05-4.22 (m, 1 H), 3.88-4.03 (m, 2 H), 3.56-3.73 (m, 1 H), 3.36-3.46 (m, 2 H), 1.22 (s, 3 H); ¹³C (100 MHz, CDCl₃) δ ppm 168.3 (s), 165.8 (s), 151.3 (s), 137.7 (s), 134.7 (s), 134.1 (s), 129.0 (d), 128.9 (d), 127.6 (d), 111.8 (d, 2 C), 66.4 (t), 60.5 (t), 56.2 (t), 35.88 (s), 21.59 (q); IR (neat) 3389, 3273, 3218, 2941, 2875, 2842, 1628, 1608, 1556, 1520 cm⁻¹; HRMS found *m/z* 338.1607 [M+H]⁺, calcd for C₁₈H₂₀N₅O₂ 338.1612; mp. 216-219 °C.

Fractions 5, 6, 7, 8, 19 and 20 were evaporated to give a clear oil (1.52g), which was dissolved methanol (15 mL) to give a solution was purified by MDAP. Sodium bicarbonate was added to MDAP fractions, in order to obtain a neutral pH for storage. Fractions of similar purity were combined and evaporated to dryness to give a solid. The solid was triturated and treated with water (30 mL) and gently heated, the slurry was filtered and washed with water (10 mL) at ambient temperature and dried under vacuum. The dried solid was dissolved in 1:1 dichloromethane/methanol (20 mL) and the hot solution was filtered through filter paper, which was washed with 1:1 dichloromethane/methanol (10 mL). The filtrate was evaporated to dryness under reduced pressure to give a foam which was dried overnight at 50 °C under vacuum to give (4-(2-amino-[1,2,4]triazolo[1,5-*a*]pyridin-5-yl)phenyl)(3-(hydroxymethyl)-3-methylazetidin-1-yl)methanone **167** (0.79 g, 15%); spectroscopic data was consistent with authentic sample.

5 References

1. Mok, C. C.; Lau, C. S. Pathogenesis of systemic lupus erythematosus. *Journal of Clinical Pathology* **2003**, *56*, 481-490.
2. Rahman, A.; Isenberg, D. A. Systemic Lupus Erythematosus. *N Engl J Med* **2008**, *358*, 929-939.
3. <http://www.nhs.uk/Conditions/Lupus/Pages/Introduction.aspx>. 2014.
4. Manning, G.; Whyte, D. B.; Martinez, R.; Hunter, T.; Sudarsanam, S. The Protein Kinase Complement of the Human Genome. *Science* **2002**, *298*, 1912-1934.
5. Patrick, G. L. *An Introduction to Medicinal Chemistry*; 4th Edition ed.; 2009.
6. Clark, J. D.; Flanagan, M. E.; Telliez, J. B. Discovery and Development of Janus Kinase (JAK) Inhibitors for Inflammatory Diseases. *J. Med. Chem.* **2014**, *57*, 5023-5038.
7. Kisseleva, T.; Bhattacharya, S.; Braunstein, J.; Schindler, C. W. Signaling through the JAK/STAT pathway, recent advances and future challenges. *Gene* **2002**, *285*, 1-24.
8. Liu, Y.; Gray, N. S. Rational design of inhibitors that bind to inactive kinase conformations. *Nat Chem Biol* **2006**, *2*, 358-364.
9. Mesa, R. A.; Yasothan, U.; Kirkpatrick, P. Ruxolitinib. *Nat Rev Drug Discov* **2012**, *11*, 103-104.
10. News in brief. *Nat Rev Drug Discov* **2012**, *11*, 895.
11. Fridman, J. S.; Scherle, P. A.; Collins, R.; Burn, T. C.; Li, Y.; Li, J.; Covington, M. B.; Thomas, B.; Collier, P.; Favata, M. F.; Wen, X.; Shi, J.; McGee, R.; Haley, P. J.; Shepard, S.; Rodgers, J. D.; Yeleswaram, S.; Hollis, G.; Newton, R. C.; Metcalf, B.; Friedman, S. M.; Vaddi, K. Selective Inhibition of JAK1 and JAK2 Is Efficacious in Rodent Models of Arthritis: Preclinical Characterization of INCB028050. *The Journal of Immunology* **2010**, *184*, 5298-5307.
12. Norman, P. Selective JAK inhibitors in development for rheumatoid arthritis. *Expert Opin. Investig. Drugs* **2014**, 1-11.
13. Van Rompaey, L.; Galien, R.; van der Aar, E. M.; Clement-Lacroix, P.; Nelles, L.; Smets, B.; Lepescheux, L.; Christophe, T.; Conrath, K.; Vandeghinste, N.; Vayssiere, B.; De Vos, S.; Fletcher, S.; Brys, R.; van 't Klooster, G.; Feyen, J. H. M.; Menet, C. Preclinical Characterization of GLPG0634, a Selective Inhibitor of JAK1, for the Treatment of Inflammatory Diseases. *The Journal of Immunology* **2013**, *191*, 3568-3577.

14. Hajduk, P. J.; Bures, M.; Praestgaard, J.; Fesik, S. W. Privileged Molecules for Protein Binding Identified from NMR-Based Screening. *J. Med. Chem.* **2000**, *43*, 3443-3447.
15. Carini, D. J.; Duncia, J. V.; Aldrich, P. E.; Chiu, A. T.; Johnson, A. L.; Pierce, M. E.; Price, W. A.; Santella, J. B.; Wells, G. J. Nonpeptide angiotensin II receptor antagonists: the discovery of a series of N-(biphenylmethyl)imidazoles as potent, orally active antihypertensives. *J. Med. Chem.* **1991**, *34*, 2525-2547.
16. Larsen, R. D.; King, A. O.; Chen, C. Y.; Corley, E. G.; Foster, B. S.; Roberts, F. E.; Yang, C.; Lieberman, D. R.; Reamer, R. A. Efficient Synthesis of Losartan, A Nonpeptide Angiotensin II Receptor Antagonist. *J. Org. Chem.* **1994**, *59*, 6391-6394.
17. Ullmann, F.; Bielecki, J. Ueber Synthesen in der Biphenylreihe. *Ber. Dtsch. Chem. Ges.* **1901**, *34*, 2174-2185.
18. Tamao, K.; Sumitani, K.; Kumada, M. Selective carbon-carbon bond formation by cross-coupling of Grignard reagents with organic halides. Catalysis by nickel-phosphine complexes. *J. Am. Chem. Soc.* **1972**, *94*, 4374-4376.
19. Corriu, R. J. P.; Masse, J. P. Activation of Grignard reagents by transition-metal complexes. A new and simple synthesis of trans-stilbenes and polyphenyls. *J. Chem. Soc., Chem. Commun.* **1972**, 144a.
20. Negishi, E.; King, A. O.; Okukado, N. Selective carbon-carbon bond formation via transition metal catalysis. 3. A highly selective synthesis of unsymmetrical biaryls and diarylmethanes by the nickel- or palladium-catalyzed reaction of aryl- and benzylzinc derivatives with aryl halides. *J. Org. Chem.* **1977**, *42*, 1821-1823.
21. Milstein, D.; Stille, J. K. Palladium-catalyzed coupling of tetraorganotin compounds with aryl and benzyl halides. Synthetic utility and mechanism. *J. Am. Chem. Soc.* **1979**, *101*, 4992-4998.
22. Miyaura, N.; Yanagi, T.; Suzuki, A. The Palladium-Catalyzed Cross-Coupling Reaction of Phenylboronic Acid with Haloarenes in the Presence of Bases. *Synth. Commun.* **1981**, *11*, 513-519.
23. Suzuki, A. Cross-Coupling Reactions Of Organoboranes: An Easy Way To Construct C-C Bonds (Nobel Lecture). *Angew. Chem. Int. Ed.* **2011**, *50*, 6722-6737.
24. Negishi, E. Magical Power of Transition Metals: Past, Present, and Future (Nobel Lecture). *Angew. Chem. Int. Ed.* **2011**, *50*, 6738-6764.
25. Johansson Seechurn, C. C. C.; Kitching, M. O.; Colacot, T. J.; Snieckus, V. Palladium-Catalyzed Cross-Coupling: A Historical Contextual

Perspective to the 2010 Nobel Prize. *Angew. Chem. Int. Ed.* **2012**, *51*, 5062-5085.

26. Kumada, M.; Tamao, K.; Sumitani, K. Phosphine-Nickel Complex Catalyzed Cross-Coupling of Grignard Reagents with Aryl and Alkenyl Halides: 1,2-Dibutylbenzene [Benzene, 1,2-di-*n*-butyl-]. *Org. Synth.* **1978**, *58*, 127.
27. Bold, G.; Fässler, A.; Capraro, H. G.; Cozens, R.; Klimkait, T.; Lazdins, J.; Mestan, J.; Poncioni, B.; Rösel, J.; Stover, D.; Tintelnot-Blomley, M.; Acemoglu, F.; Beck, W.; Boss, E.; Eschbach, M.; Hürlimann, T.; Masso, E.; Roussel, S.; Ucci-Stoll, K.; Wyss, D.; Lang, M. New Aza-Dipeptide Analogues as Potent and Orally Absorbed HIV-1 Protease Inhibitors: Candidates for Clinical Development. *J. Med. Chem.* **1998**, *41*, 3387-3401.
28. Banno, T.; Hayakawa, Y.; Umeno, M. Some applications of the Grignard cross-coupling reaction in the industrial field. *J. Organomet. Chem.* **2002**, *653*, 288-291.
29. Pérez-Balado, C.; Ormerod, D.; Aelterman, W.; Mertens, N. Development of a Concise Scaleable Synthesis of 2-Chloro-5-(pyridin-2-yl) Pyrimidine via a Negishi Cross-Coupling. *Org. Process Res. Dev.* **2007**, *11*, 237-240.
30. Ragan, J. A.; Raggon, J. W.; Hill, P. D.; Jones, B. P.; McDermott, R. E.; Munchhof, M. J.; Marx, M. A.; Casavant, J. M.; Cooper, B. A.; Doty, J. L.; Lu, Y. Cross-Coupling Methods for the Large-Scale Preparation of an Imidazole-Thienopyridine: Synthesis of [2-(3-Methyl-3H-imidazol-4-yl)-thieno[3,2-*b*]pyridin-7-yl]-(2-methyl-1H-indol-5-yl)-amine. *Org. Process Res. Dev.* **2003**, *7*, 676-683.
31. Boyer, I. J. Toxicity of dibutyltin, tributyltin and other organotin compounds to humans and to experimental animals. *Toxicology* **1989**, *55*, 253-298.
32. Lipton, M. F.; Mauragis, M. A.; Maloney, M. T.; Velely, M. F.; VanderBor, D. W.; Newby, J. J.; Appell, R. B.; Daus, E. D. The Synthesis of OSU 6162: Efficient, Large-Scale Implementation of a Suzuki Coupling. *Org. Process Res. Dev.* **2003**, *7*, 385-392.
33. Miyaura, N.; Yamada, K.; Suzuki, A. A new stereospecific cross-coupling by the palladium-catalyzed reaction of 1-alkenylboranes with 1-alkenyl or 1-alkynyl halides. *Tetrahedron Lett.* **1979**, *20*, 3437-3440.
34. Miyaura, N.; Suzuki, A. Stereoselective synthesis of arylated (*E*)-alkenes by the reaction of alk-1-enylboranes with aryl halides in the presence of palladium catalyst. *J. Chem. Soc., Chem. Commun.* **1979**, *0*, 866-867.

35. Miyaura, N.; Suzuki, A. Palladium-Catalyzed Cross-Coupling Reactions of Organoboron Compounds. *Chem. Rev.* **1995**, *95*, 2457-2483.
36. Aliprantis, A. O.; Canary, J. W. Observation of Catalytic Intermediates in the Suzuki Reaction by Electrospray Mass Spectrometry. *J. Am. Chem. Soc.* **1994**, *116*, 6985-6986.
37. Fauvarque, J.-F.; Pflüger, F.; Troupel, M. Kinetics of oxidative addition of zerovalent palladium to aromatic iodides. *J. Organomet. Chem.* **1981**, *208*, 419-427.
38. Fitton, P.; McKeon, J. E. Reactions of tetrakis(triphenylphosphine)palladium(0) with olefins bearing electron-withdrawing substituents. *Chem. Commun. (London)* **1968**, 4-6.
39. Fitton, P.; Rick, E. A. The addition of aryl halides to tetrakis(triphenylphosphine)palladium(0). *J. Organomet. Chem.* **1971**, *28*, 287-291.
40. Grushin, V. V.; Alper, H. Transformations of Chloroarenes, Catalyzed by Transition-Metal Complexes. *Chem. Rev.* **1994**, *94*, 1047-1062.
41. Hamann, B. C.; Hartwig, J. F. Sterically Hindered Chelating Alkyl Phosphines Provide Large Rate Accelerations in Palladium-Catalyzed Amination of Aryl Iodides, Bromides, and Chlorides, and the First Amination of Aryl Tosylates. *J. Am. Chem. Soc.* **1998**, *120*, 7369-7370.
42. Old, D. W.; Wolfe, J. P.; Buchwald, S. L. A Highly Active Catalyst for Palladium-Catalyzed Cross-Coupling Reactions: Room-Temperature Suzuki Couplings and Amination of Unactivated Aryl Chlorides. *J. Am. Chem. Soc.* **1998**, *120*, 9722-9723.
43. Littke, A. F.; Fu, G. C. A Convenient and General Method for Pd-Catalyzed Suzuki Cross-Couplings of Aryl Chlorides and Arylboronic Acids. *Angew. Chem. Int. Ed.* **1998**, *37*, 3387-3388.
44. Littke, A. F.; Dai, C.; Fu, G. C. Versatile Catalysts for the Suzuki Cross-Coupling of Arylboronic Acids with Aryl and Vinyl Halides and Triflates under Mild Conditions. *J. Am. Chem. Soc.* **2000**, *122*, 4020-4028.
45. Christmann, U.; Vilar, R. Monoligated Palladium Species as Catalysts in Cross-Coupling Reactions. *Angew. Chem. Int. Ed.* **2005**, *44*, 366-374.
46. Wolfe, J. P.; Singer, R. A.; Yang, B. H.; Buchwald, S. L. Highly Active Palladium Catalysts for Suzuki Coupling Reactions. *J. Am. Chem. Soc.* **1999**, *121*, 9550-9561.

47. Braga, A. A. C.; Morgon, N. H.; Ujaque, G.; Lledós, A.; Maseras, F. Computational study of the transmetalation process in the Suzuki–Miyaura cross-coupling of aryls. *J. Organomet. Chem.* **2006**, *691*, 4459-4466.
48. Sicre, C.; Braga, A. A. C.; Maseras, F.; Cid, M. M. Mechanistic insights into the transmetalation step of a Suzuki–Miyaura reaction of 2(4)-bromopyridines: characterization of an intermediate. *Tetrahedron* **2008**, *64*, 7437-7443.
49. Jover, J.; Fey, N.; Purdie, M.; Lloyd-Jones, G. C.; Harvey, J. N. A computational study of phosphine ligand effects in Suzuki–Miyaura coupling. *J. Mol. Catal. A: Chem.* **2010**, *324*, 39-47.
50. Amatore, C.; Jutand, A.; Le Duc, G. Kinetic Data for the Transmetalation/Reductive Elimination in Palladium-Catalyzed Suzuki–Miyaura Reactions: Unexpected Triple Role of Hydroxide Ions Used as Base. *Chem. Eu. J.* **2011**, *17*, 2492-2503.
51. Carrow, B. P.; Hartwig, J. F. Distinguishing Between Pathways for Transmetalation in Suzuki–Miyaura Reactions. *J. Am. Chem. Soc.* **2011**, *133*, 2116-2119.
52. Wright, S. W.; Hageman, D. L.; McClure, L. D. Fluoride-Mediated Boronic Acid Coupling Reactions. *J. Org. Chem.* **1994**, *59*, 6095-6097.
53. Amatore, C.; Jutand, A.; Le Duc, G. The Triple Role of Fluoride Ions in Palladium-Catalyzed Suzuki–Miyaura Reactions: Unprecedented Transmetalation from [ArPdFL₂] Complexes. *Angew. Chem. Int. Ed.* **2012**, *51*, 1379-1382.
54. Gillie, A.; Stille, J. K. Mechanisms of 1,1-reductive elimination from palladium. *J. Am. Chem. Soc.* **1980**, *102*, 4933-4941.
55. Ozawa, F.; Hidaka, T.; Yamamoto, T.; Yamamoto, A. Mechanism of reaction of trans- diarylbis(diethylphenylphosphine)palladium(II) complexes with aryl iodides to give biaryls. *J. Organomet. Chem.* **1987**, *330*, 253-263.
56. Mann, B. E.; Musco, A. Phosphorus-31 nuclear magnetic resonance spectroscopic characterisation of tertiary phosphine palladium(0) complexes: evidence for 14-electron complexes in solution. *J. Chem. Soc., Dalton Trans.* **1975**, 1673-1677.
57. Amatore, C.; Pfluger, F. Mechanism of oxidative addition of palladium(0) with aromatic iodides in toluene, monitored at ultramicroelectrodes. *Organometallics* **1990**, *9*, 2276-2282.
58. <http://www.sigmaaldrich.com/>. 2014.

59. Amatore, C.; Jutand, A.; M'Barki, M. A. Evidence of the formation of zerovalent palladium from Pd(OAc)₂ and triphenylphosphine. *Organometallics* **1992**, *11*, 3009-3013.
60. Amatore, C.; Jutand, A.; Khalil, F.; M'Barki, M. A.; Mottier, L. Rates and mechanisms of oxidative addition to zerovalent palladium complexes generated in situ from mixtures of Pd⁰(dba)₂ and triphenylphosphine. *Organometallics* **1993**, *12*, 3168-3178.
61. Lennox, A. J. J.; Lloyd-Jones, G. C. Selection of boron reagents for Suzuki-Miyaura coupling. *Chem. Soc. Rev.* **2014**, *43*, 412-443.
62. Li, W.; Nelson, D. P.; Jensen, M. S.; Hoerrner, R. S.; Cai, D.; Larsen, R. D.; Reider, P. J. An Improved Protocol for the Preparation of 3-Pyridyl- and Some Arylboronic Acids. *J. Org. Chem.* **2002**, *67*, 5394-5397.
63. Khotinsky, E.; Melamed, M. Die Wirkung der magnesiumorganischen Verbindungen auf die Borsäureester. *Ber. Dtsch. Chem. Ges.* **1909**, *42*, 3090-3096.
64. Gerbino, D. C.; Mandolesi, S. D.; Schmalz, H. G.; Podestá, J. C. Introduction of Allyl and Prenyl Side-Chains into Aromatic Systems by Suzuki Cross-Coupling Reactions. *Eur. J. Org. Chem.* **2009**, *2009*, 3964-3972.
65. Molander, G. A.; Trice, S. L. J.; Dreher, S. D. Palladium-Catalyzed, Direct Boronic Acid Synthesis from Aryl Chlorides: A Simplified Route to Diverse Boronate Ester Derivatives. *J. Am. Chem. Soc.* **2010**, *132*, 17701-17703.
66. Molander, G. A.; Trice, S. L. J.; Kennedy, S. M.; Dreher, S. D.; Tudge, M. T. Scope of the Palladium-Catalyzed Aryl Borylation Utilizing Bis-Boronic Acid. *J. Am. Chem. Soc.* **2012**, *134*, 11667-11673.
67. Ishiyama, T.; Murata, M.; Miyaura, N. Palladium(0)-Catalyzed Cross-Coupling Reaction of Alkoxydiboron with Haloarenes: A Direct Procedure for Arylboronic Esters. *J. Org. Chem.* **1995**, *60*, 7508-7510.
68. Ishiyama, T.; Ishida, K.; Miyaura, N. Synthesis of pinacol arylboronates via cross-coupling reaction of bis(pinacolato)diboron with chloroarenes catalyzed by palladium(0)-tricyclohexylphosphine complexes. *Tetrahedron* **2001**, *57*, 9813-9816.
69. Molander, G. A.; Biolatto, B. Efficient Ligandless Palladium-Catalyzed Suzuki Reactions of Potassium Aryltrifluoroborates. *Org. Lett.* **2002**, *4*, 1867-1870.
70. Molander, G.; Canturk, B. Organotrifluoroborates and Monocoordinated Palladium Complexes as Catalysts – A Perfect Combination for

Suzuki–Miyaura Coupling. *Angew. Chem. Int. Ed.* **2009**, *48*, 9240-9261.

71. Vedejs, E.; Fields, S. C.; Schrimpf, M. R. Asymmetric transformation in synthesis: chiral amino acid enolate equivalents. *J. Am. Chem. Soc.* **1993**, *115*, 11612-11613.
72. Lennox, A. J. J.; Lloyd-Jones, G. C. Preparation of Organotrifluoroborate Salts: Precipitation-Driven Equilibrium under Non-Etching Conditions. *Angew. Chem. Int. Ed.* **2012**, *51*, 9385-9388.
73. Butters, M.; Harvey, J. N.; Jover, J.; Lennox, A. J.; Lloyd-Jones, G. C.; Murray, P. M. Aryl Trifluoroborates in Suzuki–Miyaura Coupling: The Roles of Endogenous Aryl Boronic Acid and Fluoride. *Angew. Chem. Int. Ed.* **2010**, *49*, 5156-5160.
74. Batey, R. A.; Quach, T. D. Synthesis and cross-coupling reactions of tetraalkylammonium organotrifluoroborate salts. *Tetrahedron Lett.* **2001**, *42*, 9099-9103.
75. Knapp, D. M.; Gillis, E. P.; Burke, M. D. A General Solution for Unstable Boronic Acids: Slow-Release Cross-Coupling from Air-Stable MIDA Boronates. *J. Am. Chem. Soc.* **2009**, *131*, 6961-6963.
76. Gillis, E. P.; Burke, M. D. Multistep Synthesis of Complex Boronic Acids from Simple MIDA Boronates. *J. Am. Chem. Soc.* **2008**, *130*, 14084-14085.
77. Moon, J.; Lee, S. Palladium catalyzed-dehalogenation of aryl chlorides and bromides using phosphite ligands. *J. Organomet. Chem.* **2009**, *694*, 473-477.
78. Zawisza, A. M.; Muzart, J. Pd-catalyzed reduction of aryl halides using dimethylformamide as the hydride source. *Tetrahedron Lett.* **2007**, *48*, 6738-6742.
79. Kuivila, H. G.; Reuwer, J.; Mangravite, J. A. Electrophilic displacement reactions: XV. Kinetics and mechanism of the base-catalyzed protodeboronation of areneboronic acids. *Can. J. Chem.* **1963**, *41*, 3081-3090.
80. Kong, K. C.; Cheng, C. H. Facile aryl-aryl exchange between the palladium center and phosphine ligands in palladium(II) complexes. *J. Am. Chem. Soc.* **1991**, *113*, 6313-6315.
81. O'Keefe, D. F.; Dannock, M. C.; Marcuccio, S. M. Palladium catalyzed coupling of halobenzenes with arylboronic acids: Role of the triphenylphosphine ligand. *Tetrahedron Lett.* **1992**, *33*, 6679-6680.

82. Leadbeater, N. E.; Resouly, S. M. Suzuki aryl couplings mediated by phosphine-free nickel complexes. *Tetrahedron* **1999**, *55*, 11889-11894.
83. Nadri, S.; Azadi, E.; Ataei, A.; Joshaghani, M.; Rafiee, E. Investigation of the catalytic activity of a Pd/biphenyl-based phosphine system in the Ullmann homocoupling of aryl bromides. *J. Organomet. Chem.* **2011**, *696*, 2966-2970.
84. Shao, L.; Du, Y.; Zeng, M.; Li, X.; Shen, W.; Zuo, S.; Lu, Y.; Zhang, X. M.; Qi, C. Ethanol-promoted reductive homocoupling reactions of aryl halides catalyzed by palladium on carbon (Pd/C). *Appl. Organometal. Chem.* **2010**, *24*, 421-425.
85. Hassan, J.; Hathroubi, C.; Gozzi, C.; Lemaire, M. Preparation of unsymmetrical biaryls via palladium-catalyzed coupling reaction of aryl halides. *Tetrahedron* **2001**, *57*, 7845-7855.
86. Moreno-Mañas, M.; Pérez, M.; Pleixats, R. Palladium-Catalyzed Suzuki-Type Self-Coupling of Arylboronic Acids. A Mechanistic Study. *J. Org. Chem.* **1996**, *61*, 2346-2351.
87. Garrett, C.; Prasad, K. The Art of Meeting Palladium Specifications in Active Pharmaceutical Ingredients Produced by Pd-Catalyzed Reactions. *Adv. Synth. Catal.* **2004**, *346*, 889-900.
88. Kallman, N. J.; Liu, C.; Yates, M. H.; Linder, R. J.; Ruble, J. C.; Kogut, E. F.; Patterson, L. E.; Laird, D. L. T.; Hansen, M. M. Route Design and Development of a MET Kinase Inhibitor: A Copper-Catalyzed Preparation of an N1-Methylindazole. *Org. Process Res. Dev.* **2014**, *18*, 501-510.
89. Ennis, D. S.; McManus, J.; Wood-Kaczmar, W.; Richardson, J.; Smith, G. E.; Carstairs, A. Multikilogram-Scale Synthesis of a Biphenyl Carboxylic Acid Derivative Using a Pd/C-Mediated Suzuki Coupling Approach. *Org. Process Res. Dev.* **1999**, *3*, 248-252.
90. Villa, M.; Cannata, V.; Rosi, A.; Allegrini, P. Method for removing heavy metals from organic compounds solution by treatment with cysteine or N-acylcysteine. WO9851646A1, 1998.
91. Prashad, M.; Liu, Y.; Repiç, O. An Expedient Synthesis of 1-(4-Chlorophenyl)-3,3-dimethyl-2-butanone by a Ligand-Free Palladium-Catalyzed α -Arylation of Pinacolone: Scale-Up and Effect of Base Concentration. *Adv. Synth. Catal.* **2003**, *345*, 533-536.
92. Tang, W.; Patel, N. D.; Wei, X.; Byrne, D.; Chitroda, A.; Narayanan, B.; Sienkiewicz, A.; Nummy, L. J.; Sarvestani, M.; Ma, S.; Grinberg, N.; Lee, H.; Kim, S.; Li, Z.; Spinelli, E.; Yang, B. S.; Yee, N.;

- Senanayake, C. H. Synthesis of a Sodium–Hydrogen Exchange Type 1 Inhibitor: An Efficient Cu-Catalyzed Conjugated Addition of a Grignard Reagent to an Acetyl Pyridinium Salt. *Org. Process Res. Dev.* **2013**, *17*, 382-389.
93. Prashad, M.; Hu, B.; Har, D.; Repic, O.; Blacklock, T.; Acemoglu, M. Efficient and Practical Syntheses of (R)-(5-Amino-2,3-dihydro-1H-inden-2-yl)-carbamic Acid Methyl Ester. *Adv. Synth. Catal.* **2001**, *343*, 461-472.
94. Pandarus, V.; Gingras, G.; Béland, F.; Ciriminna, R.; Pagliaro, M. Process Intensification of the Suzuki–Miyaura Reaction over Sol–Gel Entrapped Catalyst SiliaCat DPP-Pd Under Conditions of Continuous Flow. *Org. Process Res. Dev.* **2014**.
95. Liégault, B.; Lapointe, D.; Caron, L.; Vlassova, A.; Fagnou, K. Establishment of Broadly Applicable Reaction Conditions for the Palladium-Catalyzed Direct Arylation of Heteroatom-Containing Aromatic Compounds. *J. Org. Chem.* **2009**, *74*, 1826-1834.
96. Lafrance, M.; Fagnou, K. Palladium-Catalyzed Benzene Arylation: Incorporation of Catalytic Pivalic Acid as a Proton Shuttle and a Key Element in Catalyst Design. *J. Am. Chem. Soc.* **2006**, *128*, 16496-16497.
97. Schipper, D. J.; Campeau, L.-C.; Fagnou, K. Catalyst and base controlled site-selective sp² and sp³ direct arylation of azine N-oxides. *Tetrahedron* **2009**, *65*, 3155-3164.
98. Larivée, A.; Mousseau, J. J.; Charette, A. B. Palladium-Catalyzed Direct C–H Arylation of *N*-Iminopyridinium Ylides: Application to the Synthesis of (±)-Anabesine. *J. Am. Chem. Soc.* **2008**, *130*, 52-54.
99. Amatore, M.; Gosmini, C. Efficient Cobalt-Catalyzed Formation of Unsymmetrical Biaryl Compounds and Its Application in the Synthesis of a Sartan Intermediate. *Angew. Chem. Int. Ed.* **2008**, *47*, 2089-2092.
100. Mesganaw, T.; Garg, N. K. Ni- and Fe-Catalyzed Cross-Coupling Reactions of Phenol Derivatives. *Org. Process Res. Dev.* **2012**, *17*, 29-39.
101. Hatakeyama, T.; Nakamura, M. Iron-Catalyzed Selective Biaryl Coupling: Remarkable Suppression of Homocoupling by the Fluoride Anion. *J. Am. Chem. Soc.* **2007**, *129*, 9844-9845.
102. Vallée, F.; Mousseau, J. J.; Charette, A. B. Iron-Catalyzed Direct Arylation through an Aryl Radical Transfer Pathway. *J. Am. Chem. Soc.* **2010**, *132*, 1514-1516.

103. Chouteau, F. Unpublished Work, 2011.
104. Fletcher, S. R.; Menet, C. J. M.; Van Rompaey, L. J. C. Novel Compounds Useful For The Treatment of Degenerative and Inflammatory Diseases. WO2010/10187, 2010.
105. Welch, C. J.; Leonard, W. R.; Henderson, D. W.; Dorner, B.; Childers, K. G.; Chung, J. Y. L.; Hartner, F. W.; Albanese-Walker, J.; Sajonz, P. Adsorbent Screening Using Microplate Spectroscopy for Selective Removal of Colored Impurities from Active Pharmaceutical Intermediates. *Org. Process Res. Dev.* **2008**, *12*, 81-87.
106. Wehrstedt, K. D.; Wandrey, P. A.; Heitkamp, D. Explosive properties of 1-hydroxybenzotriazoles. *J. Hazard. Mater.* **2005**, *126*, 1-7.
107. Chemburkar, S. R.; Bauer, J.; Deming, K.; Spiwek, H.; Patel, K.; Morris, J.; Henry, R.; Spanton, S.; Dziki, W.; Porter, W.; Quick, J.; Bauer, P.; Donaubaue, J.; Narayanan, B. A.; Soldani, M.; Riley, D.; McFarland, K. Dealing with the Impact of Ritonavir Polymorphs on the Late Stages of Bulk Drug Process Development. *Org. Process Res. Dev.* **2000**, *4*, 413-417.
108. Beckmann, W. Seeding the Desired Polymorph: Background, Possibilities, Limitations, and Case Studies. *Org. Process Res. Dev.* **2000**, *4*, 372-383.
109. Isaad, J.; El Achari, A. Colorimetric sensing of cyanide anions in aqueous media based on functional surface modification of natural cellulose materials. *Tetrahedron* **2011**, *67*, 4939-4947.
110. Kobayashi, H.; Nakashima, K.; Ohshima, E.; Hisaeda, Y.; Hamachi, I.; Shinkai, S. Novel saccharide-induced conformational changes in a boronic acid-appended poly(L-lysine) as detected by circular dichroism and fluorescence. *J. Chem. Soc., Perkin Trans. 2* **2000**, 997-1002.
111. ICH Harmonised Tripartite Guideline *Q3A(R) Impurities in New Drug Substances*; 08.
112. *Design Expert* 7, 2014
113. Pace, V.; Hoyos, P.; Castoldi, L.; Domínguez de María, P.; Alcántara, A. R. 2-Methyltetrahydrofuran (2-MeTHF): A Biomass-Derived Solvent with Broad Application in Organic Chemistry. *ChemSusChem* **2012**, *5*, 1369-1379.
114. Department of Health and Human Services; Public Health Service *National Toxicology Program Report on Carcinogens, Twelfth Edition*; 11.

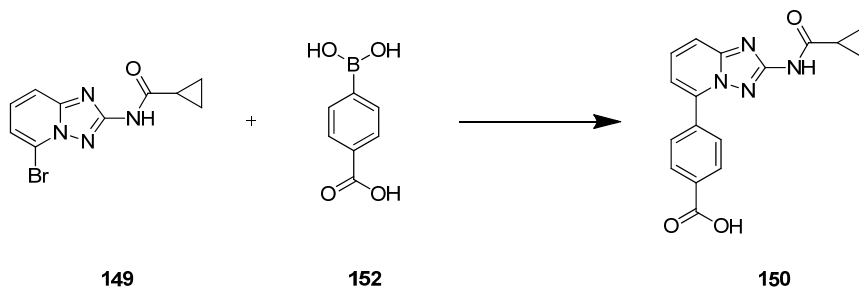
115. Corona, J. A.; Davis, R. D.; Kedia, S. B.; Mitchell, M. B. Expedited Development through Parallel Reaction Screening: Application to PTC-Mediated Knoevenagel Condensation. *Org. Process Res. Dev.* **2010**, *14*, 712-715.
116. Rosso, V. W.; Lust, D. A.; Bernot, P. J.; Grosso, J. A.; Modi, S. P.; Rusowicz, A.; Sedergran, T. C.; Simpson, J. H.; Srivastava, S. K.; Humora, M. J.; Anderson, N. G. Removal of Palladium from Organic Reaction Mixtures by Trimercaptotriazine. *Org. Process Res. Dev.* **1997**, *1*, 311-314.
117. Clark, J. H.; Macquarrie, D. J.; Mubofu, E. B. Preparation of a novel silica-supported palladium catalyst and its use in the Heck reaction. *Green Chem.* **2000**, *2*, 53-56.
118. Al-Hashimi, M.; Qazi, A.; Sullivan, A. C.; Wilson, J. R. H. Dithio palladium modified silicas – New heterogeneous catalysts for Suzuki cross-coupling reactions. *J. Mol. Catal. A: Chem.* **2007**, *278*, 160-164.
119. Richardson, J. M.; Jones, C. W. Strong evidence of solution-phase catalysis associated with palladium leaching from immobilized thiols during Heck and Suzuki coupling of aryl iodides, bromides, and chlorides. *Journal of Catalysis* **2007**, *251*, 80-93.
120. Collins, A. M.; Maslin, C.; Davies, R. J. Scale-Up of a Chiral Resolution Using Cross-Linked Enzyme Crystals. *Org. Process Res. Dev.* **1998**, *2*, 400-406.
121. Aggarwal, V. K.; Staubitz, A. C.; Owen, M. Optimization of the Mizoroki–Heck Reaction Using Design of Experiment (DoE). *Org. Process Res. Dev.* **2005**, *10*, 64-69.
122. Menet, C. J. M.; Joannigot, N.; Blanc, J.; Van Rompaey, L. J. C.; Fletcher, S. R. Novel Compounds Useful for the Treatment of Degenerative and Inflammatory Diseases. WO2010/10186, 2010.
123. Bell, K.; Sunose, M.; Ellard, K.; Cansfield, A.; Taylor, J.; Miller, W.; Ramsden, N.; Bergamini, G.; Neubauer, G. SAR studies around a series of triazolopyridines as potent and selective PI3K γ inhibitors. *Bioorg. Med. Chem. Lett.* **2012**, *22*, 5257-5263.
124. Wisdom, R. Unpublished Work, 2011.
125. Collie, L.; Denness, J. E.; Parker, D.; O'Carroll, F.; Tachon, C. Synthesis of functionalised 12-,13- and 14-membered crown ethers bearing exocyclic polymerisable groups and the binding properties and conductivities of their lithium doped polymers. *J. Chem. Soc. , Perkin Trans. 2* **1993**, 1747-1758.

126. Darensbourg, D. J.; Moncada, A. I.; Wei, S. H. Aliphatic Polycarbonates Produced from the Coupling of Carbon Dioxide and Oxetanes and Their Depolymerization via Cyclic Carbonate Formation. *Macromolecules* **2011**, *44*, 2568-2576.
127. Kong, D. L.; He, L. N.; Wang, J. Q. Synthesis of Urea Derivatives from CO₂ and Amines Catalyzed by Polyethylene Glycol Supported Potassium Hydroxide without Dehydrating Agents. *Synlett* **2010**, 1276-1280.
128. Liu, L.; Zhang, S.; Fu, X.; Yan, C. H. Metal-free aerobic oxidative coupling of amines to imines. *Chem. Commun.* **2011**, *47*, 10148-10150.
129. An, G.; Rhee, H. Oxidation of N-Benzylaldimines to N-Benzylamides by MCPBA and BF₃.OEt₂. *Synlett* **2003**, 876-878.
130. Mohamed, M. A.; Yamada, K.; Tomioka, K. Accessing the amide functionality by the mild and low-cost oxidation of imine. *Tetrahedron Lett.* **2009**, *50*, 3436-3438.
131. Hillier, M. C.; Chen, C. A One-Pot Preparation of 1,3-Disubstituted Azetidines. *J. Org. Chem.* **2006**, *71*, 7885-7887.
132. Bartholomew, D.; Stocks, M. J. A novel rearrangement reaction conversion of 3-(chloromethyl)azetididin-2-ones to azetidine-3-carboxylic acid esters. *Tetrahedron Lett.* **1991**, *32*, 4795-4798.
133. Ghorai, M. K.; Das, K.; Shukla, D. Lewis Acid-Mediated Highly Regioselective S_N2-Type Ring-Opening of 2-Aryl-N-tosylazetidines and Aziridines by Alcohols. *J. Org. Chem.* **2007**, *72*, 5859-5862.
134. Bream, R. N.; Hulcoop, D. G.; Gooding, S. J.; Watson, S. A.; Blore, C. Development of a Selective Friedel-Crafts Alkylation Surrogate: Safe Operating Conditions through Mechanistic Understanding. *Org. Process Res. Dev.* **2012**, *16*, 2043-2050.
135. Hamza, D.; Stocks, M. J.; Décor, A.; Pairedeau, G.; Stonehouse, J. P. Synthesis of Novel 2,6-Diazaspiro[3.3]heptanes. *Synlett* **2007**, 2584-2586.
136. <http://catalysts.evonik.com/product/catalysts/en/Pages/default.aspx>. 2014.
137. Padiya, K. J.; Gavade, S.; Kardile, B.; Tiwari, M.; Bajare, S.; Mane, M.; Gaware, V.; Varghese, S.; Harel, D.; Kurhade, S. Unprecedented "In Water" Imidazole Carbonylation: Paradigm Shift for Preparation of Urea and Carbamate. *Org. Lett.* **2012**, *14*, 2814-2817.
138. Engstrom, K. M.; Sheikh, A.; Ho, R.; Miller, R. W. The Stability of N,N-Carbonyldiimidazole Toward Atmospheric Moisture. *Org. Process Res. Dev.* **2014**, *18*, 488-494.

GSK CONFIDENTIAL

139. Allen, M. P.; Am Ende, C. W.; Brodney, M. A.; Dounay, A. B.; Johnson, D. S.; Petterson, M. Y.; Schwarz, J. B.; Tran, T. P. Novel Phenyl Imidazoles and Phenyl Triazoles as Gamma-Secretase Modulators. WO2010/100606, 2010.
140. Allen, J. R.; Amegadzie, A. K.; Gardinier, K. M.; Gregory, G. S.; Hitchcock, S. A.; Hoogestraat, P. J.; Jones, W. D. J.; Smith, D. L. CB1 Modulator Compounds. WO2005/66126, 2005.

6 Appendices

6.1 Route A Stage 2 Palladium Source, Base and Solvent Screen

149 (0.10g, 0.36 mmol), **152** (0.068 g, 0.41 mmol), palladium source *a* (18 μ mol) and ligand *b* (36 μ mol) were suspended in solvent *d* (0.5 mL). A solution of base *c* (0.75 mmol) in water (0.5 mL) was added and the reaction mixture was microwaved on high absorption for 15mins. The reaction mixture was sampled for HPLC analysis (Method B).

GSK CONFIDENTIAL

Entry	Palladium Source <i>a</i> Ligand <i>b</i>	Base <i>c</i>	Solvent <i>d</i>	Boronic acid 152 % PAR	Triazole 147 % PAR	168 % PAR	Aryl bromide 149 % PAR	Coupled product 150 % PAR
1	Pd(OAc) ₂ PPh ₃	KHCO ₃	Methanol	0.6	0.2	1.8	1.1	89.7
2	Pd(OAc) ₂ PPh ₃	NaOH	Methanol	0.6	0.7	2.3	0.8	87.0
3	Pd(OAc) ₂ PPh ₃	KOH	Ethanol	0.8	1.5	2.6	4.7	82.3
4	Pd(OAc) ₂ PPh ₃	Na ₂ CO ₃	Methanol	0.3	3.6	2.7	2.1	78.3
5	Pd(OAc) ₂ PPh ₃	NaOH	Ethanol	2.2	0.1	3.7	0.3	77.8
6	Pd(OAc) ₂ PPh ₃	KHCO ₃	Ethanol	0.1	0.3	3.7	9.1	76.5
7	Pd ₂ (dba) ₃ DavePhos	KHCO ₃	Ethanol	7.0	0.1	2.0	0.2	74.3
8	Pd(PPh ₃) ₄	Na ₂ CO ₃	Methanol	6.0	6.2	2.7	3.3	70.0
9	PdCl ₂ PPh ₃	K ₃ PO ₄	Methanol	0.1	0.1	7.3	0.1	68.2
10	Pd(PPh ₃) ₄	K ₃ PO ₄	Methanol	4.2	5.8	3.9	1.4	67.2
11	PdCl ₂ PPh ₃	KHCO ₃	THF		0.3	4.9	16.0	67.0
12	Pd ₂ (dba) ₃ DavePhos	K ₃ PO ₄	Ethanol	1.7	0.1	3.4	0.4	66.6
13	PdCl ₂ PPh ₃	K ₃ PO ₄	Ethanol	5.2	1.5	4.7	15.0	65.4
14	Pd ₂ (dba) ₃ DavePhos	K ₃ PO ₄	Methanol	7.6	2.3	3.7	7.1	58.0
15	PdCl ₂ PPh ₃	NaOH	Ethanol	11.6	6.0	2.7	25.9	46.3
16	Pd(PPh ₃) ₄	KOH	Methanol	11.0	12.2	2.5	14.3	45.4
17	Pd(PPh ₃) ₄	NaOH	Ethanol	12.2	12.1	2.3	25.1	40.8
18	Pd(OAc) ₂ PPh ₃	K ₃ PO ₄	CH ₂ Cl ₂	3.0	0.7	6.4	29.7	39.5
19	Pd(PPh ₃) ₄	NaOH	Ethanol	14.5	8.7	2.3	29.4	38.7
20	Pd(OAc) ₂ PPh ₃	KOH	THF	11.4	1.9	2.3	42.2	34.8
21	PdCl ₂ PPh ₃	Na ₂ CO ₃	Methanol	12.8	14.0	2.0	27.4	34.4
22	Pd(PPh ₃) ₄	Na ₂ CO ₃	Ethanol	14.1	8.4	2.1	36.3	33.9
23	PdCl ₂ PPh ₃	KOH	Methanol	21.3	8.8	2.2	32.6	29.2
24	PdCl ₂ PPh ₃	K ₃ PO ₄	THF	3.6	0.2	5.8	52.2	27.5
25	Pd ₂ (dba) ₃ DavePhos	Na ₂ CO ₃	Methanol	16.5	11.8	2.3	27.9	26.3
26	PdCl ₂ PPh ₃	KHCO ₃	Methanol	20.5	2.4	2.0	47.1	25.2
27	PdCl ₂ PPh ₃	NaOH	CH ₂ Cl ₂	2.5	8.7	2.0	57.6	21.2
28	PdCl ₂ PPh ₃	KOH	THF	14.2	2.2	3.0	55.7	16.2

GSK CONFIDENTIAL

Entry	Palladium Source <i>a</i> Ligand <i>b</i>	Base <i>c</i>	Solvent <i>d</i>	Boronic acid 152 % PAR	Triazole 147 % PAR	168 % PAR	Aryl bromide 149 % PAR	Coupled product 150 % PAR
29	Pd(OAc) ₂ PPh ₃	Na ₂ CO ₃	PhMe	26.5	0.6	2.6	44.8	15.8
30	Pd(OAc) ₂ PPh ₃	KHCO ₃	PhMe	9.9	0.3	3.6	58.7	15.6
31	Pd(OAc) ₂ PPh ₃	Na ₂ CO ₃	THF	25.8	1.0	4.0	46.0	11.0
32	Pd(PPh ₃) ₄	KHCO ₃	THF	29.9	1.5	3.3	53.7	8.4
33	PdCl ₂ PPh ₃	KHCO ₃	CH ₂ Cl ₂	21.9	0.7	7.3	48.6	8.2
34	Pd-C	NaOH	Ethanol	16.2	30.0	7.1	30.6	5.6
35	Pd-C	KHCO ₃	Ethanol	14.1	23.7	7.6	41.8	5.4
36	Pd(PPh ₃) ₄	KOH	PhMe	0.0	11.7	1.8	38.7	5.3
37	Pd ₂ (dba) ₃ DavePhos	Na ₂ CO ₃	CH ₂ Cl ₂	11.1	0.3	4.7	59.6	4.3
38	Pd(OAc) ₂ PPh ₃	NaOH	CH ₂ Cl ₂	15.0	2.7	3.0	66.5	4.0
39	Pd(OAc) ₂ PPh ₃	Na ₂ CO ₃	PhMe	32.0	1.4	4.6	50.3	3.9
40	PdCl ₂ PPh ₃	KHCO ₃	CH ₂ Cl ₂	8.0	0.4	4.3	70.8	3.5
41	Pd ₂ (dba) ₃ DavePhos	NaOH	THF	27.7	3.8	2.0	52.6	3.5
42	Pd-C	K ₃ PO ₄	Ethanol	14.4	37.7	11.7	24.7	3.3
43	Pd-C	Na ₂ CO ₃	Methanol	14.9	46.9	11.1	9.3	2.8
44	PdCl ₂ PPh ₃	NaOH	PhMe	8.4	1.3	1.7	80.6	2.6
45	Pd-C	KOH	Methanol	11.8	39.8	1.6	15.4	2.4
46	Pd-C	KOH	Ethanol	12.8	40.3	9.0	25.8	2.3
47	Pd-C	KHCO ₃	THF	18.8	23.8	15.8	35.6	2.2
48	Pd ₂ (dba) ₃ DavePhos	K ₃ PO ₄	THF	39.1	0.6	3.6	44.0	1.9
49	Pd(PPh ₃) ₄	KHCO ₃	PhMe	74.7	2.2	9.7	9.0	1.6
50	Pd ₂ (dba) ₃ DavePhos	KOH	CH ₂ Cl ₂	18.9	1.3	3.6	55.8	1.5
51	Pd ₂ (dba) ₃ DavePhos	NaOH	CH ₂ Cl ₂	12.7	4.8	2.0	61.3	1.4
52	Pd ₂ (dba) ₃ DavePhos	KHCO ₃	CH ₂ Cl ₂	14.0	0.4	4.4	53.0	1.4
53	Pd ₂ (dba) ₃ DavePhos	K ₃ PO ₄	THF	22.9	0.4	3.1	57.8	1.3
54	Pd-C	NaOH	THF	13.8	13.2	6.8	63.2	1.1
55	Pd(PPh ₃) ₄	K ₃ PO ₄	THF	31.9	0.9	4.5	50.8	0.9
56	Pd-C	Na ₂ CO ₃	THF	18.8	9.7	7.5	61.3	0.9
57	Pd(PPh ₃) ₄	NaOH	PhMe	48.6	3.5	2.7	34.3	0.9
58	Pd ₂ (dba) ₃ DavePhos	KHCO ₃	PhMe	21.5	0.7	5.6	61.5	0.8
59	Pd ₂ (dba) ₃ DavePhos	KOH	PhMe	31.2	14.2	1.8	44.3	0.7

Entry	Palladium Source <i>a</i> Ligand <i>b</i>	Base <i>c</i>	Solvent <i>d</i>	Boronic acid 152 % PAR	Triazole 147 % PAR	168 % PAR	Aryl bromide 149 % PAR	Coupled product 150 % PAR
60	Pd(PPh ₃) ₄	NaOH	CH ₂ Cl ₂	15.6	10.8	1.5	45.5	0.7
61	Pd-C	KOH	THF	21.7	20.1	7.4	47.4	0.7
62	Pd(PPh ₃) ₄	KOH	CH ₂ Cl ₂	26.3	6.3	3.2	53.0	0.7
63	Pd ₂ (dba) ₃ DavePhos	K ₃ PO ₄	PhMe	25.8	0.2	4.9	58.3	0.5
64	Pd-C	KOH	PhMe	39.1	14.7	12.2	31.2	0.5
65	Pd(OAc) ₂ PPh ₃	K ₃ PO ₄	PhMe	0.6	1.2	1.7	81.7	0.4
66	Pd-C	KOH	PhMe	35.1	9.3	8.3	44.2	0.4
67	PdCl ₂ PPh ₃	Na ₂ CO ₃	PhMe	58.2	1.7	3.8	31.2	0.4
68	Pd(PPh ₃) ₄	Na ₂ CO ₃	PhMe	74.3	2.3	4.4	15.9	0.4
69	Pd-C	Na ₂ CO ₃	CH ₂ Cl ₂	12.2	0.5	2.6	83.9	0.2
70	Pd-C	K ₃ PO ₄	CH ₂ Cl ₂	4.8	0.2	2.6	91.6	0.2
71	Pd-C	KOH	CH ₂ Cl ₂	26.2	6.0	1.0	66.8	0.0

6.2 Working Directions for Route B Processes

Working directions are written by laboratory chemist to provide a step by step guide to carrying out a chemical transformation. The working directions are used by pilot plant chemists to author the batch record used in the pilot plant synthesis. The working directions provide extra information not usually found in an experimental procedure, for example contents temperature during a distillation. The extra information is required so the synthesis run on pilot plant scale truly reflects the experimental procedure run in the laboratory.

6.2.1 Working Directions For the Preparation of IG 1
Version No: 1.1

Route: B Stage: 3

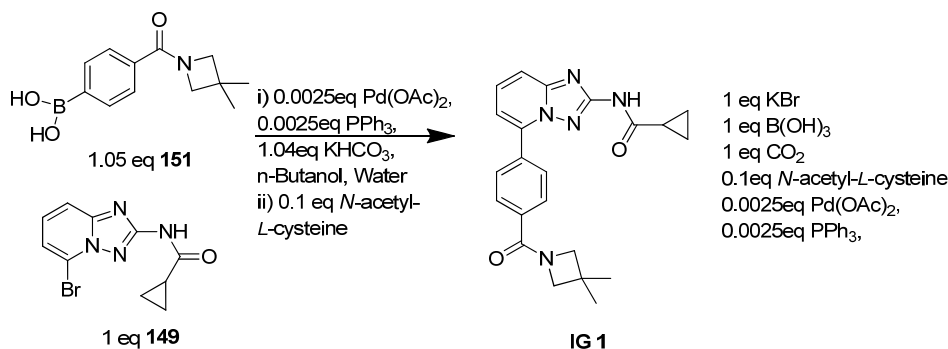
Notebook Ref: R18439/40

Reason for Change: Updated with changes following pilot plant preparation of
batch R18439/40/1

Date: 15th August 2012

Author: Erin D'Souza

Reviewer: Antonella Carangio

Process Scheme**Process Summary**

Potassium hydrogen carbonate (0.37 wt, 1.04 eq), **149** (1 eq, 1 wt), **151** (0.87 wt, 1.05 eq), palladium(II) acetate (0.002 wt, 0.0025 eq), triphenylphosphine (0.0023 wt, 0.0025 eq) are charged to the CLR. *n*-Butanol (9.6 vol) and water (6.4 vol) are added and the mixture heated to reflux (93-94 °C). The organic phase is sampled for HPLC analysis. Once complete, the jacket is cooled to 70 °C and the lower aqueous phase is removed.

N-acetyl-*L*-cysteine (0.0581 wt, 0.1 eq) and water (6.4 vol) are added to the CLR and the mixture stirred for 13-21 hours. The lower aqueous phase is removed and the organic phase is washed with water (6.4 vol), then filtered through Cuno R55S cartridge (pre-wetted with *n*-butanol) to remove black tar. A wash with *n*-butanol (4 vol) carried out and the combined filtrate is transferred to a clean CLR. The organic solution is distilled under reduced pressure (jacket temperature 70 °C) to 8 volumes. *n*-Butanol (5 vol) is added and the solution is again distilled under reduced pressure down to 8 vol. After KF analysis, the slurry is distilled under reduced pressure to 6 vol and *n*-butanol (2 vol) is added. The batch is cooled to 20 °C. The slurry is aged at 20 °C for at least an hour. The slurry is filtered and washed with *n*-butanol (2 x 2 vol). The filtered solid was placed in a vacuum oven to dry at 50 °C.

Percent yield range observed: 78-88%

Procedure: (run in 250mL equipment)

1. A nitrogen flow is started in the CLR and the CLR is purged for several minutes.
2. *n*-Butanol (2 vol) was charged to the CLR.
3. **149** (1 eq, 1 wt), palladium acetate (0.0025 eq) and triphenylphosphine (0.0025 eq) were charged together in one portion to the CLR.
4. *n*-Butanol (7.6 vol) was charged to the CLR, washing in the solids from the previous step.
5. **151** (1.05 eq), and potassium bicarbonate (1.04 eq) were charged to the CLR.
6. Water (6.4 vol) was charged to the CLR, washing in the solids from the previous step.
7. The contents were stirred and heated to reflux (contents = 93-94 °C).
8. After 4 hours, a sample of the organic phase was taken for HPLC analysis (See Go/No Go Decision).
9. The contents were cooled to 70±3 °C. The stirrer was stopped and the aqueous phase was removed
10. *N*-acetyl-*L*-cysteine (0.0581 wt, 0.1 eq) and water (6.4 vol) were charged to the CLR.
11. The biphasic mixture was stirred for 13-21 hours with contents temperature at 70±3 °C.
12. The stirrer was stopped and the aqueous phase was removed.
13. Water (6.4 vol) was charged to the CLR.
14. The biphasic mixture was stirred for 60 minutes with contents temperature at 70±3 °C.
15. The stirrer was stopped and the aqueous phase was removed.
16. The organic phase was filtered through a Cuno R55S cartridge (pre-wetted with *n*-butanol).
17. The Cuno cartridge was washed with *n*-butanol (4 vol)
18. The filtrate was concentrated to 8 volumes (vacuum distillation, maximum jacket temperature 70 °C, start of distillation contents temperature 60 °C, 250 mbar)

GSK CONFIDENTIAL

19. *n*-Butanol (5 vol) was charged and the reaction mixture was concentrated to 8 volumes (vacuum distillation, end of distillation contents temperature 61 °C, 83 mbar, see Go/No Go Decision)
20. The reaction mixture was concentrated under vacuum to 6 volumes
21. *n*-Butanol (2 vol) was charged to the reaction to wash in encrustation.
22. The contents were cooled to 20 °C.
23. The slurry was stirred for at least 9 hours at 20 °C
24. The slurry was filtered and washed with *n*-butanol (2 x 30 mL, 2 x 2 vol)
25. The damp cake was dried in a vacuum oven at 50 °C (Damp cake volume 3.8 vol, see Go/No Go Decision)

Yield 78-88% theory, 108-122% w/w

Go/No Go Decision

Step 8 – A 50 µL sample of the organic phase is taken and diluted with methanol (20 mL). The solution obtained is sent for HPLC analysis using the 8 minute generic method at 232 nm.

Retention Time **149** - ~2.8 minute

Retention Time **151** - ~3.2 minutes

Retention Time **1** - ~ 4.1 minutes

149 must be below 3% area before the process can continue

Step 19 – A sample of the slurry will be taken and filtered. The filtrate will be analysed by KF analysis. Require KF <0.5% w/w water.

Step 23- eOVI analysis is carried out to determine if batch is dry. eOVI must show less than 0.5% w/w *n*-butanol in order to proceed.

Waste Stream Composition

Step 9 – 5.2 vol Aqueous waste containing ~7% w/w *n*-butanol, ~4% w/w B(OH)₃, 8% w/w KBr, and <1% w/w **151**.

GSK CONFIDENTIAL

Step 12 – 6.6 vol Aqueous waste containing ~7% w/w *n*-butanol, 0.9% w/w *N*-acetyl-*L*-cysteine and trace palladium salts.

Step 15 – 7.6 vol Aqueous waste containing ~7% *n*-butanol

Step 17 – Cuno cartridge containing trace palladium salts.

Step 18 – ~8 vol *n*-butanol containing ~6% w/w water.

Step 19 – ~5 vol *n*-butanol containing ~1% w/w water

Step: 20 - ~ 2 vol *n*-butanol

Step 24 – Mother liquors: *n*-butanol containing ~1% w/w **1**, <1% w/w triphenylphosphine and other trace organic impurities. Washes contain < 1% **1**.

Cleaning

It is recommended that water washes of the reactor vessels are carried out in between batches, as water soluble orange stains have been observed in laboratory vessels

The solubility of **1** is 26mg/mL in MeOH at room temperature going up to approximately 45mg/mL at 50 °C.

1 is stable in methanol for 8 h at reflux followed by 40 h at room temperature.

Holdpoints

Step 8 – Following a successful IPM, the stirred mixture may be cooled to 20 °C and held overnight. Crystallisation will occur, but all solids will dissolve upon heating back up to 70 °C before proceeding with step 9

Step 15 – Following removal of the aqueous phase, the stirred mixture may be cooled to 20 °C and held for 3 days. Crystallisation will occur, but all solids will dissolve

GSK CONFIDENTIAL

upon heating back up to 70 °C before proceeding with step 16. Note: it is important to check that all solids have dissolved before proceeding with Step 16.

Step 17 – Following Celite filtration and washes, the stirred mixture may be cooled to 20°C and held over the weekend. Crystallisation will occur, but most of the solids will dissolve upon heating back up to 70°C before proceeding with the distillation.

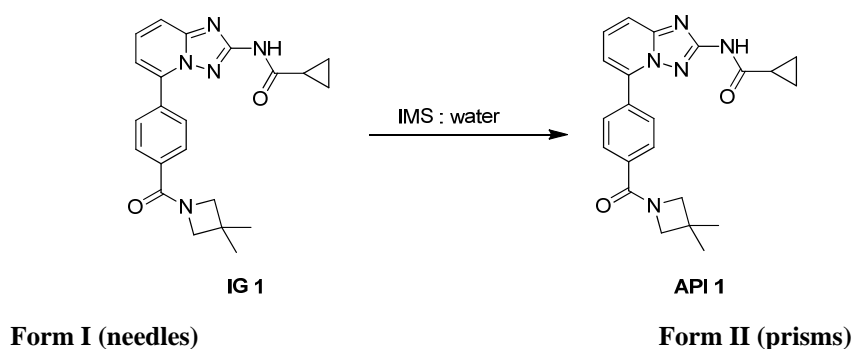
Step 18-19 – hold point suitable for up to 2 days (held over weekend)

Step 23 – The slurry may be held over the weekend at 20°C prior to filtration

6.2.2 Working Directions for Preparation of API 1

Version No: 1.0

Route: B Stage: 4

Reason for Change: new route and increase in seed temperature**Date:** 07th August 2012**Author:** Elaine Smith**Reviewed by:** Andrew Craig**Process Scheme****Process Summary**

IG 1 (1 wt) is dissolved in 4:1 v/v IMS/water (9 vol) and heated to 75±3 °C. The solution is clarified using a line wash of 4:1 v/v IMS/water (1 vol). The clarified solution is cooled to 60±3 °C over 30 minutes and seeded with API 1 (0.5% w/w). The slurry is aged over at least 1 hour. The slurry is cooled to 5±3 °C over at least 110 mins and aged for at least 2 hours. The slurry is filtered and the cake is washed with 4:1 v/v IMS/water (2 x 1.7 vol), blown down and dried under vacuum at 50 °C to give API 1 as a white to off-white solid.

Percent yield range observed: 77-84%**Min process volume: 9 volumes****Max process volume: 10 volumes**

Procedure: (run in 1L CLR)

All weights and volumes are relative to IG 1.

1. Charge IG 1 (50.0 g, 1 weight) to CLR.
2. Charge IMS (360 ml, 7.2 vol) to CLR.
3. Charge water (90 ml, 1.8 vol) to CLR
4. Heat contents to 72-75 °C and hold until complete dissolution is observed.
5. Clarify the solution into a clean, dry vessel maintaining the temperature above 60 °C and as close to 75 °C as possible. See GO/NO GO Decision.
6. Charge 4:1 v/v IMS/water (49 ml, 1 vol) to dissolution CLR.
7. Line rinse with 4:1 v/v IMS/water at 72-75 °C
8. Once transferred to the crystallizer, ensure that complete dissolution has been maintained. See GO/NO GO Decision.
9. Cool the solution to 60±3 °C at 0.5 °C/min whilst stirring at 350 rpm.
10. Seed solution with API 1 (0.25 g, 0.005 wt) as a dry solid. See GO/NO GO Decision.
11. Age slurry at 60±3 °C for at least 1 hour.
12. Cool slurry to 5±2 °C at 0.5±0. 2 °C/min whilst stirring at 350 rpm.
13. Age slurry at 5±2 °C for at least 2 hours. Take a sample of slurry for information only.
14. Isolate slurry by filtration at 5±2 °C. Take a sample of the mother liquors for information only.
15. Wash cake with 4:1 v/v IMS/water chilled to 5±2 °C (2 x 1 cake vol, 2 x 1.7 vol, 2 x 85 mL).
16. Blow cake with nitrogen for at least 1 hour.
17. Dry the product *in vacuo* at 50°C overnight. See GO/NO GO Decision.

Notes:

All steps: Use bottom jacket only for heating and cooling to minimize encrustation

GSK CONFIDENTIAL

Step 10: Due to the high density of the seed material and good flow properties, seed will be added as a dry solid but can be rinsed in with 0.04 vol of water.

Step 11: Slurry must be aged for at least 1 hour but the process can be held here for up to 2 hours if required.

Step 13: Slurry must be aged for at least 2 hours but the process can be held here overnight if required.

Step 15: Encrustation will have occurred on the agitator shaft and any other probes inside the vessel. Please try to avoid washing this material into the slurry during the washes.

Go/No Go Decision

Step 5: If crystallization has started to occur before the solution has passed through the filter, the process will need to be aborted and equipment cleaned ready for re-processing. Consult the chemist.

Step 8: If crystallization has started to occur in the crystallizer vessel due to a temperature drop during the clarification step, ensure that the solution is held at 72-75 °C until complete dissolution re-occurs before proceeding to the next step.

Step 10: After addition of the seeds, the seeds should persist in solution and initiate crystallization. If the seeds dissolve, consult the chemist.

Step 17: Sample for KF and eOVI analyses. Off load when levels of IMS $\leq 0.1\%$ w/w and water $\leq 0.05\%$ w/w.

Waste Stream Composition

Step 14: Waste stream (approx. 10 vol) consists of IMS and water (~80% v/v IMS and ~20% v/v water) containing <20 mg/mL **1**.

Step 15: Waste stream (approx 3.2 vol) consists of IMS and water (~80% v/v IMS and ~20% v/v water) containing trace **1**.

Cleaning

1 has a solubility of ~26 mg/ml in methanol at room temperature and ~45mg/mL at 50 °C. **1** is stable in methanol at a concentration of 1 mg/ml after stirring at reflux for 8 hours and stirring at room temperature for 72 hours.

7 Acknowledgments

I would like to acknowledge the following team members for their advice and assistance in carrying out experiments and analysis:

Chris Nichols – Project leader during route A development and metabolite **157** synthesis.

Antonella Carangio – Project leader during Route B development.

Neil Smith – Route B Stage 2 development (Section 2.2.1) and project leader during metabolite **167** synthesis (Section 3.3) including preparation of **185** (Section 3.3.3).

Dharmista Patel – Project analyst.

Richard Jones – ICP-AES analysis of IG **1** and API **1**.

Elaine Smith and Leanda Kindon – Recrystallisation of laboratory batches of route B IG **1** output (Section 2.2).

Daniel Tray – Route A stage 2 d-optimal design (Section 2.2.2).

Phillip Jolly – Initial route B development (Sections 2.2.2 and 2.2.3).

Katherine Wheelhouse – Assistance with palladium supported reagents and palladium scavenger reagents (Section 2.2.5) and discussions on hydrogenolysis to prepare **175** (Section 3.3.4).

Chris Hughes and Chris Messenger – Scale-up lab synthesis of IG **1**.

Alec Simpson – Identification of impurities with LC-MS (Section 2.2.8) and HRMS (Section 3.3.3).

Claire Crawford and Kate Llewellyn – Route B Stage 3 DoE analysis (Section 2.2.9).

Stuart Leach – Development of Stage 3 work-up and isolation (Section 2.2.10).

Jamie Russell, Chris McKay and Stevenage Pilot Plant technicians – Pilot plant manufacture of IG **1** and API **1**.

Mike Urquhart – Preparation of **183** (Section 3.3.3).

GSK CONFIDENTIAL

Michael Webb - Discussions on hydrogenolysis to prepare **175** (Section 3.3.4).

Chris Thickitt, Richard Horan and Hugh Clark – discussions on purification of Metabolite **167** (Section 3.3.5).

John Leahy and John Strachan – Isolation of metabolite **167** (Section 3.3.5).